CONTRIBUTION OF THE TEMPOROAMMONIC PATHWAY TO HIPPOCAMPAL PROCESSING

Thesis by

Hannah Dvorak-Carbone

in partial fulfillment of the requirements

for the degree of

Doctor of Philosophy

California Institute of Technology

Pasadena, California

1999

(Submitted April 14, 1999)

Acknowledgments

Graduate school has been the most educational experience of my life – but much of what I learned has nothing to do with rat brains. I would like to acknowledge here the invaluable support of faculty, colleagues, friends and family that has gotten me through this long and often arduous stage of my life.

Each of my committee members – Mark Konishi, Gilles Laurent, Henry Lester, Jerry Pine, and Erin Schuman – has contributed in some way to my development as a scientist. In particular, I would like to thank Jerry for providing me with the hands-on laboratory training that has left me with the confidence to tackle just about any technical problem. Erin, my thesis advisor, has always been supportive of my efforts and patient with my idiosyncrasies. Under her tutelage, I hope I have picked up some of her skill in seeing and sharing the big picture to which seemingly modest discoveries contribute.

My laboratory colleagues, past and present, in both the Pine and the Schuman labs have always made it a pleasure to come in to work, even when my experiments weren't going well. In particular, I would like to thank my friends Jeroo Sinor and Steve Potter for hours of stimulating conversations and emotional support.

I would like to thank the Howard Hughes Medical Institute for financial support in the form of a predoctoral fellowship. Thanks, too, to Novartis (formerly Ciba-Geigy) for the gift of the $GABA_B$ receptor antagonist CGP 55845A; Julie Kauer at Duke, for a biocytin staining protocol that actually worked; and Brian Christie at the Salk Institute, for sharing his recipe for whole-cell recording solution. Here at Caltech, I would like to acknowledge the help of biology grad student secretaries Liz Ayala and Janet Davis,

Mike Walsh and Tim Heitzman in the biology electronics shop, and Parandeh Kia at International Student Programs.

The class of biology graduate students with whom I entered Caltech in the fall of 1992 turned out to be a truly extraordinary group. Being a member of the "organism," the pizza class that wouldn't die, was a wonderful experience. I was lucky enough to be able to study for qualifiers with a great set of classmates: Roian Egnor, Amy Greenwood, Hyejin Kang, Kate MacLeod, Jeff Rawlings, and Brian Sullivan. Each of these people became a good friend as well as a supportive study buddy. Those sessions in BI 23 were educational, intellectually challenging, and a great deal of fun.

Extracurricular and social activities have helped keep me balanced over the years. Softball in all its incarnations (Brains not Botts, Botts not Bonobos...) and Gradiators were great fun in the summer. The late, lamented Alles Courtyard beer hour was a great way to meet people from other labs (and even other divisions). I had a lot of fun hanging out with the band Bananafish (Greg Carbone, Anna Karion, Kate MacLeod, and Mark Stopfer).

Two of my closest friendships have developed over the course of my graduate studies and have brought much joy to my life. Thanks to Andrea Dvoredsky for long swims and smug smoothies, supportive conversations and reality checks, fun times and a different perspective. Thanks to Kate MacLeod, whose steadfast friendship I have much appreciated in good times and bad.

I would never have gotten where I am today without the support and encouragement of my parents, Pavel and Antonia Dvorak. They have always motivated me to do my best, and I hope I have done so.

Finally, and most importantly, I must thank my infinitely patient, loving, and supportive husband, Greg Carbone. Without his love, encouragement, and confidence in me, I don't know how I could have made it through this grueling thing called grad school. I look forward in great anticipation to our post-Caltech life together.

Abstract

The temporoammonic (TA) pathway is the direct, monosynaptic projection from layer III of entorhinal cortex to the distal dendritic region of area CA1 of the hippocampus. Although this pathway has been implicated in various functions, such as memory encoding and retrieval, spatial navigation, generation of oscillatory activity, and control of hippocampal excitability, the details of its physiology are not well understood. In this thesis, I examine the contribution of the TA pathway to hippocampal processing. I find that, as has been previously reported, the TA pathway includes both excitatory, glutamatergic components and inhibitory, GABAergic components. Several new discoveries are reported in this thesis. I show that the TA pathway is subject to forms of short-term activity-dependent regulation, including paired-pulse and frequency-dependent plasticity, similar to other hippocampal pathways such as the Schaffer collateral (SC) input from CA3 to CA1. The TA pathway provides a strongly excitatory input to stratum radiatum giant cells of CA1. The excitatory component of the TA pathway undergoes a long-lasting decrease in synaptic strength following low-frequency stimulation in a manner partially dependent on the activation of NMDA receptors. High-frequency activation of the TA pathway recruits a feedforward inhibition that can prevent CA1 pyramidal cells from spiking in response to SC input; this spike-blocking effect shows that the TA pathway can act to regulate information flow through the hippocampal trisynaptic pathway.

Table of Contents

List of figures

Following Chapter 3 (starting page 190):

Following Chapter 4 (starting page 223):

Following the Appendix (starting page A-12):

List of tables

Abbreviations used

5-HT	5-hydroxy-tryptamine (serotonin)
ACh	acetylcholine
AHP	afterhyperpolarization
AMPA	α-amino-3-hydroxy-5-methyl-4-isoxazolepropionic acid
AP5	2-amino-5-phosphonopentanoic acid
CCh	carbachol
CNQX	6-cyano-7-nitroquinoxaline-2,3-dione
DAB	diaminobenzidine
DG	dentate gyrus
EC	entorhinal cortex
EGTA	ethylene glycol-bis(β-aminoethyl ether) N,N,N'N'-tetraacetic acid
EPSC	excitatory postsynaptic current
EPSP	excitatory postsynaptic potential
GABA	γ-aminobutyric acid
HEPES	N-[2-hydroxyethyl]piperazine-N'-[4-butanesulfonic acid]
HFS	high frequency stimulation
IPSC	inhibitory postsynaptic current
IPSP	inhibitory postsynaptic potential
ISI	interstimulus interval
LFS	low frequency stimulation
LTD	long-term depression
LTP	long-term potentiation
mAChR	muscarinic acetylcholine receptor
mGluR	metabotropic glutamate receptor
NE	norepinephrine

NMDA	*N*-methyl-D-aspartate
NS	not significant
O/A	oriens/alveus
O-LM	oriens-lacunosum-moleculare
PBS	phosphate-buffered saline
PP	perforant path
PPD	paired-pulse depression
PPF	paired-pulse facilitation
PSP	postsynaptic potential
PTP	post-tetanic potentiation
RE	nucleus reuniens thalami
SC	Schaffer collateral
SCG	superior cervical ganglion
SE	standard error
SEM	scanning electron microscopy
SLM	stratum lacunosum-moleculare
SO	stratum oriens
SP	stratum pyramidale
SR	stratum radiatum
STP	short-term potentiation
TA	temporoammonic
TBS	theta burst stimulation
TEA	tetraethylammonium

1 Introduction and literature review

All nervous systems, from the simple, diffuse neuronal nets of cnidarians, to the complex, sophisticated brains of the higher vertebrates, have basically the same function: to take in sensory information about an animal's external environment and provide motor or hormonal control commands to allow the animal to respond appropriately. In all but the simplest animals, in between these input and output systems is a neuronal network that stores information about both previous and ongoing experiences and is continually being modified to allow the animal to respond in a more adaptive way in the future; in other words, nervous systems underlie the phenomena of adaptability, flexibility, learning, and memory.

How is information represented and processed in the brain? Although there is much heterogeneity amongst the individual neurons of the nervous system, in vertebrates, individual neurons are not sufficiently specialized so that one could point to a particular neuron as being responsible for storing a particular bit of information. Rather, it is the position of that neuron in a network, and its temporal pattern of activity in relation to other neurons in that network, that give meaning to its signaling.

The brain is not a static device, reacting identically to identical inputs. On the contrary, it is a dynamically shifting network whose responses depend on its current state as well as its recent activity patterns and its developmental history. Networks in the brain are modified in an activity- or experience-dependent manner on many different time scales, from moment-to-moment changes over milliseconds to minutes, based on the recent history and activity of the network, to slow and/or long-lasting changes that can

occur and persist over the lifetime of the organism. On a short time scale, changes in input-output relations underlie processes such as behavioral decisions or retrieval of stored memories. Longer-scale changes include developmental phenomena as well as the processes of learning and long-term memory storage.

In this thesis I explore short- and long-term activity-dependent modulation, and interaction with other pathways, of a particular pathway in the mammalian nervous system: the temporoammonic (TA) projection from the entorhinal cortex (EC) to area CA1 of the hippocampus, a projection whose physiological properties and functional roles are not particularly well understood. The phenomena I describe in this pathway illustrate well the importance of temporal and spatial patterning in the nervous system. Chapter 1 provides general background regarding excitation and inhibition in neuronal networks, the importance of the hippocampus as a system for studying neural processing, and a description of what is currently known about the TA pathway. My investigations of the physiology and short-term plasticity of the TA input to hippocampus are described in Chapter 2. Chapter 3 describes my discovery and characterization of long-term depression (LTD) of synaptic transmission in the TA pathway. In Chapter 4, I describe a role for the TA pathway in regulating information flow through the hippocampus. (Chapters 3 and 4 are verbatim copies of papers published or submitted for publication, so there may be some redundancy between these and other chapters.) The contribution of my findings to our understanding of the TA pathway and hippocampal processing, and possible directions for further research, are described in Chapter 5. Finally, in the appendix, I describe another approach to understanding neuronal processing: the

neurochip, a micromachined silicon device designed to allow detailed recording and stimulation of a small network of cultured neurons.

1.1 Balancing excitation and inhibition in the brain

Synaptic connections between neurons in the brain can be classified as either excitatory or inhibitory, depending on whether their effect is to bring the postsynaptic neuron closer to or further away from action potential threshold. Clearly, this is a gross oversimplification and complications abound. For example, in a network of neurons, inhibition of another inhibitory neuron may result in a net excitation of a neuron further downstream, a phenomenon known as disinhibition. In a complicated circuit, the ultimate response of any particular neuron to a set of inputs may be impossible to predict even if all pairwise connections are understood (Harris-Warrick and Marder 1991; Dickinson and Moulins 1992; Buzsáki 1997). Following an "inhibitory," hyperpolarizing postsynaptic response, the membrane potential of a neuron may rebound above the original baseline (e.g., Buhl *et al.* 1995), even reaching action potential threshold (e.g., Crunelli and Leresche 1991; Cobb *et al.* 1995) – a net excitatory effect. Postsynaptic responses to neurotransmitters generally considered to be inhibitory can be depolarizing, actually bringing the cell closer to threshold (Michelson and Wong 1991; Taira *et al.* 1997). Nevertheless, the simple definition above is still useful as a starting point for describing neuronal circuitry. In general, in the mammalian CNS, excitatory connections between neurons are mediated by glutamatergic synapses, and inhibitory connections by γ-aminobutyric acid-mediated (GABAergic) synapses. Glutamate and GABA have not been found to be co-localized in the same neurons, allowing classification of neurons

either as excitatory (glutamatergic) principal cells, or inhibitory (GABAergic) interneurons. (It should be noted that not all principal cells are glutamatergic; the Purkinje cells of the cerebellum are a notable exception (Ito *et al.* 1964)).

The reason for the importance of excitation, of bringing neurons closer to firing action potentials, is simply that action potentials are necessary for the long-distance communication of activity in the vertebrate nervous system. Although inhibition is sometimes described as being detrimental to neuronal transmission (e.g., "Three types of inhibitory neurones provide different classes of *interference*" (my emphasis) (Andersen 1990)), inhibitory pathways have a crucial role in sculpting neuronal activity patterns. Information carried in patterns of neural activity is likely to be conveyed by both excitatory and inhibitory mechanisms. Synaptic inhibition may contribute to the generation of rhythmic oscillatory activity in the brain and provide a background or "context" for the activity of principal cells (Buzsáki 1997).

In the absence of inhibition, runaway excitation leads to seizure-like activity (e.g., Ben-Ari *et al.* 1979; Sloviter 1991; Watson *et al.* 1997) and even cell death. Conversely, an excess of inhibitory activity may also be pathological, for example, in absence or petit mal seizures (Marescaux *et al.* 1992b). A healthy and functional nervous system depends on a careful, dynamic balance of excitatory and inhibitory influences. Ways in which excitation and inhibition are mediated, regulated, and interact are described below. Many of the examples given are from the hippocampal formation, because my thesis work focused on this region of the brain.

1.1.1 Mechanisms of excitation

The primary excitatory neurotransmitter in the mammalian CNS is glutamate. Glutamatergic excitatory postsynaptic potentials (EPSPs) are mediated primarily by the α-amino-3-hydroxy-5-methyl-4-isoxazolepropionic acid (AMPA) and *N*-methyl-D-aspartate (NMDA) types of ionotropic receptors (AMPARs and NMDARs) (see Seeburg for review); a variety of metabotropic glutamate receptors (mGluRs) also exist (see Nakanishi 1992; Schoepp and Conn 1993; Pin and Duvoisin 1995 for reviews). The AMPA and NMDA receptors are both directly-gated ion channels permeable to mono-valent cations (Na^+ and K^+); therefore, activation of these receptors results in an inward, depolarizing current (Jahr and Stevens 1987). AMPAR currents have a quick, short time course (Tang *et al.* 1989; Trussell and Fischbach 1989). NMDA channels are slower to activate but stay open longer, resulting in a longer-lasting current (Lester *et al.* 1990). NMDARs also differ from (most) AMPARs in their permeability to calcium (Mayer and Westbrook 1987), a property which makes them crucial to several forms of activity-dependent plasticity (see Malenka and Nicoll 1993 for review). However, NMDA receptors are not just simple ligand-gated channels; there is also a voltage-dependent component to the NMDA response. At typical resting membrane potentials, NMDA channels are blocked by ambient levels of extracellular Mg^{2+}; this block is relieved only by membrane depolarization (Nowak *et al.* 1984). Hence, a glutamatergic EPSP will only include an NMDAR-mediated component when the depolarization due to AMPAR activation is sufficient to relieve the voltage-dependent block of the NMDAR (Herron *et*

al. 1986). This constraint allows NMDARs to act as coincidence detectors (e.g., Mel 1992; see Malenka and Nicoll 1993 for review).

Most glutamatergic, excitatory synapses are made onto the dendritic tree, rather than the soma, of postsynaptic neurons. The result of the convergence of multiple excitatory inputs onto the same postsynaptic cell depends on the location of the synapses and on the passive and active electrical properties of the postsynaptic dendritic tree. Passive cable theory predicts that EPSPs evoked distally in the dendrites will undergo electrotonic decay, decreasing in amplitude and increasing in duration and time to peak, between the dendrite and the soma (Rall 1967). Summation of EPSPs is predicted to depend on the relative locations of synaptic inputs, with EPSPs evoked in close proximity to one another summating sublinearly because of the decreased driving force due to postsynaptic depolarization; however, it has been shown experimentally that the summation of EPSP-like responses to glutamate puffs in cultured hippocampal pyramidal cells is, in fact, linear and position independent (Cash and Yuste 1998). This linearization of EPSP summation was found to be mediated by the competing effects of increased depolarization due to activation of NMDARs, and increased shunting due to voltage-activated K^+ conductances.

Active dendritic conductances can shape excitatory inputs in a number of ways (see Yuste and Tank 1996 for review). Voltage-dependent Na^+ conductances can boost EPSP-like responses to epochs of photoreleased glutamate closely spaced in time, resulting in a supralinear summation (Margulis and Tang 1998). Transient, A-type K^+ conductances can decrease EPSP amplitude (Hoffman *et al.* 1997), as can the hyperpolarization-activated K^+ current I_H (Magee 1998). Perforant path inputs to the distal

dendrites of CA3 pyramidal cells are amplified by voltage-dependent Na^+ and Ca^{2+} channels (Urban *et al.* 1998).

1.1.2 Regulation and modulation of excitation

Although excitatory synaptic transmission is most dramatically regulated by concurrent inhibitory transmission (see below, section 1.1.3, p. 10), EPSPs are also modulated by processes independent of inhibition. Activity- and state-dependent changes in the strength of excitatory synapses can modulate patterns of information flow through neuronal circuits.

Excitatory synapses undergo several forms of activity-dependent short- and long-term plasticity (see Malenka and Nicoll 1993 for review). Paired-pulse stimulation of excitatory pathways often results in an increase in the amplitude of the response to the second stimulus (Creager *et al.* 1980; Leung and Fu 1994; Debanne *et al.* 1996; Thomson 1997); this paired-pulse facilitation (PPF) is thought to be mediated presynaptically by the accumulation of calcium in the presynaptic terminal (Manabe *et al.* 1993; Thomson *et al.* 1993; Wu and Saggau 1994). However, paired-pulse stimulation sometimes results in a depression of the second response (Thomson *et al.* 1993; Thomson 1997). The balance between paired-pulse facilitation and depression appears to depend on the probability of neurotransmitter release, and hence is predicted by the size of the first response: a small response is more likely to show facilitation, while a larger response is more likely to undergo depression (Manabe *et al.* 1993; Debanne *et al.* 1996; Dobrunz and Stevens 1997). Paired-pulse responses can also be modulated by voltage-dependent conductances such as voltage-dependent K^+ and Na^+ channels (Margulis and Tang 1998) or NMDA

receptors (Thomson 1997). Paired-pulse depression of EPSPs is thought to be mediated by transient depletion of neurotransmitter at the presynaptic terminal (Galarreta and Hestrin 1998; Wang and Kaczmarek 1998).

Intermediate in time scale between paired-pulse plasticity, and the long-lasting forms of plasticity described below, are the phenomena of post-tetanic potentiation (PTP) and short-term potentiation (STP). PTP is a brief (~1 minute) increase in synaptic strength observed following intense, high-frequency stimulation of afferent pathways, and is thought to be mediated presynaptically, by means of calcium accumulation in the presynaptic terminal (Rosenthal 1969; Swandulla *et al.* 1991; Wu and Saggau 1994; see Fisher *et al.* 1997 for review). STP is less well-defined, but seems to be similar to long-term potentiation (LTP) (Hannay *et al.* 1993) but of a briefer duration.

Activity-dependent long-term plasticity of excitatory synapses has been described in several neural pathways. LTP of synaptic transmission is an increase in synaptic strength that can last for hours or days (see Bliss and Collingridge 1993; Nicoll and Malenka 1995 for review). LTP can be induced by high-frequency (tetanic) (Andersen *et al.* 1977), theta-patterned (Larson and Lynch 1986), or primed-burst stimulation (Rose and Dunwiddie 1986), as well as by pairing low-frequency inputs with direct depolarization of the postsynaptic cell (Gustafsson and Wigström 1986). Many forms of LTP are dependent on the activation of NMDARs, and the influx of Ca^{2+} into the postsynaptic cell via NMDARs and/or voltage-dependent calcium channels (Grover and Teyler 1990) seems to be a common first step in LTP induction (Lynch *et al.* 1983; Malenka *et al.* 1988; see Malenka and Nicoll 1993 for review; Neveu and Zucker 1996).

LTD of synaptic transmission is a reduction in synaptic strength that can last for hours (see Linden 1994; Bear and Abraham 1996 for review). LTD is most commonly induced by long episodes of low-frequency inputs (e.g., Dudek and Bear 1992), although other paradigms, such as trains of paired-pulse stimuli (e.g., Doyère *et al.* 1996) or asynchronous pre- and postsynaptic activity (e.g., Debanne *et al.* 1994), are also used. Calcium influx into the postsynaptic cell is also required for LTD induction (Cummings *et al.* 1996; Neveu and Zucker 1996), although the sources for this calcium can include NMDARs, various types of voltage-dependent calcium channels, mGluR activation, and release of Ca^{2+} from intracellular stores (see section 3.5, p. 183, for further discussion).

Glutamatergic transmission can also be rapidly regulated by the activation of presynaptic mGluRs. Immunocytochemical studies have demonstrated the presence of various mGluR subtypes at presynaptic terminals (Neki *et al.* 1996; Petralia *et al.* 1996; Risso Bradley *et al.* 1996). Activation of presynaptic mGluRs, which can occur during periods of high-frequency activity in which excess glutamate is more likely to spill over outside of the synaptic cleft, can inhibit further glutamate release (Burke and Hablitz 1994; Gereau and Conn 1995; Macek *et al.* 1996; Scanziani *et al.* 1997).

Excitatory neurotransmission can also be modulated by the activity of other neurotransmitter systems. Adenosine, whose concentration is elevated during ischemia or periods of intense neuronal activity (Winn *et al.* 1980), acts on presynaptically located A_1 receptors (Swanson *et al.* 1995) to reduce glutamate release (Proctor and Dunwiddie 1987; Thompson *et al.* 1992). The hippocampus receives substantial cholinergic innervation from the medial septum (see Dutar *et al.* 1995 for review). Acetylcholine

(ACh) can decrease excitatory transmission by acting on presynaptically located muscarinic ACh receptors (mAChRs) to reduce glutamate release (Kahle and Cotman 1989; Hasselmo and Schnell 1994; Gil *et al.* 1997), but it can also act on nicotinic receptors to enhance glutamatergic transmission (Gray *et al.* 1996; Gil *et al.* 1997; Radcliffe and Dani 1998). The overall excitability of pyramidal cells can also be increased by K^+ channel blockade due to mAChR activation (Cole and Nicoll 1984; Dutar *et al.* 1995). Serotonin (5-HT), which is released by fibers from the raphe nuclei (Oleskevich and Descarries 1990), has been shown reduce glutamatergic transmission in the subiculum (Boeijinga and Boddeke 1996), as well as reducing synaptic excitation of superficial layer EC neurons (Schmitz *et al.* 1995a) and CA1 pyramidal cells (Zhang *et al.* 1994).

1.1.3 Mechanisms of inhibition

Inhibitory mechanisms can be classified by the postsynaptic receptor mediating them, by the location of inhibitory synapses on the postsynaptic cell, or by the position of inhibitory influences in a neuronal circuit. These are all described below, along with descriptions of how these forms of inhibition interact with excitatory inputs.

1.1.3.1 $GABA_A$ and $GABA_B$

The primary inhibitory neurotransmitter in the mammalian central nervous system is GABA (see Krnjevic 1997 for review). Inhibitory cortical and hippocampal inter-neurons use GABA as their primary neurotransmitter. There are at least three families of GABA receptors: $GABA_A$, $GABA_B$, and $GABA_C$ (see Sivilotti and Nistri 1990 for

review). (The $GABA_C$ receptor appears to be found primarily in the retina (Bormann and Feigenspan 1995), although some of its subunits are also found throughout the brain (Enz and Cutting 1999); it will not be discussed further here.)

1.1.3.1.1 $GABA_A$

The $GABA_A$ receptor is an ionotropic receptor permeable to chloride. It is made up of several, most likely five, subunits and is related to the glycine and nicotinic cholinergic receptors (see Stephenson 1995 for review). $GABA_A$ receptors are fast, directly gated by GABA, blocked by picrotoxin and bicuculline, and activated by muscimol (see Sivilotti and Nistri 1990 for review). Because of their permeability to chloride, $GABA_A$ receptors usually carry an outward, hyperpolarizing current, taking the neuron further away from the threshold for action potential firing (Alger and Nicoll 1982; Pham and Lacaille 1996). However, since the reversal potential for chloride can be close to the resting potential of a neuron, the driving force on chloride may be quite small, and if a neuron is hyperpolarized, the $GABA_A$ response may be depolarizing (e.g., Andersen *et al.* 1980; Connors *et al.* 1988). Even in the absence of a voltage change, activation of $GABA_A$ channels may have an inhibitory effect by lowering the neuron's input resistance and shunting other, depolarizing currents (Ben-Ari *et al.* 1979; Andersen *et al.* 1980; Stelzer *et al.* 1994; Johnston *et al.* 1996). A depolarizing response after $GABA_A$ receptor activation is also sometimes observed even at resting potentials (Andersen *et al.* 1980; Wong and Watkins 1982; Newberry and Nicoll 1985; Michelson and Wong 1991); the ionic basis for this response is still poorly understood (Lambert *et al.* 1991; Thompson 1994; Taira *et al.* 1997). There is also evidence for two distinct $GABA_A$-mediated

hyperpolarizing currents, one fast, one slower (though still faster than the $GABA_B$ response), which may be mediated by different subtypes of the $GABA_A$ receptor (Pearce 1993; Banks *et al.* 1998).

1.1.3.1.2 $GABA_B$

Unlike the $GABA_A$ receptor, the $GABA_B$ receptor is not an ion channel itself; rather, it is coupled via G proteins to several downstream targets. Downstream effects of $GABA_B$ receptor activation include inhibition of voltage-dependent calcium currents (Pfrieger *et al.* 1994; Guyon and Leresche 1995; Lambert and Wilson 1996) and activation of potassium channels (Gähwiler and Brown 1985; Otis *et al.* 1993; Sodickson and Bean 1996). The $GABA_B$ response is antagonized by phaclofen (Dutar and Nicoll 1988; Karlsson and Olpe 1989), saclofen and their derivatives (Solís and Nicoll 1992), as well as more recently synthesized compounds such as CGP 55845A (Davies *et al.* 1993); baclofen is a potent agonist of the $GABA_B$ receptor (Hill and Bowery 1981; Newberry and Nicoll 1985; Davies *et al.* 1993). $GABA_B$ receptors are found at postsynaptic sites as well as on the presynaptic terminals of both glutamatergic and GABAergic neurons.

The postsynaptic $GABA_B$ response is a slow, long (hundreds of milliseconds) inhibitory postsynaptic potential (IPSP) (Lingenhöhl and Olpe 1993), mediated by a potassium conductance (Newberry and Nicoll 1984; Hablitz and Thalmann 1987; Dutar and Nicoll 1988; Solís and Nicoll 1992; Otis *et al.* 1993; Pham and Lacaille 1996; Pham *et al.* 1998). $GABA_B$ receptor activation at presynaptic sites reduces neurotransmitter release (Lanthorn and Cotman 1981; Solís and Nicoll 1992) by either direct modulation of presynaptic calcium channels (Pfrieger *et al.* 1994; Takahashi *et al.* 1998), shortening

of the action potential by modulation of I_A-type K^+ channels (Saint *et al.* 1990; but see Otis *et al.* 1993), or possibly both. Not all glutamatergic presynaptic terminals are equally susceptible to $GABA_B$-mediated inhibition of neurotransmitter release, although reported results are occasionally inconsistent. For example, baclofen strongly suppresses synaptic transmission at the Schaffer collateral (SC) input to area CA1 and has little effect on the perforant path input to dentate gyrus or the TA input to CA1 (Lanthorn and Cotman 1981; Ault and Nadler 1982; Colbert and Levy 1992). In one case, baclofen was reported to inhibit mossy fiber transmission (Lanthorn and Cotman 1981) while in another case it was reported to have no effect (Ault and Nadler 1982). In the neocortex, intracortical connections are inhibited by baclofen while thalamocortical inputs are unaffected (Gil *et al.* 1997). The effects of $GABA_B$ autoreceptor activation on GABAergic neurotransmission are described below (section 1.1.4.1, p. 23).

Heterogeneity in $GABA_B$-mediated effects may be due to multiple subtypes of $GABA_B$ receptors, multiple types of G protein coupled to the receptor, and multiple downstream effector pathways. For example, there seem to be differences in pertussis toxin sensitivity between presynaptic $GABA_B$ receptors on excitatory and inhibitory terminals, suggesting the involvement of different G proteins (see Kerr and Ong 1995 for review). The K^+ channel blocker 9-amino-1,2,3,4-tetrahydroacridine (THA) is reported to block the effects of baclofen and GABA at post- but not presynaptic receptors (Lambert and Wilson 1993a). Differences observed between responses to exogenous GABA or baclofen application (e.g., Lanthorn and Cotman 1981; Pham and Lacaille 1996; Pham *et al.* 1998) may be due to the presence of uptake mechanisms for GABA but

not baclofen (Solís and Nicoll 1992), suggesting that $GABA_B$ responses are normally limited by GABA uptake (Solís and Nicoll 1992; Isaacson *et al.* 1993).

The $GABA_B$ receptor was recently cloned (Kaupmann *et al.* 1997) and was found to be similar in structure to the mGluRs. Like other G protein-coupled receptors, the $GABA_B$ receptor has seven putative transmembrane domains. A possible GABA-binding site is found in the N-terminal extracellular domain. The cloned receptor is negatively coupled to adenylate cyclase, but does not alone cause much activation of potassium channels. $GABA_BR1$ mRNA transcripts were found to be abundant in all layers of the cortex, the principal cell layers (pyramidal and granular) of the hippocampus, as well as in the basal ganglia and the Purkinje cells of the cerebellum. A more detailed *in situ* hybridization study found that $GABA_BR1$ mRNA is found in the vast majority of neurons in the adult rat brain, with the notable exception of certain populations of GABAergic neurons (Lu *et al.* 1998). A second $GABA_B$ receptor subunit, $GABA_BR2$, has recently been identified; this subunit is homologous to $GABA_BR1$ and presumably similar in structure, with seven transmembrane domains and a GABA-binding site. Expression of both subunits is required for reconstitution of fully functional $GABA_B$ receptors with binding constants and downstream effects similar to native $GABA_B$ receptors, and the two mRNAs are expressed in overlapping populations of neurons (Jones *et al.* 1998; Kaupmann *et al.* 1998; White *et al.* 1998; Kuner *et al.* 1999). The existence of more than one type of $GABA_B$ receptor subunit may account for the heterogeneity of $GABA_B$ responses observed experimentally.

1.1.3.1.3 Comparison of $GABA_A$ and $GABA_B$ effects

It is unclear whether $GABA_A$ and $GABA_B$ responses are evoked by separate or overlapping populations of interneurons. There are many circumstances in which $GABA_A$ responses appear in the absence of $GABA_B$ responses. In hippocampus, paired recordings of presynaptic interneurons and postsynaptic pyramidal cells (Buhl *et al.* 1994a; Buhl *et al.* 1995; Vida *et al.* 1998) or loose cell-attached stimulation of interneurons (Ouardouz and Lacaille 1997) showed unitary IPSPs with no $GABA_B$ component in the postsynaptic neuron. Spontaneous inhibitory postsynaptic currents (IPSCs) recorded in dentate gyrus granule cells were mediated exclusively by $GABA_A$ receptors (Otis and Moody 1992). In neocortex, most activity from single interneurons also evoked only a $GABA_A$ IPSP in postsynaptic cells, although long, high-frequency trains of action potentials (>20 spikes, 220-250 Hz) in fast-spiking interneurons could elicit a slower, $GABA_B$-like IPSP in pyramidal cells (Thomson *et al.* 1996). No unitary IPSPs containing only a $GABA_B$ component have been reported.

Focal stimulation in stratum lacunosum-moleculare (SLM) of hippocampal area CA1 has been used to evoke $GABA_B$-mediated synaptic responses in pyramidal cells, presumably by the activation of SLM interneurons (Williams and Lacaille 1992; Benardo 1995; Miles *et al.* 1996); when glutamate is applied focally to SLM, $GABA_B$ IPSPs that are unaffected by the $GABA_A$ antagonists bicuculline or picrotoxin are observed (Williams and Lacaille 1992). However, it is not known how many interneurons were activated by this focal stimulation, or whether activated interneurons fired just one action potential or several. $GABA_B$ responses can be evoked by extracellular stimulation in any layer of hippocampus (e.g., Newberry and Nicoll 1984; Pham *et al.* 1998). "Giant"

$GABA_B$ responses can be elicited in neurons in hippocampal slices by application of the convulsant, K^+ channel blocker 4-aminopyridine (4-AP) (Segal 1987; Misgeld *et al.* 1992; Otis and Moody 1992; Pham *et al.* 1998), which apparently evokes burst firing in a subpopulation of hippocampal interneurons (Segal 1987; Misgeld *et al.* 1992). Trains of electrical stimulation were required to see a $GABA_B$-mediated inhibition of SC inputs to CA1 (Chapter 4) (Isaacson *et al.* 1993) and increased the size of the postsynaptic $GABA_B$ response in retrohippocampal neurons (Funahashi and Stewart 1998). These results suggest that high levels of activity, possibly including synchronous activation of many interneurons, are necessary to evoke a $GABA_B$-mediated response (see Mody *et al.* 1994, for review). In dissociated cultures of hippocampal CA3 neurons, $GABA_B$ receptors were activated at a much lower concentration of GABA than were $GABA_A$ receptors (Sodickson and Bean 1996), suggesting that the necessity for high levels of interneuron activity may be due to an extrasynaptic location of $GABA_B$ receptors, rather than a lower affinity for GABA. An extrasynaptic localization of $GABA_B$ receptors has been shown using immunogold labeling in cerebellar Purkinje cells (Kaupmann *et al.* 1998).

Focal bicuculline or GABA application shows, functionally, that $GABA_A$ receptors are found on both somata and dendrites in piriform cortex (Kanter *et al.* 1996), sensory cortex (Connors *et al.* 1988), and hippocampus (Newberry and Nicoll 1985; Empson and Heinemann 1995b). Current source density analysis also shows that there are $GABA_A$ responses in dendritic locations in stratum oriens (SO), stratum radiatum (SR), and SLM of hippocampus (Lambert *et al.* 1991). $GABA_A$ binding sites, as determined by quantitative autoradiography, are distributed quite evenly across the layers

of the CA1 region of the hippocampus (Chu *et al.* 1990). Some cerebellar neurons also have $GABA_A$ receptors on their axon terminals (Pouzat and Marty 1999).

Focal GABA application most readily evoked a $GABA_B$-like response at somatic and proximal dendritic sites of pyramidal cells in sensory cortex (Connors *et al.* 1988). In hippocampus, however, a larger hyperpolarizing response was observed when baclofen was applied to dendritic, rather than somatic, regions (Newberry and Nicoll 1985). It is not clear whether these results reflect a real difference between $GABA_B$ receptor distribution in cortex and hippocampus, or if the use of baclofen, for which there are no intrinsic uptake mechanisms, accounts for the difference. Quantitative autoradiography shows lower overall levels, but similar even distribution, of $GABA_B$ binding sites in hippocampal area CA1 as compared to $GABA_A$ binding sites (Chu *et al.* 1990). However, presynaptic $GABA_B$ receptors will contribute to the signal observed in the dendritic layers, making a comparison of postsynaptic $GABA_B$ receptor density in dendrites and soma difficult. Only preliminary reports exist of localization of $GABA_B$ receptors by recently-developed antibodies (Honer *et al.* 1998; Princivalle *et al.* 1998; Shigemoto *et al.* 1998); in one study, a particularly strong $GABA_B$ signal was observed in SLM, the distal dendritic region, of hippocampal area CA3 (Shigemoto *et al.* 1998).

$GABA_A$ and $GABA_B$-mediated responses likely play different roles in neuronal circuits. $GABA_A$-mediated inhibition is clearly important in preventing hyperexcitability of neuronal networks; for example, hippocampal slices exposed to the $GABA_A$ antagonist bicuculline will exhibit spontaneous epileptiform activity (e.g., Ben-Ari *et al.* 1979; Sloviter 1991), suggesting that a tonic $GABA_A$-mediated inhibition keeps excitation in check. By curbing excitatory neurotransmission, $GABA_A$-mediated inhibition may also

prevent indiscriminate potentiation of synaptic transmission. Low concentrations of $GABA_A$ antagonists are often used to help promote the induction of LTP in the rat hippocampal slice (Gustafsson and Wigström 1986; Kelso *et al.* 1986; Kauer *et al.* 1988; Malenka *et al.* 1988), and LTP is enhanced by the blockade of $GABA_A$ receptors (Wigström and Gustafsson 1983). Associative interactions between the medial and lateral perforant pathways in dentate gyrus were enhanced by blockade of $GABA_A$-mediated inhibition, suggesting that this inhibition normally limits the spread of excitatory effects (Tomasulo *et al.* 1993). Fast, $GABA_A$-mediated IPSPs are well suited for "robust suppression of activity with fine temporal control" (Connors *et al.* 1988). $GABA_A$ IPSPs can also limit the back-propagation of action potentials into dendrites, thus regulating changes in intracellular Ca^{2+} concentration and distribution (Tsubokawa and Ross 1996). Dendritically-located $GABA_A$ receptors can limit the contribution of NMDA receptors to EPSPs by hyperpolarizing the cell membrane and preventing alleviation of the voltage-dependent block of NMDA receptors by Mg^{2+} (Kanter *et al.* 1996), although $GABA_B$ IPSPs can also have this effect (Morrisett *et al.* 1991); this may have important implications for NMDAR-dependent synaptic plasticity (section 1.1.5.2, p. 34). The effects of $GABA_A$-mediated inhibition will depend on the location of the postsynaptic receptors (section 1.1.3.2, p. 19).

$GABA_B$-mediated inhibition may have a more subtle effect on neuronal excitability. In cortex, there is apparently a background level of $GABA_B$-mediated inhibition controlling excitation, since microiontophoresis of the $GABA_B$ antagonist CGP 35348 into sensorimotor cortex *in vivo* results in a modest increase in spontaneous firing rates (Andre *et al.* 1992). The $GABA_B$ antagonist CGP 55845A can increase the amplitude of

unitary IPSCs evoked by single stimulation of CA1 interneurons, showing that in hippocampus there is a tonic level of presynaptic $GABA_B$ inhibition of interneurons (Ouardouz and Lacaille 1997). In an animal model of epilepsy, slices taken from seizing animals showed a total lack of pre- or postsynaptic $GABA_B$ inhibition, suggesting that $GABA_B$-mediated inhibition normally acts as an "emergency brake" for excitatory activity (Mangan and Lothman 1996). Conversely, blockade of $GABA_B$ receptors by phaclofen can suppress post-tetanic disinhibition in the dentate gyrus (Mott *et al.* 1990). The $GABA_B$ agonist baclofen can have both antiepileptic and proepileptic effects (see Kerr and Ong 1995 for review). $GABA_B$ receptors are particularly implicated in absence epilepsy (Bernasconi *et al.* 1992; Marescaux *et al.* 1992a). $GABA_B$-mediated inhibition can increase the threshold for action potential firing (Connors *et al.* 1988), decrease the net depolarizing effect of EPSPs (Buonomano and Merzenich 1998) (section 1.1.5.1, p. 31), and block spiking due to excitatory inputs (Chapter 4).

1.1.3.2 Somatic, axo-axonic, and dendritic inhibition

The effect of inhibitory inputs onto a neuron will depend on whether the inhibitory synapses are located at the soma, axon initial segment, or dendrites of the postsynaptic neuron. Interneurons, which are very heterogeneous (Lorente de Nó 1934; Parra *et al.* 1998), can be classified into a small number of categories based on their axonal arborization and postsynaptic targets. For example, in the hippocampus, axo-axonic or "chandelier" cells preferentially innervate the axon initial segment of post-synaptic neurons (Somogyi *et al.* 1983; Li *et al.* 1992; Buhl *et al.* 1994b); basket cells form axon plexuses around the somata of postsynaptic targets (Lorente de Nó 1934;

Ribak and Seress 1983; Buhl *et al.* 1995; Cobb *et al.* 1997); and other cell types, including bistratified cells (Buhl *et al.* 1994a; Cobb *et al.* 1997), oriens-lacunosum-moleculare (O-LM) interneurons (Maccaferri and McBain 1995; Yanovsky *et al.* 1997; Katona *et al.* 1999), and perforant path- and Schaffer-associated SLM interneurons (Vida *et al.* 1998) have axonal arborizations in the dendritic layers of the hippocampus. It has been noted that interneurons targeting the axon or soma tend to have dendrites spanning multiple layers, and thus can be activated by a variety of inputs, while interneurons targeting dendrites tend to have more restricted dendritic arborizations and are thus likely to be activated only by activity in specific pathways (Freund and Buzsáki 1996, p. 372).

In order for neurons to communicate with one another, action potentials must be generated. Action potential generation depends on the interaction of all the excitatory and inhibitory inputs converging onto a neuron over a certain time; when a threshold potential at the spike initiation zone is reached, an action potential is produced. The spike initiation zone is generally thought to be located in the soma or action initial segment (see Stuart *et al.* 1997 for review), though sodium spikes can also be initiated in dendritic regions (Turner *et al.* 1991; see Yuste and Tank 1996 for review; Golding and Spruston 1998). The location of inhibitory inputs relative to other inputs and to the spike initiation zone will determine their effect.

When spikes are initiated at the soma or axon, axo-axonic or somatic inhibitory synapses will have a "veto" or global effect on the postsynaptic neuron. Regardless of the location of excitatory inputs, inhibition at the axon or soma can take the membrane potential further away from action potential threshold and thus inhibit or delay action potential firing (Miles *et al.* 1996).

Dendritic inhibition can have a much more restricted or input-specific effect than somatic or axo-axonic inhibition. Much theoretical work has been devoted to the idea that inhibitory inputs restricted to particular parts of the dendritic tree, or interposed between excitatory inputs and the spike initiation zone at the soma, can selectively nullify excitatory inputs to parts of the dendritic tree, resulting in an "AND NOT" computation (i.e., excitation goes through only in the absence of inhibition) being performed (Koch *et al.* 1983; Koch *et al.* 1990). The discovery of active membrane properties in dendrites (see Johnston *et al.* 1996; Yuste and Tank 1996 for review) has added new complexity to the possible effects of inhibitory dendritic inputs. Spikes initiated in dendrites of hippocampal pyramidal cells *in vivo* can be reduced by synaptic inhibition (Buzsáki *et al.* 1996), and dendritic calcium spikes *in vitro* can be suppressed by dendritic inhibition (Miles *et al.* 1996). Backpropagation of action potentials into the dendritic tree, which can be an important retrograde signal of neuronal activity (see Stuart *et al.* 1997 for review), can be blocked by $GABA_A$ IPSPs in dendrites (Tsubokawa and Ross 1996). If the spike initiation zone is located in the dendrites, rather than at the soma, dendritic inhibition can have a veto effect similar to that mediated by basket and axo-axonic cells.

1.1.3.3 Feedback and feedforward inhibition

Inhibitory components of neuronal circuits can be classified as feedforward or feedback, depending on their position relative to excitatory pathways (see Buzsáki 1984 for review). For example, excitatory afferents to a brain region may make synapses onto both principal cells and interneurons in that region; if the interneurons then go on to make

synapses onto the pyramidal cells, feedforward inhibition will occur. Feedback inhibition is seen when principal cells activate local interneurons which then make reciprocal connections back onto the same population of principal cells, possibly even the same individual cells.

Some interneurons seem to be specialized for either feedforward or feedback inhibition, while other interneurons can be involved in both types of circuits. For example, in area CA1, SLM interneurons appear not to receive recurrent excitatory input from pyramidal cells, and therefore subserve only a feedforward inhibitory function (Lacaille and Schwartzkroin 1988b), while certain interneurons in stratum oriens are activated both by afferents from CA3 as well as by feedback connections from pyramidal cells, thus mediating both feedforward and feedback inhibition (Lacaille *et al.* 1988). Other stratum oriens interneurons may be activated in only a feedback manner (Maccaferri and McBain 1995).

1.1.4 Regulation and modulation of inhibition

Inhibition can be regulated at many levels (see Thompson 1994 for review). Inhibitory responses themselves undergo various forms of activity-dependent regulation; interneurons may be differentially recruited by afferent activity; activation of interneurons may be modulated by long-term plasticity of synapses onto interneurons; and interneurons themselves are subject to inhibitory innervation.

1.1.4.1 Short-term plasticity of inhibitory transmission

Inhibitory responses (IPSPs or IPSCs) undergo a form of short-term activity-dependent plasticity known as paired-pulse depression (PPD), where repeated stimulation of inhibitory inputs results in a decrease in IPSP/C amplitude (Ben-Ari *et al.* 1979; McCarren and Alger 1985; Deisz and Prince 1989; Thompson and Gähwiler 1989; Davies *et al.* 1990; Williams and Lacaille 1992; Ling and Benardo 1994). PPD is mediated by $GABA_B$ autoreceptors (Davies *et al.* 1990; Roepstorff and Lambert 1994), although a $GABA_B$-independent component of PPD, possibly due to synaptic vesicle depletion, has also been observed (Lambert and Wilson 1994; Wilcox and Dichter 1994; Fortunato *et al.* 1996). Synaptic vesicle depletion is likely to be particularly important during long periods of interneuron activation (Galarreta and Hestrin 1998). Although most studies of PPD have focused on $GABA_A$ responses, $GABA_B$ responses are also depressed with repeated stimulation (Pacelli *et al.* 1991; Williams and Lacaille 1992; Otis *et al.* 1993; Ling and Benardo 1994; Jones 1995). Not all evoked IPSPs undergo $GABA_B$-mediated depression; for example, in CA3, a subpopulation of inhibitory inputs onto the somata of pyramidal cells are unaffected by baclofen (Lambert and Wilson 1993b). Some inhibitory neurons, such as cerebellar stellate and basket cells, have presynaptic $GABA_A$ autoreceptors (Pouzat and Marty 1999), suggesting another possible mechanism for activity-dependent regulation: reduction of GABA release due to hyperpolarization by activation of presynaptic $GABA_A$ receptors.

Inhibitory responses evoked by paired-pulse stimulation do not always show depression. Paired-pulse facilitation of unitary IPSCs evoked by hippocampal inter-neurons was observed when the initial response size was smaller than average (Ouardouz

and Lacaille 1997), suggesting that a phenomenon similar to paired-pulse facilitation of excitatory responses (Debanne *et al.* 1996), possibly mediated by residual calcium in the presynaptic terminal, can exist in inhibitory terminals as well.

1.1.4.2 Long-term plasticity of synapses onto interneurons

It has been clearly demonstrated that synapses onto pyramidal cells in the hippocampus can be potentiated in an activity-dependent manner (section 1.1.2, p. 7). However, the question of whether synapses onto hippocampal interneurons show the same sort of plasticity is more controversial. Attempts to induce plasticity in synapses onto interneurons have had mixed results. It may be, as is so often the case with experiments done in hippocampal slices, that the results are very dependent on the exact conditions used in the experiment.

Because of the sparseness of interneurons in the hippocampus, as compared to pyramidal cells, it is impossible to study plasticity of synapses onto interneurons by means of field recordings. Rather, it is necessary to record from individual interneurons with either sharp or whole-cell electrodes. Some of the conflict between reported results may be due to differences between these two techniques, since intracellular factors necessary for synaptic plasticity may be washed out during whole-cell recording; on the other hand, when perforated-patch and regular whole-cell recordings were compared directly, no differences were observed (Maccaferri and McBain 1996).

Even when recording from single interneurons, it is necessary to distinguish between direct potentiation or depression of the actual synapses made onto the interneurons, and indirect or "passive propagation" of LTD or LTP of excitatory connections

whose effects are seen in interneurons because of the feedback connections from pyramidal cells onto interneurons (Maccaferri and McBain 1995; Maccaferri and McBain 1996). It has proven difficult to induce LTP of monosynaptic connections onto a variety of interneuron types, including basket and bistratified cells of SR (McMahon and Kauer 1997b) (although these experiments were performed in high concentrations of Mg^{2+}, which may block NMDARs) and stratum oriens/alveus (O/A) interneurons (Maccaferri and McBain 1996).

Synapses onto different types of interneurons may also vary in their capacity for plasticity. For example, in an experiment using tetanic presynaptic stimulation paired with postsynaptic depolarization, LTP was induced in O/A interneurons but not in SLM interneurons (Ouardouz and Lacaille 1995). Differences between interneurons are even observed in the passive propagation of LTD/LTP via feedback connections; for example, vertical and horizontal interneurons in SO showed passive propagation of potentiation, but SR interneurons did not (Maccaferri and McBain 1996).

The input specificity of LTP observed in pyramidal cells (see Schuman 1997 for review) may be due to the fact that excitatory synapses are made onto individual spine heads, and the electrical and biochemical isolation between individual spines may limit non-specific spread of plasticity between excitatory synapses. Since interneurons tend not to be spiny, this may compromise their ability to undergo input-specific plasticity. Tetanic stimulation applied to independent SC inputs to interneurons of stratum pyramidale (SP) in CA1 resulted in every possible combination of homo- and hetero-synaptic LTP and LTD, suggesting that, indeed, input specificity is not seen in long-term plasticity in interneurons (Cowan *et al.* 1998). Similarly, in an experiment where tetanic

stimulation of afferents resulted in potentiation of the field response but depression of the response recorded in an interneuron, this depression was not specific to the tetanized pathway (McMahon and Kauer 1997b).

A recent study designed to resolve the controversy about plasticity in interneurons points to temperature as a contributing factor. The same tetanic stimulus applied to afferents onto interneurons of SR had no effect at room temperature but resulted in LTP when the experiment was performed at 34 °C (Franks *et al.* 1998).

Plasticity in interneurons may be very different in mechanism to that seen in pyramidal cells. Hippocampal interneurons apparently lack some of the signaling molecules critical to plasticity in pyramidal cells, including calcineurin (Ca^{2+}/calmodulin-dependent protein phosphatase 2B) and Ca^{2+}/calmodulin-dependent protein kinase IIα (Sík *et al.* 1998). One possible alternative mechanism for plasticity of inputs onto interneurons is an activity-dependent facilitation of currents through Ca-permeable AMPARs due to relief from polyamine block (Rozov *et al.* 1998; see commentary by McBain 1998).

1.1.4.3 Differential recruitment of interneurons

The balance between excitation and inhibition will be affected by the relative effectiveness of afferent inputs in recruiting excitatory principal cells or inhibitory interneurons to fire action potentials.

In the dentate gyrus, tetanic stimulation of the commissural or perforant paths resulted in changes in recruitment of hilar interneurons, with a net change in inhibitory efficacy in this circuit (Tomasulo and Steward 1996). In CA1, excitatory postsynaptic

currents (EPSCs) onto SLM interneurons are decreased more quickly and completely by anoxia than are EPSCs onto pyramidal cells, suggesting a selective loss of recruitment of interneurons; this inhibition of EPSCs in SLM interneurons is apparently mediated by presynaptic adenosine A_1 receptors (Congar *et al.* 1995). In dentate gyrus (DG), however, a hypoxic loss of interneuron recruitment is apparently mediated by mGluRs (Doherty and Dingledine 1997).

Long-term plasticity may also affect interneuron recruitment. In area CA1 of the hippocampus, tetanic stimulation of Schaffer collaterals results in LTP of inputs onto pyramidal cells, but LTD of the EPSP/C onto SR interneurons (bistratified or basket cells), suggesting a decreased recruitment of interneurons following otherwise potentiating stimuli (McMahon and Kauer 1997b).

1.1.4.4 Long-term plasticity of inhibitory synapses

Thus far, there seems to be little, or conflicting, evidence for LTP or depression of IPSPs themselves (i.e., presynaptic changes in GABA release or postsynaptic changes in responsiveness to GABA). Suppression of inhibition has been described as a contributor to LTP of excitatory neurotransmission (Chavez-Noriega *et al.* 1990; Stelzer *et al.* 1994). It is possible that the decrease in IPSP amplitude observed may have been due to a depression of feedforward recruitment of interneurons (McMahon and Kauer 1997b), although in one study (Stelzer *et al.* 1994) a potentiation of EPSPs in interneurons was observed.

Long-term enhancement of excitatory synaptic transmission in hippocampus evoked by activation of mGluRs was shown to be dependent on a reduction in GABA-

ergic inhibition, and monosynaptic IPSPs evoked by stimulation in the presence of AMPAR and NMDAR antagonists were shown to be reduced by mGluR agonists; the decrease in IPSP amplitude was blocked by application of a G protein activator to the postsynaptic neuron, showing that mGluR activation can decrease the responsiveness of neurons to GABA (Liu *et al.* 1993). A similar effect has been observed in response to NMDAR activation, where an observed reduction of the response to ionophoretically applied GABA suggested a postsynaptic change in GABA sensitivity (Stelzer *et al.* 1987).

1.1.4.5 Inhibitory and modulatory effects on interneurons

Inhibitory interneurons are themselves subject to control by inhibitory innervation. In the hippocampus, a subpopulation of interneurons apparently targets other interneurons exclusively (see Freund and Buzsáki 1996, pp. 372-377, for review). Ultrastructural data shows that GABAergic, inhibitory synapses are made onto interneurons (e.g., see Freund and Antal 1988; Cobb *et al.* 1997; Gulyás *et al.* 1998a). Paired recordings show that hippocampal interneurons, including basket cells (Cobb *et al.* 1997), SLM interneurons (Lacaille and Schwartzkroin 1988b; Cobb *et al.* 1997), and O/A interneurons (Lacaille *et al.* 1988) innervate both pyramidal cells and other interneurons, as well as making autapses. Spontaneous IPSCs can be recorded in a variety of hippocampal interneurons, including O-LM cells, bistratified cells, trilaminar cells, SR, and SLM interneurons (Atzori 1996; Hájos and Mody 1997). Extracellular stimulation of afferent pathways can elicit IPSPs in many types of hippocampal interneurons, including SLM interneurons (Lacaille and Schwartzkroin 1988a; Williams *et al.* 1994; Morin *et al.*

1996) (section 2.3.3.2, p. 100), O/A interneurons (Morin *et al.* 1996), CA3 SLM and hilar interneurons (Misgeld and Frotscher 1986), and interneurons near SP (Morin *et al.* 1996).

In addition to inhibitory inputs from local interneurons, interneurons may receive inhibitory innervation from other areas of the brain. For example, GABAergic afferents from the septum specifically target CA3 hippocampal interneurons (Freund and Antal 1988), resulting in a net disinhibition of CA3 pyramidal cells (Tóth *et al.* 1997).

Like excitatory neurotransmission, inhibitory neurotransmission can also be modulated by the activity of other neurotransmitter systems. Unlike glutamatergic terminals, GABAergic terminals appear not to be regulated by presynaptic adenosine receptors (Thompson *et al.* 1992). The overall excitability of interneurons can be increased by ACh acting on both muscarinic and nicotinic (Frazier *et al.* 1998) receptors (see Vizi and Kiss 1998 for review), although different populations of interneurons may show differential responses to ACh (Xiang *et al.* 1998). Norepinephrine acting on α_1- and β-adrenoceptors can also excite various types of interneurons (Bergles *et al.* 1996). Serotonin has a variety of effects on inhibitory neurotransmission, including a selective presynaptic inhibition of interneurons mediating the $GABA_B$ IPSP in hippocampal area CA3 (Oleskevich and Lacaille 1992), inhibition of CA1 interneurons via presynaptic 5-HT_{1A} receptors (Schmitz *et al.* 1995b), and a general excitation of CA1 interneurons via 5-HT_3 receptors (Ropert and Guy 1991). Opioid peptides can also have a modulatory effect on inhibitory transmission. GABA release in hippocampal interneurons is inhibited by activation of opioid receptors (Cohen *et al.* 1992; Lambert and Wilson

1993b). μ- and δ-opioid receptors also mediate a postsynaptic inhibition of interneurons by opioid peptides (Bramham and Sarvey 1996; Svoboda and Lupica 1998). Finally, the intrinsic firing patterns of interneurons can be affected by neuromodulators; for example, interneurons in prefrontal cortex can be converted from firing a few spikes followed by a plateau, to fast-spiking trains, by dopamine (via D1/D5 receptors) (Gorelova and Yang 1998). Inhibitory responses can also be reduced by the activation of presynaptic mGluRs on interneuron axon terminals (Burke and Hablitz 1994; Gereau and Conn 1995).

1.1.5 Frequency dependence of neuronal activity

Synaptic transmission occurs when an action potential reaches an axon terminal and triggers the release of neurotransmitter. As we have seen, the postsynaptic effect of that neurotransmitter depends on the context in which it is received. Synapses are not activated in isolation, but rather as members of a huge number of inputs converging on a postsynaptic neuron. In addition to this spatial integration, temporal integration is also important, since presynaptic spikes also do not occur isolated in time. *In vivo* recordings show that some neurons, such as so-called "theta" cells (now known to be interneurons), fire at high frequencies (Ranck 1973); other neurons, generally principal cells such as pyramidal cells of the hippocampus (Kandel and Spencer 1961; Ranck 1973; Otto *et al.* 1991) and granule cells of the dentate gyrus (Jung and McNaughton 1993), fire in high-frequency bursts sometimes known as complex spikes. What are the postsynaptic consequences of presynaptic burst activity, or other temporal patterns of inputs? We have seen already how excitatory and inhibitory inputs interact, and how repetitive

stimulation can modulate excitatory or inhibitory neurotransmission. Here the interaction of excitatory and inhibitory transmission during repetitive activation will be described.

1.1.5.1 Frequency dependence of synaptic transmission

Frequency-dependent synaptic transmission involves an interplay between excitation and inhibition, and facilitation and depression of both excitatory and inhibitory responses. It has long been recognized that paired-pulse depression of inhibition (section 1.1.4.1, p. 23) underlies some of the facilitation seen in the excitatory response (Ben-Ari *et al.* 1979; Wigström and Gustafsson 1981; Nathan and Lambert 1991; Pacelli *et al.* 1991). EPSPs evoked in hippocampal pyramidal cells by extracellular stimulation are normally limited in amplitude and duration by concurrently activated $GABA_A$-mediated inhibition (e.g., see Turner 1990). When repeated stimuli are presented, $GABA_A$-mediated IPSPs are depressed and their effect on the EPSP is reduced, resulting in a larger, broader EPSP (Nathan and Lambert 1991; Pacelli *et al.* 1991; Davies and Collingridge 1993; Davies and Collingridge 1996; Buonomano and Merzenich 1998). This facilitation was confirmed to be dependent on $GABA_B$ receptors by the use of baclofen, which selectively enhanced the first EPSP (Nathan and Lambert 1991), and by the use of $GABA_B$ antagonists, which abolished the facilitatory effect (Davies and Collingridge 1993; Davies and Collingridge 1996; Buonomano and Merzenich 1998). It should be noted that, because the second EPSP arrives during a $GABA_B$-mediated hyper-polarization, its amplitude relative to the original baseline may still be less than that of the first EPSP (Buonomano and Merzenich 1998).

Even in the absence of underlying inhibition, repeated stimulation of an excitatory pathway can result in a variety of outcomes. In dual intracellular recordings from pairs of pyramidal cells in neocortical slices, each of four possible patterns of response was observed: PPF or PPD with the second EPSP the same shape as the first, and PPF or PPD with the second EPSP broadened by NMDAR activation. Even at synapses that showed facilitation of the second EPSP, the third EPSP was usually depressed. Meanwhile, at synapses made by pyramidal cells onto interneuron, a strong, NMDA-independent PPF which could persist for seconds was always observed. It was noted that these patterns relate well to natural firing patterns of pyramidal cells, which generally burst briefly before slowing down. For synapses onto pyramidal cells, PPD would make continued fast firing ineffective, whereas for synapses onto interneurons, slow firing would lead to effective transmission because of the long-lasting PPF. A frequency-dependent switch in recruitment, with pyramidal cells recruited at low frequencies and interneurons at high frequencies, would also be possible (Thomson 1997).

There exist other examples of repetitive stimulation at various frequencies resulting in differential recruitment of neuron of different types, hence shifting the balance between excitation and inhibition. In the EC, synaptic transmission is frequency-dependent. For example, stimuli that evoke IPSPs in EC layer II cells when applied singly, at widely-spaced intervals, will instead evoke spikes if applied at moderately high frequencies (5-10 Hz) (Finch *et al.* 1986), presumably owing to an activity-dependent depression of inhibition. Similar results have been seen in EC layer III cells, which show frequency facilitation at 3 Hz (Jones 1995). Further characterization of this phenomenon revealed a difference between the two layers, with layer II cells preferentially activated at

input frequencies above 5 Hz, whereas layer III cells fired most at input frequencies below 10 Hz (Gloveli *et al.* 1997b). In the hippocampus, repetitive stimulation of the SC input to area CA1 resulted in a transition from simple EPSP responses to complex spike bursts in the postsynaptic cells (Thomas *et al.* 1998).

Another example of frequency-dependent regulation of the balance between excitation and inhibition is suggested by the observation that during prolonged firing of cortical excitatory or inhibitory cells at 20 Hz, unitary EPSCs were reduced to a lower steady-state amplitude than unitary IPSCs. This suggests that in periods of high neuronal activity, inhibition will predominate over excitation, allowing a dynamic equilibrium to be reached (Galarreta and Hestrin 1998).

Greater complexity is seen when frequency dependence of synaptic transmission is studied in a polysynaptic pathway. The effects of changes at each synapse in the pathway will be combined in some fashion that may not be predictable from the properties of each individual synapse. For example, frequency dependence of synaptic transmission through the hippocampal trisynaptic pathway *in vivo*, from perforant path to CA1 (section 1.3.1, p. 44), was compared to that of the monosynaptic SC input to CA1. When stimulation frequency was increased from 0.1 to 1.0 Hz, the trisynaptic response showed a much greater facilitation than did the SC response, a result made even more striking by the fact that transmission at the first synapse in the trisynaptic pathway (perforant path to dentate gyrus) was actually depressed by repeated stimulation (Herreras *et al.* 1987). Conversely, in slice, the trisynaptic response showed less frequency facilitation than the monosynaptic SC response, though pharmacological enhancement of excitation or reduction of inhibition did selectively enhance the trisynaptic response, suggesting that

the balance of excitation and inhibition was affected by the slicing procedure (Sirvio *et al.* 1996).

1.1.5.2 Importance of frequency in synaptic plasticity

The magnitude and direction of synaptic plasticity are highly dependent on the temporal pattern, including the frequency, of the stimulus paradigm used to induce plasticity. For example, in the SC pathway in hippocampus, 1 Hz stimulation causes LTD (e.g., Dudek and Bear 1992), 200 Hz stimulation causes LTP (e.g., Grover and Teyler 1990). A variety of results is observed at intermediate frequencies. For example, LTP can be induced by stimulation frequencies as low as 10 Hz (Andersen *et al.* 1977; Aihara *et al.* 1997) or 5 Hz (Thomas *et al.* 1998), whereas in other experiments, 5 Hz stimulation caused LTD (Bolshakov and Siegelbaum 1994). In general, there appears to be a threshold level of postsynaptic activity, above which LTP is induced, and below which LTD is induced (Artola and Singer 1993); the level of this threshold can itself be changed by previous activity, which may account for some of the variability observed in long-term plasticity experiments (Abraham and Bear 1996).

Frequency-dependent activation of NMDARs and activity-dependent disinhibition appear to be key to the induction of LTP by various stimulation protocols. Most of the stimulus paradigms used to evoke LTP involve high-frequency activity, whether in a long train (tetanus, e.g., 10-50 Hz for 10-15 s (Andersen *et al.* 1977); 200 Hz for 0.5 s (Grover and Teyler 1990); or 100 Hz for 1 s (Kantor *et al.* 1996)), in a burst pattern (e.g., theta, 4 pulses at 100 Hz, repeated at 200 ms intervals (Larson and Lynch 1986)), or the so-called primed-burst protocol (one pulse followed 170 ms later by four pulses at 100 Hz) (Rose

and Dunwiddie 1986)). As noted previously, LTP induction generally requires the activation of postsynaptic NMDARs, which are subject to a voltage-dependent block. High-frequency synaptic inputs are necessary for summation of EPSPs mediated by non-NMDA glutamate receptors to depolarize postsynaptic neurons sufficiently to relieve the NMDAR block and allow Ca^{2+} influx (Herron *et al.* 1986; Collingridge *et al.* 1988). Short-term, activity-dependent depression of $GABA_A$-mediated inhibition may also transiently increase levels of synaptic excitation (Pacelli *et al.* 1991; Davies and Collingridge 1996; Buonomano and Merzenich 1998) which in turn may underlie the potency of theta and primed-burst stimulation paradigms in inducing LTP (Larson and Lynch 1986; Davies *et al.* 1991; Mott and Lewis 1991; Thomas *et al.* 1998).

1.2 Why study the hippocampus?

1.2.1 Hippocampal function

The hippocampus is believed to play an important role in learning and memory (see Eichenbaum *et al.* 1992) as well as in spatial navigation (Barnes 1988; see Muller 1996 for review). Although there may be species differences in the relative importance of these functions, they are by no means mutually exclusive (e.g., see Levy 1989). The distinction is clouded somewhat by the fact that many tests of learning in rodents use tasks dependent upon spatial navigation (e.g., Morris *et al.* 1986).

1.2.1.1 Learning and memory

1.2.1.1.1 Clinical and behavioral results

The idea that the hippocampus plays a crucial role in learning and memory dates back to at least the 1950s, when Scoville and Milner (1957) described the consequences of bilateral hippocampal removal in patient HM. Although his intelligence, working memory, and memory of most events prior to the surgery remained intact, after the operation HM was no longer able to form new memories. This suggested that the hippocampus plays a time-limited role in information storage, being necessary for the formation, but not the long-term storage, of memories. Subsequent studies have confirmed and extended this idea (see Squire and Zola-Morgan 1991; Eichenbaum *et al.* 1992). For example, in monkeys, a temporally graded amnesia was observed following removal of the hippocampus (Zola-Morgan and Squire 1990). In humans, MRI imaging has shown a correlation between hippocampal abnormalities and amnesia (Press *et al.* 1989). In rats, hippocampal lesions have been shown to impair learning both in spatial (e.g., Morris *et al.* 1982) and in non-spatial (e.g., Bunsey and Eichenbaum 1996) tasks, and activity of hippocampal neurons has been correlated with task-specific features of non-spatial tasks (Ranck 1973; Hampson *et al.* 1993; Wood *et al.* 1999).

1.2.1.1.2 Synaptic plasticity: long-term potentiation (LTP) and depression (LTD)

The hippocampus has also been used as a model system for the study of long-lasting synaptic plasticity (Siegelbaum and Kandel 1991; Malenka 1994), a phenomenon considered to be a possible neural substrate for learning and memory. As described above

(section 1.1.2, p. 7), LTP and LTD are long-lasting increases or decreases, respectively, of synaptic strength, generally induced by patterned activity, pharmacological manipulations, or a combination of the two. Parallels between the conditions required for learning and the conditions required for LTP are very suggestive of a functional link between the two phenomena. For example, many learning tasks involve an association between two inputs; LTP shows the property of associativity in that a weak input can be potentiated by close temporal association with a stronger input (Barrionuevo and Brown 1983; Levy and Steward 1983; Kelso *et al.* 1986). Learning tasks are fairly input-specific, although some generalization may occur; LTP is input-specific (Andersen *et al.* 1977; White *et al.* 1988), although some spreading to nearby synapses (on the same or neighboring neurons) may occur (Schuman and Madison 1994). Learning requires a threshold level of input; LTP will not be induced if input levels are too low (Leung *et al.* 1992; Aihara *et al.* 1997). Finally, learning can be modulated by motivational state; LTP induction and maintenance can be affected by neuromodulators (Huerta and Lisman 1993; Derrick and Martinez 1996; Thomas *et al.* 1996).

Early speculations about the connection between long-term plasticity and learning took the simplistic view that if the increases in synaptic strength after LTP were related to remembering, then the decreases in synaptic strength LTD must mean erasing memories, or forgetting. Indeed, in many synapses at which it is difficult to induce LTD, a reversal of LTP, also known as depotentiation, can be induced by stimulus paradigms that cause LTD at other synapses (Wagner and Alger 1995; see Wagner and Alger 1996 for review). Specific depotentiation of previously potentiated synapses may indeed affect memory storage. More generally, however, some sort of downregulation of synaptic strength, as

seen in LTD, is critical to models of learning to prevent saturation of the strength of synapses in a network (e.g., McClelland and Goddard 1996).

1.2.1.1.3 Connection between in vitro *and* in vivo *data*

Despite theoretical considerations and much suggestive evidence, the link between LTP and learning is still somewhat controversial (e.g., see Eichenbaum and Otto 1993; Shors and Matzel 1997). One way to make a connection is to see whether manipulations that affect LTP also affect learning. Some pharmacological manipulations that block LTP also interfere with learning (e.g., Morris *et al.* 1986), but other studies show that it is possible to block LTP pharmacologically without preventing learning (Bannerman *et al.* 1995; Saucier and Cain 1995). Gene knockout techniques have also shown simultaneous disruptions of LTP and of spatial learning (e.g., Grant *et al.* 1992; Silva *et al.* 1992), but these techniques may cause general impairments that reduce performance on learning tasks without necessarily being specific to learning. Other gene knockout experiments have shown impaired LTP without impairment of spatial learning (Huang *et al.* 1995; Nosten-Bertrand *et al.* 1996); these experiments also suggest that perhaps not all hippocampal pathways contribute to spatial learning.

Attempts have been made to establish a connection between LTP and learning by trying to saturate LTP by electrical stimulation *in vivo*, then see if learning is prevented. Results have been contradictory (see Bliss and Richter-Levin 1993 for review) and caveats abound; it is hard to believe that the sort of stimulation required to saturate LTP throughout the hippocampus would not have other, severe effects on function. Other studies have looked for LTP- or LTD-like changes in synaptic strength following natural

learning experiences (e.g., Hargreaves *et al.* 1990). This is like looking for a needle in a haystack, since any particular learning experience is likely to involve plasticity of only a small subset of hippocampal connections, and there is currently no way to measure LTP *in vivo* other than coarsely stimulating afferent pathways and looking for changes in population responses. Nevertheless, experiments using exposure to new environments, which may result in broader modifications than would more restricted learning tasks, have shown an increase in evoked responses in the dentate gyrus (Green *et al.* 1990), increases in dendritic spine density (suggestive of new synapse formation) (Moser *et al.* 1994), and reversal of previously-established LTP in area CA1 (Xu *et al.* 1998).

Evidence for a connection between LTD and learning is sparse. Some pharmacological manipulations, such as blockade of NMDA receptors, that prevent LTD induction also prevent LTP induction; it could, therefore, be argued that disruptions in learning observed in experiments like those described above are due to deficits in LTD, rather than LTP. A deficit in LTP, but not LTD, was seen in mutant mice in which the γ subunit of protein kinase C had been knocked out; these mice were only mildly impaired in spatial learning (Abeliovich *et al.* 1993a; Abeliovich *et al.* 1993b). One interpretation of this result is that intact LTD is sufficient, in the absence of LTP, to mediate learning; however, slices of the mutant mice did show robust LTP when an alternative stimulation paradigm was used (Abeliovich *et al.* 1993a), suggesting that LTP may well have occurred *in vivo*, since it is unknown under what conditions LTP is induced naturally (or, indeed, whether it ever is). It has proven difficult to induce LTD *in vivo* (Staubli and Scafidi 1997), and the extended 1 Hz stimulation paradigm is con-

sidered to be particularly unphysiological. However, LTD can also be induced by more irregular low-frequency stimulation (Dudek *et al.* 1996), possibly a more physiological paradigm.

1.2.1.2 Spatial navigation

A considerable body of evidence supports the idea that the hippocampus plays a role in spatial navigation. As mentioned above, many spatial learning tasks are disrupted by hippocampal lesions. Since the 1970s, it has been recognized that the firing patterns of hippocampal principal cells *in vivo* are modulated by the location of the animal in space (O'Keefe and Dostrovsky 1971; see Muller 1996 for review).

In rodents, many populations of temporal lobe neurons, including neurons in EC (Mizumori *et al.* 1992; Quirk *et al.* 1992; Stewart *et al.* 1992), dentate gyrus (Jung and McNaughton 1993), CA3 (Muller and Kubie 1989; Barnes *et al.* 1990) and CA1 (O'Keefe and Dostrovsky 1971; Mizumori *et al.* 1989; Muller and Kubie 1989; Barnes *et al.* 1990; Wilson and McNaughton 1993) are found to fire preferentially when the animal is in a particular location in its environment; such cells are therefore known as place cells. The firing patterns of place cells in CA1 are sufficient to predict the animal's trajectory, showing that they can provide an ensemble code for space (Wilson and McNaughton 1993). Although there is no obvious topographical mapping between the outside world and the anatomical localization of place cells within the hippocampus, recent evidence suggests the existence of a distorted, fractured map with a definable topological transformation between physical and hippocampal space (Deadwyler and Hampson 1998). Firing patterns of place cells during exploratory behavior may be "replayed" during

sleep, suggesting a possible consolidation of spatial memories (Wilson and McNaughton 1994; Skaggs and McNaughton 1996).

A recent report shows that primates also have place cells; neurons with firing patterns modulated by location were recorded throughout the hippocampus and para-hippocampal gyrus of monkeys performing real and virtual translocation tasks (Matsumura *et al.* 1999). Imaging studies have shown that the hippocampus is active during spatial tasks in humans (Maguire *et al.* 1997; O'Keefe *et al.* 1998).

1.2.2 Hippocampal dysfunction

Hippocampal damage is found in conjunction with several neurological disorders, including epilepsy and Alzheimer's disease. Understanding the basic physiology of the hippocampus may shed light on the pathology of the disease state. Conversely, the relationship between the exact nature of hippocampal damage and the neurological consequences may lend insight into the role of different pathways in the healthy hippocampus.

1.2.2.1 Epilepsy

Epilepsy is a neurological disorder characterized by periodic seizures correlated with excessive neuronal discharge within the nervous system (Penfield and Jasper 1954). The hippocampus, perhaps because of its recurrent connectivity, is particularly prone to seizure activity and plays a prominent role in temporal lobe epilepsy (see Lothman *et al.* 1991; Bradford 1995 for review). Seizure-like activity can be induced in the hippo-campal slice preparations by manipulations of the bathing medium, such as low Ca^{2+},

zero Mg^{2+}, or high K^+ concentrations, allowing the slice to be used as an *in vitro* system for studying the cellular and molecular mechanisms of epilepsy (see McNamara 1994 for review). The physiology of hippocampal slices taken from normal and epileptic animals can also be compared to examine the changes seen in the epileptic condition (e.g., Mangan and Lothman 1996; Scharfman *et al.* 1998).

1.2.2.2 Alzheimer's

The neuropathology of Alzheimer's disease, a form of senile dementia, is known to involve hippocampal damage, to the point that Alzheimer's disease has even been referred to as a "hippocampal dementia" (Ball *et al.* 1985). Considerable damage is seen in the temporal lobes of victims of Alzheimer's disease, including substantial cell loss in layers II, III and IV of EC, the major source of afferents to hippocampus; degeneration of the perforant path, the connection between EC and hippocampus; cell loss in areas CA1 and subiculum; neurofibrillary tangles in layer II of EC and CA1; and neuritic plaques in layer III of EC, the molecular layer of dentate gyrus and subiculum, and the CA1 pyramidal cell layer (Van Hoesen *et al.* 1986). *In vivo* MRI studies show a correlation between hippocampal atrophy and severity of Alzheimer's disease (De Leon *et al.* 1996).

1.2.3 The hippocampal slice as an experimental preparation

Several aspects of hippocampal anatomy make the transverse hippocampal slice (Skrede and Westgaard 1971) a particularly useful *in vitro* preparation. Hippocampal slices can be routinely kept alive for 8+ hours after slicing and even longer (up to 30 hours) under special conditions (Kantor *et al.* 1996). The simple, three-layered structure

of the hippocampus, with all the principal cell bodies packed into a single layer (granule cells in stratum granulosum of the dentate gyrus, pyramidal cells in SP of areas CA3 and CA1), makes field recordings easy to interpret and intracellular recordings from principal cells easy to obtain. Because of the roughly lamellar organization of the major excitatory pathways through the hippocampus (Andersen *et al.* 1971; but see Amaral and Witter 1989; Paré and Llinás 1994), a substantial portion of the circuitry is preserved in the slice, allowing studies of network properties. Responses of neurons in slice are similar to those recorded *in vivo* (Schwartzkroin 1975). The clear laminar organization of these excitatory pathways allows selective stimulation and recording of different pathways, as will be seen below.

As in any *in vitro* preparation, some of the complexity of the intact *in vivo* system will be lost. For example, although the trisynaptic loop (section 1.3.1, p. 44) is fairly well preserved in transverse slices, certain other pathways (e.g., inhibitory circuitry (Schwartzkroin 1975; Lacaille and Schwartzkroin 1988a); associational connections between CA3 pyramidal cells (Lorente de Nó 1934; Skrede and Westgaard 1971)) may have a more longitudinal organization and therefore their contribution to network interactions will be reduced by the slicing procedure. Diffuse neuromodulatory pathways, which arise from subcortical nuclei, may also be missing from the slice preparation (although, for example, cholinergic axons from the medial septum survive in the hippocampal slice (Cole and Nicoll 1984)). Care must be taken to prepare healthy, uniform slices, since many properties of slices will vary with the method of preparation and maintenance (Aitken *et al.* 1995; Lipton *et al.* 1995; Watson *et al.* 1997). However,

provided all these factors are taken into consideration, the slice can be a very useful preparation for studying the hippocampal circuitry (Amaral and Witter 1989).

1.3 Hippocampal circuitry and the temporoammonic pathway

1.3.1 The trisynaptic circuit

The fundamental information processing pathway in the hippocampus is usually considered to be the trisynaptic circuit, in which the EC sends a perforant path projection to the granule cells of the dentate gyrus, which send mossy fibers to the pyramidal cells of the CA3 region, which send Schaffer collaterals to the CA1 pyramidal cells, which then project back to the subiculum and deep layers of the EC (Ramón y Cajal 1911; Andersen *et al.* 1971; Brown and Zador 1990) (Figure 1). These projections are all glutamatergic and excitatory (Andersen 1975; Misgeld 1988), and trisynaptic responses can be recorded in CA1 following stimulation of the perforant path *in vivo* (Andersen *et al.* 1966; Herreras *et al.* 1987; Kamondi *et al.* 1988) or *in vitro* (Iijima *et al.* 1996; Sirvio *et al.* 1996). Within each region there are local GABAergic interneurons which provide feed-forward and feedback inhibition (e.g., see Ribak and Seress 1983; Lacaille *et al.* 1989; Woodson *et al.* 1989; Freund and Buzsáki 1996).

1.3.2 The temporoammonic pathway

The trisynaptic pathway is not the only route of information flow through the hippocampus (Brown and Zador 1990). In particular, there is a direct projection from EC to area CA1, effectively bypassing the first two stages of the conventional circuit (Andersen *et al.* 1966) (Figure 1). This projection is known as the temporoammonic

pathway (Ramón y Cajal 1911) because of its origins in the EC (in the temporal lobe) and its termination in CA1, part of the *cornu ammonis* of the hippocampus. In many cases (Lorente de Nó 1934; Doller and Weight 1982; Witter *et al.* 1989; Colbert and Levy 1992; Empson and Heinemann 1995b; Otmakhova and Lisman 1999), the term "perforant path" is used to refer to all projections, including the TA pathway, from EC to hippocampus, which pass through (perforate) the subiculum. However, since the term "perforant path" is so commonly used to refer only to the projection from EC to dentate gyrus, it needs to be qualified when used to refer to the projection to CA1. Given this potential confusion, and given that the projection to CA1 is now known to consist of a separate population of axons from the dentate gyrus projection, the term temporoammonic is useful for distinguishing between the two pathways.

1.3.2.1 Anatomy

The projection from EC to hippocampus arises in the superficial layers of the EC. Perforant path (PP) axons from stellate excitatory projection neurons in layer II of the EC project to the molecular layer of the dentate gyrus and to the apical dendrites of CA3 pyramidal cells; meanwhile, TA axons from pyramidal cells of layer III of the EC project to SLM of CA1 (Steward and Scoville 1976). Both sets of axons course together in the angular bundle before entering the hippocampus (Witter *et al.* 1989).

In the PP projection to dentate gyrus and CA3, the mediolateral axis of the EC maps onto the proximodistal axis of the dendritic field (Witter *et al.* 1989). In other words, more medial areas of the EC project to the proximal dendrites (nearest the cell body) of dentate gyrus granule cells and CA3 pyramidal cells, and more lateral areas of

the EC project to the more distal dendrites. Thus, each granule or CA3 pyramidal cell may receive input from across a broad area of EC.

In the rat TA projection to CA1, on the other hand, the axons are not segregated along the length of the dendrites but terminate fairly uniformly throughout SLM, although there may be a tendency to greater innervation of the inner half of SLM (Witter *et al.* 1988). However, there is a topographic mapping along the transverse axis of the hippocampus: the medial fibers terminate preferentially in the proximal part of CA1, i.e., that closest to CA2, while the more lateral fibers terminate in the more distal part of CA1, i.e., nearer the subiculum (Witter *et al.* 1989). Compared to the fairly diffuse projections along the trisynaptic circuit (Amaral and Witter 1989), this mapping is pretty much point to point (Tamamaki and Nojyo 1995); however, the relatively wide dendritic spread of pyramidal cell dendrites in SLM (Ishizuka *et al.* 1995) may reduce the specificity of this mapping.

The ultrastructure of the synapses formed by TA axons in CA1 has been studied by *Phaseolus vulgaris* leucoagglutinin labeling of the EC (Desmond *et al.* 1994). More than 90% of the synapses observed were asymmetric (i.e., excitatory) and were made onto spines, suggesting that they are contacting CA1 pyramidal cells directly, since hippocampal interneurons are generally aspinous. TA axons also make synaptic contacts onto dendritic shafts of parvalbumin-containing basket and chandelier cells (interneurons) in area CA1 (Kiss *et al.* 1996). TA axons also contain peptide neuromodulators such as cholecystokinin and enkephalin (Fredens *et al.* 1984). The metabotropic glutamate receptor subtype mGluR2 is highly expressed in SLM and seems to be localized to the presynaptic terminals of TA axons (Neki *et al.* 1996; Petralia *et al.* 1996).

1.3.2.2 Physiology

The physiology of the TA projection to CA1 is still unclear (Soltesz and Jones 1995). Different groups have reported that the projection is primarily inhibitory (Empson and Heinemann 1995b; Soltesz 1995), primarily excitatory (Doller and Weight 1982; Yeckel and Berger 1990), or a mixture of the two (Levy *et al.* 1995; Paré and Llinás 1995). These differences may be attributable to species differences (rat, guinea pig, rabbit), the different preparations used (*in vivo*, isolated whole-brain, slice) and the different interpretations due to recording technique (intracellular or field).

Early *in vivo* recordings, in rabbit, revealed the presence of a negative-going (excitatory) field potential in distal CA1 at monosynaptic latency to EC or perforant path stimulation (Andersen *et al.* 1966). This excitation was not found to be strong enough to discharge pyramidal cells, in contrast to the trisynaptic pathway, which could elicit a population spike in CA1. Later studies in rats also found that the monosynaptic TA input to CA1 did not evoke a population spike (Kamondi *et al.* 1988; Leung *et al.* 1995). However, single unit responses at monosynaptic latencies were recorded in response to EC axon activation *in vivo* in rats (Segal 1972) and in rabbits (Yeckel and Berger 1990), and intracellular recordings of spikes in CA1 pyramidal neurons in response to 40 Hz stimulation of the EC *in vivo* have been made (Buzsáki *et al.* 1995). Meanwhile, in another study, only IPSPs were recorded intracellularly in response to EC stimulation in CA1 pyramidal cells of anesthetized rats (Soltesz 1995). In the guinea pig, only small EPSPs or IPSPs were observed at monosynaptic latencies to stimulation of the EC in an isolated, arterially perfused whole-brain preparation (Paré and Llinás 1995).

Single-unit activity (Bragin and Otmakhov 1979; Doller and Weight 1982) and population spikes (Doller and Weight 1982) in CA1 have been reported in slice following activation of the TA pathway. However, in most *in vitro* studies, TA activity could not drive action potentials in CA1 pyramidal cells. An early study in slice showed that afferents to the outer fifth of the apical dendritic tree, roughly corresponding to SLM, were the only subset of CA1 fibers unable to evoke a population spike in CA1 pyramidal cells (Andersen *et al.* 1971). Later field recordings of TA responses in slice show a small to large sink in SLM, accompanied by a small source in SR, suggesting a depolarizing (excitatory) response in the distal dendrites of the CA1 pyramidal cells (Colbert and Levy 1992; Empson and Heinemann 1995b; Maccaferri and McBain 1995) (section 2.3.1.1, p. 83). In these recordings, the dentate gyrus was generally removed from the slice in order to avoid contamination of the small field response in SLM by volume conduction of the large PP response in stratum moleculare of the dentate gyrus (Stringer and Colbert 1994).

Intracellular recordings from pyramidal cells in slice reveal that the response to TA stimulation contains a substantial inhibitory component (Empson and Heinemann 1995b; Jones 1995) (section 2.3.2.2, p. 89). Pyramidal cells show either an EPSP followed by an IPSP, or just an IPSP, in response to TA stimulation. A small minority of cells show EPSPs exclusively, but other physiological evidence suggests that these may have been interneurons. The IPSPs include both a fast $GABA_A$ component and a slow $GABA_B$ component. The IPSPs disappear when excitatory transmission is blocked by the glutamate receptor antagonist 6-cyano-7-nitroquinoxaline-2,3-dione (CNQX), suggesting that they are disynaptic (Empson and Heinemann 1995b).

Taken as a whole, these studies show that the TA projection to CA1 includes both excitatory and inhibitory components. The limited excitation observed in slice is likely due to the loss of many excitatory fibers when the slice is cut. The farther the stimulating electrode is from the recording site, the greater this loss will be, as any excitatory fibers not running exactly parallel to the cut surface of the slice are likely to run out of the slice before reaching their target. The topography of the TA projection, with its restricted areas of innervation (Tamamaki and Nojyo 1995), will also make it difficult to evoke synchronous activity via TA input, which may explain the presence of single unit but not population spike activity in TA responses *in vivo*. The disynaptic IPSPs recorded *in vivo* and *in vitro* in response to TA stimulation demonstrate a definite inhibitory component.

1.3.2.3 Plasticity and modulation

A number of studies have attempted to determine whether the TA pathway, like the SC input to CA1, can undergo activity-dependent LTP. The results to date have been somewhat contradictory. An early *in vitro* study reported robust potentiation of a TA-evoked population spike in SP in area CA1 following a 15 s train of 15 Hz stimulation (Doller and Weight 1985); however, such population spikes are generally not observed in slice (e.g., see section 2.3.1.1, p. 83) except in experiments where no precautions were taken to isolate the TA pathway (e.g., Dahl and Lecompte 1994; Scharfman *et al.* 1998). Other *in vitro* experiments have shown that LTP of the TA pathway can be induced by high-frequency or theta-patterned stimulation only when fast GABAergic transmission is blocked by bicuculline (Colbert and Levy 1993; Hernandez *et al.* 1998; Dvorak-Carbone

and Schuman 1999); like SC LTP, this potentiation is dependent upon the activation of NMDA receptors (Hernandez *et al.* 1998; Dvorak-Carbone and Schuman 1999). One *in vivo* study, using careful current source density analysis to distinguish the TA response in CA1 from volume conduction of the PP response in dentate gyrus, found modest potentiation of the TA response following very high frequency (120 pulses at 400 Hz, repeated eight times at 10 s intervals) burst stimulation of the TA/PP tract (Leung *et al.* 1995). It seems likely that *in vivo*, the TA projection is much better preserved than in slice, and so the difficulty in potentiating the TA pathway *in vitro* may be due to insufficient postsynaptic depolarization in response to the relatively sparse remaining TA fibers.

In CA1, pairing a weak SC input with a stronger one can result in potentiation of the weaker input, a phenomenon known as associative potentiation (Barrionuevo and Brown 1983). Experiments were performed to look for associative plasticity between the TA and the SC pathways, again with somewhat contradictory results. Preliminary results suggested that paired stimulation of the TA and the SC pathways, in the presence of bicuculline, could induce mutually associative plasticity (Levy and Colbert 1992; Zhang *et al.* 1992; Levy *et al.* 1995); with inhibition intact, however, no associativity was seen (Colbert and Levy 1993). In a further study, simultaneous theta-patterned stimulation of the TA and SC pathways could inhibit LTP induction in the SC pathway (Levy *et al.* 1998). One *in vivo* study also suggests a possible associativity between TA and SC inputs in inducing LTP in the trisynaptic pathway (Buzsáki 1988).

The TA pathway has recently been shown to undergo LTD following low-frequency stimulation (Dvorak-Carbone and Schuman 1999), as described in Chapter 3.

Ten minutes of 1 Hz stimulation of the TA pathway resulted in a robust, but reversible, depression of the field TA response that was partially dependent on NMDA receptor activation and independent of inhibitory neurotransmission. Of note is the fact that TA LTD could be induced in slices from adult animals, in which it is difficult or impossible to induce LTD of the SC pathway by the same protocol.

Little is known about short-term or frequency-dependent plasticity in the TA pathway. A preliminary report showed that in combined entorhinal-hippocampal slices, stimuli at moderate frequencies (1-5 Hz) resulted in a decrease in the amplitude of the IPSP in CA1 pyramidal cells evoked by TA stimulation (Jones 1995); however, unlike the synaptic responses of EC layer II cells (Finch *et al.* 1986), the response never reversed to an excitatory one. In field recordings *in vivo*, the current sink seen in SLM following TA stimulation was shown to undergo robust paired-pulse facilitation (Leung *et al.* 1995).

The potency of synaptic transmission in the TA pathway can also be regulated on a short time scale by interaction with other pathways. For example, feedback inhibition in CA1 can selectively inhibit the excitatory response to TA input (Figure 2). Certain interneurons in stratum oriens, known as O-LM interneurons, have a particularly dense axonal arborization in SLM (McBain *et al.* 1994; Sík *et al.* 1995; Katona *et al.* 1999). Activation of CA1 pyramidal cells by alvear stimulation results in feedback activation of O-LM interneurons, and a subsequent reduction in the size of the field potential in SLM in response to TA stimulation (Maccaferri and McBain 1995). Similarly, in mice, activation of O-LM interneurons directly caused a reduction in the field TA response, although the SC response was also reduced (Yanovsky *et al.* 1997); however, in this

study, precautions were not taken to carefully isolate the TA and SC pathways. A subset of SLM interneurons also has an axonal arborization restricted to SLM, suggesting a specific targeting of TA inputs (Vida *et al.* 1998).

Excitatory transmission in the TA pathway, unlike the SC pathway, does not appear to be subject to regulation by presynaptic $GABA_B$ receptors. In the presence of the $GABA_B$ agonist baclofen, TA field responses in slice were unaffected, while SC responses were greatly reduced (Ault and Nadler 1982; Colbert and Levy 1992).

It has been recently shown that dopamine has an inhibitory effect on synaptic transmission in the TA pathway (Otmakhova and Lisman 1999) (see section 1.3.3.6, p. 63).

1.3.2.4 Natural activity patterns in the TA pathway

When the physiology of a neural pathway is being characterized by artificial stimulation, it is of interest to know what the physiological, *in vivo* activity patterns of that pathway are, so that these can be imitated. For the TA pathway, therefore, the natural firing patterns of neurons of layer III of EC need to be examined.

Determining the natural firing patterns of EC layer III cells is complicated by the fact that, *in vivo*, it is difficult to tell with any certainty in an extracellular, single-unit recording whether a particular cell belongs to layer II or layer III (Quirk *et al.* 1992; Stewart *et al.* 1992; Paré *et al.* 1995; Chrobak and Buzsáki 1998). Without this identification, it is impossible to tell whether the activity recorded will be presynaptic to the perforant path to dentate gyrus (layer II) or the TA path to CA1 (layer III). Intracellular recordings can be used with intracellular labeling to identify recorded cells (Finch *et al.*

1986), but current techniques allow intracellular recording only from anesthetized animals. *In vitro* recordings from identified EC layer III cells (Dickson *et al.* 1997; Gloveli *et al.* 1997a; Gloveli *et al.* 1997b) can also be useful in characterizing the responsiveness of neurons to synaptic inputs and their ability to fire at particular frequencies.

A variety of firing patterns have been observed in the neurons of the superficial layers (II and III) of the EC *in vivo*. During maze running, many EC neurons with place fields, like hippocampal pyramidal cells (O'Keefe and Dostrovsky 1971; Ranck 1973), fire only at low frequencies, with mean firing rates reported to be < 1 Hz (Mizumori *et al.* 1992), 7 ± 9 Hz (Quirk *et al.* 1992), or 12 ± 12 Hz (Stewart *et al.* 1992). Within each of these studies, some neurons were observed to fire at higher rates, including short periods of high-frequency (50 Hz (Stewart *et al.* 1992) or 150 Hz (Quirk *et al.* 1992)) bursting. The firing patterns of many superficial layer EC neurons are modulated at the theta (~5-10 Hz) frequency, with one action potential or a brief burst (2-8 spikes at 25-100 Hz) occurring in a fixed phase relationship to the background theta activity (Alonso and Garcia-Austt 1987; Stewart *et al.* 1992; Dickson *et al.* 1995; Chrobak and Buzsáki 1998). EC neurons were also found to fire in phase with gamma (40-100 Hz) oscillations, which were themselves modulated by theta, such that the population activity of superficial EC neurons during theta would consist of bursts (3-4 spikes) of synchronized activity at 40-100 Hz, repeated at theta frequencies (100-125 ms intervals) (Chrobak and Buzsáki 1998). Some EC layer II and III neurons were also found to fire single spikes or doublets in a fixed phase relationship to sharp waves, an EEG phenomenon observed during sleep (Paré and Llinás 1995).

The firing patterns of EC layer III neurons *in vitro* have also been characterized. In one study, EC layer III neurons fired tonically at about 2 Hz at "rest," and could be made to spike at up to 200 Hz in response to depolarizing current injection, with no tendency to fire in bursts (Dickson *et al.* 1997). In another study, EC layer III neurons were classified into four categories, including two types of projection cells, based on their morphology and electrophysiology. Type 1 projection cells responded to depolarizing current injection with long, regular trains of action potentials at up to 40 Hz, while type 2 projection cells fired slowly and irregularly at no more than 10 Hz; both types of neurons fired bursts of action potentials when activated synaptically in a slice with $GABA_A$ inhibition blocked (Gloveli *et al.* 1997a). Further characterization of these cells showed that both type 1 and type 2 cells were most effectively driven to spike by synaptic input, and could follow suprathreshold stimulation, at 10 Hz, in contrast to layer II cells which were more effectively driven by, and were capable of firing at, higher frequencies (Gloveli *et al.* 1997b). However, it is difficult to say how well these afferent inputs evoked by extracellular stimulation mimic the inputs these neurons would receive *in vivo*.

1.3.2.5 What is the function of the TA pathway?

What is the functional or behavioral role of the TA pathway? To answer this question, we need to know what the targets of the TA pathway, the CA1 pyramidal cells, do, and how the TA pathway contributes to their activity. In sensory cortical areas, firing patterns of individual neurons can be correlated with sensory inputs controllable, or at least measurable, by the experimenter (e.g., see Hubel 1982; Livingstone and Hubel 1988

for review) and these patterns can be used in conjunction with studies of cortical networks to discover how those patterns arise (e.g., see Gilbert 1993). Similarly, in motor cortical areas, neuronal activity can be correlated with movements made by the animal (e.g., see Georgopoulos 1991, for review). However, the distance of the hippocampus within the nervous system from both sensory inputs (with the exception of olfaction) and motor outputs makes it difficult to ascribe "meanings" to the activity of individual neurons.

As described above, two functions generally attributed to the hippocampus are learning and memory (section 1.2.1.1, p. 36) and spatial navigation (section 1.2.1.2, p. 40). How might the TA input contribute to hippocampal processing in these functions?

We are a long way from understanding how memories are encoded in the brain, and so ideas about how the TA pathway may contribute to learning and memory functions mostly come from models of the hippocampus as an associative network. An idea common to such models is that the CA1 region is a site of convergence of two parallel streams of information flow from the EC, one direct via the TA pathway, one further processed through the trisynaptic pathway and arriving via the SC projection. All of these models require that the SC and TA inputs have excitatory effects on CA1 pyramidal cells, though their relative weights can be modulated and their regions of action restricted.

One computational model of hippocampal function postulates that the activity of CA1 pyramidal cells can act either as a representation of current events or as a predictor of future ones, with the current representation mediated by the TA input and the predicted representation mediated by the SC input (Levy 1989). This model requires that the TA

input to CA1 have a strong enough excitatory component to discharge CA1 pyramidal cells, a question still in dispute (section 1.3.2.2, p. 47). To accommodate the observations that the TA input is not strongly excitatory, at least on a broad scale, a revised version of this model has been proposed (Levy *et al.* 1995; Levy *et al.* 1998) in which the TA input is postulated to excite only a small subpopulation of CA1 pyramidal cells while inhibiting others.

Another version of this model of the hippocampus as an associative memory network suggests that associations between SC and TA activity are stored in the weights of the SC synapses onto CA1 pyramidal cells (Hasselmo and Schnell 1994). A prediction of this model is that cholinergic input can switch the network between learning and recall functions, and prevent interference between previously stored and newly learned associations, by varying the relative efficacy of synaptic transmission in the two inputs. It was shown that, indeed, in the presence of ACh, SC responses were selectively suppressed while TA responses were unaffected (Hasselmo and Schnell 1994). A further elaboration of this model (Hasselmo *et al.* 1996) suggests that activation of presynaptic $GABA_B$ receptors may also be used to selectively suppress SC inputs; as previously mentioned, SC responses are suppressed by the $GABA_B$ agonist baclofen while TA responses are unaffected (Ault and Nadler 1982; Colbert and Levy 1992). A similar, larger-scale model (McClelland and Goddard 1996) also postulates an important role for the TA projection in recall, and also requires that TA input be strong enough to make CA1 pyramidal cells fire.

At an even more abstract level, it may be said that if something affects LTP, it can affect learning and memory (section 1.2.1.1.3, p. 38). Since properly timed theta-

patterned activity in the TA pathway can prevent the induction of LTP in the SC pathway (Levy *et al.* 1998), one could speculate that the TA pathway can regulate the encoding of memories.

There is evidence to suggest that input from the TA pathway may contribute to, or even be sufficient for, place specificity of CA1 place cells. Neurons in the superficial layers of EC have spatially-selective firing properties (Mizumori *et al.* 1992; Quirk *et al.* 1992; Stewart *et al.* 1992). In one experiment, the place specificity of CA3 pyramidal cells, thought to be the primary input to CA1 pyramidal cells, was eliminated when the medial septum was inactivated with tetracaine; however, CA1 pyramidal cells retained their spatial selectivity, suggesting that the monosynaptic input from EC may be sufficient for establishing place fields in CA1 (Mizumori *et al.* 1989). More support for the idea that spatial selectivity in CA1 is not established by the input from CA3 comes from a study in which place fields were found to predict, with a definite lead time, the future location of the rat; CA1 place cells had a longer lead time (i.e., fired earlier) than CA3 place cells, suggesting that their spatial selectivity may not have been dependent on CA3 input (Muller and Kubie 1989). In another experiment, destruction of a majority of dentate granule cells by colchicine injection severely impaired spatial learning, but spared the spatial selectivity of place cell firing; however, in this case, the EC input to CA3 was spared and may have contributed to spatial selectivity of the CA3 and CA1 pyramidal cells (McNaughton *et al.* 1989).

Another way of looking at the role of the TA pathway is to compare the circumstances under which neural activity in the EC is transmitted to hippocampus by either the mono- or the trisynaptic pathways. For example, the responses in DG, CA3 and CA1 to

stimulation of the angular bundle (containing the PP and TA axons) during various behavioral states were recorded in freely-moving rats. It was found that the trisynaptic pathway was by far most efficacious in slow-wave sleep, whereas during other states (still, alert awakeness, REM sleep, or voluntary movement) angular bundle stimulation evoked little response in CA1 (Winson and Abzug 1978). Acoustic or tactile stimuli presented to rats could produce a larger response in SLM than in DG, suggesting greater activity in the TA than the PP pathway (Buzsáki *et al.* 1995). A study of changes in metabolic activity of downstream regions following EC lesions found a greater decrease in glucose utilization in CA1 SLM than in the molecular layer of dentate gyrus, suggesting that the TA pathway is at least as active as the perforant path (Jørgensen and Wright 1988). Other studies have suggested the presence of a frequency-dependent switch between transmission via the mono- or trisynaptic routes (see Jones 1993, for review). Differential responses of EC neurons in various layers to different frequencies of synaptic input (Jones 1993; Gloveli *et al.* 1997b) suggest that at low frequencies, the monosynaptic pathway will dominate, while at higher frequencies the trisynaptic pathway will be more greatly recruited. This prediction is further supported by the observation of frequency facilitation in the trisynaptic pathway (Herreras *et al.* 1987).

The TA pathway may also contribute to the generation of oscillatory field activity in CA1 at both theta (Buzsáki *et al.* 1995) and higher frequencies (Charpak *et al.* 1995). Laminar analysis of oscillations shows a large peak of theta power near the hippocampal fissure, which disappears when the EC is lesioned, suggesting a contribution of synaptic currents from the TA pathway to hippocampal theta (Bragin *et al.* 1995; Buzsáki *et al.* 1995; Ylinen *et al.* 1995b; but see Vinogradova 1995). In the absence of theta, 40 Hz

oscillations were observed in the hippocampus of the anesthetized guinea pig, and were not abolished by sectioning the SC pathway, again suggesting a contribution of synaptic currents from the TA pathway (Charpak *et al.* 1995).

Observations from neuropathology can also contribute to our understanding of the role of the TA pathway under normal conditions. The hippocampus and surrounding limbic regions are a common focus for temporal lobe epilepsy in humans (Bradford 1995), and many animal models of temporal lobe epilepsy have been developed. A common feature of many of these models is the selective loss of layer III neurons in the EC (e.g., Scharfman *et al.* 1998; Wu and Schwarcz 1998). Human neuropathology data also show a selective loss of EC layer III cells in epileptics (Du *et al.* 1993). Since epileptic seizure activity is associated with uncontrolled neuronal excitation, these data suggest that the inhibitory component of the TA pathway, in normal conditions, acts as a gate controlling and limiting activity in the hippocampus (see Chapter 4). Meanwhile, a study of EC tissue from Alzheimer's patients showed a great decline in layer II neurons (Lippa *et al.* 1992). Together, these data suggest that a balance between monosynaptic and trisynaptic inputs from EC to hippocampus is critical for normal function.

In vitro studies, especially when placed into the context of *in vivo* observations, can also suggest roles for the TA pathway in hippocampal processing. As discussed above, there is *in vitro* evidence for both an excitatory and an inhibitory component to the TA input to CA1. The potency of excitation elicited by the TA pathway *in vitro* appears to be greatly reduced compared to the *in vivo* situation, limiting the experiments that can be done to elucidate the contribution of this component. Inhibition evoked by TA stim-

ulation in slice is more robust, allowing a more detailed characterization of this inhibition in controlling hippocampal output (Chapter 4).

1.3.3 Other inputs to SLM

1.3.3.1 Nucleus reuniens thalami

Anterograde and retrograde tracing techniques reveal a substantial projection from nucleus reuniens thalami (RE) (also known as the medioventral nucleus (Jones 1985)) to SLM of CA1, as well as the molecular layer of the subiculum and layers I and III of EC (Herkenham 1978; Wouterlood *et al.* 1990; Dolleman-Van Der Weel and Witter 1996). Since the TA projection to SLM originates in layer III of EC, the RE projection may interact with the TA pathway both at its site of origin and at its site of termination; however, separate populations of RE neurons target EC and CA1 SLM (Dolleman-Van Der Weel and Witter 1996). RE axon terminals contain spherical synaptic vesicles and form asymmetric synapses onto dendritic spines or shafts, suggesting an excitatory input (Wouterlood *et al.* 1990). Extracellular recordings *in vivo* of responses in CA1 to RE stimulation revealed a current sink in SLM and a current source in SR, consistent with an excitatory input to the distal dendrites of CA1 pyramidal cells (Dolleman-Van der Weel *et al.* 1997). Population spikes were never observed in response to this input, suggesting that the effect on pyramidal cells is only a subthreshold excitation. However, in a few cases, single-unit activity could be recorded in SR or SO at a fixed latency from RE stimulation, suggesting that the RE input could cause SR or SO interneurons to spike.

The role of the RE input to hippocampus in normal conditions is not known. Interestingly, the nucleus is relatively much smaller in primates than in rodents (Jones 1985). The projection from RE to hippocampus can contribute to limbic seizure activity; microinjection of NMDA into the RE of rats causes convulsive seizures and limbic kindling (Hirayasu and Wada 1992b; Hirayasu and Wada 1992a). This role of the RE projection to SLM in promoting seizures stands in contrast to the finding that the TA projection to SLM is selectively missing in seizure conditions (Du *et al.* 1993; Scharfman *et al.* 1998; Wu and Schwarcz 1998), suggesting that the excitatory component of the RE projection dominates the inhibitory component. Little is known about the natural activity patterns of RE neurons, although a preliminary *in vitro* study showed a tendency of RE neurons to fire bursts of spikes in response to synaptic activation, current injection, or NMDA application (Miyahara *et al.* 1998).

1.3.3.2 Amygdala

The amygdala is known to be strongly connected with the hippocampus (Papez 1937; Lopes da Silva *et al.* 1990) and is involved in certain learning tasks, especially those involving fear and other affective factors (e.g., McDonald and White 1993; Rogan *et al.* 1997; see Maren and Fanselow 1996 for review). Recent anatomical studies have shown that the amygdala projects primarily to SLM of area CA1 (Petrovich *et al.* 1997). A more detailed study showed that the lateral and accessory basal nuclei of the amygdala project to SLM of CA1 in the temporal end of the hippocampus; these same nuclei also project to EC layer III, providing parallel mono- and disynaptic projections from amygdala to SLM of CA1 (Pikkarainen *et al.* 1999)

1.3.3.3 Inferotemporal cortex

In monkey, horseradish peroxidase injections labeled a reciprocal connection between SLM of area CA1 and the ventral TE area of inferotemporal cortex (Yukie and Iwai 1988). Area TE is involved in visual memory, so a connection with hippocampus is not unexpected.

1.3.3.4 Medial septum

The hippocampus receives a dense cholinergic and sparse GABAergic innervation from the medial septum (see Dutar *et al.* 1995 for review), with choline acetyltransferase-positive axon terminals found particularly densely at the CA1 SR/SLM border (Matthews *et al.* 1987). Although the GABAergic projection selectively targets hippocampal interneurons, few SLM neurons receive GABAergic synapses from the septal projection (Freund and Antal 1988). ACh can trigger theta activity in the hippocampus (see Vinogradova 1995 for review), even in slice (Konopacki *et al.* 1987), through its action on mAChRs. ACh can also selectively block SC, but not TA, excitatory transmission in the hippocampus (Hasselmo and Schnell 1994).

1.3.3.5 Locus ceruleus

Noradrenergic axons from the locus ceruleus terminate particularly densely in SLM, more densely than in SR, with a greater density at the temporal end of the hippocampus (Oleskevich *et al.* 1989). Norepinephrine (NE) lowers the firing rate of pyramidal cells by depolarizing interneurons and increasing the frequency of IPSPs (Bergles *et al.* 1996). There is one published report regarding possible effects of NE on the TA

response (Nejtek and Dahl 1997); no effect was found, but the data presented were unconvincing. The question of whether NE affects TA neurotransmission remains open.

1.3.3.6 Median raphe

Serotonergic axons from the median raphe terminate somewhat more densely in SLM than in SR, with no clear gradient along the septo-temporal axis (Oleskevich and Descarries 1990). Serotonergic axons appear to selectively target interneurons (Freund *et al.* 1990). Serotonin increases the magnitude of a low-threshold transient calcium current in SLM interneurons; this current may cause these neurons to switch from a tonic firing mode to repetitive bursting (Fraser and MacVicar 1991). SR/SLM interneurons were depolarized and made more excitable by serotonin acting on 5-HT_3 receptors (McMahon and Kauer 1997a).

There is also evidence for a dopaminergic input to the hippocampus, which was once thought to originate from the ventral tegmental area but rather appears to arise from a subpopulation of neurons of the raphe nuclei (Reymann *et al.* 1983; Pohle *et al.* 1984). Dopamine has been recently shown to have a strong inhibitory effect on the field TA response in SLM (Otmakhova and Lisman 1999).

1.3.4 Other distinctive properties of SLM

The clear segregation of afferents to CA1 between SR and SLM (Amaral and Witter 1989; Tamamaki and Nojyo 1995) suggests that SLM may be distinct from SR in other ways, as well.

The G protein-gated, inwardly-rectifying K^+ channel GIRK is found in the dendrites of CA1 pyramidal cells, with particularly high levels of expression in SLM (Ponce *et al.* 1996; Drake *et al.* 1997). Recordings in cultures of CA3 neurons suggest that $GABA_B$ receptors can activate a GIRK-like channel (Sodickson and Bean 1996).

Anatomical evidence suggests that the innervation of pyramidal cell dendrites is lesser in SLM than in SR. Reconstructions of CA1 pyramidal cells show that they have more than twice as much total dendritic length in SR than in SLM (Amaral *et al.* 1990; Ishizuka *et al.* 1995), even though the dendritic plexus in SLM is wider than that in SR (Ishizuka *et al.* 1995). The density of synapses made onto dendrites in SLM is approximately 50% that of SR, with a much larger fraction made onto dendritic shafts or somata than onto dendritic spines (Andersen *et al.* 1971); spine densities in SLM also drop off dramatically compared to SR (Ishizuka *et al.* 1995).

SLM contains a high density of interneurons (Ramón y Cajal 1893), whose properties are described in the next section.

1.3.5 SLM interneurons

In rats, there is a relatively dense concentration of interneurons near the border of SLM and SR. (In contrast, in humans, SLM interneurons are more dispersed throughout the layer (Zhang *et al.* 1998).) Until recently, these interneurons were considered to be a relatively homogenous population (e.g., see Kunkel *et al.* 1988; Lacaille and Schwartzkroin 1988b; Williams *et al.* 1994). A recent, more thorough study has allowed a categorization of interneurons in this region (Vida *et al.* 1998). Based on morphology, four types of SLM interneurons were described: basket cells, whose axons ramify primarily in

SP, and dendrites range from SLM to SO; SC-associated interneurons, with axons mostly in SR and SO, dendrites mostly in SLM and SR; PP-associated interneurons, with axons mostly in SLM, dendrites mostly in SLM and SR; and neurogliaform interneurons, with dense, compact axonal and dendritic arbors. Another study, looking specifically at interneurons staining for vasoactive intestinal polypeptide, found a population of neurons with profuse dendritic arborization in SLM and axons innervating SR (Acsády *et al.* 1996). Dendrites of SLM interneurons are smooth and spineless but have a beaded or varicose appearance (Lacaille and Schwartzkroin 1988a; Williams *et al.* 1994; Khazipov *et al.* 1995; Morin *et al.* 1996; Vida *et al.* 1998) (section 2.3.3.1, p. 97).

As a group, SLM interneurons have a resting potential of about -55 to -60 mV (Lacaille and Schwartzkroin 1988a; Khazipov *et al.* 1995; Morin *et al.* 1996; Vida *et al.* 1998) and tend not to be spontaneously active (Lacaille and Schwartzkroin 1988a; Khazipov *et al.* 1995). There is little or no spike frequency accommodation during brief depolarizing current injections (Lacaille and Schwartzkroin 1988a; Khazipov *et al.* 1995), although spiking may be irregular or stop entirely during a prolonged depolarization (Vida *et al.* 1998) (section 2.3.3.1, p. 97). In general, the response to hyperpolarizing current injection begins with a sag followed by recovery to a less hyperpolarized level (Lacaille and Schwartzkroin 1988a; Williams *et al.* 1994; Morin *et al.* 1996). Rebound (anode break) firing may be seen following the end of a hyperpolarizing step (Lacaille and Schwartzkroin 1988a; Williams *et al.* 1994).

There is some evidence for low voltage activated calcium channels that may underlie bursting activity seen when SLM interneurons are depolarized from a hyper-

polarized state (Lacaille and Schwartzkroin 1988a). In acutely-dissociated interneurons from SLM of 3-4 week old rats, a low-threshold calcium current enhanced by activation of mAChRs and 5-HT receptors, but depressed by $GABA_B$ receptor activation with baclofen, is observed (Fraser and MacVicar 1991). However, recordings from SLM interneurons *in situ* in slices from 14-18 day old rats showed no low voltage activated calcium channels, but did reveal N-, L-, and P/Q-type high voltage activated calcium conductances which were inhibited by baclofen (Lambert and Wilson 1996); other whole-cell recordings in slice have also not provided any evidence of low-threshold calcium channels (Williams *et al.* 1994).

SLM interneurons, like other hippocampal interneurons (Geiger *et al.* 1995), have a calcium-permeable form of the AMPA type of ionotropic glutamate receptor (Isa *et al.* 1996; Carmant *et al.* 1997; Carmant *et al.* 1998) and also express the α_7 nicotinic AChR subunit (Séguéla *et al.* 1993; Alkondon *et al.* 1998), which has a particularly high permeability to calcium (Séguéla *et al.* 1993). SLM interneurons also express at least two types of delayed-rectifier potassium channels. One is sustained, insensitive to 4-AP, and blocked by external and internal tetraethylammonium (TEA); the other is slowly-inactivating, and blocked by 4-AP and external TEA (Chikwendu and McBain 1996). SLM interneurons also have a small, transient A-type current which is less prominent than that seen in other hippocampal interneurons (Chikwendu and McBain 1996). In the presence of the mAChR agonist carbachol, SLM interneurons depolarize and show membrane potential oscillations at theta frequencies (Chapman and Lacaille 1998). SLM interneurons are also excited by serotonin acting on $5\text{-}HT_3$ receptors (McMahon and Kauer 1997a) and have high levels of $5\text{-}HT_3$ receptor mRNA (Tecott *et al.* 1993).

Responsiveness of SLM interneurons to afferent inputs has been studied in the hippocampal slice preparation, with somewhat divergent results. In transverse slices, stimulation in SR (Williams *et al.* 1994) (section 2.3.3.2, p. 100) or in any layer, from alveus to the molecular layer of the dentate gyrus (Lacaille and Schwartzkroin 1988a) could elicit EPSPs in SLM interneurons. This excitation could bring the cell to threshold for action potential firing (Lacaille and Schwartzkroin 1988a; Williams *et al.* 1994) and stimulation in SLM could evoke bursts of action potentials (Lacaille and Schwartzkroin 1988a). The EPSPs included a fast, AMPAR-mediated component as well as a slower component that was partially sensitive to the NMDA antagonist 2-amino-5-phosphonopentanoic acid (AP5), with contributions also made by voltage-dependent conductances. SLM interneurons do not appear to be activated in a feedback manner by CA1 pyramidal cells (Lacaille and Schwartzkroin 1988b).

SLM interneurons also receive inhibitory inputs. In longitudinal slices, a multi-phasic response starting with an IPSP and followed by one or more depolarization-hyperpolarization sequences was observed following stimulation in any layer (Lacaille and Schwartzkroin 1988a). IPSPs were also sometimes observed following the EPSP evoked by stimulation in SR in the transverse slice (Williams *et al.* 1994) (section 2.3.3.2, p. 100). Spontaneous IPSCs have been observed in whole-cell recordings from SLM interneurons (Atzori 1996; Hájos and Mody 1997).

SLM interneurons make inhibitory synapses onto CA1 pyramidal cells. Ultra-structural studies in guinea pig show symmetric contacts made by axons of SLM inter-neurons onto spiny and smooth dendrites in SR and SLM of CA1 as well as the outer two-thirds of the molecular layer of DG (Lacaille and Schwartzkroin 1988b). Paired

recordings from SLM interneurons and pyramidal cells show a hyperpolarizing response in pyramidal cells when the interneurons are made to fire by means of depolarizing current injection; the $GABA_A$-mediated IPSPs evoked by single action potentials in the interneuron are very small (< 0.5 mV), but can summate to sizable IPSPs when a train of action potentials is elicited in the interneuron (Lacaille and Schwartzkroin 1988b; Vida *et al.* 1998). The $GABA_A$ IPSPs evoked by SLM interneurons may be longer and slower than those evoked by other interneurons (Buhl *et al.* 1994a; Ouardouz and Lacaille 1997), suggesting they may be mediated by a different type of $GABA_A$ receptor (Pearce 1993). Focal stimulation in SLM, either by electrical stimulation or by focal application of glutamate, can result in small IPSPs or IPSCs in pyramidal cells (Williams and Lacaille 1992; Benardo 1995; Ouardouz and Lacaille 1997; Chapman and Lacaille 1998). In some cases, a $GABA_B$-mediated component is observed (Williams and Lacaille 1992; Benardo 1995); it is not known what the firing pattern of the stimulated SLM interneurons was during these responses. SLM interneurons can also innervate other interneurons; a paired recording showed an SLM interneuron making an inhibitory synapse onto a bistratified cell as well as a pyramidal cell (Cobb *et al.* 1997)

In addition to SLM interneurons, other CA1 interneurons have dendrites in SLM and are therefore likely to be activated by afferents to SLM. Vertically-oriented O/A interneurons (McBain *et al.* 1994), SP basket cells (Sík *et al.* 1995; Han 1996), and chandelier cells, which have a dense tuft of dendrites in SLM (Li *et al.* 1992; Buhl *et al.* 1994b), may all be activated by SLM afferents. An ultrastructural study has shown that basket and chandelier cells receive synapses from TA axons (Kiss *et al.* 1996).

Figure 1. Neuronal pathways of the entorhinal cortex-hippocampus loop. EC, entorhinal cortex; DG, dentate gyrus; CA3 and CA1, fields of the Ammon's horn; sub, subiculum.

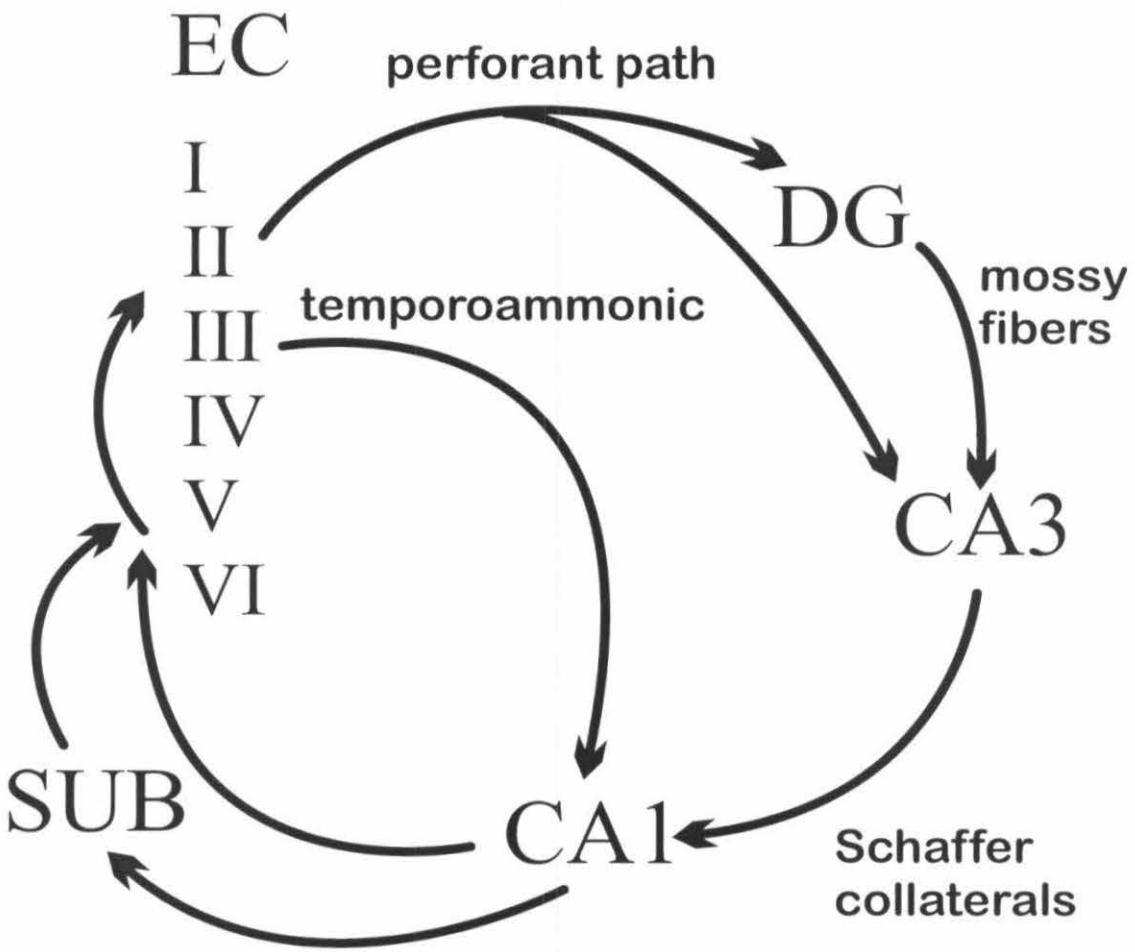
EC
perforant path
I
II
III
IV
V
VI
DG
mossy
fibers
temporoammonic
CA3
SUB
CA1
Schaffer
collaterals

Figure 2. Schematic of SC and TA inputs to CA1, and interneurons mediating feedforward and feedback inhibition. Excitatory pathways are indicated by pointed arrows and inhibitory pathways by flat-ended arrows. The temporoammonic pathway makes excitatory connections onto the distal dendrites of CA1 pyramidal cells (pyr) as well as SLM interneurons (SLM). SLM interneurons mediate feedforward inhibition onto pyramidal cells. Schaffer collateral inputs make excitatory connections onto pyramidal cells and interneurons such as basket cells (B). Pyramidal cells make excitatory connections onto basket and O-LM interneurons (O-LM), both of which mediate feedback inhibition; basket cells target the somata of pyramidal cells, while O-LM interneurons target the distal dendrites. Many other types of interneurons exist, but are not shown.

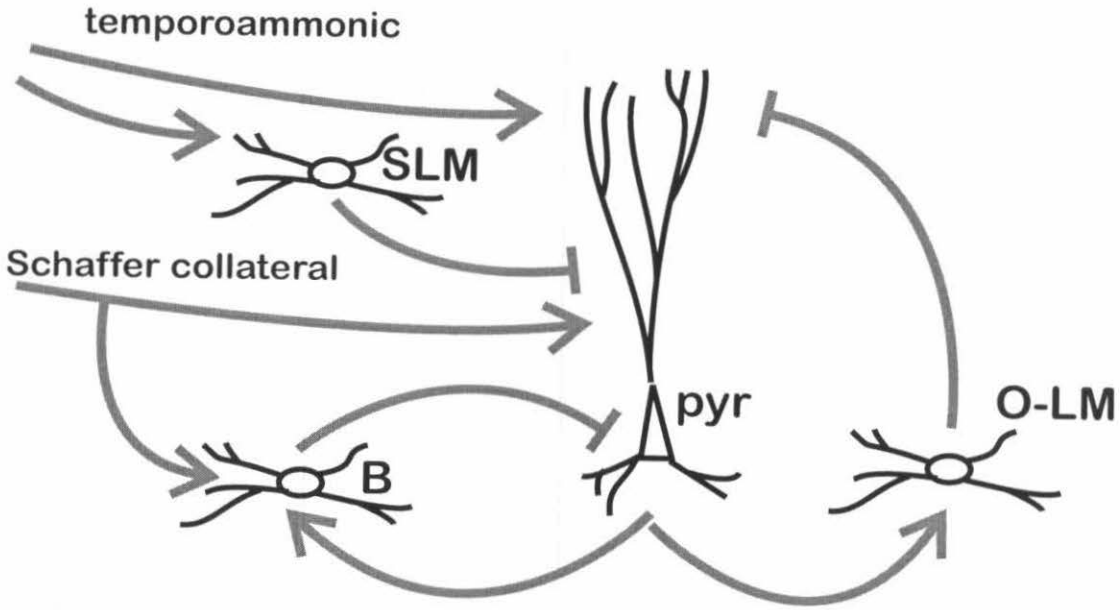
temporoammonic
SLM
Schaffer collateral
pyr
O-LM
B

2 Baseline responses and short-term plasticity of the SC and TA pathways

2.1 Introduction

As described in the opening chapter (section 1.3.2.2, p. 47), the physiology of the TA input to area CA1 of the hippocampus is, as yet, poorly understood (Soltesz and Jones 1995). Anatomical studies show that TA axons arising in layer III of the EC terminate in SLM of CA1 (Steward and Scoville 1976) and that these axons make excitatory synapses primarily onto the dendrites of pyramidal neurons (Desmond *et al.* 1994), although synapses are also made onto interneurons (Desmond *et al.* 1994; Kiss *et al.* 1996). Field recordings *in vitro* (Colbert and Levy 1992) and *in vivo* (Leung *et al.* 1995) confirm the presence of a current sink in the distal dendritic region of CA1 following stimulation of the TA pathway. However, some reports suggest that the TA input is sufficiently excitatory to activate pyramidal cells in CA1 (Yeckel and Berger 1990), while others suggest that the input has a primarily inhibitory effect (Empson and Heinemann 1995b; Paré and Llinás 1995).

In this chapter, I describe the results of my own investigations into the physiology of the TA input to CA1. I describe the development of a hippocampal slice preparation in which TA and SC responses can be unambiguously recorded. I describe and compare field potential responses to stimulation of the two pathways, as well as responses recorded intracellularly in pyramidal cells, SR/SLM interneurons, and SR giant cells. TA field

potential responses in the slice have previously been described (Colbert and Levy 1992), as have the intracellular responses of pyramidal cells to TA stimulation (Empson and Heinemann 1995b). Although responses to stimulation in SLM have been described for SR/SLM interneurons (Lacaille and Schwartzkroin 1988a; Williams *et al.* 1994), these studies did not focus on the TA pathway as a primary input to these neurons. SR giant cells have only recently been described as a discrete neuronal population in the hippocampus (Gulyás *et al.* 1998b) and their responses to stimulation in various hippocampal layers have not previously been characterized.

Short-term plasticity phenomena, such as paired-pulse facilitation and depression, and frequency-dependent synaptic transmission, are a way of regulating the efficacy of synaptic inputs on a moment-to-moment basis (see Chapter 1). Since information processing depends on the relationship between inputs and outputs of a neuronal network, any changes in the relative strengths of different inputs will affect the computation performed by the network. Although short-term plasticity in the SC pathway has been well characterized (e.g., Creager *et al.* 1980; Davies and Collingridge 1996), short-term plasticity in the TA pathway has not been thoroughly investigated. Trains of stimuli at various frequencies can be used to probe short-term plasticity processes. I compare here the field and intracellular responses to repeated stimulation of the TA and SC pathways. Some of these results have been reported in abstract form (Dvorak and Schuman 1996; Dvorak and Schuman 1997).

My investigations of long-term plasticity in the TA pathway are described in Chapter 3.

2.2 Methods

2.2.1 Slice preparation

Slices were prepared from 6-8 week old male Sprague-Dawley rats. All use of animals was performed according to the guidelines of the Caltech Institutional Animal Care and Use Committee. Rats were decapitated following Halothane anesthesia, and the brain rapidly removed to ice-cold, oxygenated artificial cerebrospinal fluid (ACSF: 119 mM NaCl; 2.5 mM KCl; 1.3 mM $MgSO_4$; 2.4 mM $CaCl_2$; 1.0 mM NaH_2PO_4; 26.2 mM $NaHCO_3$; 11.0 mM glucose). The dorsal surface of the posterior half of each hemisphere was glued onto the stage of a cooled oscillating tissue slicer (OTS-3000-04; FHC) and covered with chilled ACSF. 500 μm slices were cut, with the optimal slices (as assessed visually, by ease of identification of distinct layers, as well as electrophysiologically, by the presence of robust field potentials) generally found 4-4.5 mm below the ventral surface. The extraneous cortical and subcortical tissue was gently dissected away with the small end of a spatula. A small number of early experiments were done on slices prepared with a Stoelting tissue chopper. The slices rested in an interface chamber at room temperature for at least one hour before experiments were started. Further micro-dissection (see section 2.3.1.1, p. 83) was performed either in ice-cold ACSF during slice preparation, or in the recording chamber prior to the start of the experiment. All electro-physiology was done with the slices submerged and constantly perfused with oxygenated ACSF at room temperature (~20 °C).

2.2.2 Electrophysiology

2.2.2.1 Stimulation and field recording

Bipolar tungsten electrodes, either concentric or paired needles, were used for stimulation. One electrode was placed in SR to stimulate the Schaffer collaterals, the other in SLM to stimulate the TA pathway (Figure 3). Stimulation currents were 100 μs long, monophasic, and ranged from 10-100 μA in the SC pathway and 30-200 μA in the TA pathway. Stimulus intensities were selected to produce submaximal field responses with no population spike. Field recordings were made with low-resistance (< 5 MΩ) micropipettes filled with 3M NaCl.

2.2.2.2 Intracellular recording

Intracellular recordings from pyramidal cells were made using sharp electrodes whose resistance was 100-200 MΩ when filled with 2 M potassium acetate (KAc) or cesium acetate (CsAc). Sharp electrode recordings were made "blind" by advancing the electrode through SP until a penetration was achieved. The voltage reading of the electrode was zeroed with the electrode in the bath, and the bridge was balanced before penetration and rebalanced after penetration. Membrane potential was estimated by subtracting the potential observed in the bath after the electrode was withdrawn from the cell. Capacitance compensation was applied after penetration. Pyramidal cells were identified by the presence of spike frequency accommodation in response to positive current injection. All experiments were performed in current clamp mode, with the cell

at its resting potential or with a small hyperpolarizing current applied to prevent spontaneous spiking.

2.2.2.3 Whole-cell recording

Whole-cell electrodes had a resistance of about 5 MΩ when filled with potassium methyl sulfate-based intracellular solution (125 mM $KMeSO_4$ (City Chemical Corp., Jersey City, NJ), 9 mM HEPES, 3.6 mM NaCl, 90 μM EGTA, 4 mM Mg-ATP, 300 μM Li-GTP, and 25 mM phosphocreatine; for most recordings, the solution also contained 0.2-0.4% biocytin). A few early experiments were performed using a potassium gluconate-based whole-cell solution (130 mM K-gluconate, 1 mM $MgCl_2$, 10 mM NaCl, 2 mM ATP, 0.3 mM GTP, 10 mM HEPES, and 0.4 mM EGTA); recordings from these cells was not noticeably different from those using the $KMeSO_4$-based solution, and so the data were combined. Whole-cell recordings were made under visual guidance on an Olympus BX50WI upright microscope equipped with a MTI VE1000 CCD camera. Positive pressure was applied to the electrode solution while advancing towards the targeted neuron, in order to keep debris off the electrode as well as to "clean" the surface of the neuron (Edwards 1995). A gigaseal was obtained under voltage-clamp conditions by applying slight negative pressure; the patch was then clamped down to -60 mV and whole-cell configuration was achieved by applying further negative pressure to rupture the patch. Series resistance was measured by balancing the bridge in current clamp mode; series resistance in included experiments was always less than 30 MΩ. Neurons included for analysis had resting potentials negative to -50 mV (estimated following withdrawal of the electrode), fired overshooting action potentials, and had input resis-

tances of 562 ± 35 MΩ (n = 41). All experiments were performed in current-clamp mode, with the cell at its resting potential; in some cases, hyperpolarizing or depolarizing currents were applied to look at voltage-dependent phenomena.

2.2.2.4 Drugs applied

Drugs were applied by dilution of concentrated stock solutions into the perfusion medium. Stock solutions were made up in water. CGP 55845A was a kind gift from Novartis (Basel, Switzerland); CNQX and 2-OH-saclofen were obtained from RBI (Natick, MA); all other drugs were obtained from Sigma (St. Louis, MO).

2.2.3 Data acquisition and analysis

2.2.3.1 Hardware

All recordings were made using an Axoclamp 2A or 2B (Axon Instruments, Foster City, CA). Recordings were low-pass filtered at 3 kHz. The voltage signals were further amplified (final amplification: 1000X for field recordings, 100X for intracellular and whole-cell recordings), digitized at 1 – 10 kHz and acquired directly to the hard drive of a Pentium-class PC-compatible computer using an AT-MIO-D series data acquisition board and BNC-2080 interface (National Instruments, Austin, TX).

2.2.3.2 Software

Data were acquired using a software suite, Neurosense, originally written in LabVIEW (National Instruments) by former Caltech undergraduate Chou Hung, subsequently modified by Caltech undergraduate Brian Taba (to allow acquisition of data

during patterned stimulation) and by me (to allow acquisition of longer epochs of data, as well as to allow "on-the-fly" specification of stimulus patterns to be applied). Preliminary analysis of data was also performed in Neurosense. Further analyses were done in Origin (Microcal Software, Inc., Northampton, MA) and Excel (Microsoft Corp., Redmond, WA).

2.2.3.3 Analysis

Measurements of field and intracellular responses were performed on traces created by averaging 3-10 responses. EPSP and IPSP amplitudes were measured relative to the baseline membrane potential immediately prior to the stimulus artifact. Initial slopes of field or intracellular EPSPs were determined by fitting a straight line to approximately the first half of the rising phase of the EPSP (after the fiber volley, if present, in the case of field potentials).

All numerical values are presented as mean ± standard error (SE); error bars in figures are SE.

The statistical significance of comparisons between means was assessed using Student's t-test. The paired t-test was used if comparisons were made within a slice or a cell; unpaired t-tests were used otherwise.

2.2.3.3.1 Paired-pulse plasticity

For measurements of short-term plasticity of field potentials during paired-pulse stimulation, the ratio of the size of the response of the second stimulus to the size of the response of the first stimulus was calculated; this ratio represented the level of PPF if greater than 1, or the level of PPD if less than 1. For field recordings, the best measure of

response size is the initial slope of the field EPSP, since, unlike the amplitude, it is unaffected by changes in inhibition or by the onset of a population spike. The slope is also a better measure when the second stimulus occurs before the response to the first stimulus has returned to the original baseline. However, in some cases (e.g., when the field EPSP was very small), the amplitude was used, as indicated.

When paired-pulse plasticity is measured intracellularly, under current clamp recording conditions, the analysis of response amplitudes is complicated by the fact that the second stimulus may come before the cell has recovered back to resting potential after the first stimulus. When this is the case, the data must be analyzed in a way that accounts for this. In order to most clearly describe the difference between the first and second responses, the data were analyzed in the following way. For fast responses (EPSPs and $GABA_A$-mediated IPSPs) the peak amplitude of the second response was not measured from the original baseline; rather, the membrane potential at the onset of the second response was used as the baseline for that response. The ratio of the amplitudes of the second to the first response was used as a measure of paired-pulse plasticity. For EPSPs, initial slope of the synaptic response was also used as an alternative measure of response size. For the slow, $GABA_B$-mediated IPSP, where the second stimulus generally came prior even to the peak of the first response, the peak amplitude following the second stimulus, relative to the original baseline, was compared to the $GABA_B$ component of the response to a single stimulus.

2.2.3.3.2 Frequency-dependent synaptic transmission

For analysis of frequency-dependent synaptic transmission, the times and amplitudes of the peaks of each EPSP were recorded, with the time to peak measured relative to each stimulus artifact, and the peak amplitude measured relative to the baseline membrane potential prior to the first stimulus in the train. To compare responses between cells, peak amplitudes were calculated relative to the amplitude of the response to the first stimulus. The difference in amplitudes, rather than the ratio, was used because it is the approach to action potential threshold that is of significance to neuronal signaling. In general, three responses to any particular pattern of stimulation were averaged together and this average response was measured. Responses in which the neuron fired one or more action potentials were left out of this averaging, because the average of a graded response, such as a subthreshold EPSP, and an all-or-nothing response, such as an action potential, does not give a meaningful result. Also, responses evoked subsequent to an action potential will be affected by the activation of voltage-dependent phenomena by the action potential.

EPSP peaks could always be resolved at stimulation frequencies $\leq$ 15 Hz. At higher frequencies, peaks could not always be resolved. Such responses were not included in the analysis of frequency-dependent synaptic transmission.

2.2.4 Staining procedures

For morphological reconstructions of pyramidal cells, the intracellular electrode solution contained ~4% biocytin. For morphological reconstructions of interneurons and SR giant cells, the whole-cell recording solution included ~0.4% biocytin. In order to

prevent non-specific staining of damaged neurons at the slice surface, the tip of the whole-cell electrode was filled with biocytin-free solution, and the electrode was then back-filled with biocytin-containing solution.

After completion of the electrophysiology experiments, slices were fixed in 4% paraformaldehyde in phosphate-buffered saline (PBS) at 4 °C for at least 3 days. Thin (70 μm) sections were cut on a vibratome (Series 3000, Technical Products International, St. Louis, MO) and rinsed in PBS. The sections were incubated in an endogenous peroxidase blocker (10% MeOH, 3.5% H_2O_2 in PBS) for 1.5 hours and rinsed again in PBS. Next, sections were incubated in 2% BSA and 0.25% Triton X-100 in PBS for 45 minutes, followed by a wash in 2% BSA in PBS. Slices were then incubated in an avidin-HRP solution (ABC solution, Vectastain Kit PK-6100, Vector Labs, Burlingame, CA) for 2 hours. After rinsing in PBS, slices were incubated in a solution of diaminobenzidine (DAB) (10 mg/20 mL PBS) with cobalt chloride (.03%) and nickel ammonium sulfate (.02%) for 30 minutes; 0.0004% H_2O_2 was then added and slices were incubated until the stained neurons appeared (2-30 min). Slices were once again rinsed in PBS, mounted onto subbed slides, dehydrated in increasing alcohols, cleared in xylene, and coverslipped with Permount.

Filled neurons were observed using 20-63X objectives on a Zeiss Axioplan upright microscope equipped with a drawing tube, which was used to reconstruct the approximate neuronal morphology. Reconstructions are strictly qualitative and no attempt was made to measure process length or correct for tissue shrinkage.

2.3 Results

2.3.1 Field responses

2.3.1.1 Baseline field responses

In order to study the contribution of the TA pathway to hippocampal network interactions, it is necessary to establish a system in which it is possible to stimulate TA axons in isolation and record a response uncontaminated by other pathways. Since SC and TA axons are restricted to SR and SLM, respectively (Amaral and Witter 1989), stimulation in SR or SLM should activate only SC or TA axons, respectively. This can be confirmed by recording field responses to both SC and TA stimulation in both SR and SLM. If the pathways are being activated independently, stimulation of SC should result in a current sink (and hence a negative-going field EPSP) in SR with an accompanying current source (positive-going field EPSP) in SLM; conversely, TA stimulation should result in a negative-going field EPSP in SLM along with a positive-going field EPSP in SR (Colbert and Levy 1992; Empson and Heinemann 1995b) (Figure 3). These criteria were always used to assess proper electrode placement in the experiments described in this thesis. To further ensure isolation of the TA pathway, a cut was made through SR, near the subiculum, perpendicular to the cell body layer (Maccaferri and McBain 1995) to minimize the chance of antidromic activation of SC axons by the stimulating electrode in SLM.

Stimulation in SLM will activate the perforant path projection to dentate gyrus as well as the TA projection to CA1. The projection to dentate gyrus results in a much

larger current sink, and hence field potential, than the TA projection (Leung *et al.* 1995). Recordings of the TA response in SLM could therefore easily be contaminated by volume conduction of the potential evoked in dentate gyrus by the activation of the perforant path. Therefore, the dentate gyrus was removed from the slice in all experiments (Colbert and Levy 1992; Empson and Heinemann 1995b) (Figure 3).

Clean TA responses were generally harder to obtain and required higher stimulation strengths than SC responses, an observation consistent with published findings (Colbert and Levy 1992; Otmakhova and Lisman 1999). I experimented with various methods of slice preparation to optimize TA responses. One way of preparing hippocampal slices is to dissect the hippocampus out from under the overlying cortex, stretch it out on a flat surface, and cut slices using a manual tissue chopper. TA responses can be recorded in such a slice (Colbert and Levy 1992). However, other published reports suggested that the TA pathway may be better preserved using a different cutting angle, resulting in slices that include a portion of EC as well as hippocampus proper (Dreier and Heinemann 1991; Empson and Heinemann 1995b); such slices can only be prepared on a vibratome. I found that such slices cut on a vibratome had more robust responses both in the TA and the SC pathways than did slices prepared on the chopper. I also compared the anatomy and physiology of slices cut at various levels of the brain, from the more ventral regions near the temporal lobe, to the more dorsal regions near the septum. I found that SLM was wider, and TA responses more robust, in slices obtained from the temporal end of the hippocampus.

There exist reports in the literature of population spikes evoked in slice by activation of the TA pathway (Doller and Weight 1982; Doller and Weight 1985; Scharfman

et al. 1998). Although I often made field recordings in SR, where population spikes in SC responses can be readily recorded, I never observed a population spike in SR or SLM in response to TA stimulation. I performed a few experiments in which I recorded field responses in SP, where a population spike can most readily be recorded. Only by using a stimulation strength much larger than usual (500 μA instead of 100 – 200 μA) could I obtain the smallest trace of a population spike in response to TA stimulation (Figure 4).

In some field recordings, the negative-going, excitatory phase of the response was followed by a positive-going phase. This positive-going field potential may have reflected the outward currents evoked by monosynaptic, feed-forward and feedback inhibition and may have thus been a field IPSP (Lambert *et al.* 1991; Arai *et al.* 1994); however, this was never tested pharmacologically.

2.3.1.2 Responses to paired-pulse stimulation

Paired-pulse stimulation is used as a probe of short-term plasticity processes at the synapse (see sections 1.1.2, p. 7, and 1.1.4.1, p. 23). Short-term plasticity phenomena may be significant in controlling how the gain of a synapse varies with input frequency (section 1.1.5.1, p. 31) and allowing the postsynaptic neuron to differentiate between isolated and grouped or "bursty" presynaptic inputs (Lisman 1997). Paired-pulse plasticity has been well characterized in the SC pathway (e.g., Davies and Collingridge 1996) but has not been studied in the TA pathway. I examined the responses to paired-pulse stimulation of both the TA and the SC pathways at interstimulus intervals (ISIs) of 25, 50, 100, 200, 400 and 800 ms (Figure 5). In both pathways, facilitation of the initial

slope of the field EPSP was observed at ISIs ≤ 200 ms. Maximal facilitation was observed at an ISI of 100 ms (SC paired-pulse ratio, 1.23 ± 0.05, n = 15; TA paired-pulse ratio, 1.60 ± 0.07, n = 35). The facilitation of the TA response at 100 ms ISI was significantly greater than that of the SC response ($p < 0.01$).

At longer ISIs, the TA response remained facilitated, while the SC response showed paired-pulse depression. At 800 ms ISI, the longest interval tested, the paired-pulse ratio for the SC response was 0.90 ± 0.01 (significantly different from 1, $p < 0.01$, n = 14) and the paired-pulse ratio for the TA response was 1.12 ± 0.03 (significantly different from 1, $p < 0.01$, n = 24); the difference between the TA and SC paired-pulse responses was highly significant ($p < 0.0001$). I noticed a negative correlation between the size of the initial field response and the magnitude of the observed facilitation, as has been previously noted for SC responses in pyramidal cells (Manabe *et al.* 1993). Since one factor affecting whether paired-pulse responses will undergo facilitation or depression is the probability of vesicle release (Manabe *et al.* 1993; Debanne *et al.* 1996), and small initial responses may reflect low vesicle release probability, I wondered whether the difference in initial response sizes could explain the differences observed between the SC and the TA paired-pulse responses. In general, baseline SC responses were significantly larger than baseline TA responses (SC mean initial slope, -0.12 ± .02 mV/ms, n = 15; TA mean initial slope, -0.058 ± 0.006 mV/ms, n = 35, $p < 0.001$).

To test this hypothesis directly, I performed a series of experiments in which I varied the stimulation strength (and hence the size of the initial response) while taking paired-pulse measurements at ISIs of 50 and 800 ms. At very low stimulus strengths, the small size of the field response, along with the low sampling rate, made accurate deter-

mination of initial slope difficult. Therefore, I made comparisons of amplitudes as well as slopes, since at low stimulus strengths the amplitudes are not likely to be greatly affected by inhibition or by population spikes. As predicted, a negative correlation was observed between initial response size and paired-pulse plasticity, with paired-pulse facilitation decreasing with increasing response size (Figure 6). This dependence was much more pronounced at 50 ms ISI than at 800 ms ISI.

Paired-pulse response ratios in the SC and TA pathways at 50 ms ISI were very similar (Figure 6). To see whether the difference in SC and TA paired-pulse plasticity at 800 ms ISI was due only to initial size of the first response, I compared TA and SC responses of similar sizes in the same slices. At low slope values (SC mean initial slope, -0.034 ± 0.005 mV/ms, $n = 9$; TA mean initial slope, -0.037 ± 0.006 mV/ms, $n = 9$), there was no significant difference between the paired-pulse ratios (SC paired-pulse slope ratio $= 1.01 \pm 0.05$, $n = 9$; TA paired-pulse slope ratio $= 0.92 \pm 0.06$, $n = 9$). However, when paired-pulse responses were compared by measuring amplitudes at low stimulus strengths (SC mean amplitude, -0.18 ± 0.03 mV, TA mean amplitude, -0.19 ± 0.02 mV, $n = 9$), a significant difference was observed: the TA response showed slight, but not statistically significant, facilitation (paired-pulse amplitude ratio, 1.12 ± 0.03, $n = 9$, NS different from no effect) while the SC response showed slight depression (paired-pulse amplitude ratio, 0.91 ± 0.01, $n = 9$, significantly different from no effect ($p < 0.01$)) (difference between SC and TA paired-pulse ratios significant, $p < 0.05$).

In some field responses, a positive-going component could be observed following the field EPSP; this was likely a field IPSP. The amplitude of the field IPSP was also measured during the paired-pulse stimulation paradigm, and a paired-pulse plasticity ratio

calculated. In both the SC and TA responses, the field IPSP showed facilitation at ISIs of 10 – 100 ms, and depression at ISIs of 400 – 800 ms (Figure 5). At 200 ms ISI, the TA IPSP was facilitated, while the SC IPSP was unchanged. Where both responses were facilitated, the TA response showed greater facilitation than the SC response; conversely, where both responses were depressed, the TA response showed less depression than the SC response.

2.3.2 Pyramidal cells – intracellular recordings

2.3.2.1 Electrophysiological properties and morphology

Recordings were made from 71 different pyramidal cells, using KAc-filled electrodes. The mean resting potential of the neurons was -63.7 ± 0.7 mV (n = 71) and the mean input resistance was 103 ± 6 MΩ (n = 61). Trains of action potentials evoked by depolarizing current injection showed considerable spike frequency accommodation and small afterhyperpolarizations (AHPs) following each action potential (Figure 7A).

Some early intracellular recordings were made with CsAc in the electrode rather than KAc. These neurons had a mean resting potential of -68.4 ± 1.4 mV (significantly lower than KAc recordings, $p < 0.01$, n = 33) and a mean input resistance of 154 ± 12 MΩ (significantly higher than KAc recordings, $p < 0.0001$, n = 31). The higher input resistance may be due to the blockade of K^+ channels by Cs^+ (Hille 1992, p. 131), while the more negative resting potential remains unexplained.

A few pyramidal cells were filled with biocytin and reconstructed. Their morphology was typically pyramidal (Ramón y Cajal 1911; Ishizuka *et al.* 1995), with a

vertically-oriented soma, apical dendrites densely arborizing in SR and SLM, basal dendrites arborizing in SO, spines visible on dendrites, and axon running in SO and alveus (Figure 7B).

2.3.2.2 Responses to SC and TA stimulation

Stimulation strengths were set so as to evoke a subthreshold, submaximal EPSP at the cell body. SC stimulation by means of a stimulating electrode in SR, near CA3, almost always (69/71 neurons) evoked an EPSP; in many cases (51/71 neurons), a subsequent slow IPSP was also recorded (Table 1) (Figure 8A). In a smaller number of neurons (38/71), a fast IPSP was also seen; in 25 cases, both a fast and a slow IPSP could be distinguished. Responses to TA stimulation, with the stimulating electrode in the subicular end of SLM, were similar but smaller and slower (Table 1) (Figure 8A). The smaller amplitude and longer time to peak of the TA compared to the SC EPSPs is consistent with the more distal location of TA synapses on the pyramidal cell dendrites; dendritic filtering may have this effect on synaptic potentials (Rall 1967). Very occasionally, stimulation of either pathway would result in no visible EPSP.

Responses recorded with CsAc electrodes were very similar to responses recorded from KAc electrodes (Table 1). SC responses included a fast EPSP (30/31 neurons; time to peak significantly slower than KAc recordings, $p < 0.0001$; $n = 30$) followed by a slow IPSP, with a fast IPSP (time to peak, 44 ± 9 ms; peak amplitude, -4.8 ± 0.4 ms; $n = 2$) occasionally distinguishable. TA responses also consisted of a fast EPSP (time to peak, 43.1 ± 3.1 ms; peak amplitude, 2.6 ± 0.2 mV; time to peak significantly slower than KAc recordings, $p < 0.0001$, $n = 31$) followed by a slow IPSP (time to peak, 298 ± 17 ms; peak

amplitude, -1.0 ± 0.2 ms; n = 14). It is unclear why the time course of EPSPs in CsAc recordings would be slower than in KAc recordings; possibly, the EPSP is normally truncated by activation of voltage-dependent or $GABA_B$-activated K^+ channels. Although Cs^+ should block $GABA_B$-activated K^+ channels, a slow IPSP was still observed in most CsAc recordings; it is possible that Cs^+ was not diffusing out into the dendrites where these channels may be located. It is hard to make a meaningful comparison of IPSP amplitudes because of the varying stimulation strength and possible variation in inhibitory innervation between slices.

Monosynaptic IPSPs were evoked by proximal stimulation of either pathway in the presence of the AMPA receptor antagonist CNQX (10 μM) and the NMDA receptor antagonist AP5 (50 μM). Stimulation of either input evoked clearly biphasic IPSPs (Table 2) (Figure 8B). The pharmacology of IPSPs was determined by the addition of GABA antagonists to the bath. When the $GABA_A$ antagonist bicuculline (20 μM) was added to the bath in the absence of glutamate antagonists, the time to peak and amplitude of both the early EPSP and the late IPSP in the response to TA stimulation were increased (Figure 8C). Depending on the position of the stimulating electrode, TA IPSPs could be purely disynaptic, disappearing when the glutamate antagonists CNQX (10 μM) and AP5 (50 μM) were added to the bath, or partially monosynaptic, persisting even in the presence of CNQX and AP5. Once the stimulating electrodes were positioned to elicit a monosynaptic IPSP, the early component could be blocked by the addition of 20 μM bicuculline (Figure 8D). Addition of the $GABA_B$ antagonist 2-OH saclofen (100 μM) caused a partial block of the late component of the IPSP (Figure 8D), and a full

block could be obtained with the more potent $GABA_B$ antagonist CGP 55845A (data not shown, but see section 4.4.1, p. 211).

I attempted to determine the reversal potentials of the monosynaptic IPSP components by changing the membrane potential of the cell with current injection. However, because of the poor space clamp of the cell, the membrane potential recorded at the soma is unlikely to be an accurate reflection of that at the dendrites where synapses are located. The late component of the monosynaptic IPSP was particularly difficult to reverse. In general, the reversal potential of the early ($GABA_A$) component was about 15 mV less negative than that of the late ($GABA_B$) component. Reversal potentials for IPSPs evoked in SR were less negative than those for IPSPs evoked in SLM (Figure 9); this likely reflects the effects of space clamp, as the synapses activated by SLM stimulation are likely to be farther from the soma than those activated by stimulation in SR.

In order to be able to study the TA and SC EPSPs in isolation, especially for measurements of paired-pulse plasticity, I tried to pharmacologically isolate the EPSPs by recording in the presence of 20 μM bicuculline and 100 μM 2-OH-saclofen. However, in the absence of all inhibition, pyramidal cells were very prone to spontaneous spiking or spiking in response to any level of TA or SC stimulation.

It should be noted that all responses were very variable, not just between cells, but from sweep to sweep in a single cell. The standard errors given reflect an average across experiments, but do not represent the intra-experimental variation.

2.3.2.3 Responses to paired-pulse stimulation

Responses of individual pyramidal cells to paired-pulse stimulation of the TA and SC pathways showed a great deal of variability, both from cell to cell as well as within trials on a single cell. Further variability was caused by the fact that some paired-pulse responses were recorded with KAc electrodes, whereas others were done with CsAc electrodes.

Paired-pulse plasticity of the EPSP component of the TA and SC responses in normal ACSF was tested at ISIs of 10, 25, 50, 100, 200, 400, 600 and 800 ms. Although differences were observed between recordings made with KAc or CsAc electrodes, they did not occur in a consistent pattern (with one exception: SC EPSP slope facilitation was robust in CsAc recordings, but not present in KAc recordings) and so the data were pooled. The paired-pulse plasticity patterns of TA and SC EPSPs were remarkably similar (Figure 10). Facilitation can be seen most clearly in the EPSP slope measurement, with both TA and SC responses showing facilitation of the initial EPSP slope at ISIs up to 200 ms, with no facilitation or depression observed at longer ISIs. The apparent dip in facilitation observed at ISIs of 25 and 50 ms in the EPSP amplitude ratio measurement can be accounted for by the measurement method. The amplitude of the second EPSP was measured from its onset, which at these ISIs would have been near the peak of the first EPSP. A ratio of ~1 at 25 ms ISI shows that summation of EPSPs was approximately linear.

Paired-pulse plasticity of the slow, $GABA_B$-mediated IPSP was measured at ISIs of 10, 25, 50, 100, 200, 400 and 600 ms, also in the absence of pharmacological agents, in the same responses used for measuring paired-pulse plasticity of EPSPs. Again, SC

and TA responses were very similar. In both responses, approximately linear summation of the IPSP was observed at ISIs ≤ 100 ms. At 400 ms ISI, the first and second IPSPs were approximately equal in amplitude, and at 600 ms ISI, some depression was seen in the TA, but not the SC, response.

IPSPs evoked monosynaptically, by proximal stimulation in the presence of glutamate antagonists, were used to assess paired-pulse plasticity in the fast, $GABA_A$-mediated IPSP. At short ISIs (10 and 25 ms), an almost linear summation of IPSPs was observed. At longer ISIs, depression was observed, with the IPSP sometimes becoming depolarizing, especially in the SC response, resulting in a negative paired-pulse ratio (Figure 10). $GABA_A$ responses are known to undergo paired-pulse depression by means of presynaptic $GABA_B$ autoreceptors (e.g., Davies *et al.* 1990), but the reversal of polarity of IPSPs observed here suggests that changes in driving force played an important role as well.

No results were obtained for paired-pulse plasticity of isolated EPSPs, in the presence of GABA blockers, because virtually any paired stimulation resulted in an action potential.

2.3.2.4 Responses to trains of SC and TA inputs

As discussed in section 1.1.5.1 (p. 31), a frequency dependence of synaptic transmission is observed in many neural pathways. Understanding how neurons respond to inputs at various frequencies is key to understanding what patterns of physiological activity will contribute to information flow in a particular neural pathway. Trains of

stimuli at various frequencies can be used to probe the frequency dependence of synaptic transmission.

As noted for paired-pulse stimulation, there was a great deal of variability of responses from trial to trial both within and between individual neurons, but some consistent patterns were observed.

2.3.2.4.1 EPSPs

Intracellular responses of 17 pyramidal cells to trains of TA and SC stimuli in the following patterns were recorded: 4 stimuli at 5 Hz, 9 stimuli at 10 Hz, and 10 stimuli at 15, 25, 50 and 100 Hz. All experiments were performed in normal ACSF, with inhibitory and excitatory transmission intact, to observe the interplay between the excitatory and inhibitory, as well as facilitating and depressing, components of the response (Buonomano and Merzenich 1998). In none of the cells in which frequency-dependent responses were systematically studied did TA stimulation evoke an action potential, although such cells were occasionally observed at other times. Responses to SC stimulation, however, were often sufficiently large to evoke action potentials. Note that responses in which the cell fired an action potential were not included in this analysis, which may suggest that facilitating responses were overlooked. However, in a slice with inhibition intact, the firing of CA1 pyramidal cells will recruit feedback inhibition which will affect responses to subsequent stimuli. Furthermore, I observed that in responses with spikes, the probability of spike firing did not seem to increase over the course of the burst; on the contrary, neurons that did spike in response to SC stimulation tended to do so early in the stimulus train (data not shown).

In general, in both TA and SC responses, a reduction in peak EPSP amplitude was observed over the course of a stimulus train (Figures 11, 12). At stimulation frequencies of 10, 15, and 25 Hz, facilitation (summation) was sometimes observed between the second and first responses, but third and subsequent responses were almost always smaller than the second. This appears to be primarily due to the long $GABA_B$-mediated IPSP on which the EPSPs were riding. TA EPSPs, which were particularly small compared to TA-evoked IPSPs, often reached a maximum amplitude below the original resting potential of the cell when arriving during the IPSP (Figure 12).

In one experiment, the response of a pyramidal cell to trains of SC and TA stimulation in the presence of the $GABA_B$ antagonist CGP 55845A was recorded (data not shown). Under these conditions, the SC response showed facilitation at frequencies of 5-15 Hz, often firing action potentials, but at higher frequencies (25-100 Hz), depression of SC EPSPs occurred. TA responses were depressed at all stimulation frequencies, but the responses stayed close to the original membrane potential rather than riding on a large, hyperpolarizing IPSP.

The times to peak of the TA EPSPs were quite variable from response to response, and often difficult to measure because of the low, broad EPSP. At a stimulation frequency of 5 Hz, the time to peak of TA responses in most cases showed a clear increase, but at higher stimulation frequencies, no clear pattern was apparent (Figure 12). In contrast, the time to peak of SC responses showed a clear increase at all stimulation frequencies (Figure 11). This change in time to peak likely reflects the onset of $GABA_B$ autoreceptor-mediated inhibition of the fast, $GABA_A$-mediated IPSP (Buonomano and Merzenich 1998), which normally limits the time course of the EPSP (Turner 1990).

2.3.2.4.2 IPSPs

In the paired-pulse stimulation experiments, the slow IPSP component of both the SC and the TA response was sometimes greatly increased by application of a second stimulus. This slow IPSP component was further increased by longer, higher-frequency stimulation.

Peak IPSP amplitude was measured in 16 pyramidal cells for responses to trains of ten SC or TA stimuli (bursts) at frequencies of 15, 25, 50, and 100 Hz. Responses in which the cell fired in response to burst stimulation were left out of the analysis, because a spike AHP may have contributed to the hyperpolarizing component of the response. Burst stimulation resulted in a substantial amplification of the inhibitory component of the response, especially in the TA pathway; the SC-evoked IPSP showed less amplification, likely because of its higher initial amplitude. The SC IPSP reached a maximum of 1.7X the baseline value when evoked with 50 Hz stimulation (n = 9), whereas the TA IPSP could be increased to about 4X its initial value with 50 or 100 Hz stimulation (n = 15, 13) (Figure 13). However, the SC IPSP was larger than the TA IPSP; for example, after a 100 Hz burst, the SC IPSP had an amplitude of -7.4 ± 0.5 mV (n = 9), whereas the TA IPSP had an amplitude of -3.6 ± 0.5 mV (n = 14). The burst-evoked IPSP was mediated by $GABA_B$ receptors (see Chapter 4).

IPSPs evoked in pyramidal cells by TA burst stimulation underwent a further form of short-term plasticity when TA bursts were themselves repeated. When bursts of TA stimulation were repeated at short intervals, the evoked IPSPs decreased in amplitude. This phenomenon was characterized with burst stimulation

(10 stimuli at 100 Hz) of the TA pathway repeated at intervals of 1, 5, 10, 15, 20, 30, 60 or 120 seconds. At intervals of 30 seconds or less, a definite decrease in IPSP amplitude was observed; this decay was well fit by a single exponential (Figure 14). The time constant of this decay ranged from 3.6 ± 0.3 s (n = 8) at an ISI of 1 s, to 192 ± 104 s (n = 3) at an ISI of 30 s. At all ISIs, the time constant of decay was equal to 4-7X the ISI, meaning that the response would decrease to 37% of its original size after 4-7 repetitions of the burst stimulus. At an ISI of 60 s, a small decay was sometimes observed (n = 3); no change in the size of the IPSP was observed when TA bursts were repeated at 120 s intervals (n = 3). Recovery from IPSP decay was not systematically tested for ISIs > 1 s, but took about 5 minutes. For 1 s ISIs, the IPSP recovered to 60 ± 6% of the original response size 1 min after a train of 10 bursts (n = 3), and to 85 ± 5% of the original response size 2 min after a train of 10 bursts (n = 5). This IPSP decay may have been due to decreasing recruitment of interneurons (e.g., see Congar *et al.* 1995), activity-dependent inhibition of GABA release via $GABA_B$ autoreceptors (e.g., see Davies *et al.* 1990), synaptic vesicle depletion (e.g., see Liu and Tsien 1995; Stevens and Tsujimoto 1995; Galarreta and Hestrin 1998), or some combination of these factors.

2.3.3 SR/SLM interneurons – whole-cell recordings

2.3.3.1 Electrophysiological properties and morphology

Whole-cell recordings were made from 41 different interneurons, of which 27 were successfully filled with biocytin and reconstructed, although the axon was some-

times lost. Eight interneurons were in SLM proper, 14 were at the SR/SLM border, and 19 were in distal SR, as determined by direct observation when selecting cells for recording. (Under our observation conditions, SLM is distinctly darker than SR.) Interneurons had a mean resting potential of -68.6 ± 1.5 mV (n = 39) and fired action potentials 72.9 ± 2.2 mV (n = 27) in amplitude. Their mean input resistance was 562 ± 35 MΩ (n = 29). A variety of spiking patterns was seen in response to a 500 ms depolarizing current injection pulse: a few spikes followed by a plateau (4/41) (Figure 15A), a longer train followed by a plateau (9/41) (Figure 15B), irregular spiking (12/41) (Figure 15C), or fast spiking (14/41) (Figure 15D). Twenty-one out of 41 interneurons showed an undershoot after a step depolarization, 17 showed a sag during hyperpolarization, and 40 had a prominent spike AHP.

Some cells that were at first presumed to be interneurons, based on the location of their cell bodies well outside of SP, turned out to have intrinsic membrane properties and morphologies similar to pyramidal cells. These neurons appear to correspond to the recently described stratum radiatum giant cells (Gulyás *et al.* 1998b) and are analyzed separately below; they are not included in the above numbers.

Interneurons were generally quiet at rest, with few spontaneous action potentials. In three interneurons, depolarizing and hyperpolarizing current injections were used along with recordings of long (5 s) periods of background activity, in the absence of stimulation, to look for voltage-dependent oscillations in membrane potential. As previously reported (Williams *et al.* 1994), at hyperpolarized membrane potentials, depolarizing spontaneous postsynaptic potentials (PSPs), likely polarity-reversed IPSPs, were observed. At depolarized potentials, membrane potential oscillations and/or

spontaneous action potential firing were observed in two out of three cells, similar to previous reports (Williams *et al.* 1994; Chapman and Lacaille 1999) (Figure 16). The recording conditions and variability of the oscillations did not permit a rigorous analysis, but the approximate oscillation frequency of 1-3 Hz was similar to previously reported recordings at room temperature (Chapman and Lacaille 1999).

The morphology of recovered interneurons was highly variable and difficult to classify because of the varying degrees of success in reconstruction. In particular, axonal arborizations were not reconstructed sufficiently well to categorize the neurons into previously-described families (Vida *et al.* 1998). Cell bodies were round, fusiform, oblong, triangular, or irregular. Both dendrites and axons were usually very varicose or beaded; dendrites were much finer than those of giant cells or pyramidal cells. All recovered interneurons had processes in SR, and most (22/27) had processes in SLM; 12/27 had processes extending to SP and 8/27 had processes entering SO. One interneuron was observed to have a process crossing the hippocampal fissure, like some previously-described SLM interneurons with processes leaving CA1 and entering the dentate gyrus (Lacaille and Schwartzkroin 1988a; Vida *et al.* 1998). It is likely that such processes would have been lost in some neurons because of the removal of the dentate gyrus during slice preparation. When the axon could be clearly identified, it most commonly ramified profusely throughout a broad extent of SR. The most common dendritic arborizations were either a horizontal distribution, with dendrites running along the SR/SLM border (e.g., Figure 15E), or a stellate arrangement, with long, straight dendrites extending in various directions, often as far as SP or SO (e.g., Figure 15F). The total extent of recovered processes was generally at least 500 μm along the long axis of the slice.

2.3.3.2 Responses to SC and TA stimulation

Based on their morphology, SR/SLM interneurons are likely to be innervated by both TA and SC axons, and so their responses to TA and SC inputs were recorded. Of particular interest was their responsiveness to TA input, since I was interested in identifying interneurons mediating the inhibitory component of the TA pathway. The responses of interneurons to synaptic input were quite heterogeneous. Responses averaged over all groups are presented in Table 1. Interneurons were categorized into three groups based on their responses to TA stimulation: unresponsive, inhibited, and excited.

Unresponsive: In 14 out of 41 interneurons, the response to TA stimulation was either so small as to be undistinguishable from background, or consisted solely of an action potential driven directly by the stimulating electrode, rather than by synaptic input. Nine of these interneurons responded to SC stimulation with an EPSP (time to peak, 19.2 ± 2.3 ms; peak amplitude, 4.4 ± 0.5 mV). It is unclear why some SR/SLM interneurons, whose dendrites in many cases arborized in SLM, were completely unresponsive to TA stimulation. It is possible that slices were not always cut at an optimal angle for preserving TA axons; also, in some cases, the cut made through SR to prevent antidromic SC activation may have also cut some axons in SLM.

Inhibited: Three interneurons responded solely with an IPSP to TA stimulation. However, this may have been due to the fact that these recordings were made with the stimulating electrode further away from the recording site than usual. As discussed in the context of field responses to TA stimulation (section 2.4.1, p. 108), more distal stimulation may selectively lead to a loss of excitatory transmission.

Excited: The remaining 24 interneurons showed a distinct EPSP in response to TA stimulation. These interneurons had fairly similar TA and SC responses. These interneurons responded to SC stimulation with a fast EPSP (time to peak, 20.7 ± 1.3 ms; peak amplitude, 7.0 ± 0.8 mV, n = 21) rarely followed by a small IPSP (time to peak, 350 ± 150 ms; peak amplitude, -1.0 ± 0.1 mV; n = 3); the TA response included a fast EPSP (time to peak, 19.5 ± 1.6 ms; peak amplitude, 5.2 ± 0.6 mV; n = 24) also rarely followed by a small IPSP (time to peak, 531 ± 44 ms; peak amplitude, -0.6 ± 0.1 mV; n = 4) (Figure 17A). Since these interneurons were located near the border of SR and SLM, the SC and TA afferents innervating these layers likely make synapses with similar distributions of distance from the cell body. Therefore, both sets of inputs would be subject to similar amounts of dendritic filtering, which could account for their similar amplitudes and times to peak.

The variation with membrane potential of the synaptic responses of interneurons was not studied systematically, but certain observations were made. In seven otherwise unresponsive or excited interneurons, depolarization revealed an IPSP in synaptic response that was not apparent at the neuron's resting potential (Figure 17B). In four interneurons, a slower depolarizing component was observed following the fast EPSP (Figure 17C). In some cases, this may have represented an NMDAR and/or voltage-dependent channel mediated depolarization; in other cases, when this phenomenon was observed at lower resting potentials, this may have been a polarity-reversed slow IPSP (Williams *et al.* 1994). The cause of a very slow, long-lasting (seconds) depolarization developing after the end of high-frequency SC stimulation (Figure 17D) remains unknown, though it

bore certain resemblances to a Ca^{2+}-dependent, mGluR-activated slow, non-specific cationic current previously reported in hippocampal neurons (Congar *et al.* 1997).

In at least three interneurons, responses to TA and/or SC stimulation appeared to include multiple EPSPs at discrete latencies (Figure 18). The origins of these multiple EPSPs are unclear, but the delays between responses suggest activation of some kind of polysynaptic pathway. In one such case, the regular ACSF was replaced with a high-divalent solution (5 mM Mg^{2+} and 5 mM Ca^{2+}, instead of the regular 1.3 mM Mg^{2+} and 2.4 mM Ca^{2+}) in order to selectively reduce polysynaptic activity (Berry and Pentreath 1976). During application of the high-divalent solution, the number of putative poly-synaptic events was greatly reduced (Figure 18).

2.3.3.3 Responses to trains of SC and TA inputs

The responsiveness of interneurons to different input frequencies will contribute to the overall frequency dependence of synaptic transmission in neural pathways that include a feed-forward inhibitory component. To characterize frequency-dependent responses in interneurons, the same trains of stimuli that were applied to pyramidal cells (4 stimuli at 5 Hz, 9 stimuli at 10 Hz, and 10 stimuli at 15, 25, 50 and 100 Hz) were applied to 11 interneurons. The most striking difference between the responses of interneurons and of pyramidal cells was the much smaller inhibitory component in the interneuron response: an IPSP in response to TA burst stimulation was seen in only 1/11 interneurons, and small IPSPs in response to SC burst stimulation (-1.4 ± 0.4 mV after a stimulus train of 10 stimuli at 50 Hz) were seen in 5/11 interneurons. Although it is possible

that IPSPs were not observed because of insufficient activation of inhibitory inputs, this seems unlikely, because stimulus strengths were not systematically different from those that evoked IPSPs in pyramidal cells or SR giant cells. It is also possible that IPSPs, particularly those mediated by $GABA_A$ receptors, were not as readily apparent because of the more negative resting potential of interneurons, compared to pyramidal cells.

SC EPSPs in interneurons were generally depressed with repeated stimulation, regardless of initial amplitude or stimulation frequency (Figure 19). Repeated TA EPSPs could show either facilitation or depression, with facilitation prevalent at lower stimulation frequencies (5 or 10 Hz) while depression dominated at higher frequencies (15 or 25 Hz) (Figure 20). The initial response size did not appear to be significant in determining whether a response would facilitate or depress. The apparent lack of facilitation at higher frequencies may have been due to the removal from the analysis of cells which always fired action potentials in response to repeated TA stimulation (see below and Figure 21).

In contrast to pyramidal cell responses, SC EPSPs in interneurons showed no consistent patterns in times to peak with repeated stimulation. If anything, a net decrease in time to peak was observed between the first and second EPSPs in a train at stimulation frequencies of 10, 15 or 25 Hz (Figure 19). TA EPSP times to peak showed no consistent pattern (Figure 20).

Interneurons were much more likely than pyramidal cells to be driven to fire action potentials in response to TA input. Of the 11 interneurons whose frequency-

dependent responses were systematically tested, four showed sufficient facilitation to reach action potential threshold (see Figure 21 for two examples).

Since the TA input to CA1 may be important in inducing theta oscillations (Buzsáki *et al.* 1995), I tested the response of five interneurons to theta-patterned stimulation: a burst of five pulses at 100 Hz, repeated nine times at 5 Hz, with the whole series repeated at 15 s intervals. In two interneurons, the action potentials evoked by theta-patterned stimulation appeared to be directly driven by the stimulating electrode, rather than synaptically evoked; this was verified in one interneuron when spikes were still evoked in the presence of the glutamate antagonists CNQX and AP5. In two interneurons, the level of postsynaptic depolarization decreased greatly both from burst to burst as well as over the repeated trains of theta stimulation; in a third interneuron, the theta-patterned input resulted in action potentials whose frequency increased with repeated trains. SLM interneurons therefore appear to be heterogeneous in their responsiveness to theta-patterned input.

2.3.4 Stratum radiatum giant cells – whole-cell recordings

2.3.4.1 Electrophysiological properties and morphology

Several neurons recorded in distal SR and SLM resembled pyramidal cells both in physiology and in morphology, and are likely to correspond to the recently-described SR giant cells (Gulyás *et al.* 1998b). (The abbreviation RGC used in this previous report is unfortunate, because of its well-established use as an abbreviation for retinal ganglion cell; I will use "SR giant cell" to avoid confusion.) These neurons had an average resting

potential of -66.9 ± 2.1 mV (n = 12), input resistance of 116 ± 9 mV (n = 12), and action potentials 85.2 ± 4.1 mV in amplitude (n = 10). These neurons generally showed a moderate amount of spike-frequency accommodation in response to depolarizing current injection, with an undershoot following repolarization, sag current during hyperpolarizing current steps, and no prominent AHP following action potentials (Figure 22C), features reminiscent of pyramidal cells rather than interneurons. The morphology (10 cells) was similar to that previously described (Gulyás *et al.* 1998b); neurons had one or two thick apical dendrites with profuse dendritic arborization in SR and SLM (Figure 22A, B). Six neurons had no "basal" dendrites, similar to the previously-described SR giant cell morphology (Gulyás *et al.* 1998b). Dendritic spines could be observed when cells were viewed at high magnification.

2.3.4.2 Responses to SC and TA stimulation

Responses of SR giant cells to SC stimulation were similar to those of pyramidal cells: a fast EPSP followed by a slow IPSP (Table 1) (Figure 23A). The excitatory component of the response was mediated by glutamate and was eliminated in the presence of the AMPA receptor antagonist CNQX (10 μM) and the NMDA receptor antagonist AP5 (50 μM) (Figure 23B). The TA response had a much larger excitatory component than that seen in pyramidal cells, while the IPSP was quite small (Table 1). Fast IPSPs, however, were evident at depolarized membrane potentials (Figure 23C). EPSPs evoked in SR giant cells by TA or SC stimulation were similar in amplitude and time to peak, consistent with the greater proximity of TA inputs to the soma in SR. Directly-driven

depolarization to action potential threshold, or antidromic driving of spikes, was never observed in SR giant cells.

2.3.4.3 Responses to trains of SC and TA inputs

Frequency dependence of synaptic transmission was also examined in SR giant cells. The same trains of stimuli that were applied to pyramidal cells and interneurons (see section 2.3.2.4, p. 94) were applied to 5 SR giant cells. Like pyramidal cells and unlike interneurons, SR giant cells showed an enhanced IPSP in response to burst stimulation, with 4/5 SR giant cells showing a distinct inhibitory response to TA and/or SC burst stimulation. For example, a train of 10 stimuli at 50 Hz applied to the SC pathway resulted in an IPSP of -4.6 ± 2.3 mV (n = 3); the same pattern applied to the TA pathway resulted in an IPSP of -3.2 ± 1.2 mV (n = 3). The presence of robust IPSPs, compared to those observed in interneurons, suggests that the lack of IPSPs in interneuron recordings was not due simply to washout of some crucial intracellular factor during whole-cell recording; however, it is possible that the different morphology of interneurons and giant cells makes them differentially susceptible to washout. The underlying $GABA_B$ IPSP in SR giant cells did not come to dominate the excitatory responses to trains of TA stimuli, probably because of the greater initial amplitude of these EPSPs. SC EPSPs sometimes increased from the first to the second response, followed by a decrease (Figure 24). TA EPSPs showed consistent increases in amplitude from the first to the second response and often from the second to the third response as well, followed by a slow decrease (Figure 25). The times to peak of TA responses showed no consistent pattern, while the times to peak of SC EPSPs increased over the course of stimulus trains at 5 or 10 Hz (similar to

the responses seen in pyramidal cells) but showed no change at 15 or 25 Hz (Figures 24, 25).

2.4 Discussion

2.4.1 Comparison of TA and SC inputs to CA1

The TA and SC inputs to area CA1 of the hippocampus are similar in many ways. Both comprise a population of glutamatergic axons, the TA axons terminating in SLM, the SC axons in SR. Stimulation of either pathway results in an excitatory postsynaptic response, which can be recorded as a field EPSP in the appropriate dendritic layer, and as an intracellular EPSP in CA1 pyramidal cells. However, at least in slice, the SC input has a greater excitatory effect than the TA input; stimulation of the SC pathway can elicit a population spike in CA1, while even high-frequency TA stimulation rarely brings pyramidal cells to action potential threshold. The ineffectiveness of the TA excitatory input is likely due to the location of the TA synapses on the distal dendrites of CA1 pyramidal cells, far away from the soma and spike initiation zone. This distal dendritic location is reflected in the longer time to peak of TA compared to SC EPSPs. Although the synaptic conductances, and hence local EPSPs, are likely to follow a similar time course, electrotonic filtering of the distal TA input through the dendritic membrane will result in a slower response (Rall 1967). In CA3 pyramidal cells, voltage-dependent conductances "boost" the EPSPs evoked by perforant path input to SLM of that region (Urban *et al.* 1998); I did not observe such a phenomenon in CA1, but nor did I systematically look for it. However, the absence of a boosting mechanism would be consistent

with the idea that the EC input to CA1 is not as strongly excitatory as the EC input via the perforant path to CA3 (Wu and Leung 1998).

The relative weakness of the excitatory component of the TA input to CA1 has certain implications for our understanding of the role of this pathway in hippocampal information processing. Many models of information storage and retrieval in the hippocampus require a strongly excitatory monosynaptic input from EC to CA1 (Levy 1989; Hasselmo *et al.* 1996; McClelland and Goddard 1996), and the TA input must provide sufficient excitation to fire CA1 pyramidal cells if it is to evoke place-specific firing patterns in these cells in the absence (Mizumori *et al.* 1989) or in advance of (Muller and Kubie 1989) CA3 input. How can such models be reconciled with the present observation that the TA input is only weakly excitatory? It should be noted that the field TA response recorded *in vivo* can be substantial (Buzsáki *et al.* 1995) and that TA stimulation can discharge CA1 pyramidal cells at monosynaptic latencies (Yeckel and Berger 1990). In slice, many excitatory axons may be lost if they do not run parallel to the plane of the slice. Furthermore, the restricted topography of the TA pathway (Tamamaki and Nojyo 1995) could result in only a small subset of CA1 pyramidal cells being strongly innervated by a particular set of TA axons. My very occasional observation of pyramidal cells that could be made to fire action potentials in response to TA input (data not shown) also supports the idea that strong excitatory TA inputs to CA1 are present, but sparse.

Paired-pulse plasticity of the excitatory component of the TA and SC pathways is also similar, with field responses to either input showing facilitation at ISIs up to 200 ms, as has been previously reported for the SC pathway (e.g., see Creager *et al.* 1980). Paired-pulse facilitation of a current sink in SLM of CA1 evoked by stimulation of the

TA path *in vivo* has been previously observed, but only a 50 ms ISI was tested (Leung *et al.* 1995). The degree of facilitation observed in the TA pathway was greater than that seen in the SC pathway, but that was most likely due to the smaller initial size of the TA response. Paired-pulse plasticity is known to vary inversely with probability of synaptic vesicle release, with a second response likely to show facilitation when the first response is small, and depression when the first response is large (Debanne *et al.* 1996). Intracellular recordings also showed a similar pattern of EPSP facilitation during paired-pulse stimulation of the SC and TA pathways, including slope measurements where changes in inhibition are unlikely to be a factor. These observations suggest that there are no major differences in neurotransmitter release mechanisms in TA and SC axons.

In addition to an excitatory response, stimulation of the SC or TA pathway also elicited a biphasic inhibition including both $GABA_A$ and $GABA_B$ components, as has been previously observed (e.g., SC response, Newberry and Nicoll 1984; TA response, Empson and Heinemann 1995b). Both $GABA_A$ and $GABA_B$ components were prominent in the SC response, while a distinct $GABA_A$ component was rarely seen in the TA response. However, this does not necessarily mean that TA stimulation cannot evoke a $GABA_A$ response. The TA EPSP could be enhanced by addition of the $GABA_A$ antagonist bicuculline (e.g., see Figure 8), suggesting that a $GABA_A$ component is indeed present. The slower TA EPSP, compared to the SC EPSP, may be more likely to mask the $GABA_A$ IPSP component of the TA response. In the presence of glutamate antagonists, both $GABA_A$ and $GABA_B$ IPSPs could be evoked by proximal stimulation in either SR or SLM.

I used trains of TA and SC stimuli to look at the frequency dependence of synaptic transmission in these two inputs to CA1. Changes in response during repetitive synaptic activity can involve many different phenomena: summation of PSPs, which may be sublinear due to decreases in driving force as the response brings the membrane potential closer to the reversal potential for the synaptic conductance, or supralinear if voltage-dependent channels are activated, boosting the response (e.g., Margulis and Tang 1998); simple linear combinations of PSPs, including both fast and slow EPSPs and IPSPs, which may be differentially recruited by different afferent activity patterns; paired-pulse facilitation of EPSPs by means of residual Ca^{2+} in the presynaptic terminal (Manabe *et al.* 1993; Thomson *et al.* 1993; Wu and Saggau 1994); paired-pulse depression of PSPs by means of synaptic vesicle depletion (Lambert and Wilson 1994; Wilcox and Dichter 1994; Fortunato *et al.* 1996; Galarreta and Hestrin 1998; Wang and Kaczmarek 1998); and paired-pulse depression of IPSPs mediated by $GABA_B$ autoreceptors on the presynaptic terminal (e.g., Davies *et al.* 1990).

In order to look at the interplay between these phenomena, I measured the peak amplitudes and times to peak of the EPSPs evoked by trains of TA and SC stimuli. EPSP peak amplitudes were measured relative to the peak of the response to the first EPSP, and as a difference rather than as a ratio, in order to describe whether the later responses were bringing the cell closer or farther from action potential threshold (Buonomano and Merzenich 1998). Similar patterns were observed in both SC and TA inputs, with repeated stimulation resulting in an overall decrease in the peak amplitudes of later EPSPs in the train (Figures 11, 12). This appeared to be primarily due to the fact that later EPSPs were arriving on top of a concurrently activated, strongly hyperpolarizing $GABA_B$-mediated

IPSP, as has been observed in CA3 and auditory cortex (Buonomano and Merzenich 1998). When trains of SC inputs did drive pyramidal cells to spike, action potentials were generally seen during the first few responses in the train (data not shown), further suggesting that inhibition was dominant in this response and could rapidly curtail excitation, as has previously been shown (Turner 1990). The times to peak of SC, but not TA, EPSPs increased during repetitive stimulation, suggesting that EPSPs early in the train were curtailed by $GABA_A$ IPSPs which were themselves depressed by repeated stimulation (Buonomano and Merzenich 1998). The observation that the times to peak of TA EPSPs did not change in a consistent way with repeated stimulation suggests that $GABA_A$ IPSPs do not play a significant role in shaping the TA response; however, it may just reflect the fact that the TA EPSP is already broad and slow to peak due to dendritic filtering.

Little has been previously reported about the frequency dependence of synaptic transmission in the TA pathway. In one report, stimulation in layer V of the medial EC in a combined hippocampal-EC slice resulted in only a biphasic inhibitory response, with no EPSP component, in CA1 pyramidal cells; repeated stimulation at 1-5 Hz resulted in a decrease in both components of the IPSP, especially the $GABA_B$-mediated one, but no higher stimulation frequencies were tested (Jones 1995). I observed a similar decrease in the TA-evoked $GABA_B$ IPSP with paired-pulse stimulation at 600 ms ISI (Figure 10) as well as with repeated burst stimulation at 1 Hz (Figure 14). The effect of depression of the TA-evoked IPSP on hippocampal processing is explored further in Chapter 4.

An apparent dominance of inhibition over excitation in the TA response has been noted before (Empson and Heinemann 1995b; Levy *et al.* 1995). This suggests an impor-

tant role for the TA pathway in modulation of hippocampal output. IPSPs evoked by activation of the TA pathway can reduce SC-evoked excitation (Colbert and Levy 1992; Empson and Heinemann 1995b). I found that IPSPs evoked by burst stimulation of the TA pathway were able to prevent SC input from making pyramidal cells fire; this spike-blocking phenomenon is characterized in Chapter 4.

2.4.2 SR/SLM interneurons

The presence of a substantial IPSP component in the TA response implies the presence of hippocampal interneurons that are activated by TA inputs. I chose to study SR/SLM interneurons, which are ideally positioned to receive synaptic input from the TA pathway, although other interneurons in CA1 may also be activated by this pathway (e.g., see Kiss *et al.* 1996).

The properties of SR/SLM interneurons reported here correspond well with previously published reports, each performed under somewhat different conditions and in different preparations (Lacaille and Schwartzkroin 1988b; Lacaille and Schwartzkroin 1988a; Williams *et al.* 1994; Khazipov *et al.* 1995; Vida *et al.* 1998). The mean resting potential in our recordings, about -69 mV, was substantially lower than the -55 to -66 mV reported elsewhere. This may be due to differences in recording conditions, and may also be due to the fact that I estimated resting potential by subtracting the potential recorded in the bath after breaking the seal from the potential recorded during the experiment. This bath potential was nearly always positive and, if it were not present throughout the experiment, would bias calculated membrane potentials towards more negative values.

Measured input resistances can only be compared to other whole-cell recordings, since sharp electrode recordings give lower estimates for input resistance, owing to the leak current around the electrode in the absence of the gigaohm seal created during whole-cell recording. The input resistances I observed were about 200 MΩ greater than those previously reported (Williams *et al.* 1994; Khazipov *et al.* 1995), although there was a very high variance both in our results and in the previously published reports. The higher resistance observed in our recordings may be due, once again, to differences in recording conditions, or it may be related to the more negative membrane potential; it is possible that fewer channels are open at this relatively hyperpolarized membrane potential.

Other intrinsic membrane properties of SR/SLM interneurons were similar to those previously described. Injection of depolarizing current elicited a train of action potentials with prominent AHPs, consistent with all previous reports (Kawaguchi and Hama 1988; Lacaille and Schwartzkroin 1988a; Williams *et al.* 1994; Khazipov *et al.* 1995; Vida *et al.* 1998). A long AHP was observed following spiking during a depolarizing current step, as previously reported (Vida *et al.* 1998). I observed various patterns of spike frequency accommodation (Figure 15), very similar to those shown elsewhere (Vida *et al.* 1998) and consistent with other reports (Kawaguchi and Hama 1988; Williams *et al.* 1994; Khazipov *et al.* 1995). In one previous study (Lacaille and Schwartzkroin 1988a), SR/SLM interneurons were reported to show little spike-frequency accommodation, but short (100 ms) depolarizing currents were used, and spike frequency accommodation can take longer than 100 ms to develop (e.g., Figure 15, and Vida *et al.* 1998). In some cases (data not shown) I observed a delay before the first

action potential in a train evoked by depolarizing current, as seen in the hyperpolarization-induced "burst mode" of spiking described previously (Lacaille and Schwartzkroin 1988a; Williams *et al.* 1994). As previously reported (Lacaille and Schwartzkroin 1988a; Williams *et al.* 1994), a "sag" in the membrane potential was present in the response to a hyperpolarizing current step, possibly mediated by slowly-activating, inwardly-rectifying potassium conductances.

Responses of SR/SLM neurons to extracellular stimulation in various layers have previously been described (Lacaille and Schwartzkroin 1988a; Williams *et al.* 1994). In the transverse slice, stimulation in virtually any area of the hippocampus – alveus, SR, SLM, stratum moleculare of the dentate gyrus, or area CA3 – resulted in an EPSP that could produce one or more action potentials (Lacaille and Schwartzkroin 1988a). IPSPs, however, were observed only about half the time (Williams *et al.* 1994) or not at all (Lacaille and Schwartzkroin 1988a) in response to stimulation in transverse slices. However, SR/SLM interneurons do receive inhibitory innervation, since more proximal stimulation could evoke $GABA_A$ and $GABA_B$ IPSCs (Khazipov *et al.* 1995) or IPSPs (Williams *et al.* 1994), and extracellular stimulation in the longitudinal slice evoked robust IPSPs (Lacaille and Schwartzkroin 1988a). I, too, often did not observe IPSPs in response to SR or SLM stimulation (Table 1; Figure 17). I rarely observed spiking and, unlike previous reports (Lacaille and Schwartzkroin 1988a; Williams *et al.* 1994), never observed burst spiking in SR/SLM interneurons in response to single stimulation of SC or TA inputs. Many interneurons were not at all responsive to either SC or TA inputs, perhaps reflecting the heterogeneity of their dendritic arborizations.

Responses of SR/SLM interneurons to trains of presynaptic activity have not previously been described. In response to trains of SC stimuli, most interneurons showed facilitation of responses to the first few stimuli in a train, followed by a decrease or a plateau (Figure 19). Unlike the responses of pyramidal cells, interneuron responses were not dominated by the appearance of a large, hyperpolarizing $GABA_B$ IPSP. Some TA responses showed a similar pattern of facilitation followed by depression over the course of a train, while others showed a persistent facilitation, particularly at lower stimulation frequencies (5-10 Hz; Figure 20). Several interneurons could be driven to fire action potentials by means of repeated synaptic input from the TA pathway (Figure 21). The tendency towards facilitation or depression did not show a dependence on the size of the initial response. The strongly facilitatory responses seen in some TA-interneuron connections were similar to connections observed between individual pyramidal cells and interneurons in neocortex, which also showed greater facilitation than connections between pyramidal cells (Thomson 1997).

2.4.3 SR giant cells

In the course of doing interneuron recordings, I found that some cells in SR/SLM were not interneurons, but a different type of neuron, apparently the same as the SR giant cells described by Gulyás *et al.* (1998b). Just like interneurons, the SR giant cells I recorded had a more negative resting potential than previously reported, -67 mV compared to -53 mV. I also observed a lower input resistance, 116 MΩ, compared to 197 MΩ. In other ways, the giant cells I recorded were similar to those in the previous study, with overshooting action potentials, small spike AHPs, spike frequency accommodation

during a depolarizing current pulse, and a sag in the voltage response to a hyperpolarizing current step (Figure 22) (Gulyás *et al.* 1998b). The morphology of SR giant cells was also very similar to the previous report.

The synaptic responses of SR giant cells have not previously been described in detail; in one previous study of LTP of non-pyramidal neurons in CA1, SR giant cells responded with a large EPSP to stimulation in SR (Maccaferri and McBain 1996), consistent with my observations. Unlike pyramidal cells, SR giant cells had robust responses to TA input (Figures 23, 25), likely due to the closer location of the giant cells' somata to the synaptic sites. Fast and slow IPSPs were observed in synaptic responses (Figure 23), showing that SR giant cells receive inhibitory input mediated by $GABA_A$ and $GABA_B$ receptors. TA and SC responses in SR giant cells showed similar patterns in responses to trains of inputs, with initial facilitation followed by later plateau or depression; TA responses showed a somewhat greater tendency towards facilitation than SC responses. Unlike pyramidal cells, however, a clear-cut increase in time to peak of the SC response was observed only at low frequencies; in the TA response, no consistent pattern in time to peak was observed.

The observation of large TA EPSPs in SR giant cells suggests that these neurons may be easily excited by TA activity, and indeed, in some cases, action potential firing in response to single TA stimuli was observed (data not shown). This suggests another aspect to the hippocampal circuitry that has not yet been explored. The axon collaterals of SR giant cells make asymmetric, hence probably excitatory, synaptic contacts onto dendritic spines and shafts in SO, including many dendrites identified as belonging to interneurons (Gulyás *et al.* 1998b), suggesting a possible role in feedforward inhibition

via the SC or TA pathways. SR giant cells, along with conventional pyramidal cells, project out of the hippocampus to the olfactory bulb (Van Groen and Wyss 1990; Gulyás *et al.* 1998b), though the possible function of this projection is unclear. Other possible downstream targets of SR giant cells have not yet been identified.

2.4.4 Contribution of the TA pathway to hippocampal processing

As seen here and explored further in Chapter 4, the TA input to area CA1 of the hippocampus has a predominantly inhibitory effect. However, given the large number of glutamatergic synapses made by TA axons onto pyramidal cells (Desmond *et al.* 1994), the robust field EPSPs evoked in SLM by temporoammonic stimulation (Figure 3) (Colbert and Levy 1992), and the occasional observations of pyramidal cell firing in response to TA input (e.g., Yeckel and Berger 1990), it seems likely that a role for TA-mediated excitation exists as well.

The excitatory component of the TA input may enhance SC LTP in an associational manner (Levy *et al.* 1995), although in a subsequent study, SC LTP was actually reduced when TA inputs were stimulated simultaneously with SC inputs (Levy *et al.* 1998). There may exist conditions under which the EPSPs evoked in the distal dendrites by TA activity are boosted, perhaps by voltage-dependent conductances, in a manner similar to that seen in the perforant path input to CA3 (Urban *et al.* 1998). Finally, it is likely that the responsiveness of CA1 pyramidal cells *in vivo* will be very different from that seen in the slice preparation, where many inputs, background activity, and neuromodulatory influences are missing. It is possible that a pyramidal cell already somewhat

depolarized by other synaptic inputs will be more responsive to TA input than a quiet cell *in vitro*. *In vivo* recordings suggest that under certain conditions, the synaptic response to TA input to CA1 may be even greater than the response in dentate gyrus to perforant path input (Buzsáki *et al.* 1995). Further discussion of the potential roles of the TA pathway is found in Chapter 5.

Because of the small size of the TA EPSP recorded intracellularly, it would seem that the best way of characterizing the excitatory component of the TA input to CA1 is by looking at the field response in SLM. I used this approach to look at long-term plasticity in the temporoammonic pathway (Chapter 3).

Table 1. Intracellularly recorded synaptic responses in ACSF

	V_m (mV)	n	R_{in} (MΩ)	n	EPSP time to peak (ms)	EPSP peak amplitude (mV)	n	Fast IPSP time to peak (ms)	Fast IPSP peak amplitude (mV)	n	Slow IPSP time to peak (ms)	Slow IPSP peak amplitude (mV)	n
Pyramidal cells, KAc, SC responses	-63.7 ± 0.7	71	103 ± 6	61	14.4 ± 0.5	7.0 ± 0.4	67	77.0 ± 3.0	-5.1 ± 0.3	38	274.9 ± 9.4	-3.8 ± 0.3	51
Pyramidal cells, KAc, TA responses	"	"	"	"	30.9 ± 1.1	1.5 ± 0.1	60	82 ± 10	-2.1 ± 0.5	9	276 ± 10	-1.3 ± 0.1	59
Pyramidal cells, CsAc, SC responses	-68.4 ± 1.4	33	154 ± 12	31	25.4 ± 1.5	5.0 ± 0.3	30	44 ± 9	-4.8 ± 0.4	2	279 ± 19	-1.8 ± 0.6	13
Pyramidal cells, CsAc, TA responses	"	"	"	"	43.1 ± 3.1	2.6 ± 0.2	31	-	-	0	298 ± 17	-1.0 ± 0.2	14
SR/SLM interneurons, SC responses*	-68.6 ± 0.2	39	562 ± 5	41	20.3 ± 1.1	6.2 ± 0.6	31	59.0 ± 9.5	-1.8 ± 0.5	3	488 ± 28	-1.0 ± 0.1	5
SR/SLM interneurons, TA responses*	"	"	"	"	19.5 ± 1.6	5.2 ± 0.6	24	35.0 ± 7.0	-1.6 ± 0.8	2	544 ± 30	-0.6 ± 0.1	6
SR giant cells, SC responses	-67 ± 2	12	116 ± 9	12	18.2 ± 1.7	8.4 ± 0.9	12	-	-	0	262 ± 39	-1.7 ± 0.5	11
SR giant cells, TA responses	"	"	"	"	25.1 ± 1.7	5.0 ± 0.7	12	-	-	0	352 ± 41	-0.6 ± 0.1	10

* IPSP data were not determined in SR/SLM interneurons for 11 SC responses and 12 TA responses out of 41 cells. No IPSPs were observed in 22 SC responses and 21 TA responses in SR/SLM interneurons. TA EPSP responses are from only those cells described in the text as "excited" (section 2.3.3.2).

Table 2. Monosynaptic IPSPs in pyramidal cells, recorded in 10 μM CNQX and 50 μM AP5

	Fast IPSP time to peak (ms)	Fast IPSP peak amplitude (mV)	n	Slow IPSP time to peak (ms)	Slow IPSP peak amplitude (mV)	n
KAc electrode, SR responses	63 ± 20	-3.2 ± 0.7	5	329 ± 25	-1.8 ± 0.5	5
KAc electrode, SLM responses	78 ± 8	-2.7 ± 1.2	5	301 ± 16	-2.0 ± 0.3	4
CsAc electrode, SR responses	65.5 ± 2.6	-2.7 ± 0.5	6	308 ± 25	-3.1 ± 0.2	5
CsAc electrode, SLM responses	67.8 ± 4.6	-2.5 ± 0.6	6	373 ± 27	-3.1 ± 0.5	5

Figure 3. *A*, Microdissected slice recording configuration for field temporoammonic (TA) responses, recorded in stratum lacunosum-moleculare (SLM), and field Schaffer collateral (SC) responses, recorded in stratum radiatum (SR). The dentate gyrus and CA3 regions, shown in dotted lines, are dissected away before starting the experiment. A cut is made through stratum radiatum in distal CA1 to prevent antidromic SC stimulation from contaminating the TA response. *B*, Representative field potentials showing negative-going fields in SR in response to SC stimulation, and in SLM in response to TA stimulation; meanwhile, positive-going fields are seen in SR in response to TA stimulation and in SLM in response to SC stimulation. Scale bar: 0.2 mV / 30 ms.

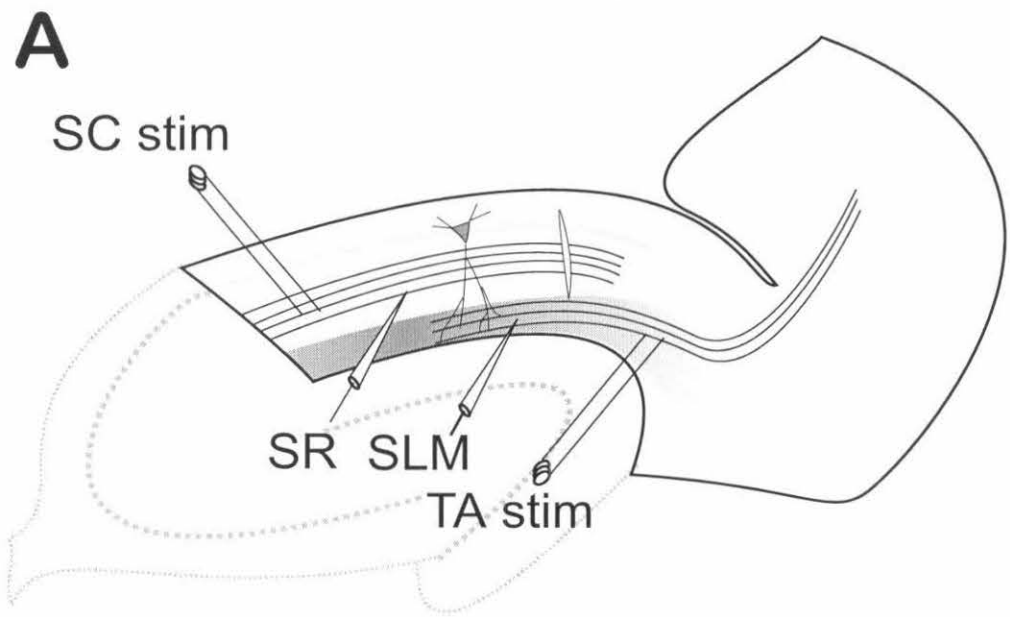
A
SC stim
SR
SLM
TA stim

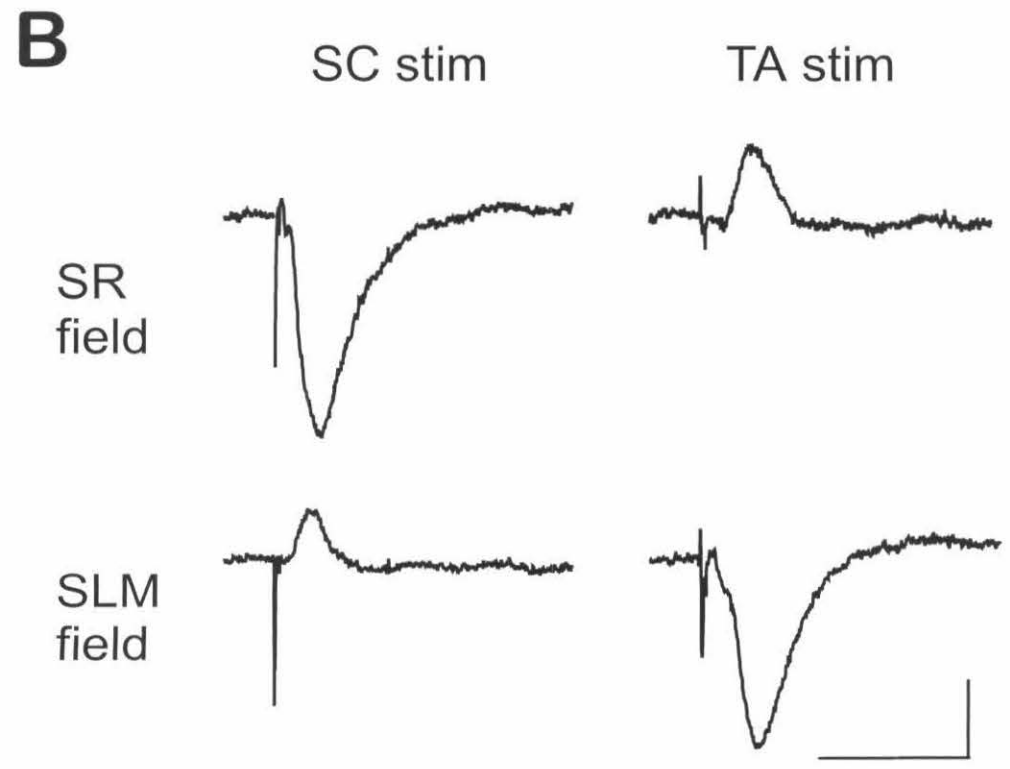
B
SC stim
TA stim
SR
field
SLM
field

Figure 4. TA stimulation evokes, at most, a very small population spike in stratum pyramidale (SP). Two examples of sets of field recordings where SC stimulation evoked a robust population spike in SP while a much larger TA stimulus evoked only a very small population spike as well as a moderately-sized field EPSP in stratum lacunosum-moleculare (SLM). Vertical arrows indicate population spikes; * indicates fiber volley in TA response. Stimulus artifacts digitally removed for clarity; vertical lines indicate time of stimulus.

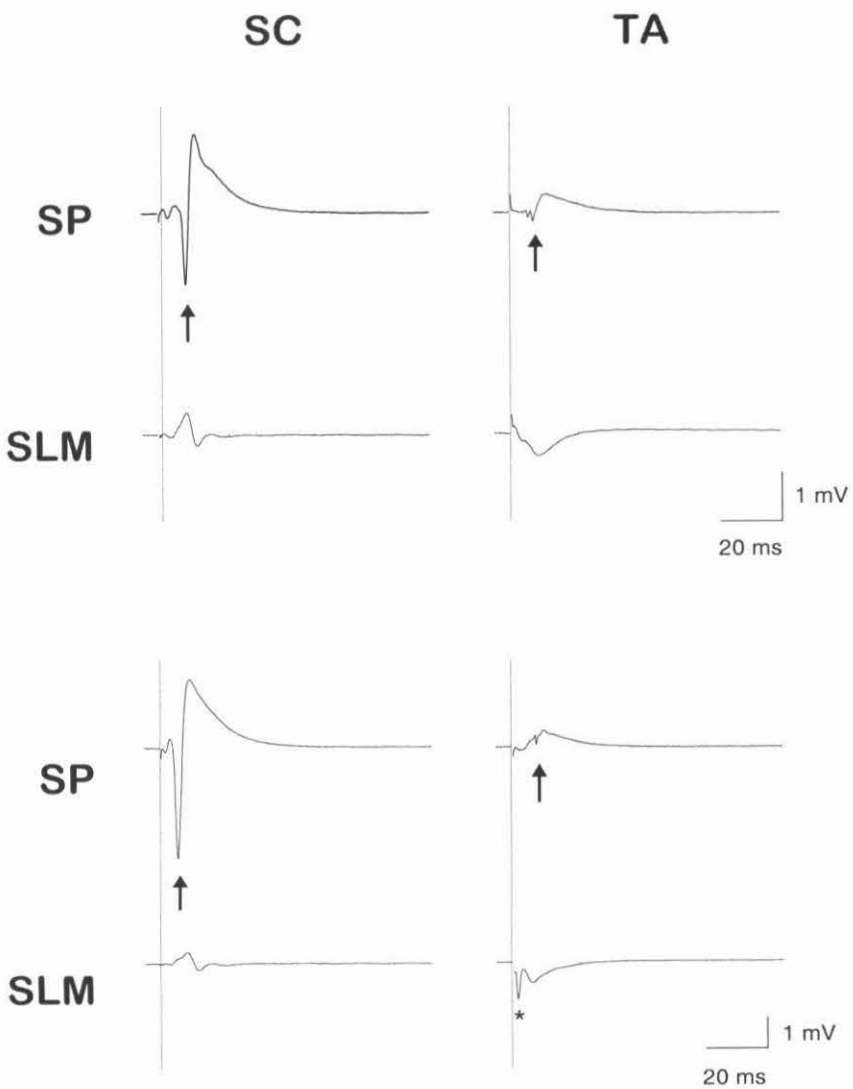
SC
TA
SP
SLM
1 mV
20 ms
SP
SLM
*
1 mV
20 ms

Figure 5. Paired-pulse plasticity in field responses to SC and TA stimulation.

Both the field EPSPs and the field IPSPs evoked by TA (filled circles) and SC (open triangles) stimulation show paired-pulse facilitation at short (≤ 200 ms) interstimulus intervals (ISIs); at longer ISIs, TA responses remain facilitating while SC responses show depression. Top, representative sweeps of SC and TA responses with first and second responses at each ISI overlaid; first response is black, second is red. At 10 and 25 ms ISI, pre-stimulus baseline is distorted because the response to the first stimulus had not yet returned to baseline.

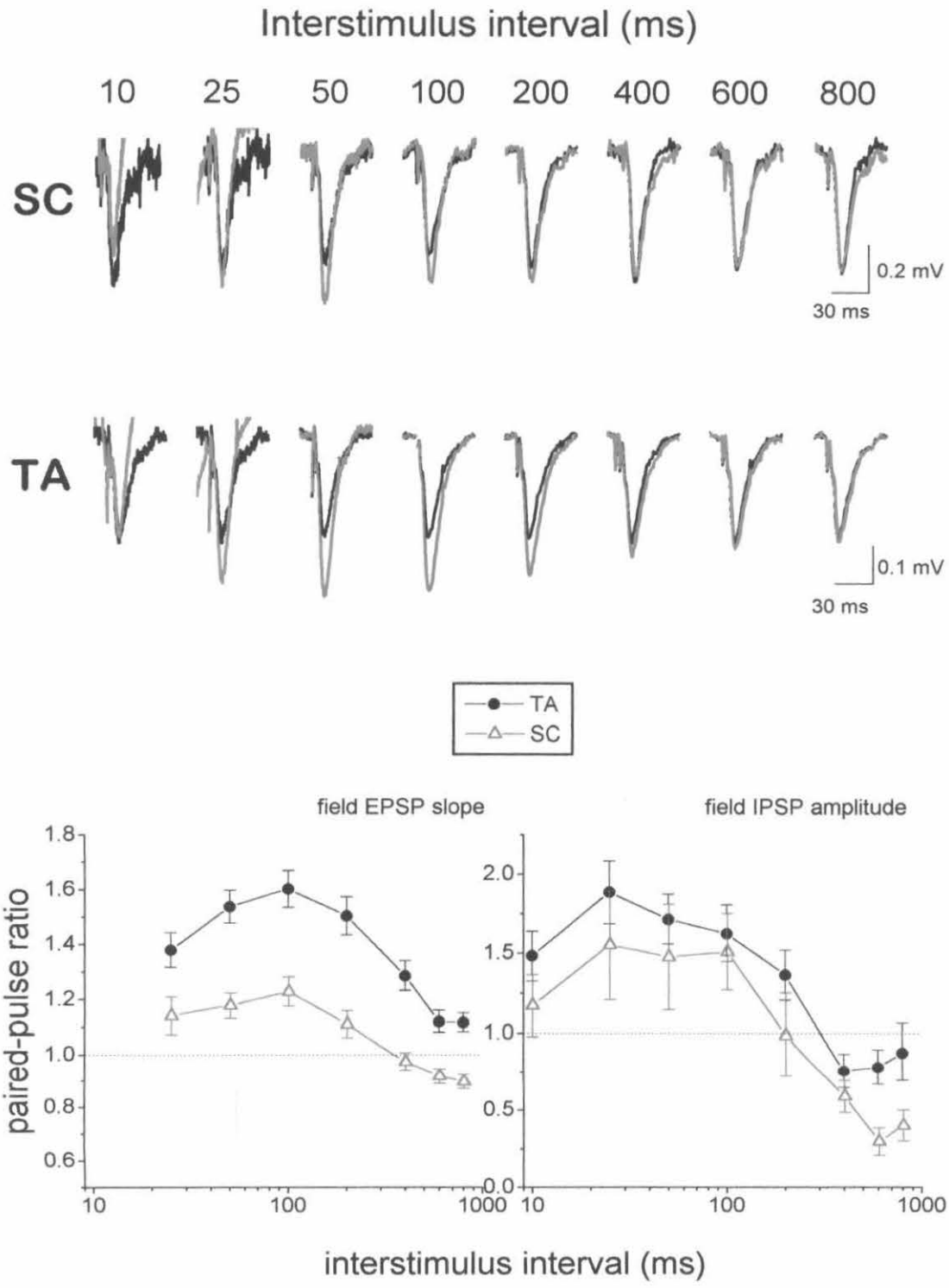
Interstimulus interval (ms)
10
25
50
100
200
400
600
800
SC
0.2 mV
30 ms
TA
0.1 mV
30 ms
TA
SC
field EPSP slope
field IPSP amplitude
paired-pulse ratio
1.8
1.6
1.4
1.2
1.0
0.8
0.6
2.0
1.5
1.0
0.5
0.0
10
100
1000
interstimulus interval (ms)

Figure 6. Negative correlation between initial field response size and paired-pulse plasticity ratio. Using either amplitude (left) or field EPSP slope (right) to measure paired-pulse plasticity, facilitation is more likely when the initial response is small, and depression more likely when the initial response is large. This pattern holds for both TA (filled circles) and SC (open triangles) responses, at 50 (top) and 800 (bottom) ms ISI.

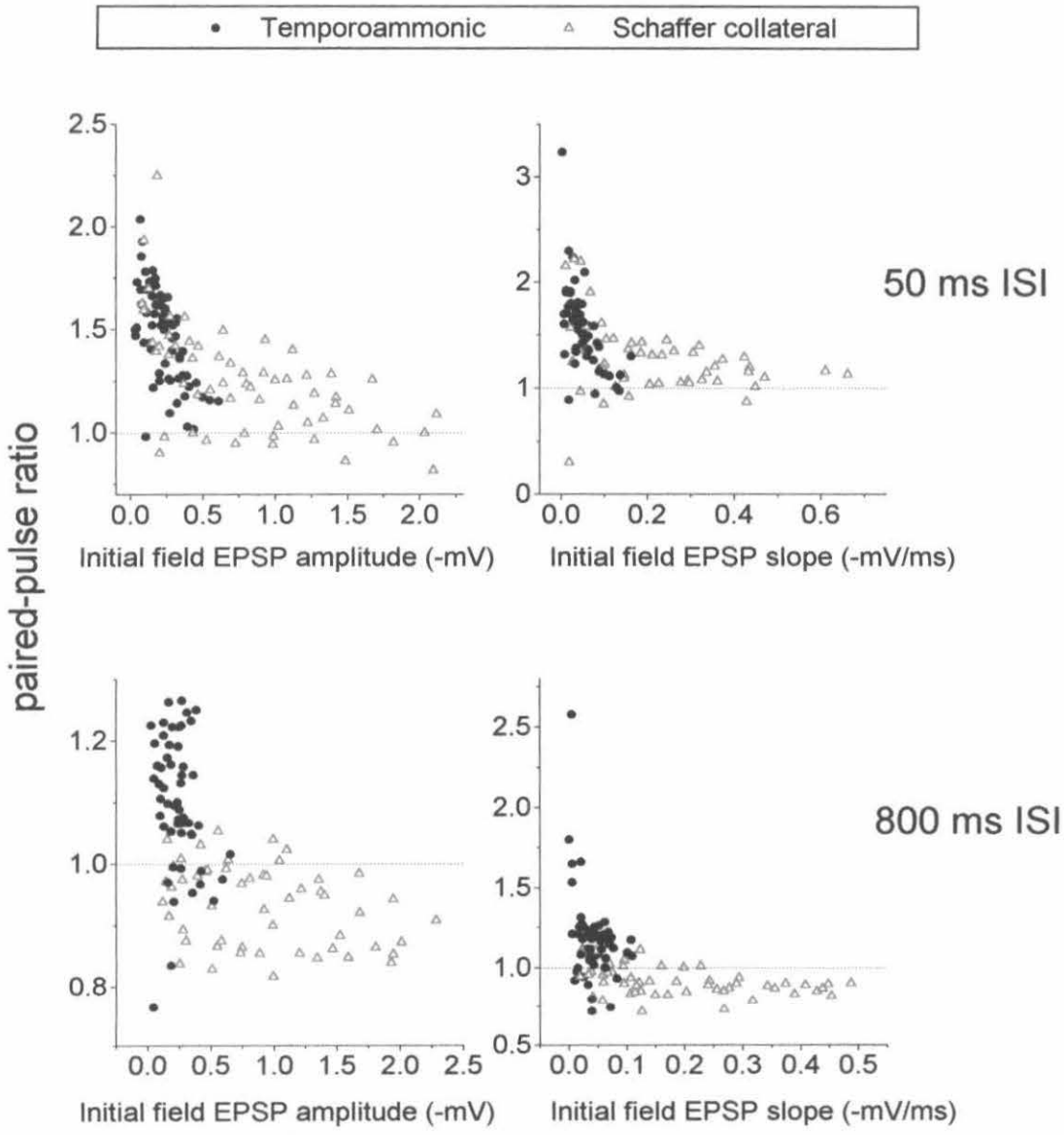
Temporoammonic
Schaffer collateral
paired-pulse ratio
50 ms ISI
800 ms ISI
Initial field EPSP amplitude (-mV)
Initial field EPSP slope (-mV/ms)
Initial field EPSP amplitude (-mV)
Initial field EPSP slope (-mV/ms)

Figure 7. Intrinsic electrophysiological properties and morphology of pyramidal cells. *A*, examples of responses to depolarizing and hyperpolarizing current injection in two cells. Vertical scale is top value for responses to depolarizing current, middle value for current steps, bottom value for responses to hyperpolarizing current. *B*, example of a biocytin-filled pyramidal cell; the long process in SO is likely to be an axon. Dendrites were profusely spiny, but the spines are not illustrated.

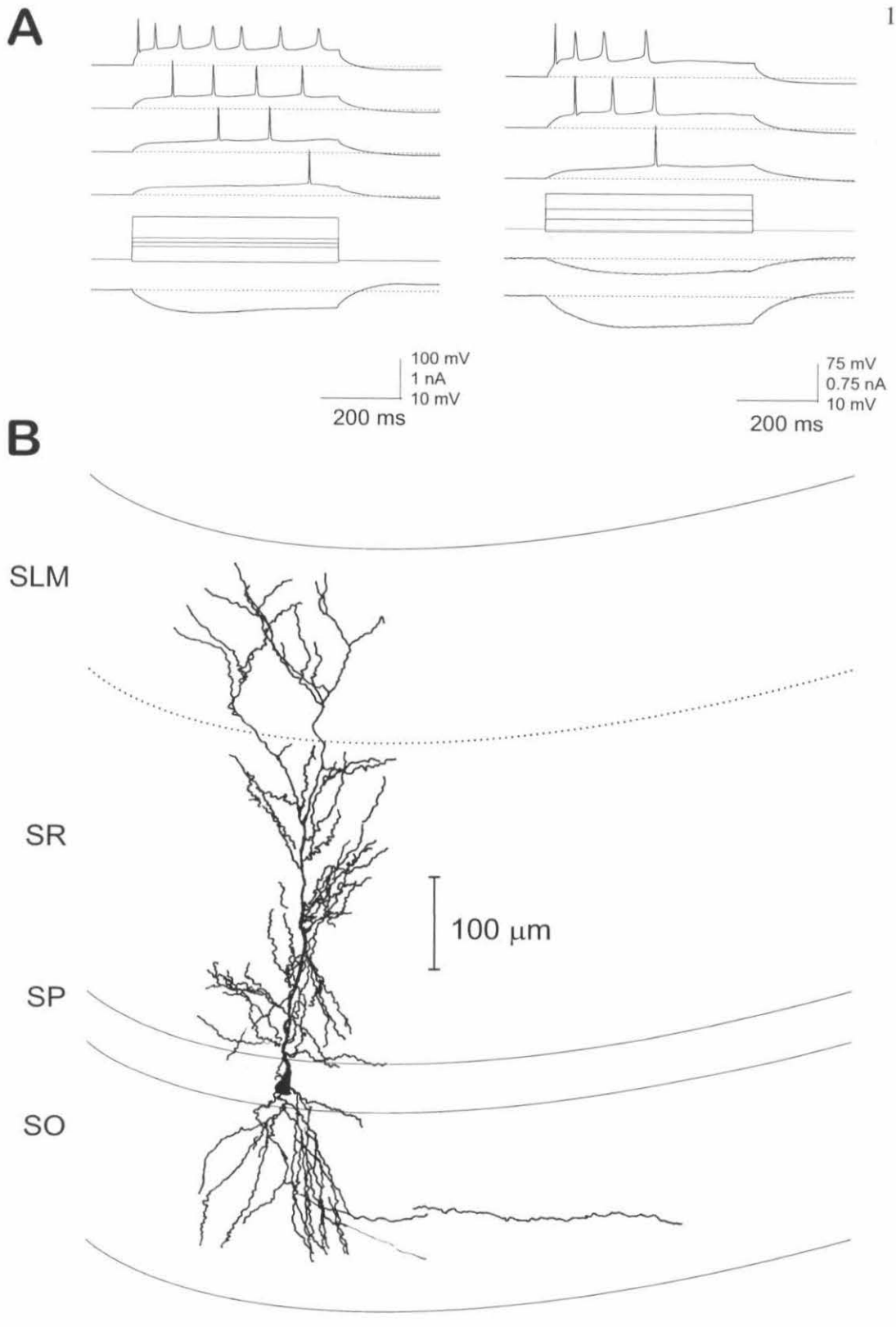
A
100 mV
1 nA
10 mV
200 ms
75 mV
0.75 nA
10 mV
200 ms
B
SLM
SR
SP
SO
100 µm

Figure 8. Pharmacology of TA and SC postsynaptic responses in pyramidal cells. *A*, responses to SC (left, black) and TA (middle, red) responses in one pyramidal cell in normal ACSF; the two responses are shown overlaid at right. *B*, monosynaptic IPSP responses of one pyramidal cell to SC (left, black) and TA (right, red) stimulation in the presence of the glutamate receptor antagonists CNQX (10 μM) and AP5 (50 μM); the two responses are shown overlaid at right. *C*, effect of the GABAA antagonist bicuculline (bic) (20 μM) (middle, red) on the TA response (left, black); the two responses are shown overlaid at right. *D*, left, black, monosynaptic IPSP evoked by TA stimulation in the presence of CNQX and AP5; middle, effect of bicuculline (20 μM; blue trace) and the $GABA_B$ antagonist 2-OH-saclofen (sac; 100 μM; red trace) on the monosynaptic IPSP; right, all responses overlaid. Scale bars, -2 mV / 400 ms.

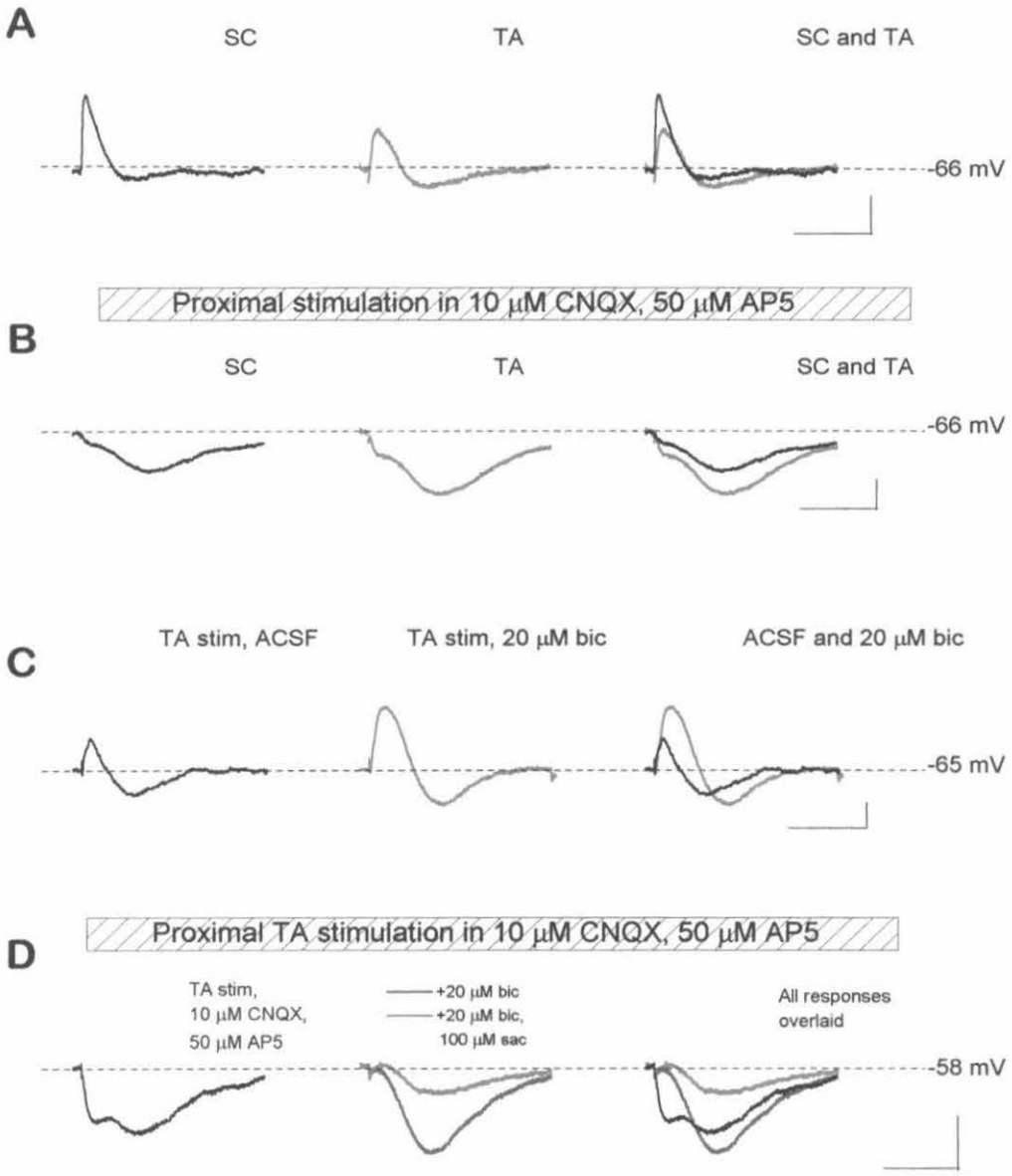
A
SC
TA
SC and TA
-66 mV
Proximal stimulation in 10 μM CNQX, 50 μM AP5
B
SC
TA
SC and TA
-66 mV
C
TA stim, ACSF
TA stim, 20 μM bic
ACSF and 20 μM bic
-65 mV
D
Proximal TA stimulation in 10 μM CNQX, 50 μM AP5
TA stim,
10 μM CNQX,
50 μM AP5
+20 μM bic
+20 μM bic,
100 μM sac
All responses
overlaid
-58 mV

Figure 9. Determination of the reversal potential of monosynaptic IPSPs in pyramidal cells. Left, top, pyramidal cell responses to SC stimulation in the presence of 10 μM CNQX and 50 μM AP5 at various membrane potentials; bottom, linear fits to amplitudes of the early (open squares) and late (filled circles) components of the response. Right, same except stimulation was of the TA pathway.

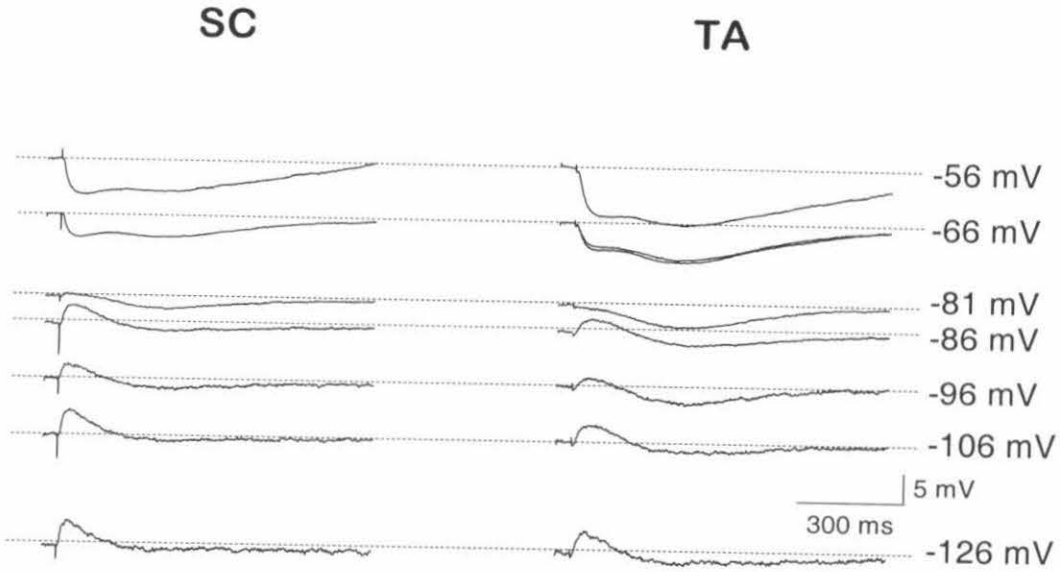
SC
TA
-56 mV
-66 mV
-81 mV
-86 mV
-96 mV
-106 mV
5 mV
300 ms
-126 mV

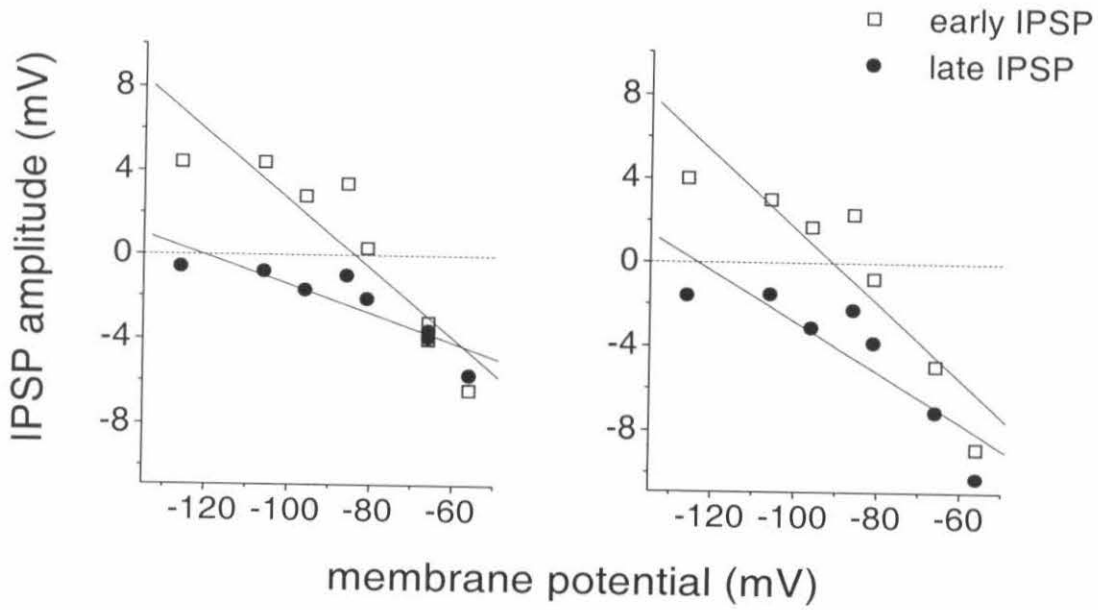
early IPSP
late IPSP
IPSP amplitude (mV)
8
4
0
-4
-8
-120 -100 -80 -60
membrane potential (mV)

Figure 10. Paired-pulse plasticity ratios of intracellular responses to TA and SC stimulation. For EPSP and fast IPSP amplitudes, the amplitude of the second response is measured relative to the membrane potential at the onset of the response; for the slow IPSP, the amplitude of the total response relative to the original baseline is measured.

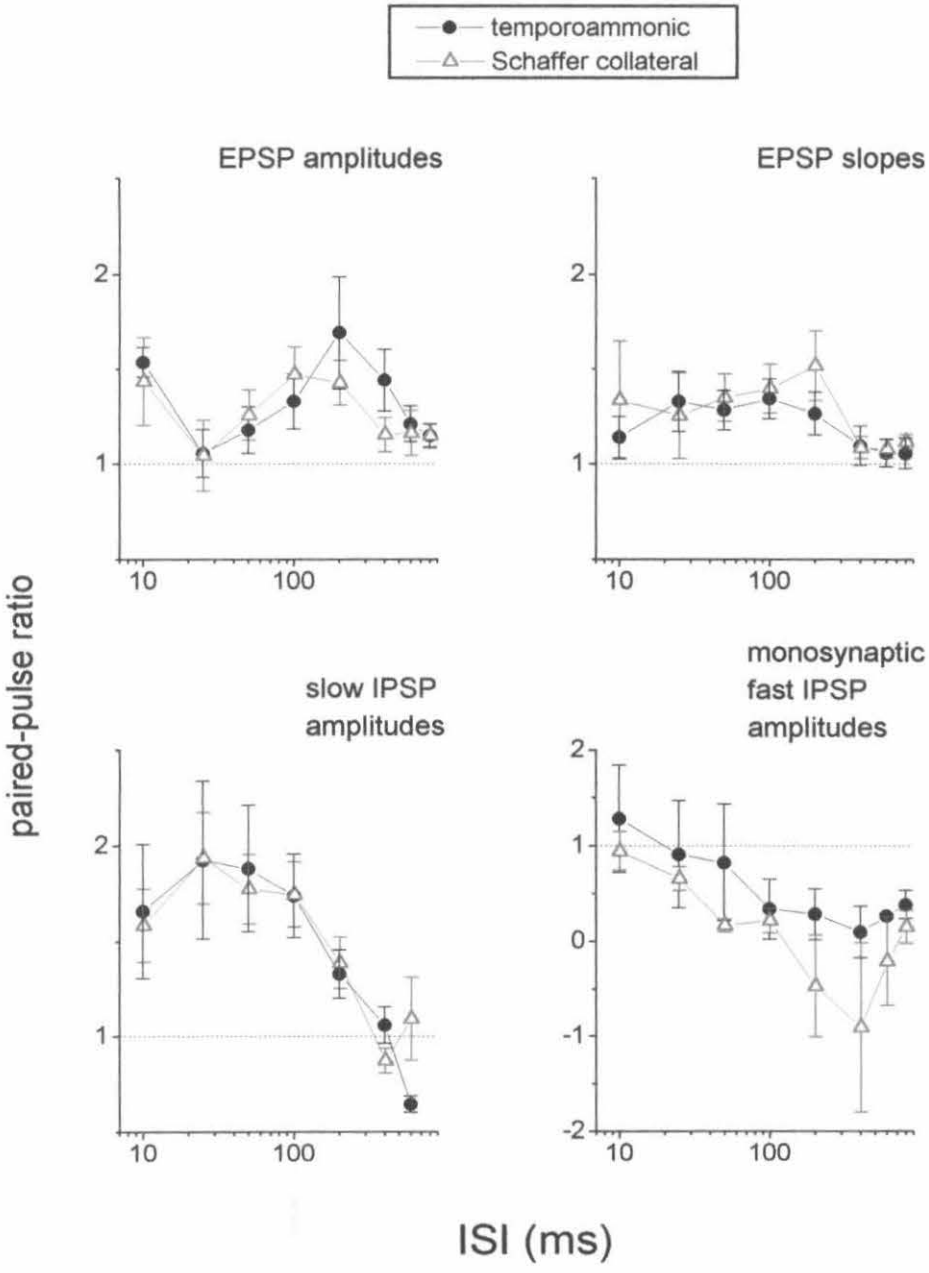
temporoammonic
Schaffer collateral
EPSP amplitudes
EPSP slopes
slow IPSP amplitudes
monosynaptic fast IPSP amplitudes
paired-pulse ratio
ISI (ms)
10
100
1
2
0
-1
-2

Figure 11. Frequency dependence of the response of a pyramidal cell to SC stimulation. *A*, times to peak for each EPSP relative to each stimulus, at 5, 10, 15 and 25 Hz. *B*, peak amplitudes for each EPSP relative to the first, at 5, 10, 15 and 25 Hz. *C*, representative traces of the pyramidal cell response to SC stimulation at 5, 10, 15 and 25 Hz.

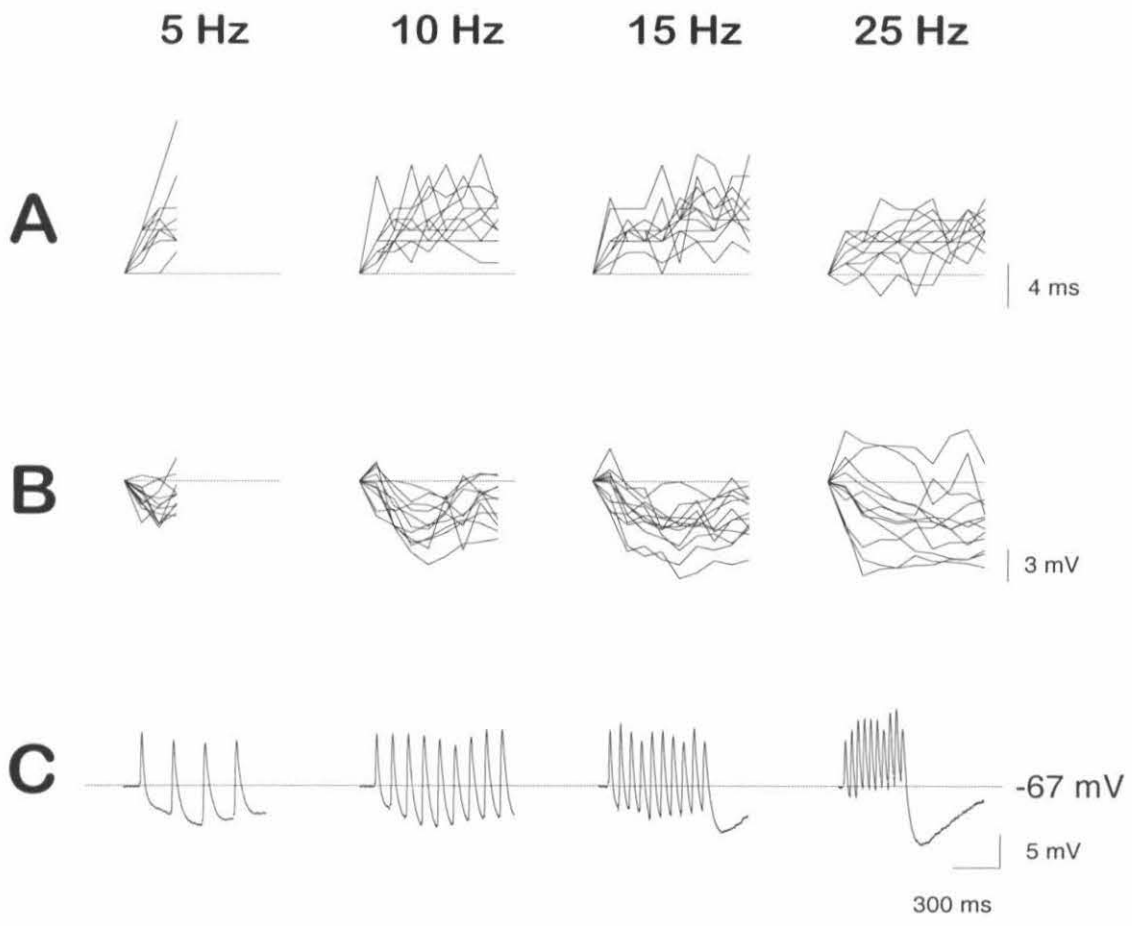
5 Hz
10 Hz
15 Hz
25 Hz
A
4 ms
B
3 mV
C
-67 mV
5 mV
300 ms

Figure 12. Frequency dependence of the response of a pyramidal cell to TA stimulation. *A*, times to peak for each EPSP relative to each stimulus, at 5, 10, 15 and 25 Hz. *B*, peak amplitudes for each EPSP relative to the first, at 5, 10, 15 and 25 Hz. *C*, representative traces of the pyramidal cell response to SC stimulation at 5, 10, 15 and 25 Hz. Data from the same cell as Figure 11.

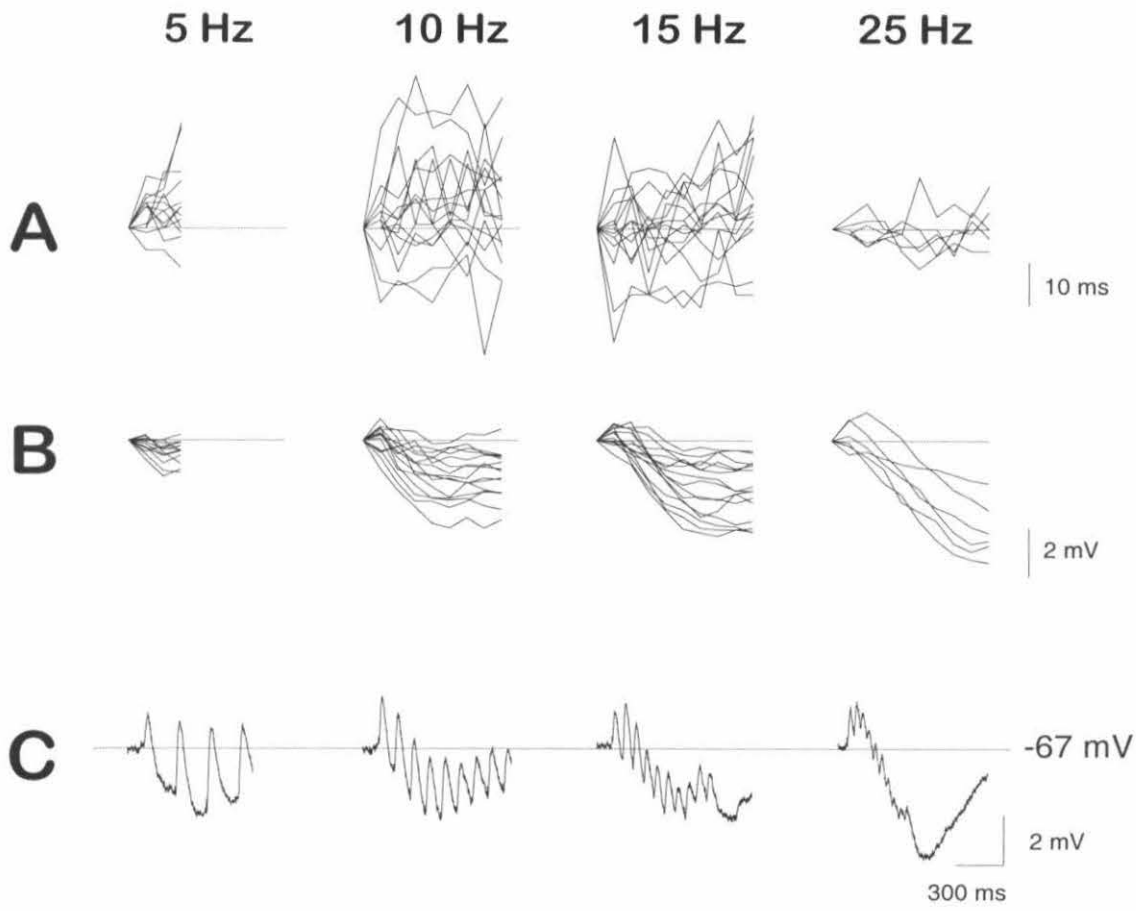
5 Hz
10 Hz
15 Hz
25 Hz
A
10 ms
B
2 mV
C
-67 mV
2 mV
300 ms

Figure 13. IPSPs evoked in a pyramidal cell by SC (top) and TA (bottom) burst stimulation.

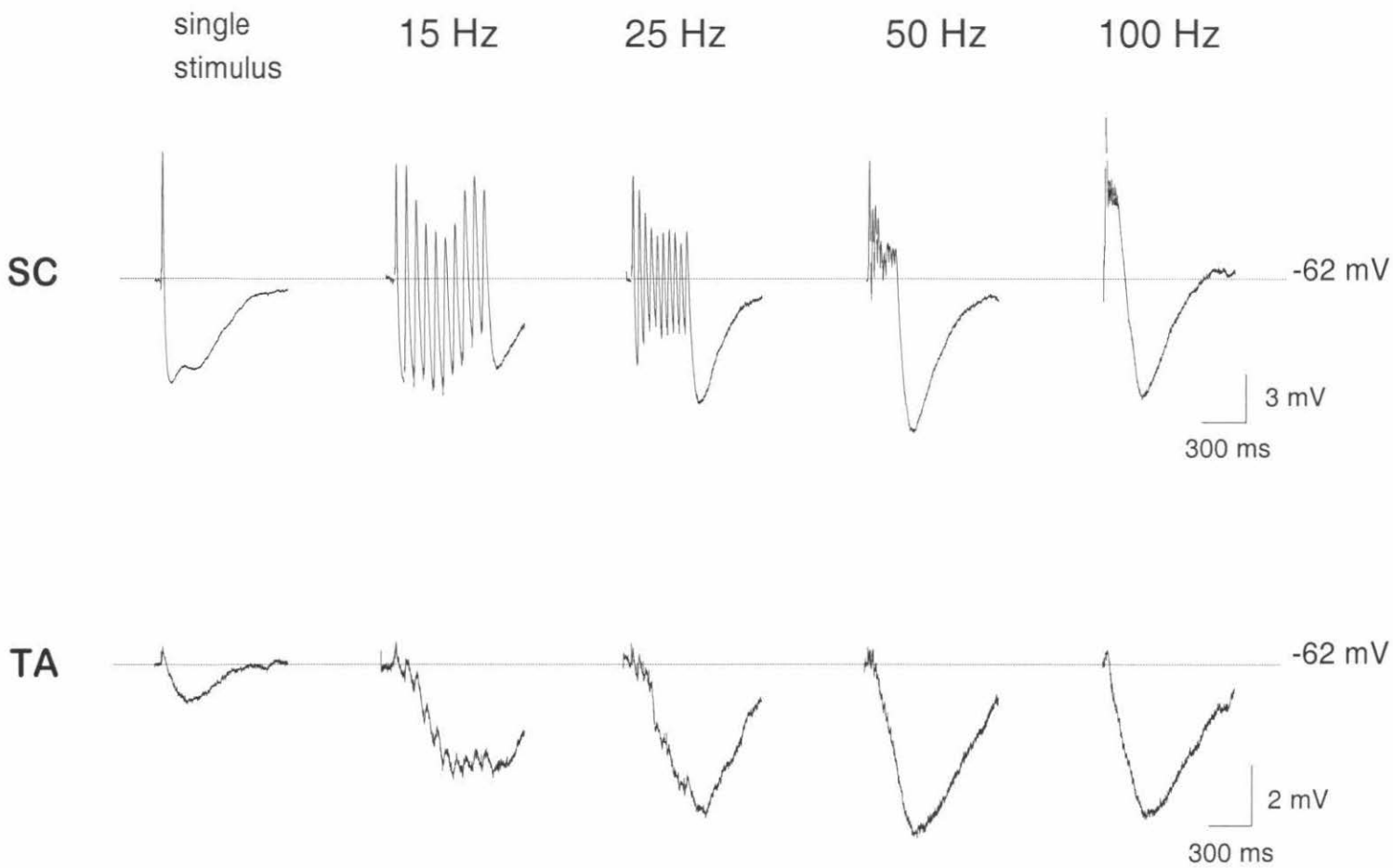
single
stimulus
15 Hz
25 Hz
50 Hz
100 Hz
SC
-62 mV
3 mV
300 ms
TA
-62 mV
2 mV
300 ms

Figure 14. Decay of the amplitude of IPSPs evoked in a pyramidal cell by TA burst (10 stimuli at 100 Hz) stimulation. TA bursts were repeated at 1, 5, 15, 30, 60 and 120 second repeats in the same cell. IPSP amplitudes were plotted versus time and fitted by an exponential decay curve.

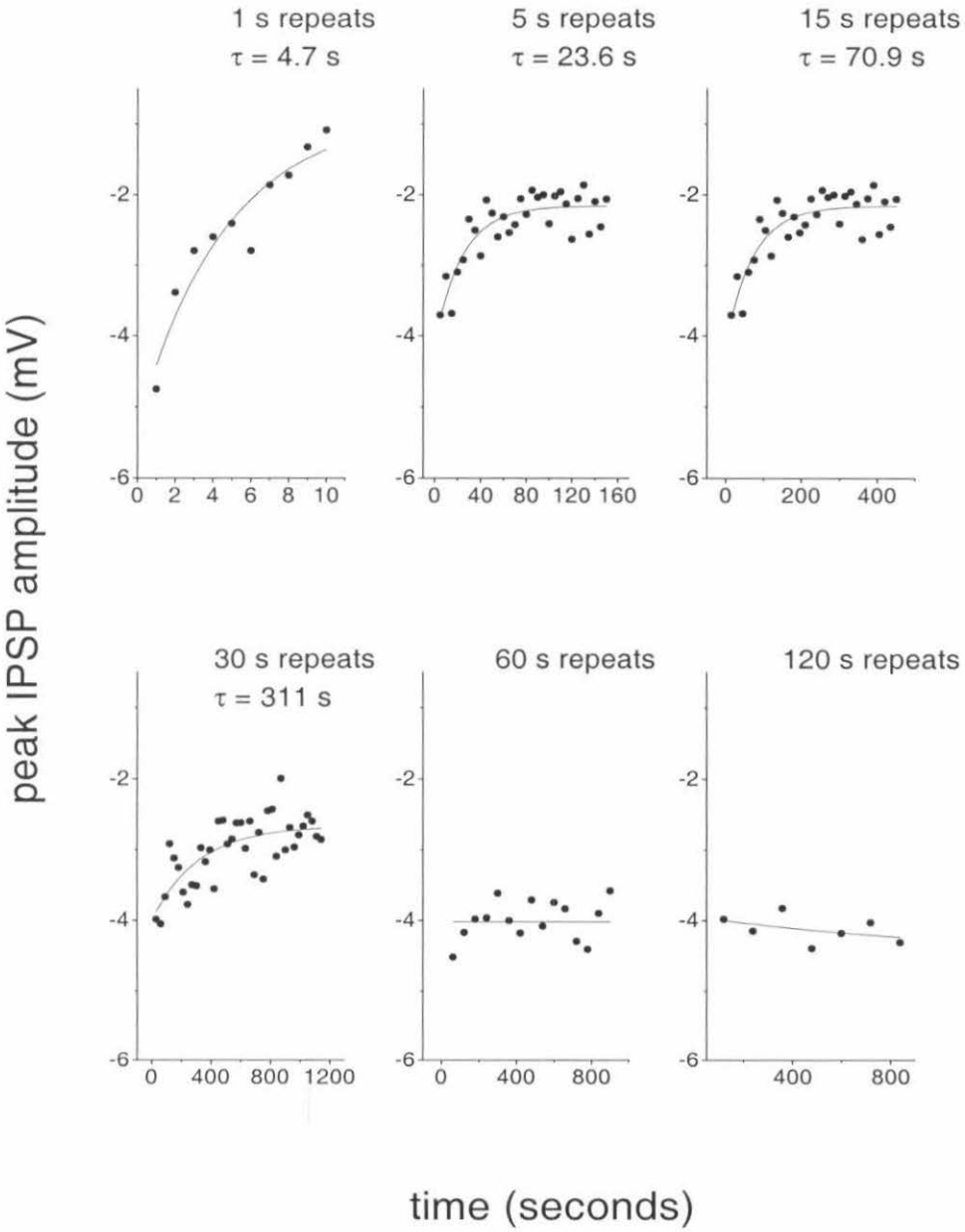
1 s repeats
τ = 4.7 s
5 s repeats
τ = 23.6 s
15 s repeats
τ = 70.9 s
30 s repeats
τ = 311 s
60 s repeats
120 s repeats
peak IPSP amplitude (mV)
time (seconds)

Figure 15. Intrinsic electrophysiological properties and morphology of SR/SLM interneurons. *A-D*, responses of four interneurons to depolarizing and hyperpolarizing current injection, illustrating the types of responses described in section 2.3.3.1 (p. 97). Vertical scale is top value for responses to depolarizing current, middle value for current steps, bottom value for responses to hyperpolarizing current. *E*, reconstruction of an interneuron with processes running horizontally along the SR/SLM border. The cell body and axon were not recovered; the presumed location of the cell body is indicated by the dotted circle. *F*, reconstruction of an interneuron with a stellate dendritic arborization. Dendrites extend from SLM to SO, and the axon ramifies profusely in SR.

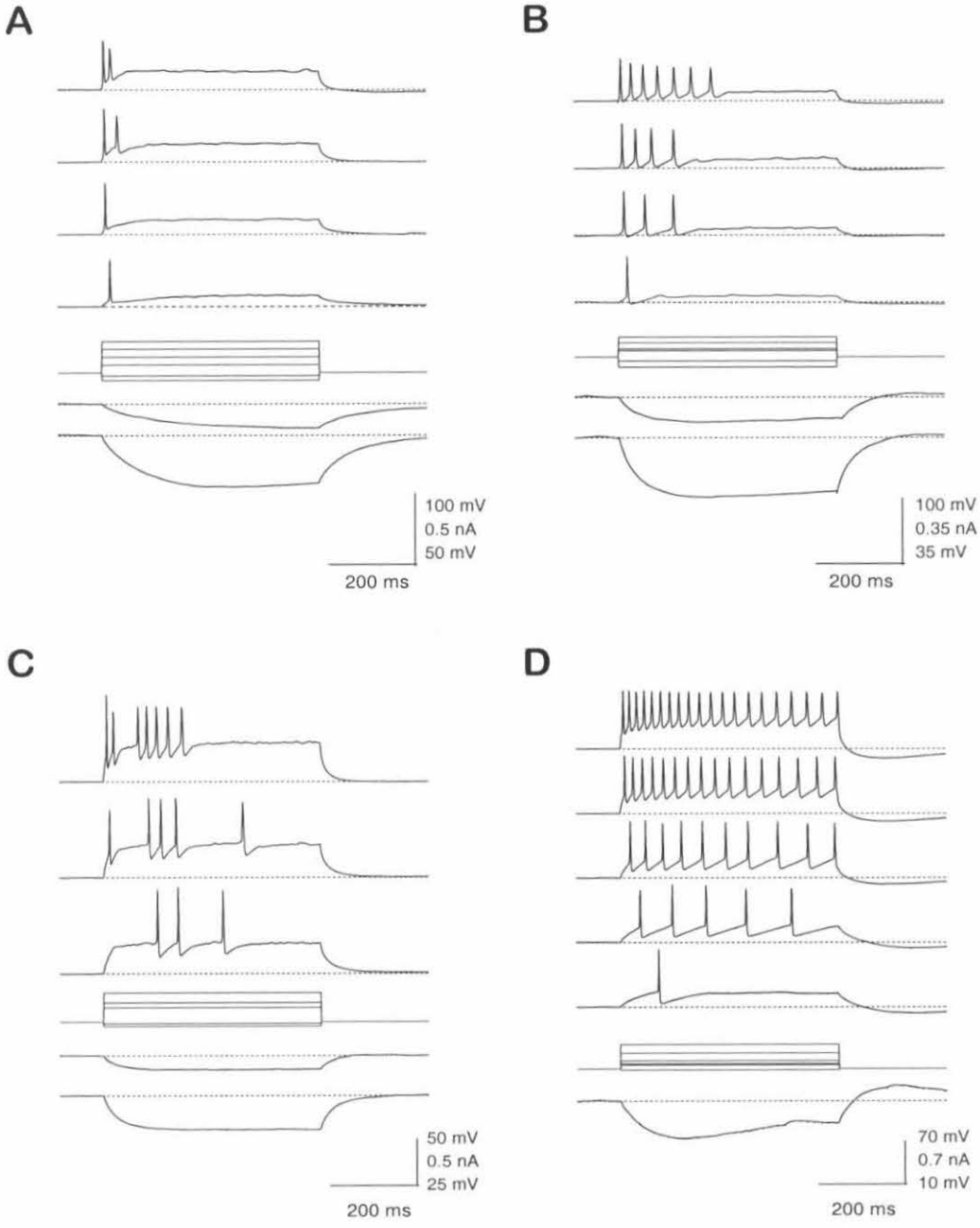
A
100 mV
0.5 nA
50 mV
200 ms
B
100 mV
0.35 nA
35 mV
200 ms
C
50 mV
0.5 nA
25 mV
200 ms
D
70 mV
0.7 nA
10 mV
200 ms

E

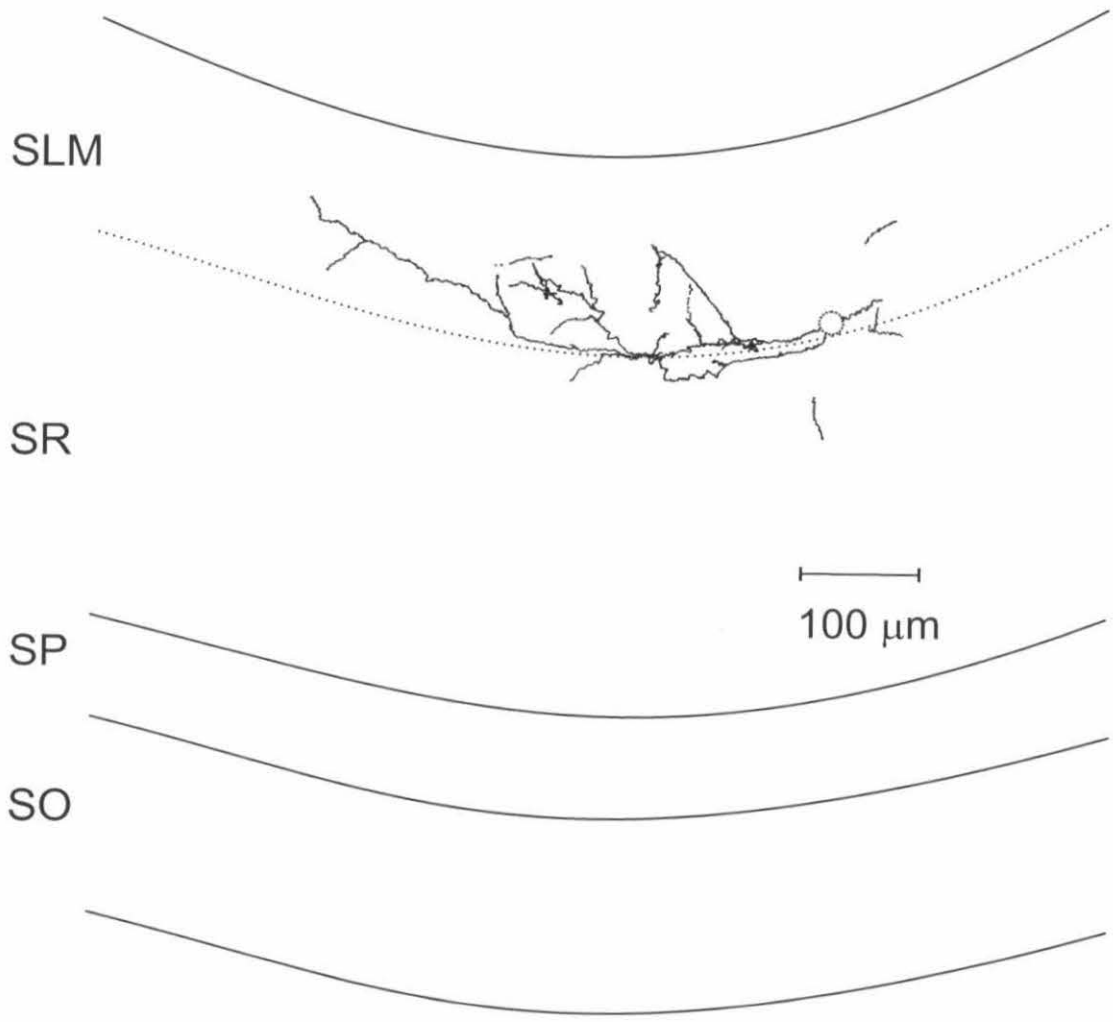

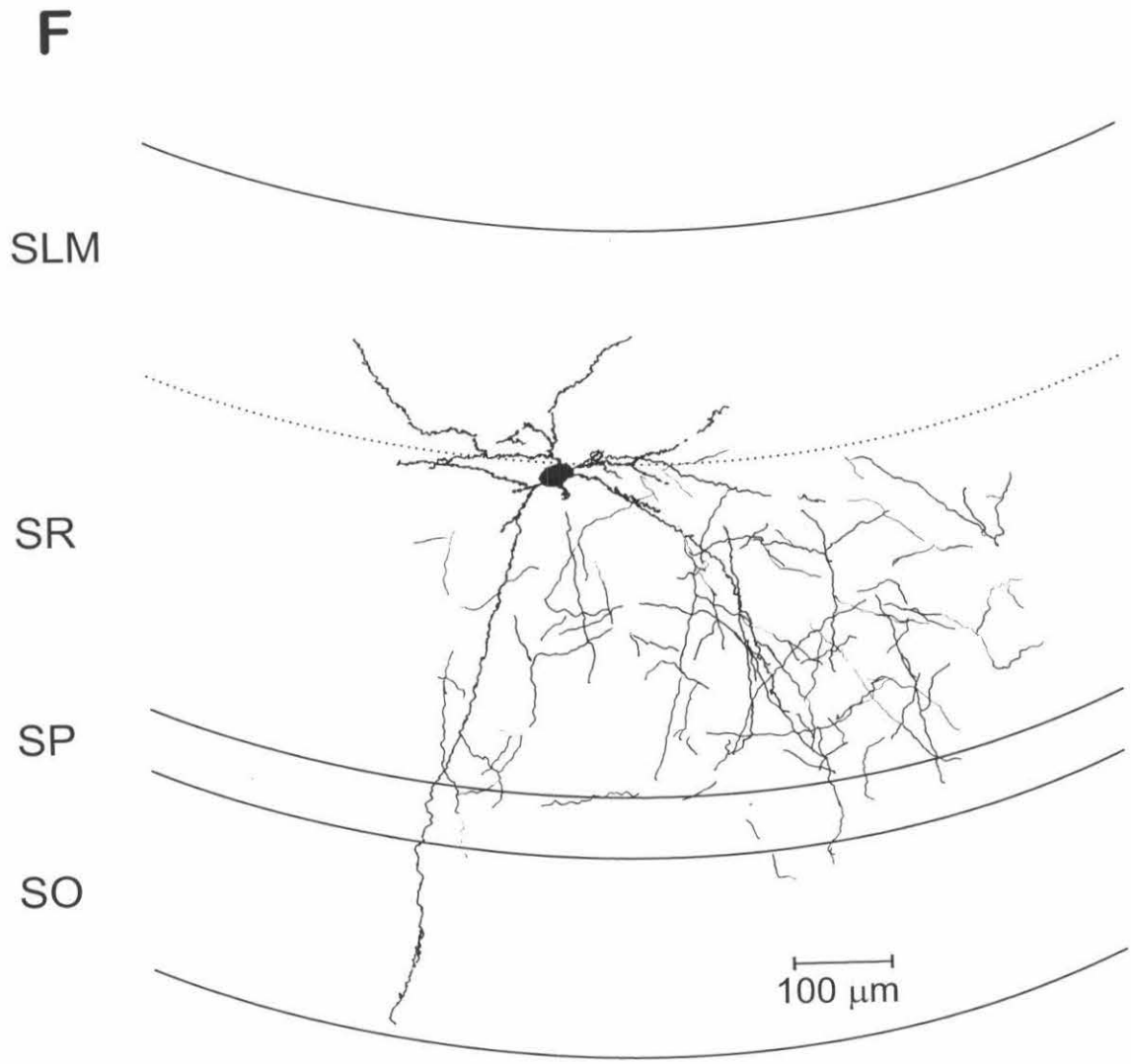
F
SLM
SR
SP
SO
100 μm

Figure 16. Voltage-dependent behavior in three SLM interneurons. At depolarized potentials, the neurons at the left and in the middle showed oscillatory behavior, while the one at right did not.

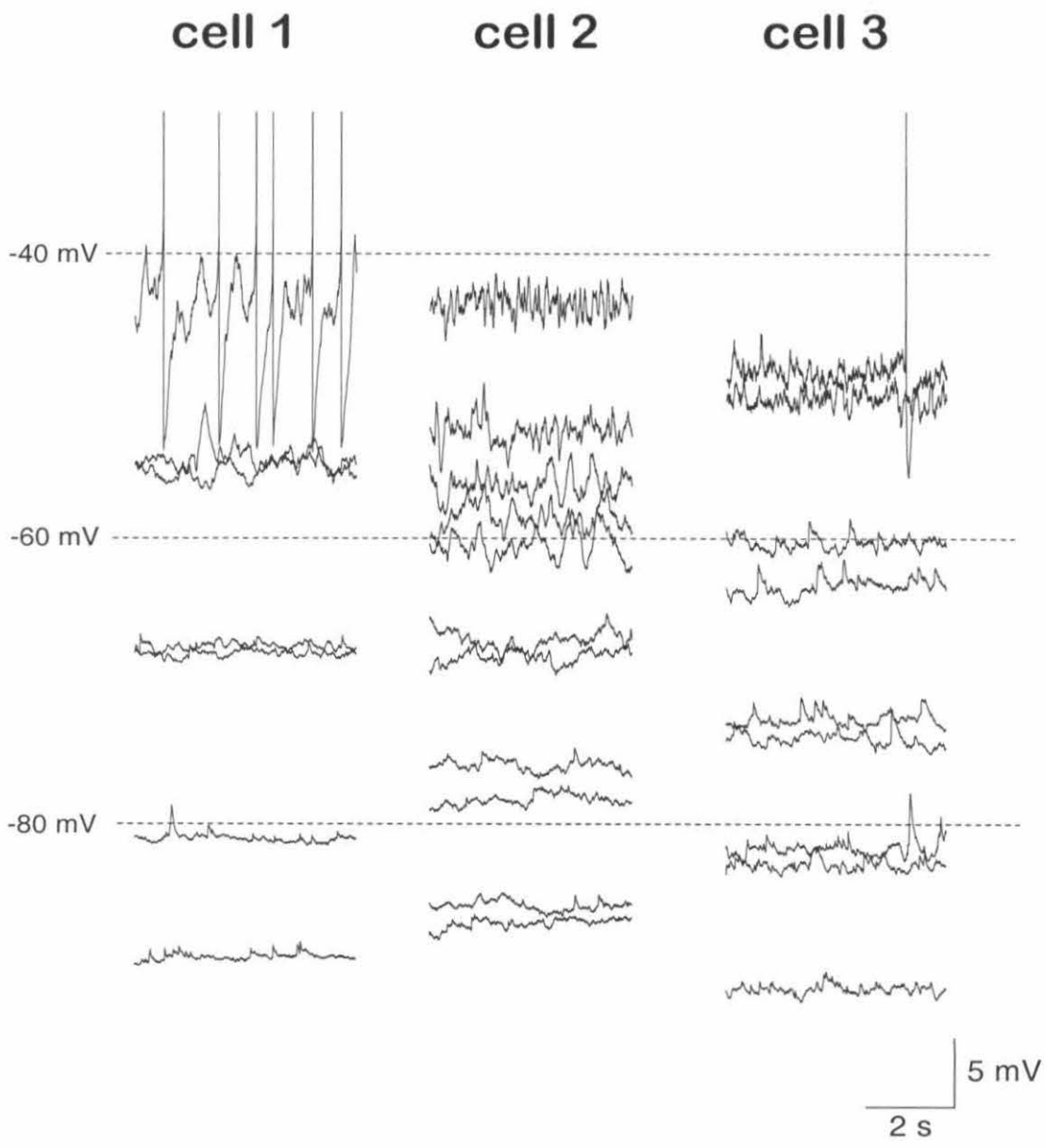
cell 1
cell 2
cell 3
-40 mV
-60 mV
-80 mV
5 mV
2 s

Figure 17. Responses of SLM interneurons to TA and SC stimulation. *A*, responses to SC (left, black) and TA (middle, red) stimulation; responses overlaid at right. *B*, voltage-dependence of SC (left) and TA (right) synaptic responses; at depolarized potentials, a fast IPSP is visible in the response. *C*, examples of voltage-dependent depolarizations following the EPSP in response to SC (left) and TA (right) stimulation, in two different interneurons. *D*, long-lasting depolarization following high-frequency stimulation in the SC pathway. Response to single stimulus, red; response to 10 stimuli at 100 Hz, black.

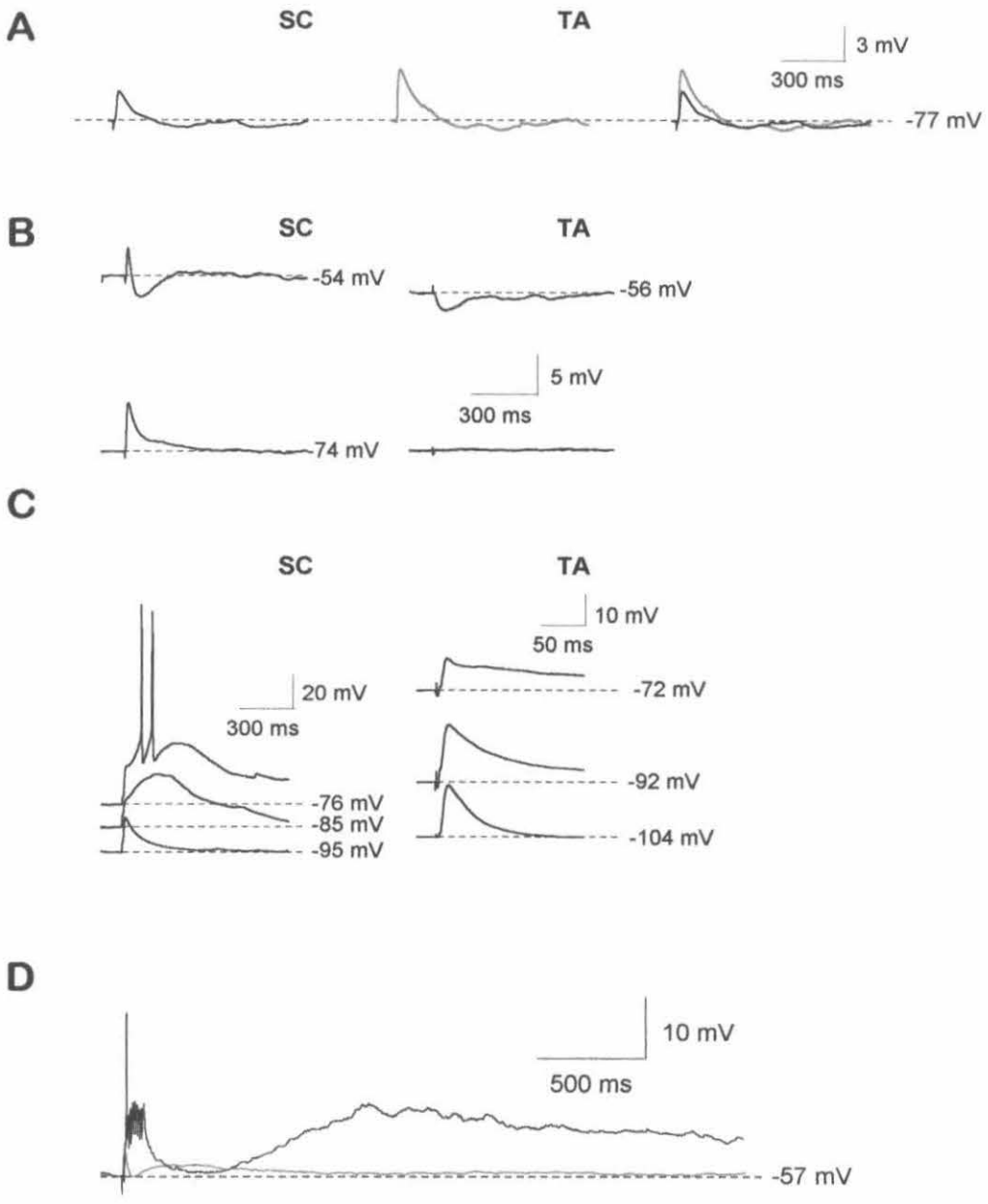
A
SC
TA
3 mV
300 ms
-77 mV
B
SC
TA
-54 mV
-56 mV
5 mV
300 ms
-74 mV
C
SC
TA
10 mV
50 ms
20 mV
300 ms
-72 mV
-76 mV
-92 mV
-85 mV
-95 mV
-104 mV
D
10 mV
500 ms
-57 mV

Figure 18. Putative polysynaptic responses in an SLM interneuron. Top, representative responses to TA (top) and SC (bottom) stimulation in regular ACSF (left), high-divalent solution (middle), and washout with regular ACSF (right). Bottom, scatter plot of the number of distinguishable EPSPs in each response to TA (top) or SC (bottom) solution; shaded bar shows period of application of high-divalent ACSF but does not compensate for delay in perfusion medium reaching the recording chamber.

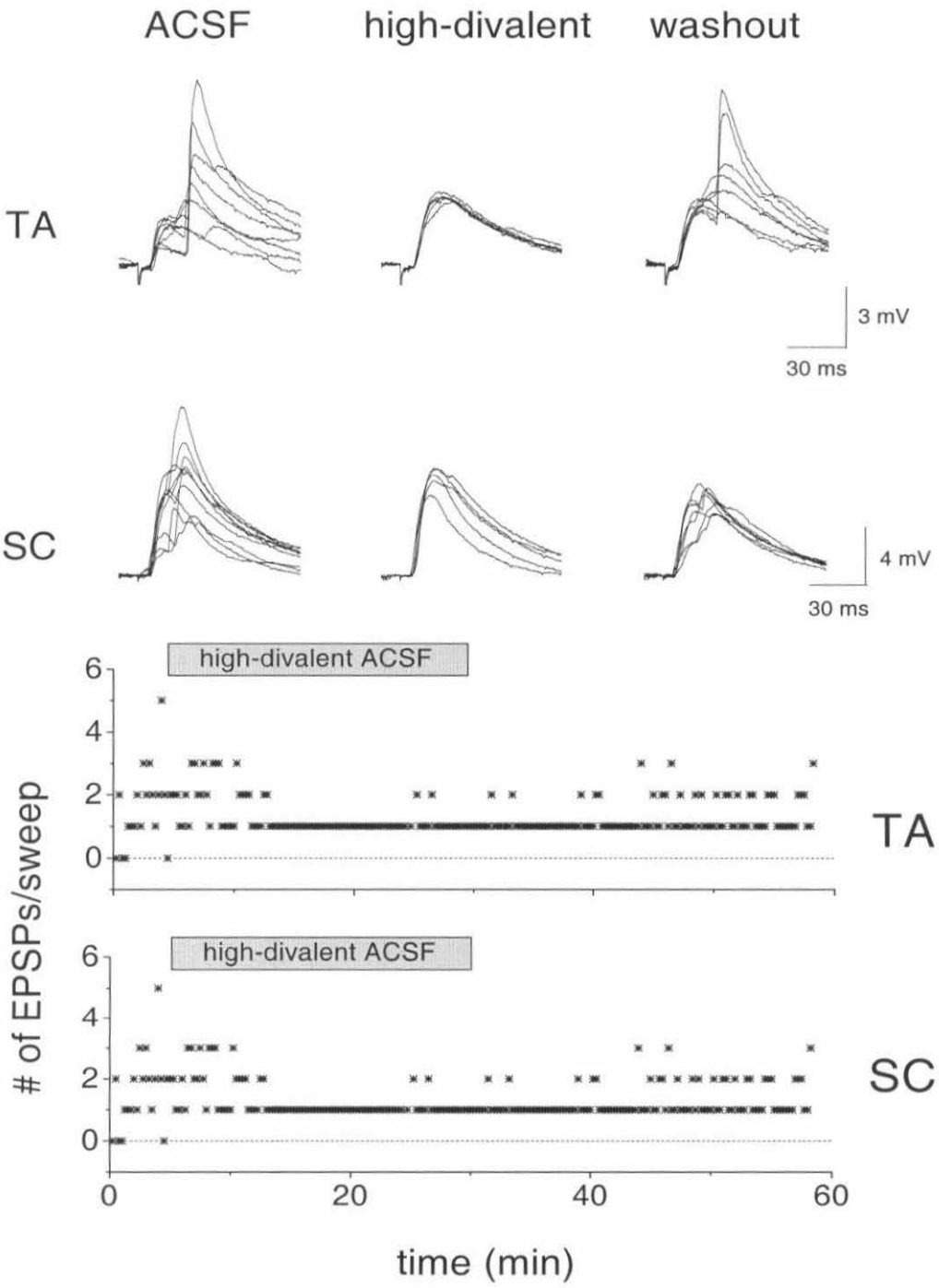
ACSF
high-divalent
washout
TA
3 mV
30 ms
SC
4 mV
30 ms
high-divalent ACSF
high-divalent ACSF
# of EPSPs/sweep
TA
SC
0
2
4
6
0
20
40
60
time (min)

Figure 19. Frequency dependence of the response of an SLM interneuron to SC stimulation. *A*, times to peak for each EPSP relative to each stimulus, at 5, 10, 15 and 25 Hz. *B*, peak amplitudes for each EPSP relative to the first, at 5, 10, 15 and 25 Hz. *C*, representative traces of the pyramidal cell response to SC stimulation at 5, 10, 15 and 25 Hz.

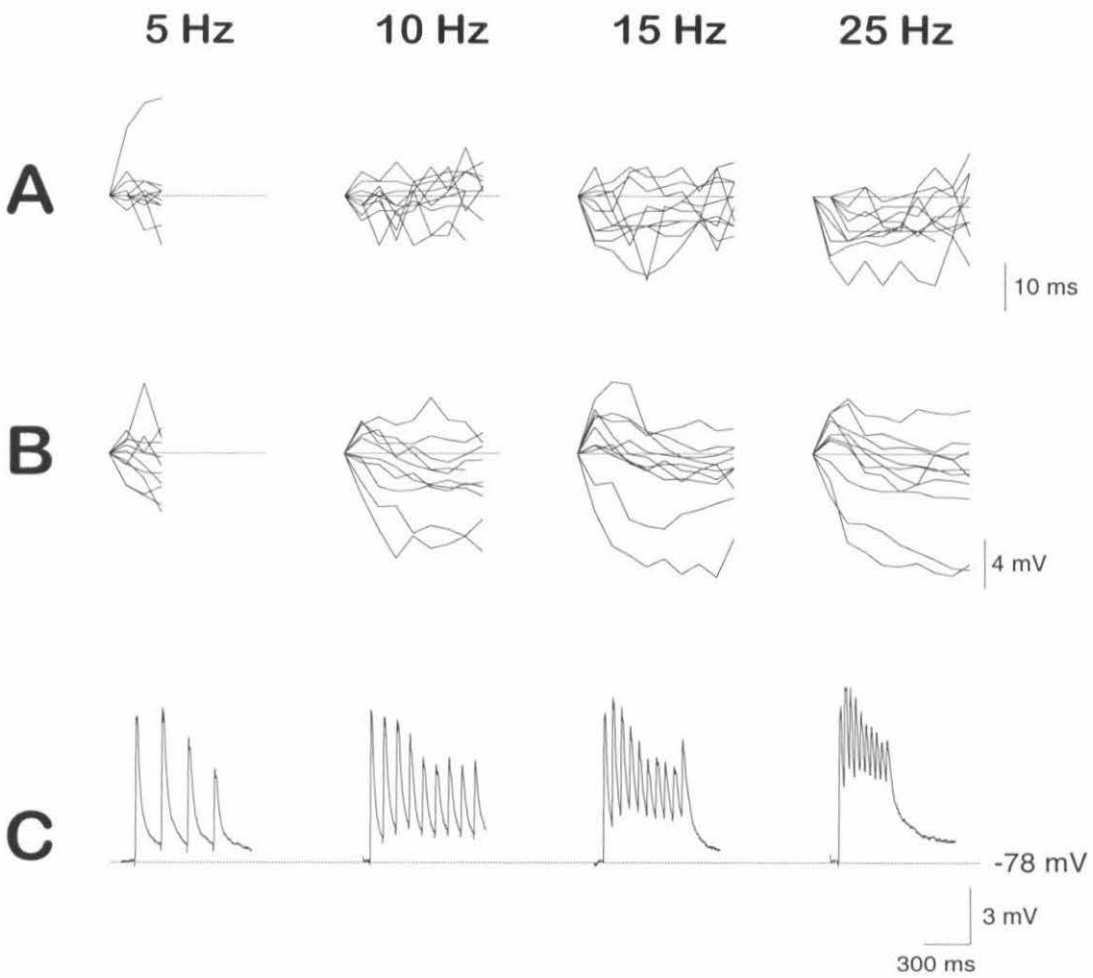
5 Hz
10 Hz
15 Hz
25 Hz
A
10 ms
B
4 mV
C
-78 mV
3 mV
300 ms

Figure 20. Frequency dependence of the response of an SLM interneuron to TA stimulation. *A*, times to peak for each EPSP relative to each stimulus, at 5, 10, 15 and 25 Hz. *B*, peak amplitudes for each EPSP relative to the first, at 5, 10, 15 and 25 Hz. *C*, representative traces of the pyramidal cell response to SC stimulation at 5, 10, 15 and 25 Hz. Data from the same cell as Figure 19.

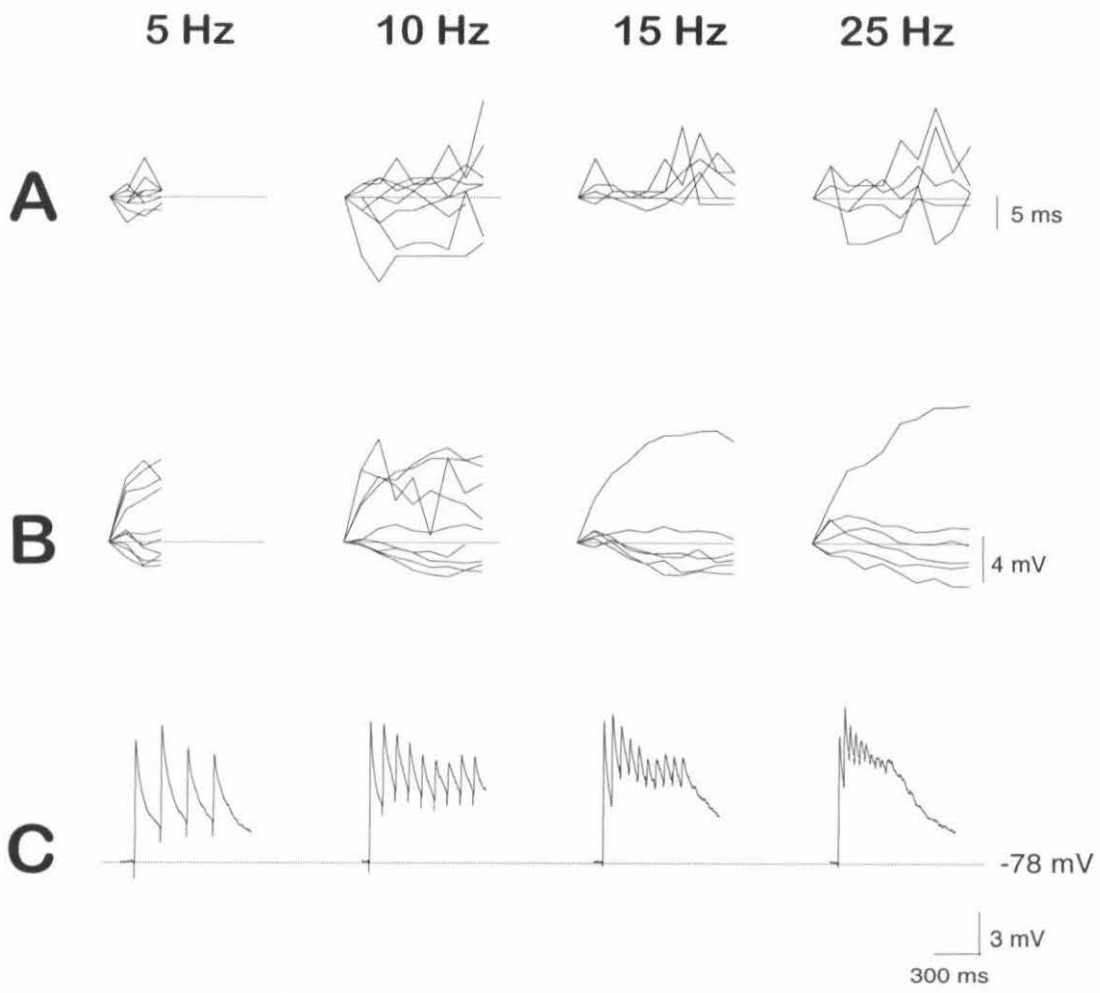
5 Hz
10 Hz
15 Hz
25 Hz
A
5 ms
B
4 mV
C
-78 mV
3 mV
300 ms

Figure 21. Two SLM interneurons (*A* and *B*) showing sufficient frequency facilitation to be driven to spike by repeated TA stimulation at various frequencies. Stimulus artifacts digitally removed for clarity.

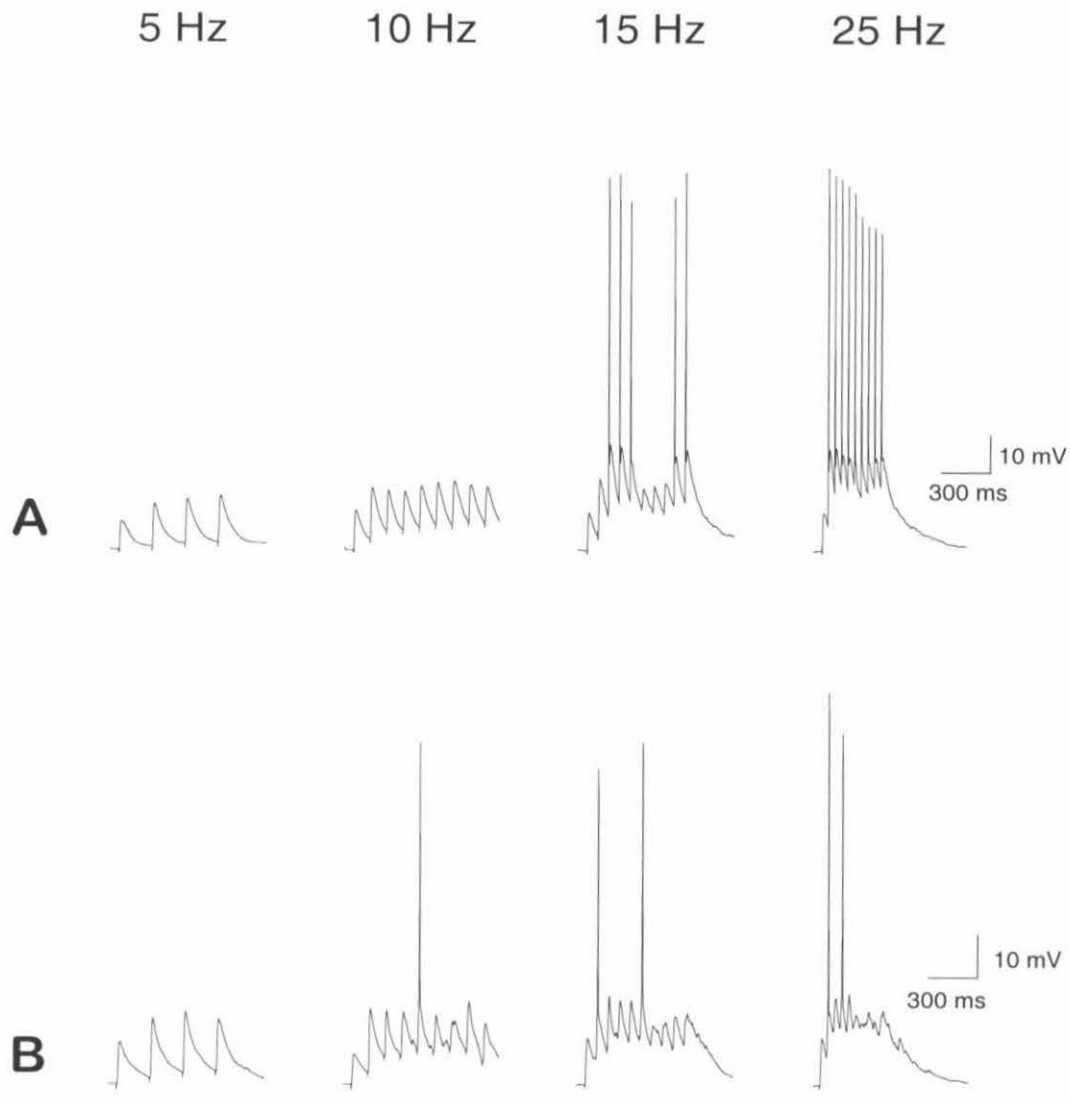
5 Hz
10 Hz
15 Hz
25 Hz
A
10 mV
300 ms
B
10 mV
300 ms

Figure 22. Intrinsic electrophysiological properties and morphology of SR giant cells. *A*, reconstruction of an SR giant cell with typical Y-shaped soma and primary dendrites. The axon of this cell was not recovered. *B*, reconstruction of an SR giant cell more closely resembling a pyramidal cell in morphology. The processes extending to SO are probably the axon and collaterals. *C*, responses of an SR giant cell to depolarizing and hyperpolarizing current injection. Vertical scale is top value for responses to depolarizing current, middle value for current steps, bottom value for responses to hyperpolarizing current.

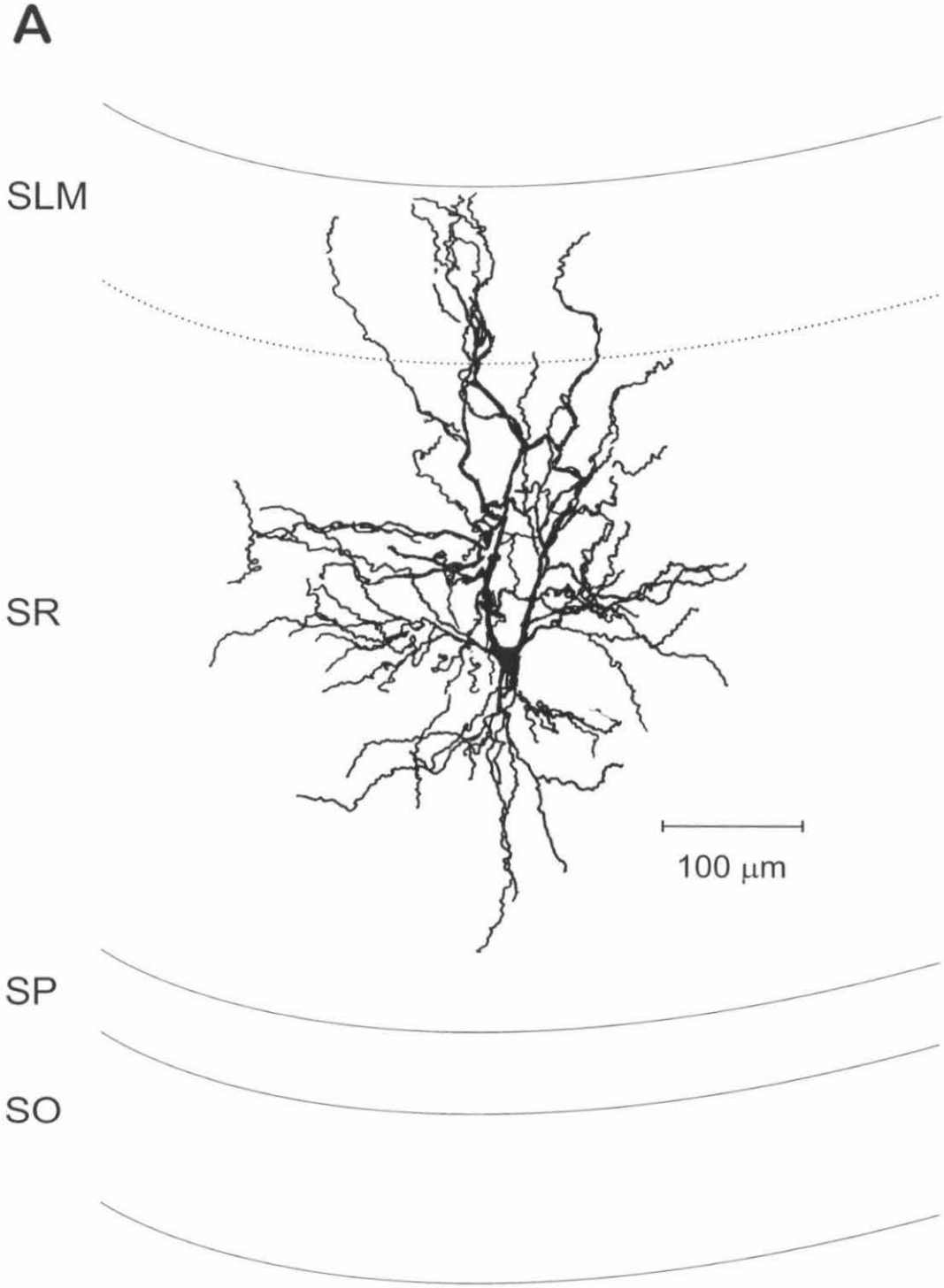
A
SLM
SR
SP
SO
100 μm

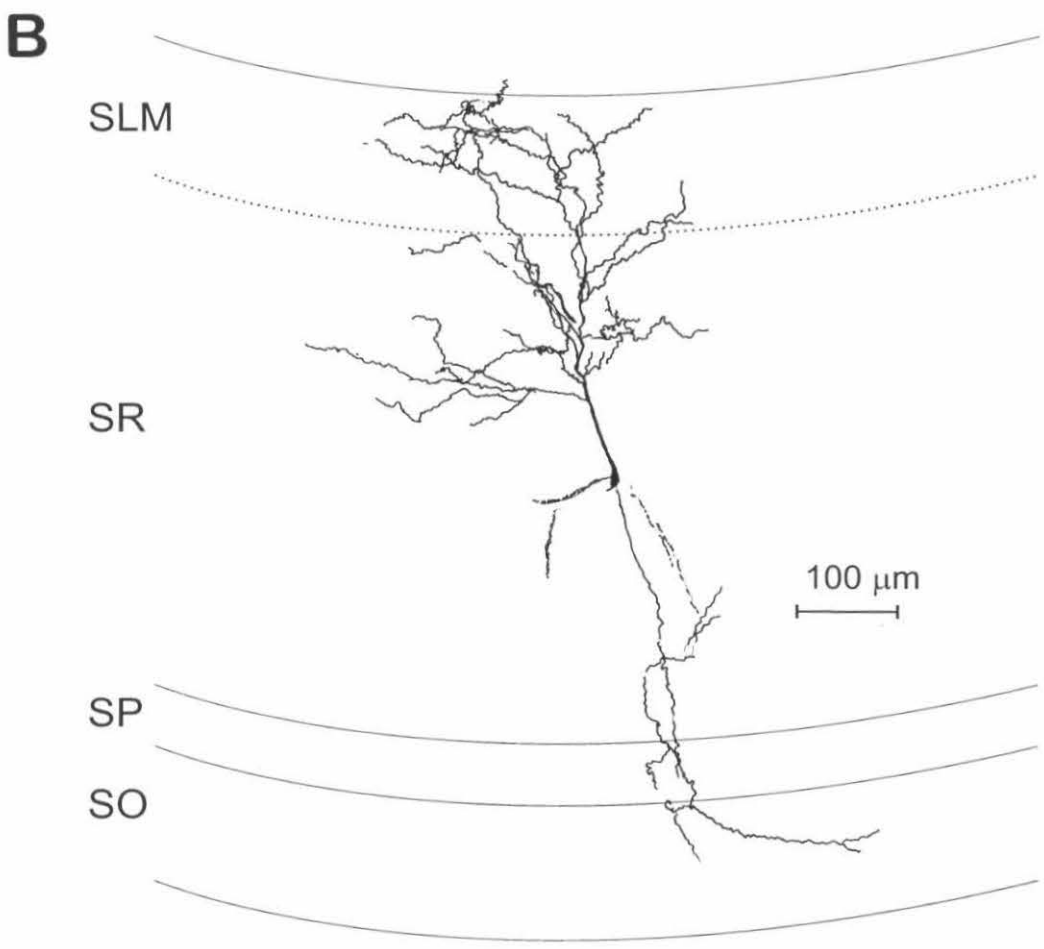
B
SLM
SR
SP
SO
100 μm

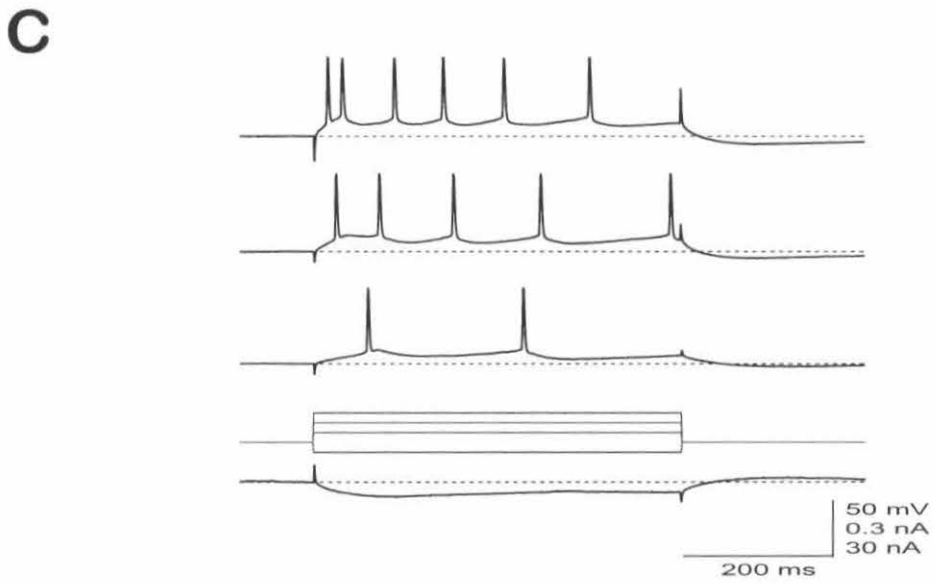
C
50 mV
0.3 nA
30 nA
200 ms

Figure 23. Responses of SR giant cells to SC and TA stimulation. *A*, responses to SC (left, black) and TA (middle, red) stimulation; responses shown overlaid at right. *B*, SC (left) and TA (right) EPSPs (black) are eliminated by the glutamate receptor antagonists CNQX (10 μM) and AP5 (50 μM) (red). *C*, voltage-dependence of PSPs in SR giant cells, showing the appearance of a fast IPSP at depolarized membrane potentials.

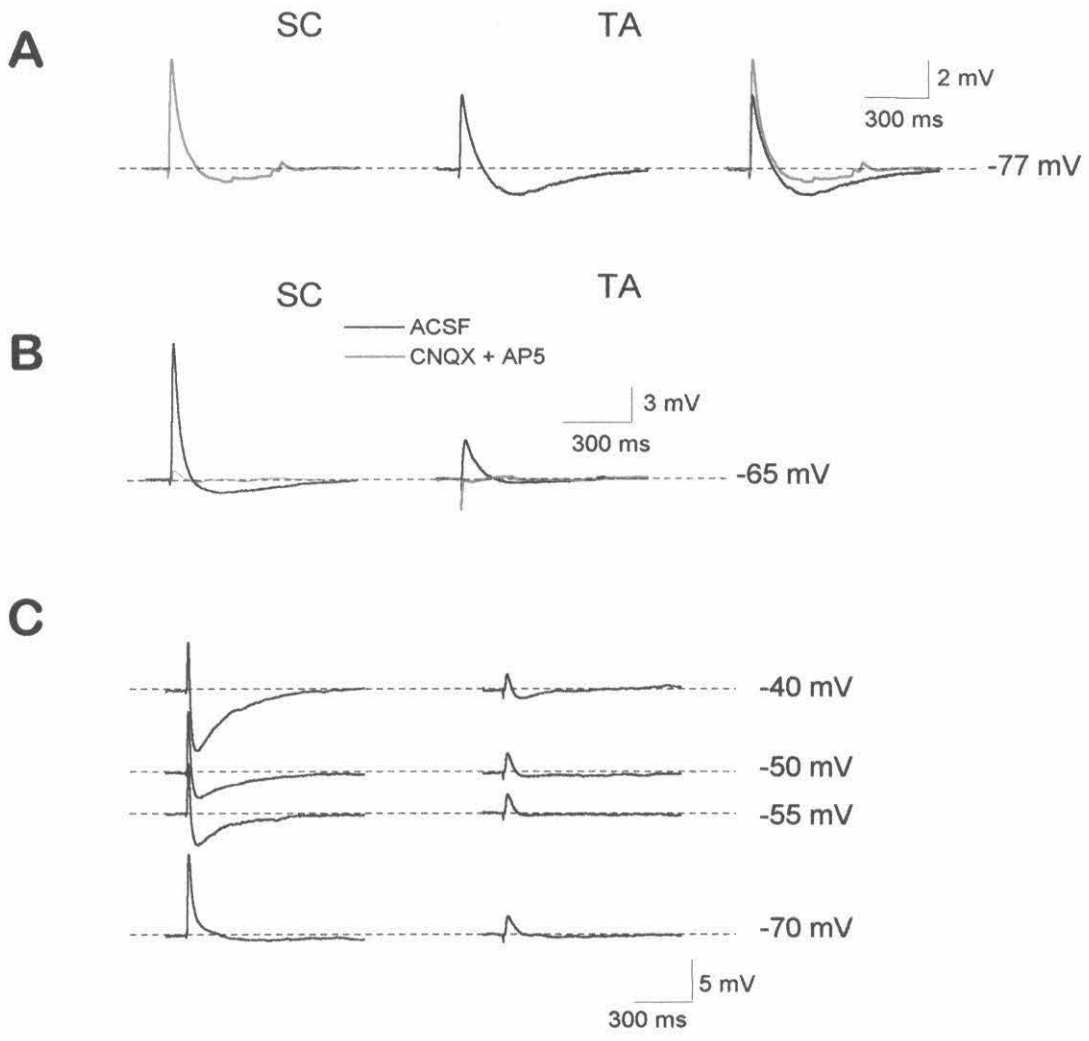
A
SC
TA
2 mV
300 ms
-77 mV
B
SC
TA
ACSF
CNQX + AP5
3 mV
300 ms
-65 mV
C
-40 mV
-50 mV
-55 mV
-70 mV
5 mV
300 ms

Figure 24. Frequency dependence of the response of an SR giant cell to SC stimulation. *A*, times to peak for each EPSP relative to each stimulus, at 5, 10, 15 and 25 Hz. *B*, peak amplitudes for each EPSP relative to the first, at 5, 10, 15 and 25 Hz. *C*, representative traces of the pyramidal cell response to SC stimulation at 5, 10, 15 and 25 Hz.

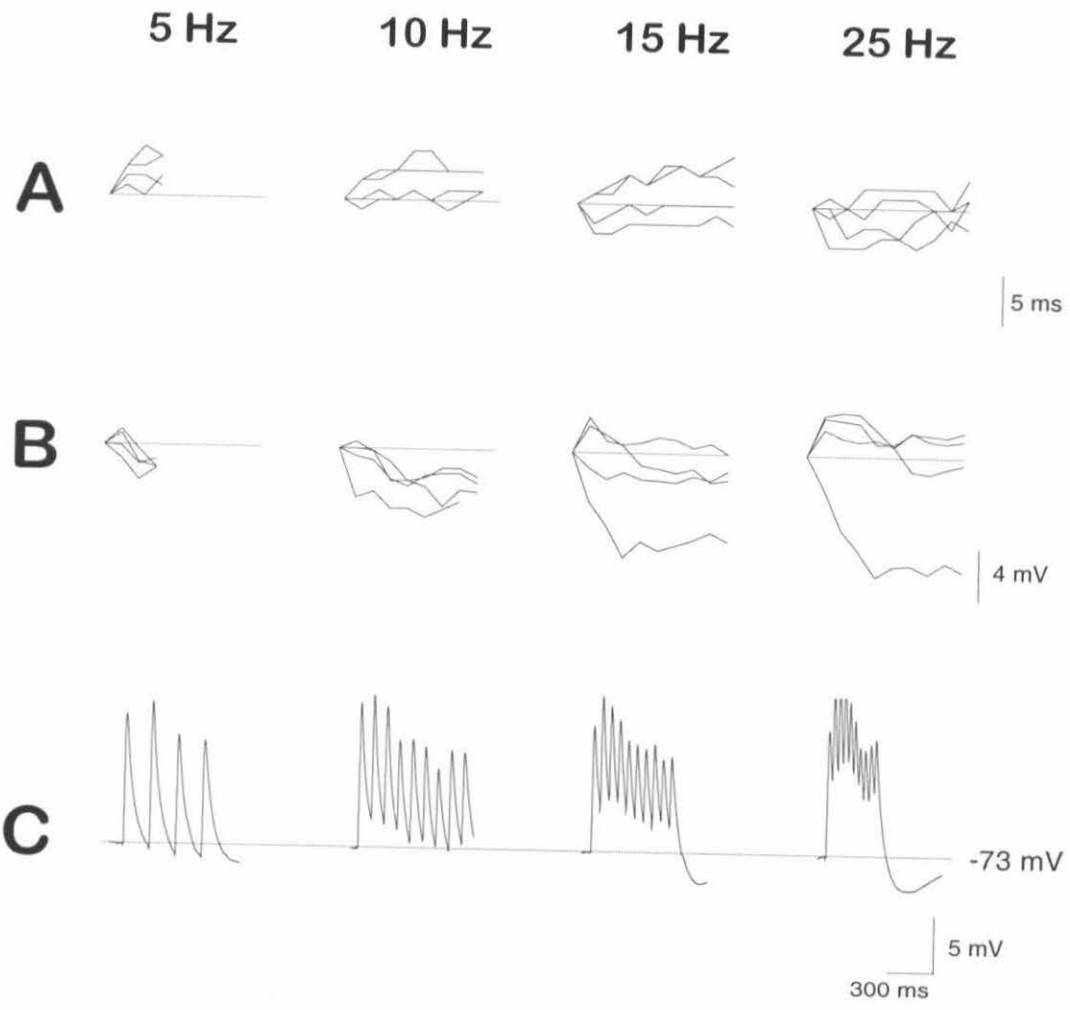
5 Hz
10 Hz
15 Hz
25 Hz
A
5 ms
B
4 mV
C
-73 mV
5 mV
300 ms

Figure 25. Frequency dependence of the response of a pyramidal cell to TA stimulation. *A*, times to peak for each EPSP relative to each stimulus, at 5, 10, 15 and 25 Hz. *B*, peak amplitudes for each EPSP relative to the first, at 5, 10, 15 and 25 Hz. *C*, representative traces of the pyramidal cell response to SC stimulation at 5, 10, 15 and 25 Hz. Data from the same cell as Figure 24.

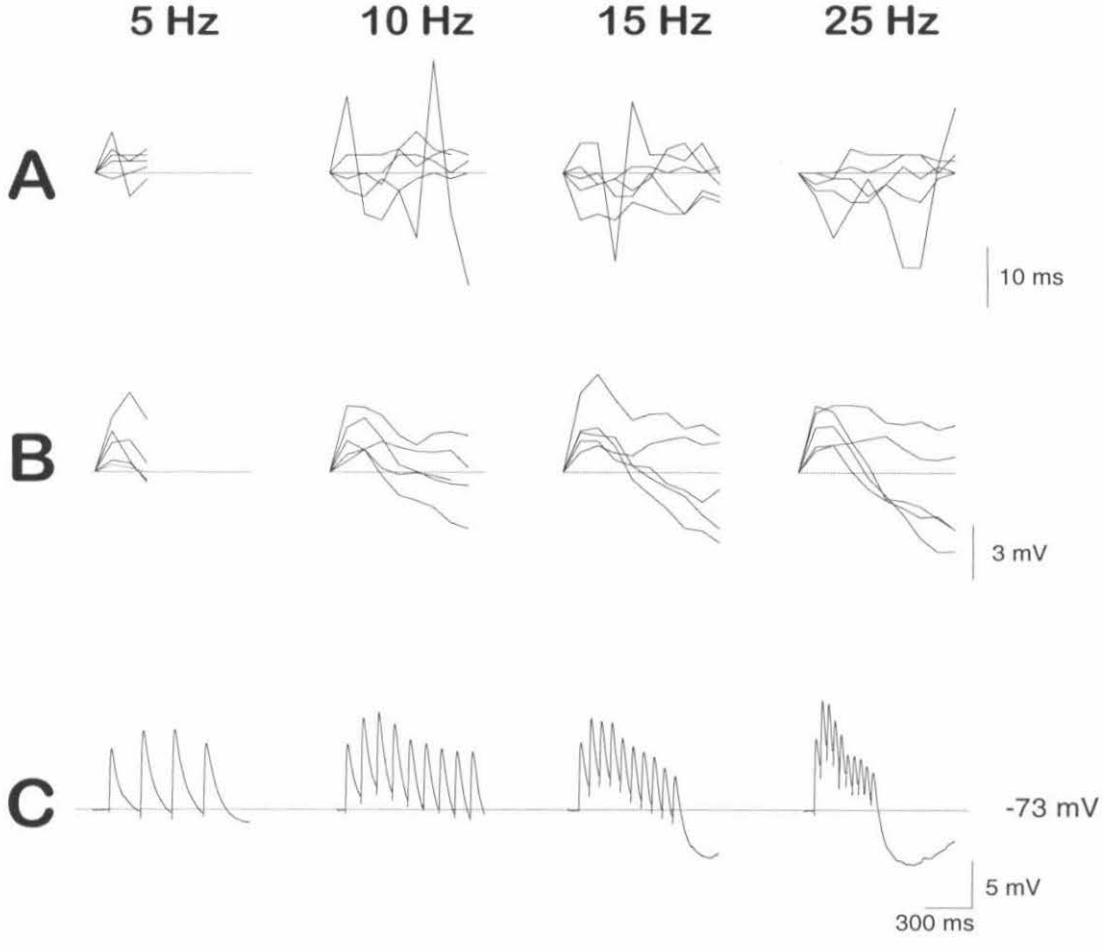
5 Hz
10 Hz
15 Hz
25 Hz
A
10 ms
B
3 mV
C
-73 mV
5 mV
300 ms

3 Long-term depression (LTD) of the temporoammonic pathway

Published: Dvorak-Carbone, H. and Schuman, E.M. 1999. Journal of Neurophysiology 81 (3):1036-1044.

3.1 Abstract

The temporoammonic pathway, the direct projection from layer III of the entorhinal cortex to area CA1 of the hippocampus, includes both excitatory and inhibitory components that are positioned to be an important source of modulation of the hippocampal output. However, little is known about synaptic plasticity in this pathway. We used field recordings in hippocampal slices prepared from mature (6-8 week old) rats to study long-term depression (LTD) in the temporoammonic pathway. Low-frequency (1 Hz) stimulation (LFS) for ten minutes resulted in a depression of the field response that lasted for at least an hour. This depression was saturable by multiple applications of LFS. LTD induction was unaffected by the blockade of either fast ($GABA_A$) or slow ($GABA_B$) inhibition. Temporoammonic LTD was inhibited by the presence of the NMDA receptor antagonist AP5, suggesting a dependence on calcium influx. Full recovery from depression could be induced by high-frequency (100 Hz) stimulation (HFS); in the presence of the $GABA_A$ antagonist bicuculline, HFS induced recovery above the original baseline level. Similarly, HFS or theta-burst stimulation (TBS) applied to naive slices caused little potentiation, whereas HFS or TBS applied in the

presence of bicuculline resulted in significant potentiation of the temporo-ammonic response. Our results show that, unlike the Schaffer collateral input to CA1, the temporoammonic input in mature animals is easy to depress but difficult to potentiate.

3.2 Introduction

The hippocampus is a brain structure that plays a critical role in learning and memory (Press *et al.* 1989; Zola-Morgan and Squire 1990; Squire and Zola-Morgan 1991; Eichenbaum *et al.* 1992). The fundamental information processing pathway in the hippocampus is usually considered to be the trisynaptic circuit, in which the entorhinal cortex sends a perforant path projection to the granule cells of the dentate gyrus, which send mossy fibers to the pyramidal cells of the CA3 region, which send Schaffer collaterals to the CA1 pyramidal cells, which then project back to the entorhinal cortex (Andersen *et al.* 1966; Brown and Zador 1990). These projections are all glutamatergic and excitatory (Andersen 1975; Misgeld 1988). Within each region there are local GABAergic interneurons which provide feed-forward and feedback inhibition (e.g., see Ribak and Seress 1983; Lacaille *et al.* 1989; Woodson *et al.* 1989; Freund and Buzsáki 1996).

However, there is more to hippocampal processing than this simple trisynaptic loop. In particular, there is a direct projection from entorhinal cortex to area CA1, effectively bypassing the first two stages of the conventional circuit. This projection has been referred to as the temporoammonic pathway (Ramón y Cajal 1911; Maccaferri and McBain 1995) because of its origins in the entorhinal cortex (in the temporal lobe) and its termination in CA1, part of the *cornu ammonis* of the hippocampus. Unlike the perforant

path, which consists of axons from stellate excitatory neurons of layer II of the entorhinal cortex, the temporoammonic pathway consists of axons from pyramidal cells of layer III of the entorhinal cortex (Steward and Scoville 1976). These temporo-ammonic axons terminate preferentially in the area of the distal dendrites of the pyramidal cells, stratum lacunosum-moleculare (SLM). These axons make asymmetric (and hence probably excitatory) synapses, more than 90% of which are onto the spines of CA1 pyramidal cells (Desmond *et al.* 1994). Temporoammonic axons also synapse onto the inhibitory basket and chandelier cells of CA1 (Kiss *et al.* 1996) and are likely to innervate the interneurons of stratum lacunosum-moleculare (Lacaille and Schwartzkroin 1988a; Vida *et al.* 1998).

There is some controversy as to whether the temporoammonic input to the hippo-campus is primarily excitatory or primarily inhibitory (see Soltesz and Jones 1995). Field recordings *in vitro* (Doller and Weight 1982; Colbert and Levy 1992) and *in vivo* (Yeckel and Berger 1990; Leung *et al.* 1995; Yeckel and Berger 1995) reveal a population excitatory postsynaptic potential (EPSP) in SLM following stimulation of the temporo-ammonic pathway, supporting the ultrastructural evidence for an excitatory input onto the distal dendrites of CA1 neurons. Intracellular recordings (Empson and Heinemann 1995b), however, show a mixed response, including a monosynaptic glutamatergic EPSP and a disynaptic inhibitory postsynaptic potential (IPSP) with both $GABA_A$ and $GABA_B$ components.

Various forms of short- and long-term plasticity have been extensively studied at all three synapses in the trisynaptic circuit of the hippocampus (Bliss and Collingridge 1993). As yet, however, relatively little is known about plasticity in the temporo-

ammonic pathway, whose activity can modulate plasticity in the Schaffer collateral pathway to CA1 (Levy *et al.* 1998) and whose position in the hippocampal circuitry suggests a potent role in the modulation of hippocampal output from CA1. A previous study reported induction of LTP in this pathway *in vitro* only when fast inhibition was blocked by addition of the $GABA_A$ antagonist bicuculline (Colbert and Levy 1993); *in vivo,* LTP of the excitatory current sink in the distal dendrites of area CA1 evoked by stimulation of the perforant path (including temporoammonic axons) was reported following tetanic stimulation (Leung *et al.* 1995). In this study we report that long-term depression (LTD) can readily be induced in the temporoammonic pathway, in slices prepared from mature rats, by means of low-frequency stimulation. Some of these results have previously appeared in abstract form (Dvorak and Schuman 1996).

3.3 Methods

3.3.1 Slice preparation

3.3.1.1 Dissection

Slices were prepared from 6-8 week old male Sprague-Dawley rats. All use of animals was performed according to the guidelines of the Caltech Institutional Animal Care and Use Committee. Rats were decapitated following Halothane anesthesia, and the brain rapidly removed to ice-cold, oxygenated artificial cerebrospinal fluid (ACSF: 119 mM NaCl; 2.5 mM KCl; 1.3 mM $MgSO_4$; 2.4 mM $CaCl_2$; 1.0 mM NaH_2PO_4; 26.2 mM $NaHCO_3$; 11.0 mM glucose). The dorsal surface of the posterior half of each hemisphere was glued onto the stage of a cooled oscillating tissue slicer (OTS-3000-04; FHC) and

covered with chilled ACSF. 500 μm slices were cut, with the optimal slices (as assessed visually, by ease of identification of distinct layers, as well as electrophysiologically, by the presence of robust field potentials) generally found 4-4.5 mm below the ventral surface. The extraneous cortical and subcortical tissue was gently dissected away with the small end of a spatula. (A small number of early experiments were done on slices prepared with a Stoelting tissue chopper. However, slices prepared on the tissue slicer had larger temporoammonic responses.) The slices were then allowed to recover in an interface chamber at room temperature for at least one hour before experiments were started. Further microdissection (see below) was performed either in ice-cold ACSF immediately following slice preparation, or in the recording chamber prior to the start of the experiment. All electrophysiology was done with the slices submerged and constantly perfused with oxygenated ACSF at room temperature.

3.3.1.2 Minislice preparation

In order to clearly isolate the temporoammonic response, it was necessary to further dissect the slice (see Figure 3). The entire dentate gyrus was removed, to eliminate the possibility of activation of the trisynaptic pathway, and to prevent contamination of a field response recorded in SLM by the much larger field elicited in dentate gyrus by concurrent activation of the perforant path. In most experiments, including all those in which bicuculline was used, CA3 was also removed to prevent induction of seizure-like activity as well as to eliminate the possibility of disynaptic activation via the perforant path projection to CA3. Also, a cut was made through stratum radiatum (SR) in distal

CA1 (near the subiculum) perpendicular to the cell body layer, in order to prevent antidromic activation of Schaffer collaterals by the stimulating electrode in SLM (see Figure 1). Schaffer collaterals do not enter SLM to any appreciable extent (Amaral and Witter 1989) so this cut cleanly isolates temporoammonic axons.

3.3.2 Electrophysiology

3.3.2.1 Field recording

Bipolar tungsten electrodes, either concentric or paired needles, were used for stimulation. One electrode was placed in SR to stimulate the Schaffer collaterals; the other in SLM to stimulate the temporoammonic pathway (Figure 3). Stimulus pulses were 100 μs long, monophasic, and ranged from 10-100 μA in the Schaffer collateral pathway and 100-200 μA in the temporoammonic pathway. Stimulus intensities were selected to produce submaximal responses with no population spike. Field recordings were made with low-resistance micropipettes filled with 3M NaCl. The Schaffer collateral response was recorded in SR and the temporoammonic response in SLM. Separation of the two pathways was further confirmed by the observation of a positive-going field potential in the other layer (Figure 3) (Colbert and Levy 1992).

The following stimulation paradigms were used: high frequency stimulation (HFS) = 100 Hz for 1 s, repeated 4X at 20-30 s intervals; theta burst stimulation (TBS) = 4 bursts of 5 pulses at 100 Hz, 200 ms between bursts, repeated 4X at 20-30 s intervals; low-frequency stimulation (LFS) = 1 Hz stimulation for 10 min. All stimulus pulses were of the same length and amplitude as test pulses. Test pulses were applied once

every 20 or 30 seconds to each pathway. The initial slope of the field potential, following the end of the fiber volley, was measured.

3.3.2.2 Drugs applied

Drugs were applied by dilution of concentrated stock solutions into the perfusion medium. Stock solutions were made up in water, with the exception of nifedipine, which was prepared in DMSO (1000X) and stored protected from light. Experiments using nifedipine were performed in low light. CGP 55845A was a kind gift from Novartis (Basel, Switzerland); all other drugs were obtained from Sigma (St. Louis, MO).

3.3.3 Data acquisition and analysis

Data were collected directly onto an IBM-compatible computer using in-house software. All numerical values are listed as mean ± SE, unless otherwise stated. Depression and potentiation were measured by taking an average of the initial slopes of the field excitatory postsynaptic potentials (fEPSPs) over ten minute periods immediately before and 20-30 or 50-60 minutes after the end of LFS, HFS, or TBS. Student's paired t-test was used to determine statistical significance for within-group comparisons; the unpaired t-test was used between groups. Results from each experimental manipulation were compared to the same control group. P values greater than 0.05 are reported in the text as not significant (NS). Points in figures represent mean ± SE across all experiments; each point is the average of data taken over five minutes. Representative traces, shown in insets, are averages of five consecutive sweeps from a representative exper-

iment, taken five minutes before LFS, HFS, or TBS, and 25 minutes after the end of LFS, HFS or TBS.

3.4 Results

3.4.1 Long-term depression

3.4.1.1 The TA field response is depressed by low frequency stimulation

When low-frequency stimulation (LFS; see Methods) was applied to the temporoammonic pathway in normal ACSF, the response was significantly depressed (Figure 26A) (mean percent of baseline at 30-40 min, 75.9 ± 3.4%, n = 26, $p < 0.0001$). This synaptic depression persisted for at least an hour (mean percent of baseline at 60-70 min, 73.7 ± 5.0%, n = 7, $p < 0.01$) and was not accompanied by any significant changes in the size of the presynaptic fiber volley (Figure 26A).

During the application of LFS to the temporoammonic pathway, the Schaffer collateral pathway was not stimulated; during the rest of the experiment, test pulses were applied to the Schaffer collateral pathway at the same frequency as to the temporoammonic pathway. Synaptic strength in the Schaffer collateral pathway was not affected while the temporoammonic response was depressed by LFS (Figure 26A) (mean percent of baseline at 30-40 min, 95.0 ± 4.7%, n = 9, NS).

LTD has also been observed following LFS of the Schaffer collateral pathway (Mulkey and Malenka 1992), but only in slices prepared from younger animals (Dudek and Bear 1993; Wagner and Alger 1995). When the LFS protocol was applied to the Schaffer collateral pathway in the present study, little or no depression was seen. On

average, a small, but not statistically significant, depression of the response was observed (Figure 26B) (mean percent of baseline at 30-40 min, 87.3 ± 6.2%, n = 8, NS); this trend was due only to results from two slices that were depressed to 55 and 65% of baseline.

To determine whether LTD of the temporoammonic pathway can be saturated, the LFS protocol was applied repeatedly, for 10 minutes every 30 minutes, either four or five times. The response asymptotically approached a level of about 30 to 50% of the original baseline (Figure 26C), reaching its maximally depressed level following 3-4 epochs of LFS.

3.4.1.2 GABA-mediated synaptic transmission is not required for TA LTD

Synaptic depression of the temporoammonic response could be induced in the absence of fast GABAergic inhibition. After the $GABA_A$ antagonist bicuculline (20 μM) was added to the perfusion solution, a slight but not significant increase in the temporo-ammonic field response was generally observed (mean percent of original response 20-25 minutes after bicuculline application, 105 ± 6%, n = 4, NS). The response was allowed to reach a steady baseline for at least 20 minutes before application of LFS. Low frequency stimulation in the presence of bicuculline induced depression of the field response (Figure 27) (mean percent of baseline at 30-40 min, 75.7 ± 2.6%, n = 20, $p < 0.0001$) that was not significantly different from that observed in control slices. This depression lasted at least an hour (mean percent of baseline at 60-70 min, 79.9 ± 3.2%, n = 14, $p < 0.001$).

Depression of the temporoammonic response was also possible in the absence of slow, $GABA_B$-mediated inhibition. Addition of the $GABA_B$ antagonist CGP 55845A (1 μM) had no significant effect on the baseline field potential elicited by temporoammonic stimulation (mean percent of original response 20-25 minutes after CGP 55845A application, 112 ± 7%, n = 5, NS). When LFS was applied in the presence of CGP 55845A, the field response was still significantly depressed (Figure 27) (mean percent of baseline at 30-40 min, 72.7 ± 3.5%, n = 5, $p < 0.01$). This amount of depression was also not significantly different from that seen in control slices.

3.4.1.3 Blockade of NMDA receptor-mediated transmission reduces TA LTD

What are the early signaling events important for establishing temporoammonic LTD? Calcium ion is an important initiator of many short- and long-term plasticity processes in neurons (Katz and Miledi 1968; Delaney *et al.* 1989; Bliss and Collingridge 1993; Neveu and Zucker 1996). LTD induction in other hippocampal pathways has been shown to be NMDA receptor-dependent (Mulkey and Malenka 1992; Cummings *et al.* 1996; Thiels *et al.* 1996). When LFS was applied to the temporoammonic pathway in the presence of the NMDA receptor antagonist DL-2-amino-5-phosphonovaleric acid (AP5; 50 μM), LTD was significantly reduced relative to control ($p < 0.05$) (Figure 28) (mean percent of baseline at 30-40 min, 90.1 ± 5.4%, n = 15, $p < 0.05$; 60-70 min, 91.2 ± 4.8%, n = 5, $p < 0.05$), although a small, but significant amount of residual depression was still observed. It is worth noting that there was variability between experiments: in about half of the experiments, AP5 treatment appeared to block LTD, whereas in the other half, it had little effect. LTD was not blocked further when higher concentrations of AP5 were

used; in the presence of 100 μM AP5, LTD was similarly reduced but not completely blocked (data not shown) (mean percent of baseline at 30-40 min, 88.3 ± 1.5%, n = 3, NS different from depression in 50 μM AP5).

In the hippocampus, some forms of heterosynaptic LTD are dependent on L-type calcium channel activation (Wickens and Abraham 1991; Christie and Abraham 1994). Homosynaptic temporoammonic LTD, however, was not blocked by the presence of the L-type calcium channel blocker nifedipine (20 μM) (data not shown; mean percent of baseline at 30-40 min, 82.6 ± 1.7%, n = 5, $p < 0.05$). The combination of nifedipine and AP5 produced slightly, although not significantly, greater inhibition of temporoammonic LTD than AP5 alone (Figure 28) (mean percent of baseline at 30-40 min, 93.4 ± 4.3% of baseline, n = 7, NS different from AP5 alone, significantly different from baseline ($p < 0.05$)). The block of temporoammonic LTD by AP5 and nifedipine was reversible; when LFS was applied again to slices 30 minutes after washout of the drugs, significant depression was observed (data not shown; mean percent of baseline at 30-40 min, 70.7 ± 4.4%, n = 7, $p < 0.0001$).

3.4.1.4 Blockade of muscarinic receptors does not affect TA LTD

In addition to the temporoammonic projection, stratum lacunosum-moleculare of CA1 also receives a substantial cholinergic input from the medial septum (Matthews *et al.* 1987). Activation of the mAChR has been implicated in other forms of hippocampal synaptic plasticity (Auerbach and Segal 1996). In order to determine whether mAChRs are involved in temporoammonic LTD, we applied LFS in the presence of 1 μM atropine. Atropine itself had no significant effect on the temporoammonic field response. In the

presence of atropine, the temporoammonic field response was depressed to the same extent as in control ACSF (Figure 29) (mean percent of baseline at 30-40 min, 75.1 ± 5.0%, n = 4, NS different from control).

3.4.2 Reversal of temporoammonic LTD

To test whether LTD in the temporoammonic pathway is reversible, high-frequency stimulation (HFS; see Methods) was applied either 30 or 60 minutes after the end of LFS. In experiments conducted in normal ACSF, HFS induced a significant recovery of the depressed synaptic response (Figure 30A) (mean percent of original baseline at 20-30 min, 89.4 ± 3.6%, n = 22, $p < 0.05$). The increase relative to the depressed baseline was 116.3 ± 3.6% of baseline (n = 22, $p < 0.001$). The reversal of LTD was even greater when HFS was applied in the presence of 20 μM bicuculline (Figure 30A) (mean percent of original baseline at 20-30 min, 115.3 ± 4.8%, n = 18, $p < 0.05$). The increase relative to the depressed baseline was 150.1 ± 9.1% of baseline (n = 18, $p < 0.0001$). This difference in response to HFS after LTD is similar to that seen when HFS was applied to naive slices (see below).

Complete reversal of temporoammonic LTD was achieved by repeated application of HFS. In normal ACSF, three applications of HFS at five-minute intervals resulted in a full recovery to the original baseline response, which persisted for an hour after the last HFS (Figure 30B) (mean percent of original baseline at 30-40 min after first HFS, 106.8 ± 9.0%, n = 5, significantly different from depressed level of 76.4 ± 4.5% ($p < 0.01$), NS different from baseline; mean percent of original baseline at 60-70 min,

103.3 ± 6.4%, n=5, significantly different from depressed level ($p < 0.01$), NS different from baseline).

3.4.3 Long-term potentiation

In several hippocampal pathways, high-frequency or theta-burst stimulation can induce long-term potentiation (LTP) (Bliss and Collingridge 1993). When HFS was applied to the temporoammonic pathway in naive slices, little potentiation of the field response was observed (Figure 31A) (mean percent of baseline at 20-30 min, 107.8 ± 7.5%, n = 7, NS). Furthermore, no potentiation was observed when theta-burst stimulation (TBS) was applied (Figure 31B; mean percent of baseline at 20-30 min, 96.3 ± 3.7%, n = 5, NS). In order for LTP to be induced, a certain level of postsynaptic depolarization must be reached in response to the excitatory input; in some pathways, this requires overcoming the inhibition that is concurrently activated (e.g., see Wigström and Gustafsson 1983; Steward *et al.* 1990). The idea that fast inhibitory transmission opposes the induction of LTP in this pathway was tested by using the $GABA_A$ antagonist bicuculline. When HFS was applied to the temporoammonic pathway in the presence of 20 μM bicuculline, significant potentiation was observed (Figure 31A) (mean percent of baseline at 20-30 min, 134.2 ± 6.8%, n = 10, $p < 0.05$). Delivery of TBS in the presence of bicuculline also resulted in significant potentiation (Figure 31B) (mean percent of baseline at 20-30 min, 118.9 ± 7.9%, n = 5, $p < 0.05$), as has been previously observed (Colbert and Levy 1993).

Long-term potentiation induced by HFS in most hippocampal pathways is dependent on the activation of NMDA receptors (Bliss and Collingridge 1993). We

tested whether the potentiation of the temporoammonic pathway seen in the presence of bicuculline required NMDA receptor activation by applying HFS in the presence of both bicuculline (20 μM) and AP5 (50 μM). Under these conditions, HFS did not induce LTP (Figure 31A) (mean percent of baseline at 20-30 min, 104.1 ± 3.3%, n = 4, NS).

3.5 Discussion

We examined the capacity for long-term synaptic modification of the temporoammonic-CA1 pathway in the hippocampus. LTD was consistently induced by simple LFS of the temporoammonic pathway in slices taken from 6-8 week old animals; the same protocol applied to the Schaffer collateral pathway resulted in little or no depression (Figure 26B). Other studies have reported an age-dependence of LTD induction in the Schaffer collateral pathway, with little or no LTD induced by LFS in slices from older animals (Dudek and Bear 1993; Wagner and Alger 1995). Unlike LTD of the Schaffer collateral response, LTD of the temporoammonic response is robust in slices prepared from adult animals. It should be noted, however, that LTD of the commissural input to CA1 has been shown in adult animals *in vivo*, though only by means of application of a paired-pulse low-frequency stimulation protocol (Thiels *et al.* 1994).

Repeated application of LFS to the temporoammonic pathway resulted in saturation of depression at a maximal level of about 40-50% of the original baseline, similar to or lower than that seen in the Schaffer collateral pathway (Mulkey and Malenka 1992; Dudek and Bear 1993). However, following cessation of LFS, the response rebounded somewhat, suggesting that there may be a "floor" below which the temporoammonic

response can be pushed only temporarily. This transient, larger depression may also be analogous to the short-term potentiation seen following tetanic stimulation, which then decays away to reveal a long-term potentiation of lesser magnitude.

LTD in the temporoammonic pathway is independent of $GABA_A$ or $GABA_B$ receptor activation. This also contrasts with Schaffer collateral LTD, where LTD induced by LFS in slices from adult animals is enhanced in the presence of the $GABA_A$ antagonist bicuculline, and LTD in young animals is inhibited by the $GABA_B$ antagonist CGP 35348 (Wagner and Alger 1995). Although stimulation of the temporoammonic pathway does clearly activate interneurons which in turn make both $GABA_A$ and $GABA_B$-mediated synapses onto CA1 pyramidal cells (Empson and Heinemann 1995b; Dvorak and Schuman 1997), depression of the monosynaptic, excitatory component of this pathway is neither enhanced nor reduced by interneuron activity. The difference between Schaffer collateral and temporoammonic LTD in terms of the involvement of inhibition may be due to the fact that stimulation in SLM may activate GABAergic pathways only disynaptically, in a feed-forward fashion (Empson and Heinemann 1995b), whereas stimulation in SR to activate the Schaffer collaterals can also directly activate axons of CA1 interneurons (e.g., see Lambert *et al.* 1991; Arai *et al.* 1995). The differences in temporal patterning of excitation and inhibition in the Schaffer collateral and temporoammonic pathways may play a role in the differential responses to LFS shown by these two pathways.

The induction of homosynaptic LTD in other pathways requires an increase in intracellular Ca^{2+} concentration, either by influx through NMDA receptors (Mulkey and Malenka 1992; Cummings *et al.* 1996) or voltage-gated calcium channels (Bolshakov and

Siegelbaum 1994; Christie *et al.* 1997), or by release from intracellular stores (Reyes and Stanton 1996). Homosynaptic LTD of the Schaffer collateral pathway is sometimes fully blocked by the NMDA receptor antagonist AP5 (Dudek and Bear 1992; Mulkey and Malenka 1992) but in other cases only a partial block is seen (Bolshakov and Siegelbaum 1994; Kemp and Bashir 1997). Homosynaptic temporoammonic LTD was significantly inhibited, relative to control slices, in the presence of 50 μM AP5, although there were some individual experiments in which AP5 did not block LTD. Similarly, in the presence of nifedipine and AP5 together, a complete block of LTD was sometimes observed, while at other times less complete inhibition was observed. NMDA receptors are found in the distal dendrites of CA1 pyramidal cells, although not as densely in SLM as in SR (Monaghan and Cotman 1985; Jarvis *et al.* 1987; Jacobson and Cottrell 1993), and an NMDA receptor-mediated response to temporoammonic stimulation has been observed physiologically (Colbert and Levy 1992; Empson and Heinemann 1995b); furthermore, LTP of the temporoammonic pathway was fully blocked by 50 μM AP5 (Figure 31). It therefore seems unlikely that the incomplete block of temporoammonic LTD by AP5 is due to an absence or paucity of NMDA receptors in SLM. Conversely, although calcium imaging studies show that some voltage-dependent calcium channels are clearly present in the distal dendrites of hippocampal pyramidal cells, L-type calcium channels are most abundant close to the soma, with much lower densities in the more distal dendrites (see Johnston *et al.* 1996). This may account for the relatively small effect of nifedipine on temporoammonic LTD. The mechanism of the induction of the residual, non-NMDA component of temporoammonic LTD remains to be elucidated. Other studies have found a contribution of calcium release from intracellular stores

(Reyes and Stanton 1996; Wang *et al.* 1997), activation of T-type calcium channels (Christie *et al.* 1997; Oliet *et al.* 1997; Wang *et al.* 1997), and mGluR activation (O'Mara *et al.* 1995; Oliet *et al.* 1997) to homosynaptic LTD at other hippocampal synapses; these calcium sources may also contribute to temporoammonic LTD.

One possible explanation for the variability between experiments in the sensitivity of temporoammonic LTD to blockade of NMDA receptors may be a difference between temporoammonic fibers arising in the lateral and medial entorhinal cortex. There are distinct physiological differences between the lateral and medial perforant path (LPP and MPP) projections to dentate gyrus (McNaughton and Barnes 1977; McNaughton 1980). The two projections may also differ in their dependence on NMDA receptor activation for LTP, at least *in vivo* (Bramham *et al.* 1991), although *in vitro* studies show no difference in NMDA receptor dependence of LTP induction (Colino and Malenka 1993). The LPP and MPP can be activated and recorded independently *in vivo* or *in vitro* by virtue of the laminar segregation of their axon terminals along the proximodistal axis of the dendrites of the granule cells of the dentate gyrus; the LPP terminates in the outer third of the molecular layer, while the MPP terminates in the middle third of the molecular layer (Witter *et al.* 1989). The temporoammonic projection, on the other hand, maps along the transverse axis of CA1, with medial fibers terminating closer to CA2 and lateral fibers closer to the subiculum (Witter *et al.* 1989). It should therefore in theory be possible to selectively record responses to either medial or lateral inputs by varying the position of the electrode along the transverse axis of the hippocampal slice. We did not systematically monitor this, but the bulk of our experiments were performed with the recording electrode somewhere in the middle of the CA1 area, where it would likely

record inputs from both pathways. We did perform a small number of experiments with two recording electrodes in SLM at either end of CA1, but observed no consistent differences in LTD expression or AP5 sensitivity (Dvorak-Carbone and Schuman, unpublished data). However, this question would likely best be resolved by *in vivo* experiments where the lateral and medial temporoammonic fibers could more unambiguously be stimulated independently.

Stratum lacunosum-moleculare, the terminal field of the temporoammonic pathway, receives a strong cholinergic input from the septum (Matthews *et al.* 1987), and muscarinic acetylcholine receptor activation has been implicated in some forms of hippocampal long-term depression (Auerbach and Segal 1996). Since stimulation directly in SLM could have activated septal axons remaining in the slice, it was important to show that the LTD observed was not due to release of ACh from septal afferents. Temporoammonic LTD was unaffected by application of the mAChR antagonist atropine (Figure 29), showing that the observed depression was not due to the activation of cholinergic inputs.

When studying synaptic depression, it is important to show that the effect of LFS on the synaptic response does not simply reflect damage to the synapses or general degradation of the slice. To monitor the health of the slice, we applied test stimuli to the Schaffer collateral pathway alternately with the test stimuli applied to the temporoammonic pathway, and observed no change in the Schaffer collateral response while the temporoammonic response was depressed (Figure 26A). The ability to reverse synaptic depression with HFS can also counter-indicate synaptic rundown or poor slice health (Mulkey and Malenka 1992; Dudek and Bear 1993). When we applied high-frequency

stimulation to a depressed temporoammonic pathway, we observed a partial recovery of the response to a level between the depressed level and the original baseline; repeated application of HFS brought the response back up to the original baseline, suggesting that the depressed temporoammonic pathway had not suffered some non-specific damage (Figure 30). Furthermore, HFS applied to the depressed pathway in the presence of bicuculline resulted in complete recovery and potentiation of the response above the original baseline level (Figure 30).

The requirement for multiple applications of HFS to bring the depressed temporoammonic response back to baseline after LTD is consistent with the lack of LTP seen in naive slices. In agreement with a previous report (Colbert and Levy 1993), we were able to potentiate the temporoammonic response in naive slices by HFS or TBS only in the presence of bicuculline. Compared to the Schaffer collateral response, the temporoammonic field response is fairly small to begin with, and might therefore require disinhibition before it can be potentiated; indeed, it has been shown that LTP cannot be induced in this pathway, even in the presence of bicuculline, if the initial response is too small (Colbert and Levy 1993). (LTP of the temporoammonic pathway in the slice preparation in the presence of intact inhibition has been shown only in a situation where the temporoammonic input was stimulated so as to elicit a population spike recorded in stratum pyramidale (Doller and Weight 1985); we have never observed population spike activity in response to temporoammonic stimulation.) The LTP that was induced by HFS of the temporoammonic pathway was dependent on the activation of NMDA receptors (Figure 31), just as so many other hippocampal pathways are (Bliss and Collingridge 1993).

The entorhinal cortex is not the only brain region to send a projection to stratum lacunosum-moleculare of area CA1. Fibers from nucleus reuniens thalami (Wouterlood *et al.* 1990; Dolleman-Van Der Weel and Witter 1996), the amygdala (Petrovich *et al.* 1997), and area TE of inferotemporal cortex (Yukie and Iwai 1988) also terminate in SLM, raising the possibility that activity in these areas might also serve to modulate or gate information flow through the trisynaptic circuit. It is worth noting that extracellular stimulation electrodes placed in SLM may well activate these fibers as well as temporoammonic axons.

The function of the temporoammonic pathway and of other inputs to SLM is not yet well understood. *In vivo* studies suggest that the temporoammonic input plays a role in the generation of theta oscillations (Buzsáki *et al.* 1995) and 40 Hz oscillations (Charpak *et al.* 1995); models of the hippocampus as a heteroassociative learning network include the temporoammonic pathway and the Schaffer collateral pathway as two distinct information-bearing inputs to CA1 (Hasselmo and Schnell 1994); and the inhibition activated by temporoammonic input may serve to gate the output of the hippocampus (Empson and Heinemann 1995b; Dvorak and Schuman 1997). Temporoammonic activity has also been shown to be capable of modulating the induction of LTP at the Schaffer collateral input to CA1 (Levy *et al.* 1998); it will be interesting to examine the impact of plasticity of the temporoammonic pathway on this heterosynaptic modulatory effect.

Figure 26. The temporoammonic field response is depressed by low-frequency stimulation (LFS = 1 Hz for 10 min). A, The temporoammonic response (solid circles) is depressed by LFS while the unstimulated Schaffer collateral response (open triangles) in the same slices is unaffected. Above, superimposed representative field potentials of the temporoammonic (TA) or Schaffer collateral (SC) responses, taken 5 min before and 35 min after LFS of the TA pathway. B, When LFS is applied to the Schaffer collateral pathway (open triangles), much less depression is seen than when LFS is applied to the temporoammonic pathway (A). Above, superimposed representative field potentials taken 5 min before and 35 min after LFS of either temporoammonic (TA) or Schaffer collateral (SC) axons. C, LTD of the temporoammonic response is saturated by repeated application of LFS. Top, a representative experiment showing saturation of LTD. Bottom, five individual experiments showing similar saturation of temporoammonic LTD. Each point represents the average slope for that experiment over the ten minutes prior to that point. In the experiment denoted by open squares, a fifth LFS period was applied at 120-130 min. Scale bars: 0.2 mV / 30 ms.

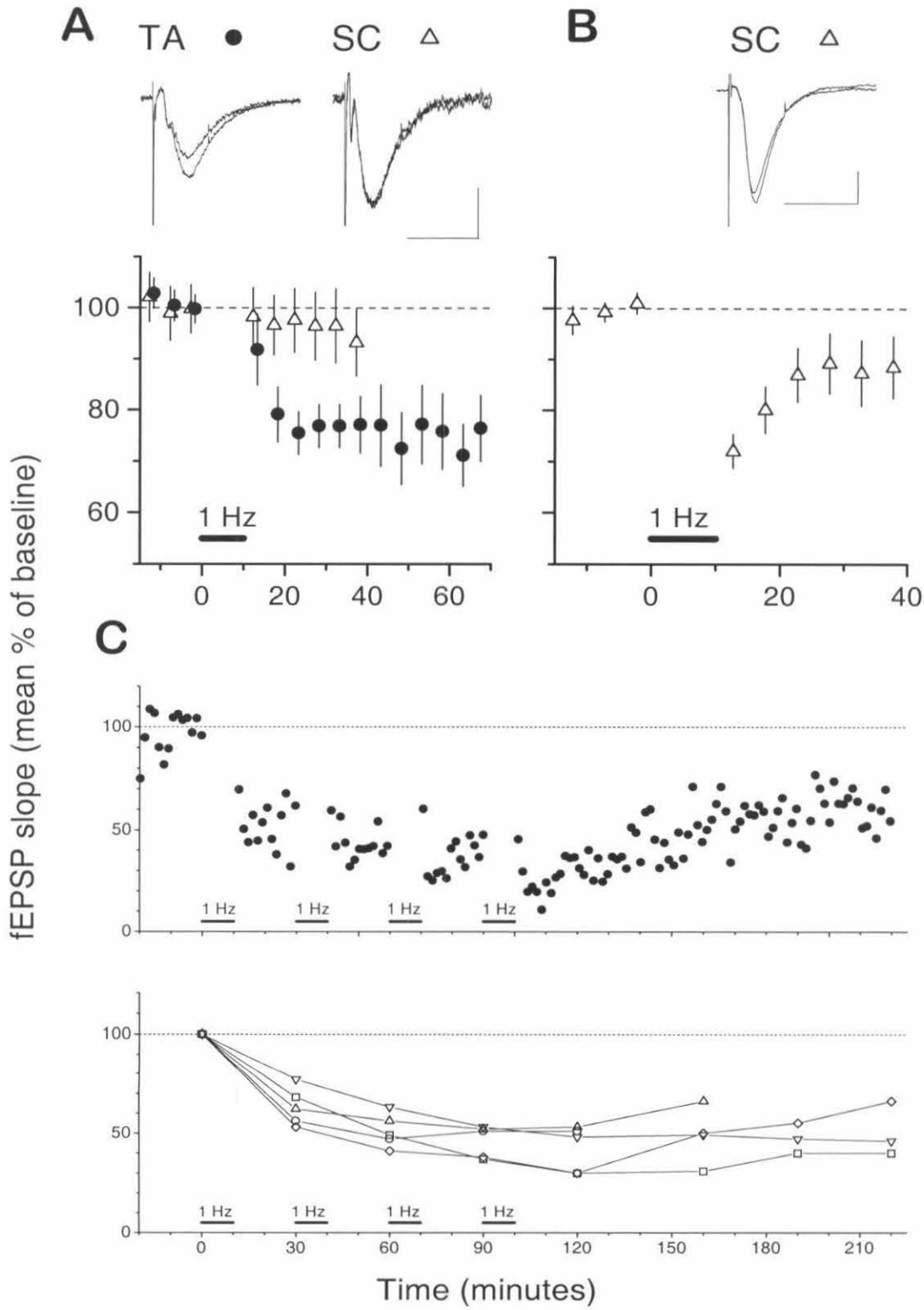
A
TA
SC
B
SC
100
80
60
1 Hz
0
20
40
60
1 Hz
0
20
40
C
fEPSP slope (mean % of baseline)
100
50
0
1 Hz
1 Hz
1 Hz
1 Hz
100
50
0
1 Hz
1 Hz
1 Hz
1 Hz
0
30
60
90
120
150
180
210
Time (minutes)

Figure 27. Temporoammonic LTD does not require intact GABAergic inhibition. The response to LFS in normal ACSF (solid circles) is not different from that seen in the presence of 20 μM bicuculline (open triangles) or 1 μM CGP 55845A (open squares). Above, superimposed representative field potentials taken 5 min before and 35 min after LFS of temporoammonic pathway in normal ACSF (control; same data as in Figure 26), 20 μM bicuculline (bic), or 1 μM CGP 55845A (CGP). Scale bar: 0.2 mV / 30 ms.

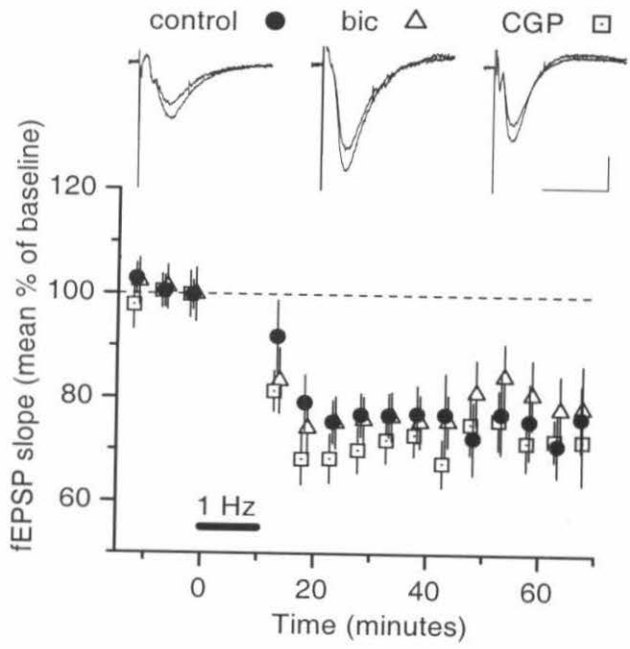
control
bic
CGP
fEPSP slope (mean % of baseline)
120
100
80
60
1 Hz
0
20
40
60
Time (minutes)

Figure 28. Temporoammonic LTD is partially dependent on NMDA receptor activation. LFS applied in the presence of 50 μM AP5 (open triangles) or 50 μM AP5 plus 20 μM nifedipine (open squares) resulted in significantly less depression than LFS applied in normal ACSF (solid circles). Above, superimposed representative field potentials taken 5 min before and 35 min after LFS of temporoammonic pathway in normal ACSF (control; same data as in Figure 26), 50 μM AP5 (AP5), or 50 μM AP5 plus 20 μM nifedipine (AP5+nif). Scale bar: 0.2 mV / 30 ms.

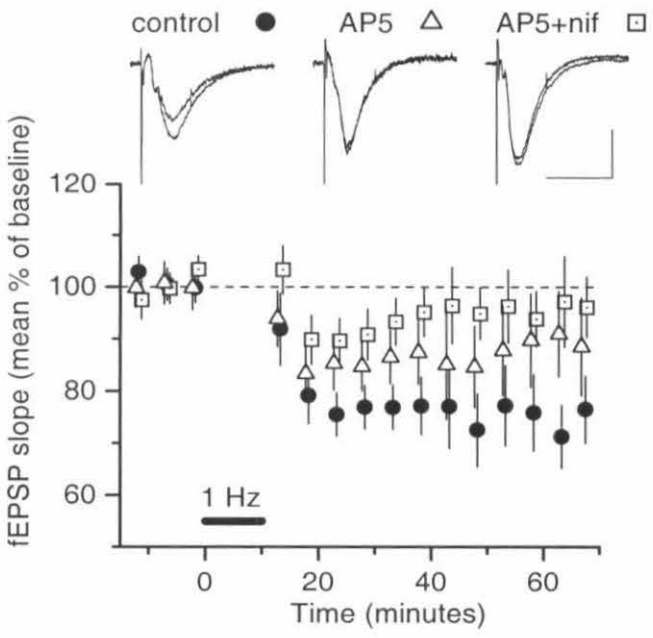
control
AP5
AP5+nif
120
100
80
60
fEPSP slope (mean % of baseline)
1 Hz
0
20
40
60
Time (minutes)

Figure 29. Temporoammonic LTD does not require activation of muscarinic acetylcholine receptors. LFS applied in the presence of 1 μM atropine (open triangles) resulted in the same amount of depression as LFS applied in normal ACSF (solid circles). Above, superimposed representative field potentials taken 5 min before and 35 min after LFS of temporoammonic pathway in normal ACSF (control; same data as in Figure 26) or 1 μM atropine (atr). Scale bar: 0.2 mV / 30 ms.

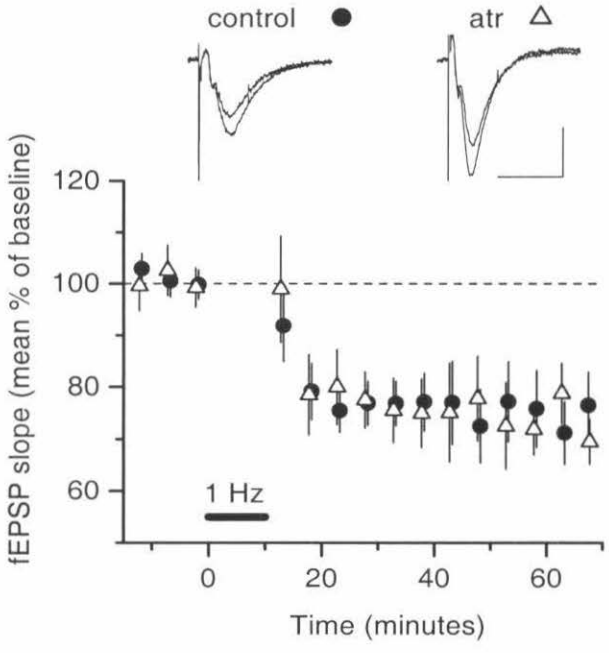
control
atr
120
100
80
60
1 Hz
0
20
40
60
Time (minutes)
fEPSP slope (mean % of baseline)

Figure 30. Temporoammonic LTD can be partially or wholly reversed by high-frequency stimulation (HFS = 100 Hz for 1 s). *A*, In normal ACSF (*solid circles*), HFS applied to the depressed temporoammonic pathway resulted in a recovery above the depressed baseline but below the original baseline (*dashed line*). In the presence of 20 μM bicuculline, HFS resulted in a potentiation significantly above the original baseline. *Above*, superimposed representative field potentials taken 5 min before and 25 min after HFS of temporoammonic pathway in normal ACSF (control) or 20 μM bicuculline (bic). *B*, Three applications of HFS at 5 min intervals result in a full recovery of the temporo-ammonic response to the original baseline. *Above*, superimposed representative field potentials taken 5 min before and 35 min after the first HFS application. Scale bar: 0.2 mV / 30 ms.

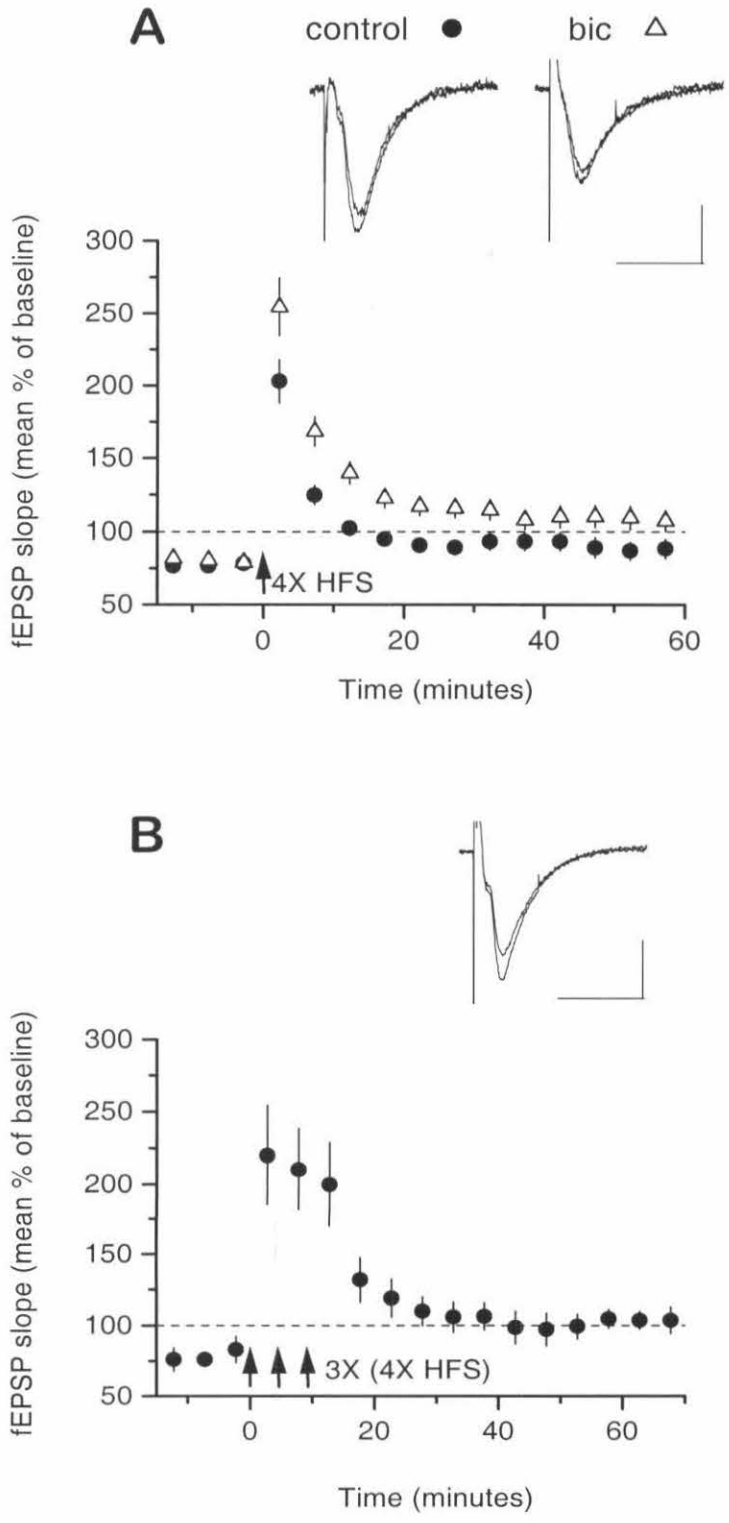
A
control
bic
fEPSP slope (mean % of baseline)
300
250
200
150
100
50
4X HFS
0
20
40
60
Time (minutes)
B
fEPSP slope (mean % of baseline)
300
250
200
150
100
50
3X (4X HFS)
0
20
40
60
Time (minutes)

Figure 31. The temporoammonic response in naive slices can be potentiated only when fast GABAergic inhibition is blocked. This potentiation requires activation of NMDA receptors. A, HFS applied in the presence of 20 μM bicuculline (open triangles) results in significant potentiation of the temporoammonic response, while the same protocol applied in normal ACSF (solid circles) results in little or no potentiation. In the presence of both bicuculline and 50 μM AP5 (open squares), no potentiation is observed. Above, super-imposed representative field potentials taken 5 min before and 25 min after HFS of temporoammonic pathway in normal ACSF (control), 20 μM bicuculline (bic), or 20 μM bicuculline plus 50 μM AP5 (bic+AP5). Scale bar: 0.2 mV / 30 ms. B, Theta-burst stimulation (TBS) potentiates the temporoammonic response only when applied in the presence of 20 μM bicuculline (open triangles); TBS in normal ACSF (solid circles) has little effect. Above, superimposed representative field potentials taken 5 min before and 25 min after TBS of temporoammonic pathway in normal ACSF (control) or 20 μM bicuculline (bic). Scale bar: 0.2 mV / 30 ms.

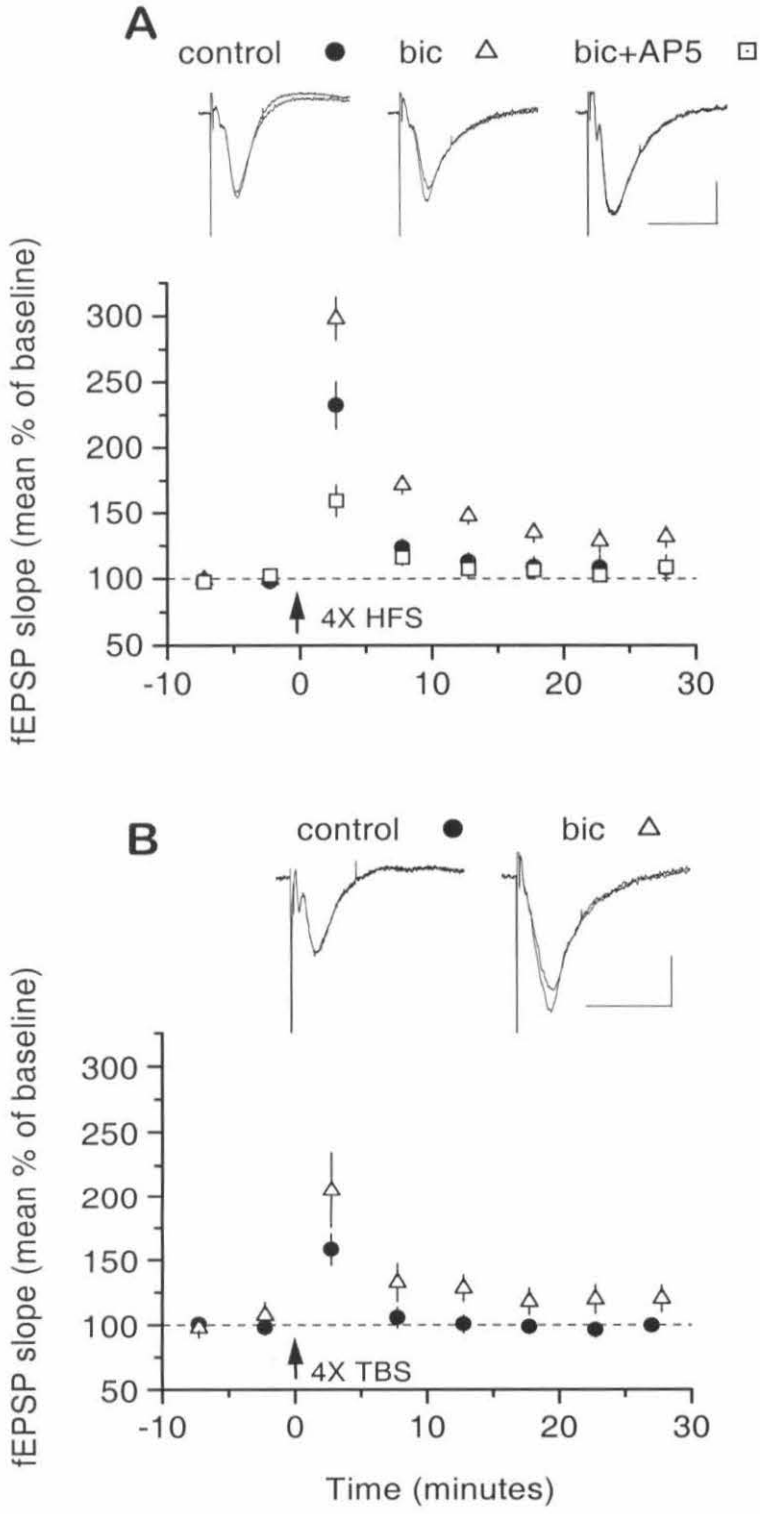
A
control
bic
bic+AP5
fEPSP slope (mean % of baseline)
300
250
200
150
100
50
4X HFS
-10
0
10
20
30
B
control
bic
fEPSP slope (mean % of baseline)
300
250
200
150
100
50
4X TBS
-10
0
10
20
30
Time (minutes)

4 Regulation of information flow through the hippocampus by the inhibitory component of the TA pathway

Submitted for publication in the Journal of Neuroscience.

Note that the neurons for which results are reported in this chapter are a subset of those described in Chapter 2.

4.1 Abstract

CA1 pyramidal cells are the primary output neurons of the hippocampus, carrying information about the result of hippocampal network processing to the subiculum and entorhinal cortex (EC) and thence out to the rest of the brain. The primary excitatory drive to the CA1 pyramidal cells comes via the Schaffer collateral (SC) projection from area CA3. There is also a direct projection from EC to stratum lacunosum-moleculare (SLM) of CA1, an input well positioned to modulate information flow through the hippocampus. High-frequency stimulation in SLM evokes an inhibition sufficiently strong to prevent CA1 pyramidal cells from spiking in response to SC input, a phenomenon we refer to as spike-blocking. We characterized the spike-blocking efficacy of burst stimulation (10 stimuli at 100 Hz) in SLM and found that it is greatest at about 300-600 ms after the burst, consistent with the time course of the slow $GABA_B$ signaling pathway. Spike-blocking efficacy increases in potency with the number of SLM stimuli in a burst, but also decreases with repeated presentations of SLM bursts. Spike-blocking was eliminated in the presence of $GABA_B$ antagonists. We have identified a candidate

population of interneurons in SLM and distal stratum radiatum (SR) which may mediate this spike-blocking effect. We conclude that the output of CA1 pyramidal cells, and hence the hippocampus, is modulated in a input pattern-dependent manner by activation of the direct pathway from EC.

4.2 Introduction

The hippocampus plays a critical role in such high-level brain functions as learning and memory (Zola-Morgan and Squire 1990; Squire and Zola-Morgan 1991; Eichenbaum *et al.* 1992; Wood *et al.* 1999) and spatial navigation (Wilson and McNaughton 1993; Muller 1996). In order for the neural computations performed by the hippocampus to be used by the rest of the brain, an output from the hippocampus to neocortex is necessary. The pyramidal cells of area CA1 are the primary population of hippocampal principal cells projecting outside of the hippocampus, with axons projecting to subiculum and entorhinal cortex (EC) as well as subcortical targets (Witter *et al.* 1989; Lopes da Silva *et al.* 1990; Van Groen and Wyss 1990; Tamamaki and Nojyo 1995). The primary excitatory input to the CA1 pyramidal cells is the Schaffer collateral (SC) projection from area CA3 (Andersen *et al.* 1966; Amaral and Witter 1989; Amaral *et al.* 1990; Lopes da Silva *et al.* 1990). CA1 pyramidal cells and their SC inputs are therefore crucial sites for the regulation of hippocampal output.

Stratum lacunosum-moleculare (SLM) of area CA1 receives a number of inputs from various other brain regions, including a direct projection from layer III of EC (Steward and Scoville 1976), as well as projections from the nucleus reuniens of the thalamus (Wouterlood *et al.* 1990) and inferotemporal cortex (Yukie and Iwai 1988).

The function of inputs to this distal dendritic region of CA1 pyramidal cells is not well understood (see Soltesz and Jones 1995). Although there is some evidence for direct excitation via the EC projection to CA1 (Yeckel and Berger 1990), there is also a strong inhibitory component (Empson and Heinemann 1995a; Paré and Llinás 1995). We investigated the effect of this inhibitory input on the activity of CA1 pyramidal cells, focusing particularly on their responsiveness to SC inputs. We find that the effectiveness of SC inputs in causing pyramidal cells to fire is greatly reduced when stratum radiatum (SR) is stimulated shortly after a burst stimulus in SLM, a phenomenon we call spike-blocking. We investigated the dependence of spike-blocking efficacy on the relative timing of the SR and SLM inputs and on the number of SLM stimuli. We also investigated whether the SLM-mediated modulation of SR inputs could itself be modulated, by examining the effects of repeated SLM bursts on spike-blocking. Some of these results have previously appeared in abstract form (Dvorak and Schuman 1997).

4.3 Methods

4.3.1 Tissue preparation

Slices were prepared by standard procedures from 6-8 week old male Sprague-Dawley rats. Rats were decapitated following Halothane anesthesia, and the brain rapidly removed to ice-cold, oxygenated artificial cerebrospinal fluid (ACSF: 119 mM NaCl; 2.5 mM KCl; 1.3 mM $MgSO_4$; 2.4 mM $CaCl_2$; 1.0 mM NaH_2PO_4; 26.2 mM $NaHCO_3$; 11.0 mM glucose). The posterior half of each hemisphere was glued, ventral side up, onto the stage of a cooled oscillating tissue slicer (OTS-3000-04; FHC, Brunswick, ME) and

covered with chilled ACSF. 500 μm slices were cut. The extraneous cortical and subcortical tissue was gently dissected away with the small end of a spatula. The slices were then allowed to recover in an interface chamber at room temperature for at least one hour before experiments were started. Further microdissection was performed in ice-cold ACSF immediately following slice preparation. All electrophysiology was done with the slices submerged and constantly perfused with oxygenated ACSF at room temperature.

To minimize the possibility of disynaptic or trisynaptic activity in CA1, the dentate gyrus and CA3 regions were dissected away from the slice, leaving a CA1 minislice. A cut was made through SR in distal CA1 (near the subiculum) perpendicular to the cell body layer, in order to prevent antidromic activation of SC axons by the stimulating electrode in SLM (Maccaferri and McBain 1995); SC axons do not enter SLM to any appreciable extent (Amaral and Witter 1989; Tamamaki and Nojyo 1995). Field potential recordings were used to verify isolated activation of axons in SR or SLM (Colbert and Levy 1992; Dvorak-Carbone and Schuman 1999).

4.3.2 Electrophysiology

Bipolar tungsten electrodes, either concentric or paired needles, were used for stimulation. One electrode was placed in SR to stimulate the SC axons; the other was used to stimulate SLM afferents on the far side of the cut. The level of SR stimulation was set such that the resultant EPSP in the pyramidal cell just barely reached spike threshold; this generally required a current of 20 – 40 μA for 100 μs. Stimulation in SLM was generally stronger, 30 – 200 μA for 100 μs.

Intracellular recordings from pyramidal cells were made using sharp electrodes whose resistance was 100-200 MΩ when filled with 2 M potassium acetate. Sharp electrode recordings were made "blind" by lowering the electrode into stratum pyramidale until a penetration was achieved. The voltage reading of the electrode was zeroed with the electrode in the bath, and the bridge was balanced before penetration and rebalanced after penetration. Capacitance compensation was applied after penetration. Neurons included for analysis had a resting potential of -62.1 ± 1.0 mV, fired overshooting action potentials, and had input resistances of 109 ± 10 MΩ (n = 28). Pyramidal cells were identified by the presence of strong spike frequency accommodation in response to positive current injection. All experiments were performed in current clamp mode; the cell was generally at its resting potential, though in a few (3/28) cases a small negative current was applied to hyperpolarize the cell and prevent it from spontaneously firing action potentials.

Whole-cell electrodes used for interneuron recordings had a resistance of about 5 MΩ when filled with intracellular solution (125 mM $KMeSO_4$ (City Chemical Corp., Jersey City, NJ), 9 mM HEPES, 3.6 mM NaCl, 90 μM EGTA, 4 mM Mg-ATP, 300 μM Li-GTP, 25 mM phosphocreatine, and 0.2-0.4% biocytin). Whole-cell recordings were made under visual guidance on an Olympus BX50WI upright microscope equipped with a MTI VE1000 CCD camera. Positive pressure was applied to the electrode solution while advancing towards the targeted neuron, in order to keep debris off the electrode as well as to "clean" the surface of the neuron (Edwards 1995). A gigaseal was obtained under voltage-clamp conditions by applying slight negative pressure; the patch was then

clamped down to -60 mV and whole-cell configuration was achieved by applying further negative pressure. Neurons included for analysis had resting potentials negative to -50 mV, fired overshooting action potentials, and had input resistances of 562 ± 5 MΩ. All experiments were performed in current-clamp mode, with the cell at its resting potential.

Drugs were applied by dilution of concentrated stock solutions into the perfusion medium. Stock solutions were made up in water. CGP 55845A was a kind gift from Novartis (Basel, Switzerland); CNQX and 2-OH-saclofen were obtained from RBI (Natick, MA); all other drugs were obtained from Sigma (St. Louis, MO).

4.3.3 Histology and reconstruction of filled neurons

For morphological reconstructions of interneurons, the whole-cell recording solution included 0.2-0.4% biocytin. In order to prevent non-specific staining of damaged neurons at the slice surface, the tip of the electrode was filled with biocytin-free solution, and the electrode was then back-filled with biocytin-containing solution.

After completion of the experiments, slices were fixed in 4% paraformaldehyde in phosphate-buffered saline (PBS) for at least 3 days. Thin (70 μm) sections were cut on a vibratome and rinsed in PBS. The sections were incubated in an endogenous peroxidase blocker (10% MeOH, 3.5% H_2O_2) in PBS for 1.5 hours and rinsed again in PBS. Next, sections were incubated in 2% BSA and 0.25% Triton X-100 in PBS for 45 minutes, followed by a wash in 2% BSA in PBS. Slices were then incubated in an avidin-HRP solution (ABC solution, Vectastain Kit PK-6100, Vector Labs, Burlingame, CA) for 2 hours. After rinsing in PBS, slices were incubated in a solution of diaminobenzidine

(DAB; 10 mg/20 mL PBS) with cobalt chloride (.03%) and nickel ammonium sulfate (.02%) for 30 minutes; 0.0004% H_2O_2 was then added and slices were incubated till the stained neurons appeared (2-30 min). Slices were once again rinsed in PBS, mounted onto subbed slides, dehydrated in increasing alcohols, cleared in xylene, and coverslipped with Permount.

Filled neurons were observed with a 63X oil-immersion objective on a Zeiss Axioplan upright microscope equipped with a drawing tube, which was used to reconstruct the approximate neuronal morphology. Reconstructions are strictly qualitative and no attempt was made to measure process length or correct for tissue shrinkage.

4.3.4 Data acquisition and analysis

Recordings were made using an Axoclamp-2A or 2B (Axon Instruments, Foster City, CA), low-pass filtered at 3 kHz, digitized at 1 kHz and collected directly onto an IBM-compatible Pentium-class computer using in-house software written in LabVIEW (National Instruments, Austin, TX). Intracellular responses displayed are averages of 3-5 individual traces.

The effectiveness of the SLM burst in blocking SR-evoked spiking was quantified as follows. Trials of SR stimulation following an SLM burst were interleaved with trials where SR stimuli were delivered in isolation. For any one test, typically, 10 SR+SLM trials were interleaved with about 25 SR-alone trials. SR-induced spike firing probabilities in the presence or absence of the SLM burst were calculated from these trials. Spike-blocking efficacy for each test condition was defined as follows:

spike-blocking efficacy = (probability of firing with SR stimulation alone) – (probability of firing with SR+SLM stimulation)

Thus, spike-blocking efficacy would reach a maximum of 1 if the cell never spiked when the SR stimulus was presented following the SLM burst and always spiked when the SR stimulus was presented in isolation, and would be 0 if the cell was equally likely to fire in the presence or the absence of the SLM burst. A negative value would be possible if the spike firing probability increased in the presence of the SLM burst. In practice, the upper bound of the measured spike-blocking efficacy was limited by the firing probability in response to SR stimulation alone. Over all tests, the firing probability in response to SR stimulation alone was 0.87 ± 0.01 ($n = 176$); therefore, a spike-blocking efficacy of ~ 0.9 would indicate maximal spike-blocking. In only one test out of 176 was the SR-alone spike firing probability less than 0.5, and in 76% of tests, the SR-alone spike firing probability was > 0.8.

All numerical values are listed as mean ± SE; error bars in bar graphs are SE. Data were analyzed and plotted using Microcal Origin. Some statistical analyses were performed in Microsoft Excel or STATISTICA for Windows (StatSoft, Inc., Tulsa, OK). A paired Student's t-test was used to test statistical significance of the spike-blocking effect, using spiking probabilities in the presence or absence of the SLM burst as the dependent variables. For multiple comparisons, e.g., comparing the effectiveness of spike-blocking at different ISIs, a repeated-measures, one-way analysis of variance (ANOVA) was performed across that subset of the data for which all levels (e.g., ISI) were tested on each neuron included in the analysis; the Neuman-Keuls test was

performed to assess the statistical significance of all pair-wise post-hoc comparisons. Results were considered significant when $p \leq 0.05$; p values > 0.05 are reported as NS.

4.4 Results

4.4.1 Burst stimulation in SLM results in a large IPSP and blocks SC-induced spiking in a $GABA_B$-dependent manner

A single stimulus in SLM usually resulted in a biphasic response in the post-synaptic pyramidal cell, with a small excitatory postsynaptic potential (EPSP) (0.9 ± 0.1 mV, peaking 31.3 ± 1.7 ms after the stimulus artifact, $n = 23$), presumably mediated by excitatory axons from layer III of EC (Empson and Heinemann 1995b), nucleus reuniens thalami (Wouterlood *et al.* 1990; Dolleman-Van Der Weel and Witter 1996), or infero-temporal cortex (Yukie and Iwai 1988), followed by a slow, small IPSP (-1.1 ± 0.1 mV, peaking 281 ± 10 ms after the stimulus artifact, $n = 28$) (Figure 32A). Burst stimulation in SLM, i.e., 10 stimuli at 100 Hz, resulted in a significantly larger IPSP (-4.4 ± 0.4 mV, peaking 391 ± 13 ms after the stimulus artifact, $p < 0.0001$, $n = 27$). (Figure 32B). This IPSP was mediated by $GABA_B$ receptors, since it was significantly reduced in the presence of the $GABA_B$ antagonist 2-OH-saclofen (100 μM; peak IPSP amplitude, -2.0 ± 0.3 mV, significantly different from the IPSP in the same cell under control conditions, $p < 0.05$, $n = 4$) and virtually eliminated in the presence of the more potent $GABA_B$ antagonist CGP 55845A (2 μM; peak IPSP amplitude -0.5 ± 0.3 mV, significantly different from the IPSP in the same cell under control conditions, $p < 0.05$, $n = 3$) (Figure 32C).

We wished to examine whether the inhibition evoked by high-frequency stimulation in SLM could have a functional effect on the output of the hippocampus, namely action potentials in CA1 pyramidal cells. SC stimulation strength in SR was set to such a level that the response was just suprathreshold for action potential generation (Figure 32D). Bursts of stimuli in SLM were tested for their ability to block spiking evoked by SR stimulation. Spike-blocking efficacy can range from 0 (no block: spiking equally likely in presence or absence of SLM stimulation) to 1 (maximal block: spikes never evoked following SLM stimulation), or be negative if spiking probability increased following SLM stimulation (see Methods). When the SR stimulus was delivered in the middle of the SLM burst-evoked IPSP, spike generation was blocked (Figure 32E); spike-blocking efficacy 400 ms following an SLM burst of 10 stimuli at 100 Hz was 0.73 $\pm$ 0.05 (n = 19). This spike-blocking effect was mediated by $GABA_B$ receptors, since spike-blocking efficacy was reduced from 0.69 $\pm$ 0.01 to 0.15 $\pm$ 0.003 in the presence of 100 μM 2-OH-saclofen ($p < 0.01$, n = 3), and was reduced from 0.82 $\pm$ 0.02 to -0.17 $\pm$ 0.03 in the presence of 2 μM CGP 55845A ($p < 0.001$, n = 3) (Figure 32F).

4.4.2 Spike-blocking efficacy is dependent on relative timing of the SLM and SR stimuli

The dependence of spike-blocking efficacy on the relative timing of SR and SLM stimulation may help to suggest under what circumstances spike-blocking may occur *in vivo*. Dependence on interstimulus interval (ISI; measured from the first stimulus in the SLM burst to the SR stimulus) was tested in 23 neurons using an SLM burst pattern of 10 stimuli at 100 Hz; ISIs measured ranged from 25 ms (with the SR stimulus thus arriving

during the SLM burst) to 1500 ms. Spike-blocking efficacy reached a maximum of 0.77 ± 0.04 (n = 19; significantly different from 0, $p < 0.00001$) at an ISI of 400 ms, a time interval consistent with the slow time course of the G protein-mediated $GABA_B$ signaling pathway (Mott and Lewis 1994; Misgeld *et al.* 1995), and dropped off at shorter or longer ISIs (Figure 33A). At 1500 ms, the spike-blocking effect was not significant (spike-blocking efficacy, 0.15 ± 0.15, NS, n = 4).

To compare spike-blocking efficacy at different ISIs, an ANOVA was performed on data from nine neurons on which ISIs of 100, 200, 400, 600 and 800 ms had been tested. There was significant variation in spike-blocking efficacy between ISIs ($F = 6.78$, $DF = 4$, $p < 0.001$). Spike-blocking efficacy at 100, 200, and 800 ms was significantly lower than that at 400 ms (Newman-Keuls test, $p < 0.01$, n = 9), and spike-blocking efficacy was also significantly lower at 800 than at 600 ms ISI (Newman-Keuls test, $p < 0.01$, n = 9). This confirms the observation that spike-blocking efficacy was greatest at intermediate ISIs.

4.4.3 Spike-blocking efficacy is dependent on the number of stimuli in the SLM burst

We sought to determine how spike-blocking efficacy varied with the number of stimuli in the SLM burst. IPSP amplitude and duration increased when the number of stimuli in the burst was increased (e.g., see Figure 33B, inset). We tested spike-blocking with single SLM stimuli as well as bursts consisting of 2 to 15 stimuli delivered at 100 Hz in nine neurons. With only a single SLM stimulus, there was no significant spike-blocking effect (spike-blocking efficacy, 0.12 ± 0.07, NS different from 0, n = 9); spike-

blocking efficacy was greatly increased by repetitive stimulation (Figure 33B). There was a significant effect of number of stimuli/burst on spike-blocking efficacy ($F = 6.04$, $DF = 8$, $p < 0.01$). One stimulus was significantly less effective in spike-blocking than three or more stimuli (Newman-Keuls test, $p < 0.05$ for all comparisons). Two stimuli were significantly less effective than eight or ten stimuli (Newman-Keuls test, $p < 0.05$). No other significant differences were observed between different numbers of stimuli.

4.4.4 Repeated presentation of the SLM burst results in a reduction of the IPSP and of spike-blocking efficacy

Having characterized the effect of SLM-evoked inhibition on excitatory SC transmission, we wished to examine whether this inhibitory effect could itself be modulated. GABA-mediated responses are known to undergo frequency-dependent depression by means of presynaptic $GABA_B$ autoreceptors (e.g., Davies *et al.* 1990). We found that repeated presentation of the SLM burst (10 stimuli at 100 Hz) at 1 Hz resulted in an exponential decay of IPSP amplitude, with a time constant of 3.7 ± 0.2 seconds ($n = 8$) (Figure 34).

Is spike-blocking efficacy modulated along with IPSP amplitude? To determine how spike-blocking efficacy varied with position in the train of SLM bursts, we used a modified stimulation paradigm. We presented 10 SC stimuli at 1 Hz alone, followed by 10 SC stimuli at 1 Hz offset by 400 ms from 10 SLM bursts at 1 Hz (Figure35A), followed by 10 SC stimuli again. This set of stimuli was repeated 5-10 times at ≥ 5 minute intervals to allow for recovery of the $GABA_B$ response. Spike-firing probability

for SC stimulation alone and in the presence of the SLM bursts was determined for each position in the train of bursts (Figure 35B; n = 8). Spike-blocking efficacy decayed in an exponential manner with repeated SLM burst stimulation, from 0.73 ± 0.07 during the first burst, to 0.08 ± 0.04 during the last burst (Figure 35C; n = 8). The time constant of this decay was 2.8 ± 0.3 seconds, similar to the time course of IPSP depression. Spike-blocking efficacy varied significantly with position in the train (repeated-measures ANOVA, $F = 11.10$, $DF = 9$, $p < 0.0001$); post-hoc analysis showed that spike-blocking efficacy was significantly greater during the first burst in the train than at any other position (Neuman-Keuls test, $p < 0.05$) and significantly greater during the second burst than in any of the fourth through tenth bursts (Neuman-Keuls test, $p < 0.05$ for all comparisons).

Because of our observation that SC spike firing probability was not constant during a train of 10 stimuli at 1 Hz (Figure 35B), we wished to verify that the apparent decrease in spike-blocking efficacy was not due, rather, to a facilitation in the SC response owing to repeated stimulation. To test this, we compared spike-blocking efficacy during the first and last SLM bursts by presenting only two SC stimuli nine seconds apart, thus occurring during the first and last IPSPs of a train of bursts. Spike-blocking efficacy was 0.87 ± 0.13 during the first burst and 0.17 ± 0.12 during the last burst, a significant difference ($p < 0.05$, $n = 3$), indicating that spike-blocking efficacy did in fact decrease over the course of the burst train.

Recovery from the decay of spike-blocking was measured by performing single probe tests two minutes following a train of SLM bursts. After two minutes, spike-blocking efficacy had returned to 0.46 ± 0.12 (n = 5) (Figure 36); spike-blocking efficacy

at five to ten minutes following the previous burst train was 0.72 ± 0.08 (n = 5), very similar to the 0.74 ± 0.05 spike-blocking efficacy observed when single bursts were tested at 400 ms ISI (compare with Figure 33A).

4.4.5 The spike-blocking effect may be mediated by SLM interneurons

We made recordings from SLM interneurons, likely mediators of this spike-blocking effect, to determine their responses to high-frequency SLM stimulation. Some interneurons were not very responsive at all to stimulation in SLM, despite having dendrites in that layer. A subset of SLM interneurons responded with a large EPSP to stimulation in SLM, and could be made to spike by repeated SLM stimulation at high frequencies; an example of such an interneuron is shown in Figure 37. Other interneurons could be driven directly (i.e., spiking due to direct depolarization or antidromic activation of the axon) by SLM stimulation. The spike-blocking effect we characterized is likely to be mediated by interneurons that were driven synaptically, as well as those that were driven directly by the stimulating electrode.

4.5 Discussion

We have shown that high-frequency stimulation in SLM can regulate the output activity of CA1 pyramidal cells in response to excitatory SR inputs. This result suggests a role for the direct projection from EC to SLM of CA1, the temporoammonic (TA) pathway (Fredens *et al.* 1984; Maccaferri and McBain 1995; Reeves *et al.* 1997), in regulation of the output of the hippocampus. Individual EC layer III neurons, whose axons are activated by SLM stimulation, can naturally fire at the high frequencies used in

this study (Finch *et al.* 1986; Gloveli *et al.* 1997a; but see Mizumori *et al.* 1992; Stewart *et al.* 1992; Dickson *et al.* 1997). EC layer II/III neurons also fire in high-frequency population bursts (Chrobak and Buzsáki 1998). A similar inhibitory phenomenon has been observed in area CA3 of the hippocampus, where a single stimulus to the perforant pathway in SLM can block spontaneous firing of CA3 pyramidal cells (Kehl and McLennan 1985a) and reduce the amplitude of a population spike evoked by subsequent stimulation of the fimbria (Kehl and McLennan 1985b).

Previous reports have suggested that the TA pathway may inhibit SC responses in area CA1 (Empson and Heinemann 1995b; Levy *et al.* 1998). However, the relative timing of SR and SLM stimulation in these studies was based on the difference in synaptic delays between the mono- and trisynaptic inputs from EC to CA1. This approach assumes that the cells of origin of the two pathways, which consist of discrete populations within EC (Steward and Scoville 1976), are active simultaneously. Because of the difficulty of identifying the layer of origin of single units recorded *in vivo* (e.g., see Quirk *et al.* 1992; Stewart *et al.* 1992; Chrobak and Buzsáki 1998), it is not known whether this is the case. Since afferent inputs are segregated to different layers of the EC (e.g., see Witter 1993), it is likely that the cells of layers II and III of EC have different activity patterns. The slow and long time course of the SLM-mediated inhibitory effect reported in our study suggests that spike-blocking may act as an overall damping of the output of the hippocampus, rather than a more synapse-specific or temporally restricted effect.

The dependence of the spike-blocking effect on $GABA_B$ receptors was confirmed by its elimination in the presence of the $GABA_B$ receptor antagonist CGP 55845A

(Figure 32). The spike-blocking effect may be mediated by presynaptic $GABA_B$ receptors located on the SC axon terminals, as seen elsewhere (e.g., Isaacson *et al.* 1993), by the hyperpolarization evoked by activation of postsynaptic $GABA_B$ receptors on the pyramidal cells (e.g., Connors *et al.* 1988), or a combination of both factors; we did not address this issue in our study.

The variation of spike-blocking efficacy with ISI is consistent with the time course of $GABA_B$-mediated phenomena (reviewed in Mott and Lewis 1994). The IPSP evoked by SLM burst stimulation peaked at 397 ± 14 ms, and spike-blocking efficacy was greatest at an ISI of 400 ms. Some spike-blocking was observed as early as 100 ms, at which point the somatic membrane potential was near its resting potential, suggesting that postsynaptic hyperpolarization may not be essential to the spike-blocking effect. At short ISIs, shunting of the SC input by the $GABA_A$ or EPSP components of the SLM response may have contributed to the spike-blocking effect. We found that the spike-blocking effect also had a longer time course than the IPSP, since there was no significant difference between spike-blocking efficacy at 400 and at 600 ms ISI, and spike-blocking could still be observed even 800-1000 ms after the SLM burst. Spike-blocking at long ISIs may have been mediated by the activation of presynaptic $GABA_B$ receptors on SC axon terminals (Isaacson *et al.* 1993).

Although spike-blocking efficacy was not directly dependent on the IPSP amplitude, the size of the IPSP still appears to be a good indicator of the amount of $GABA_B$ activation. Consistent with this, an increase in the number of stimuli in the SLM burst resulted in increases both in IPSP amplitude (and duration) and in spike-blocking efficacy. Increasing the number of SLM stimuli/burst could result both in the recruitment of

more interneurons, because of EPSP summation, and in more action potentials per interneuron. Previous studies have shown that activation of individual SLM interneurons does not result in a $GABA_B$ response visible at the soma of CA1 pyramidal cells, even when a train of action potentials is elicited in the interneuron (Ouardouz and Lacaille 1997; Vida *et al.* 1998). In general, it is believed that several interneurons must be activated to evoke a $GABA_B$-mediated response (Isaacson *et al.* 1993; Lambert and Wilson 1994; Fortunato *et al.* 1996), possibly because of a requirement for GABA "spill-over" to extrasynaptically located $GABA_B$ receptors (Isaacson *et al.* 1993).

Patterns of activity in the nervous system do not occur in a vacuum; responses to synaptic activity are conditioned by the prior history of the synapse. The balance of excitation and inhibition in the hippocampus varies constantly due to activity-dependent regulation of synaptic transmission. Here, we have shown that short-term depression of an SLM-activated spike-blocking effect can shift the balance between excitation and inhibition in the inputs onto CA1 pyramidal cells. Spike-blocking evoked by burst SLM stimulation was depressed when bursts were repeated at 1 Hz (Figures 35 and 36). Down-regulation of the inhibitory TA input may contribute to frequency-dependent facilitation of the trisynaptic pathway (Herreras *et al.* 1987). In the presence of natural patterns of activity, such as theta rhythms, the efficacy of spike-blocking could be continuously up- and downregulated. The long-term depression of excitatory TA responses following low-frequency (1 Hz) stimulation (Dvorak-Carbone and Schuman 1999) may also contribute to a re-balancing of inhibitory and excitatory transmission in this pathway.

Activity-dependent depression of inhibitory responses has been well characterized (Ben-Ari *et al.* 1979; McCarren and Alger 1985; Deisz and Prince 1989; Thompson and

Gähwiler 1989; Davies *et al.* 1990) and is mediated by $GABA_B$ autoreceptors (Davies *et al.* 1990; Roepstorff and Lambert 1994) as well as by a $GABA_B$-independent process, possibly synaptic vesicle depletion (Lambert and Wilson 1994; Fortunato *et al.* 1996). Although most studies of modulation of inhibition have focused on $GABA_A$ responses, $GABA_B$ responses are also reduced with repeated stimulation (Williams and Lacaille 1992; Ling and Benardo 1994). We found that repeated presentation of the SLM burst stimulus at 1 Hz resulted in a decrease in the IPSP amplitude along with a decrease in spike-blocking efficacy. In addition to processes intrinsic to interneuron axon terminals, a decrease in recruitment of SLM interneurons may also have contributed to the decreased IPSP size (Congar *et al.* 1995). Also, the repeated high-frequency stimulation used may have resulted in depletion of the available pool of synaptic vesicles (Liu and Tsien 1995; Stevens and Tsujimoto 1995). The slow time course of recovery from activity-dependent depression is consistent with synaptic vesicle depletion (Lass *et al.* 1973; Wiley *et al.* 1987; Liu and Tsien 1995).

Of the many different kinds of GABAergic interneurons in the hippocampus (see Freund and Buzsáki 1996 for review), the interneurons of SLM are likely candidates for mediators of the spike-blocking effect. SLM interneurons can be driven either synaptically (Figure 37) (Lacaille and Schwartzkroin 1988a; Williams *et al.* 1994) or by direct depolarization (Dvorak-Carbone and Schuman, unpublished observations) in response to stimulation in SLM. Focal stimulation in SLM has been used to evoke $GABA_B$-mediated synaptic responses in pyramidal cells, presumably by the activation of SLM interneurons (Williams and Lacaille 1992; Benardo 1995; Miles *et al.* 1996). Trains of action potentials in SLM interneurons can block action potentials from being evoked by depolarizing

current injection in pyramidal cells (Lacaille and Schwartzkroin 1988b).

Other types of interneurons may also contribute to SLM-activated spike-blocking, including vertically-oriented O/A interneurons (McBain *et al.* 1994), stratum pyramidale basket cells (Sík *et al.* 1995; Han 1996), and chandelier cells (Li *et al.* 1992; Buhl *et al.* 1994b), all of which have dendritic arborizations in SLM. Basket and chandelier cells have been identified as postsynaptic targets of TA axons (Kiss *et al.* 1996).

Under what physiological circumstances is the spike-blocking effect likely to be evoked? If SLM interneurons are indeed responsible for spike-blocking, then it needs to be determined under what circumstances they are active. SLM receives projections from layer III of EC (Steward and Scoville 1976), nucleus reuniens thalami (Dolleman-Van Der Weel and Witter 1996), inferotemporal cortex (Yukie and Iwai 1988), and amygdala (Petrovich *et al.* 1997; Pikkarainen *et al.* 1999), all of which might activate SLM interneurons. Disynaptic inhibition of CA1 pyramidal cells via the TA input has been demonstrated *in vitro* (Empson and Heinemann 1995b), and the projection from nucleus reuniens thalami has been shown to activate SLM interneurons *in vivo* (Dolleman-Van der Weel *et al.* 1997).

Burst firing of SLM interneurons may be required for spike-blocking; SLM interneurons may fire in bursts when recovering from hyperpolarization (Lacaille and Schwartzkroin 1988a), possibly due to low-threshold, transient Ca^{2+} currents (Fraser and MacVicar 1991; but see Williams *et al.* 1994). SLM interneurons are also depolarized and fire action potentials in the presence of the muscarinic acetylcholine receptor agonist carbachol (Chapman and Lacaille 1998); the SR/SLM border receives substantial cholin-

ergic innervation (Matthews *et al.* 1987), suggesting that SLM interneurons *in vivo* may be activated by cholinergic inputs.

SLM-evoked blockade of SC excitation of pyramidal cells may be important for selective regulation of excitatory inputs to CA1. Although SC inputs are a primary source of excitatory input to area CA1 (Andersen *et al.* 1966; Amaral and Witter 1989; Amaral *et al.* 1990; Lopes da Silva *et al.* 1990), under some circumstances, the TA pathway can also have a strong excitatory effect (Yeckel and Berger 1990; Buzsáki *et al.* 1995). Responses in CA1 to SC or TA inputs are differentially sensitive to the $GABA_B$ agonist baclofen, with SC field responses greatly reduced while TA responses are unaffected (Colbert and Levy 1992). A similar differential suppression of SC vs. TA inputs to CA1 in the presence of carbachol has been demonstrated (Hasselmo and Schnell 1994); such regulation is proposed to be important in switching between encoding and retrieval modes of associative memory systems (Hasselmo and Schnell 1994). $GABA_B$-mediated selective suppression of inputs to CA1, such as that shown here during SLM activity, could also mediate such a switch (Hasselmo *et al.* 1996). Other models of memory decoding in area CA1 require a strong excitatory input from the EC to CA1 (McClelland and Goddard 1996), further suggesting the importance of selective suppression of SC inputs. A test of the possible role of $GABA_B$-mediated spike-blocking in selecting between SC and TA inputs to CA1 pyramidal cells will require a better understanding of the circumstances under which TA input to CA1 is sufficiently strong to cause pyramidal cells to fire.

In conclusion, we have shown that afferent inputs to SLM, including the direct projection from EC, are ideally positioned to gate information flow through the

trisynaptic pathway by means of appropriately timed inputs. *In vivo* studies, where fiber tracts are intact and can be stimulated independently, would be helpful to determine which of the many afferents to SLM mediate the inhibitory spike-blocking effect, and under what circumstances the gating is physiologically effective.

Figure 32. Repeated stimulation in SLM results in a $GABA_B$-mediated IPSP in a CA1 pyramidal cell as well as a $GABA_B$-mediated spike-blocking effect on SC input. *A*, response to a single stimulus in SLM. *B*, burst stimulation in SLM (10 stimuli at 100 Hz) results in a larger IPSP. *C*, the IPSP is greatly reduced in the presence of the $GABA_B$ antagonist CGP 55845A (2 μM). *D*, suprathreshold stimulation of the SC axons in SR results in an action potential. *E*, the same SR stimulus applied 400 ms following the SLM burst results in a subthreshold EPSP (the spike-blocking effect). *F*, in the presence of 2 μM CGP 55845A, the spike-blocking effect is eliminated. Bars below sweeps show stimulation patterns in SR and SLM. Scale bar: 5 mV (*A-C*), 15 mV (*D-F*)/250 ms. Stimulus artifacts digitally removed for clarity.

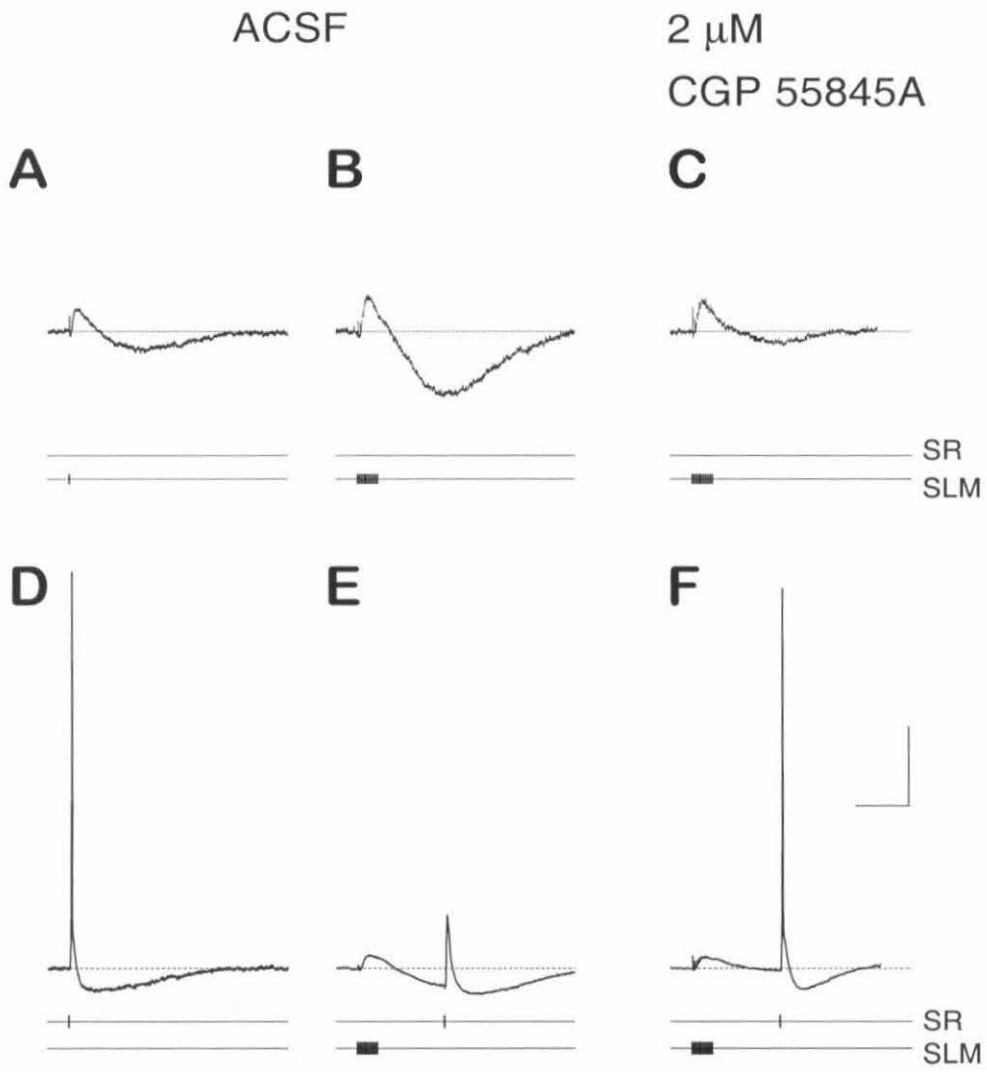
ACSF
2 μM
CGP 55845A
A
B
C
SR
SLM
D
E
F
SR
SLM

Figure 33. Spike-blocking efficacy (see Methods, section 4.3.4, p. 208) is dependent on the relative timing of SLM and SR stimulation as well as on the number of SLM stimuli in a burst. *A*, dependence on interstimulus interval (ISI), measured from the first stimulus of the SLM burst to the SR stimulus. *B*, dependence on the number of SLM stimuli in the burst. *Inset*, representative sweeps showing IPSPs in response to SLM bursts containing 1, 2, 3, 6, 8, 10, 12 and 15 stimuli. Scale bar: 4 mV/500 ms. Stimulus artifacts digitally removed for clarity.

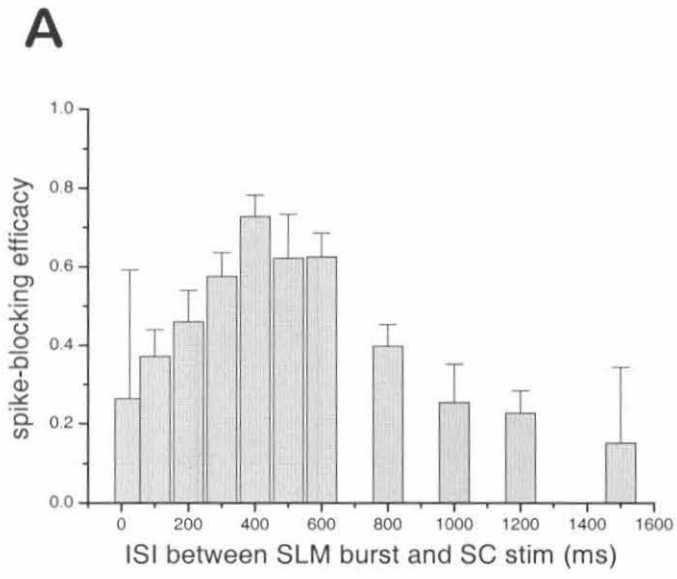
A
spike-blocking efficacy
1.0
0.8
0.6
0.4
0.2
0.0
0
200
400
600
800
1000
1200
1400
1600
ISI between SLM burst and SC stim (ms)

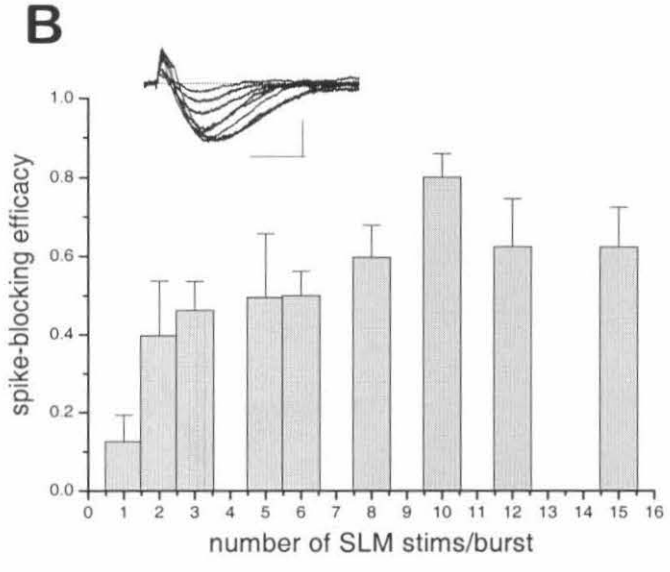
B
spike-blocking efficacy
1.0
0.8
0.6
0.4
0.2
0.0
0 1 2 3 4 5 6 7 8 9 10 11 12 13 14 15 16
number of SLM stims/burst

Figure 34. Repeated presentation of the SLM burst results in a decrease in the IPSP amplitude. *A*, SLM bursts (10 at 100 Hz) repeated 10 times at 1 Hz result in IPSPs of decreasing amplitude. Scale bar: 2 mV/2 s. *B*, the decrease in IPSP amplitude (normalized to the amplitude of the first IPSP in the train) is very well fit by a single exponential decay curve. IPSP amplitudes for eight different cells are plotted along with exponential curve fits; r^2 values range from 0.901 to 0.994. *Inset*, a representative experiment showing normalized IPSP amplitudes for the trace in the top of the figure, along with the exponential fit ($r^2 = 0.987$, $\tau = 3.7$ s).

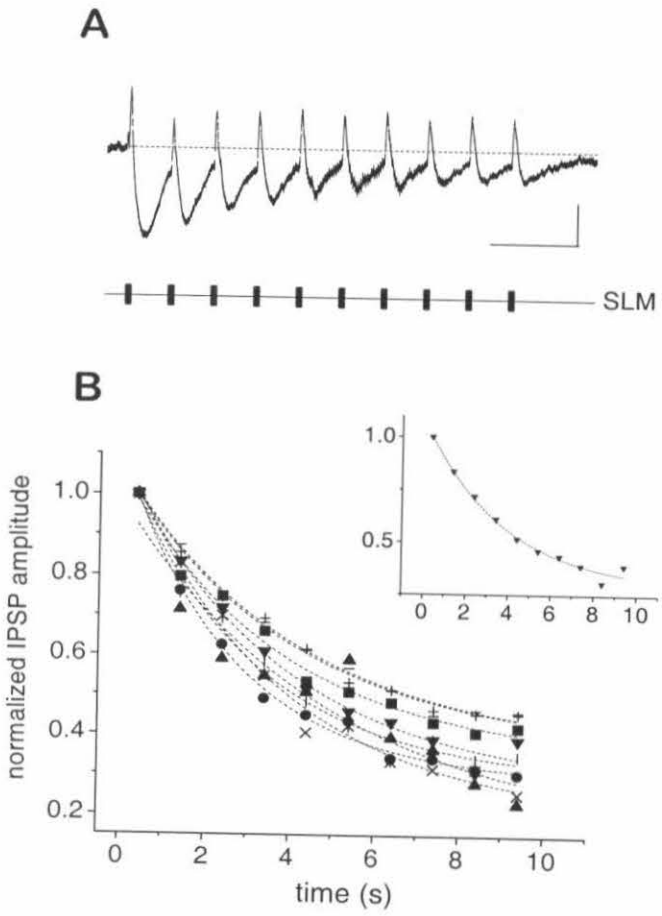
A
SLM
B
normalized IPSP amplitude
1.0
0.8
0.6
0.4
0.2
0
2
4
6
8
10
time (s)
1.0
0.5
0
2
4
6
8
10

Figure 35. Spike-blocking efficacy decreases along with the decrease in IPSP amplitude. *A*, example of a spike train elicited by 10 SC stimuli (SR) presented at 1 Hz. *B*, when the same SR train is presented with each SR stimulus arriving 400 ms after an SLM burst (10 at 100 Hz), the first spikes in the train are blocked while the remaining spikes are unaffected. Scale bar: 20 mV/2 s. *C*, Spike firing probability in the presence of the SLM bursts (dark gray bars) is reduced differentially compared to spike firing probability in the absence of SLM bursts (light gray bars) depending on position in the train. ***, significant difference, $p < 0.001$; *, significant difference, $p < 0.05$; $n = 8$. *D*, spike-blocking efficacies determined from the data in *C*. Spike-blocking efficacy decreases in a manner well fit by a single exponential ($r^2 = 0.962$, $\tau = 2.8$ s).

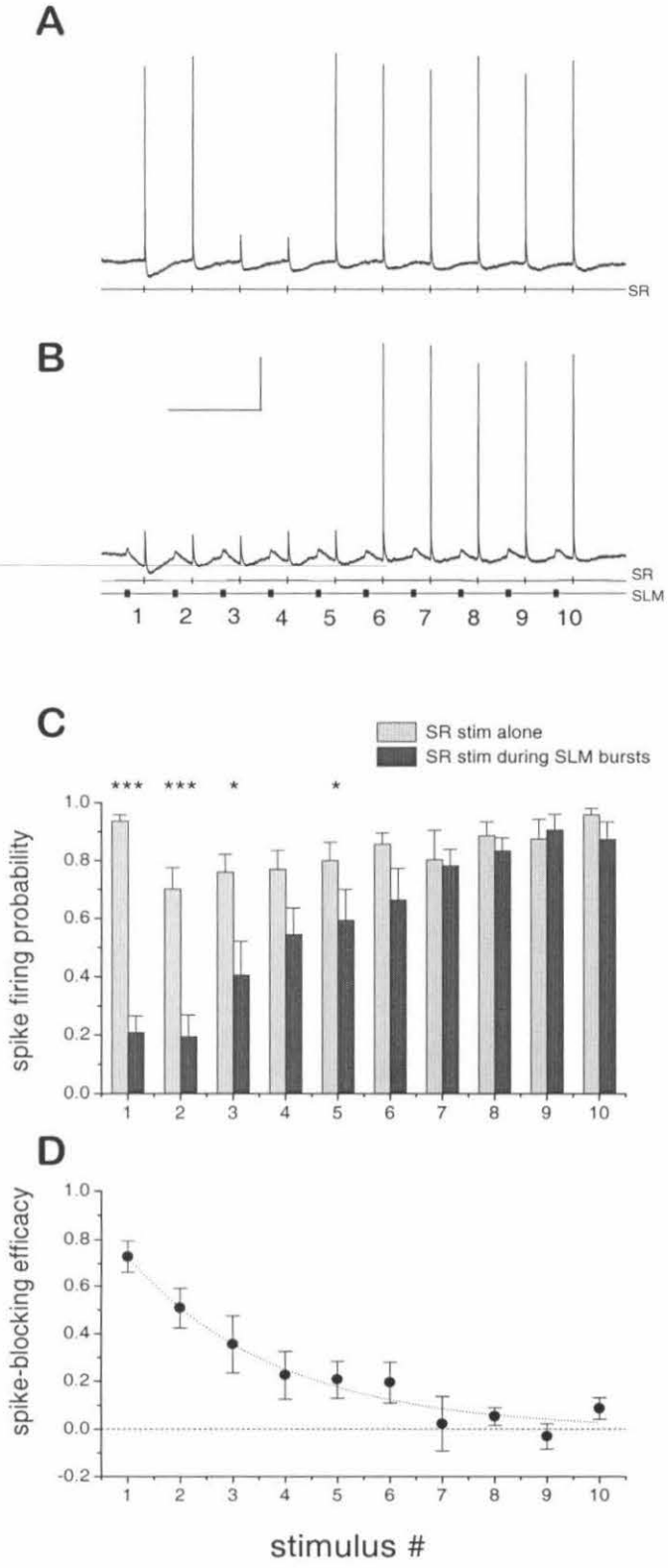
A
SR
B
SR
SLM
1 2 3 4 5 6 7 8 9 10
C
SR stim alone
SR stim during SLM bursts
*** *** * *
spike firing probability
1.0
0.8
0.6
0.4
0.2
0.0
1 2 3 4 5 6 7 8 9 10
D
spike-blocking efficacy
1.0
0.8
0.6
0.4
0.2
0.0
-0.2
1 2 3 4 5 6 7 8 9 10
stimulus #

Figure 36. Spike-blocking efficacy following trains of SLM bursts recovers over a time course of minutes. *A*, representative sweeps from a single experiment showing spike-blocking effect during repeated 1 Hz trains of SR stimuli interleaved with trains of SLM bursts. Two minutes following such trains, probe trials (single SR stimulus following single SLM burst) showed a partial recovery (e.g., 2/4 cases) of the spike-blocking effect ("2 minute recovery"). Trials repeated at ≥ 5 minute intervals showed a more complete recovery (e.g., 3/4 cases) of the spike-blocking effect ("5+ minute recovery"). Scale bar: 30 mV/300 ms (left column), 750 ms (right two columns). *B*, spike-block efficacies and exponential fit ($r^2 = 0.882$, $\tau = 3.74$ s, $n = 5$) for neurons in which recovery of spike-block efficacy was tested, along with spike-block efficacies at 2 and ≥ 5 minutes.

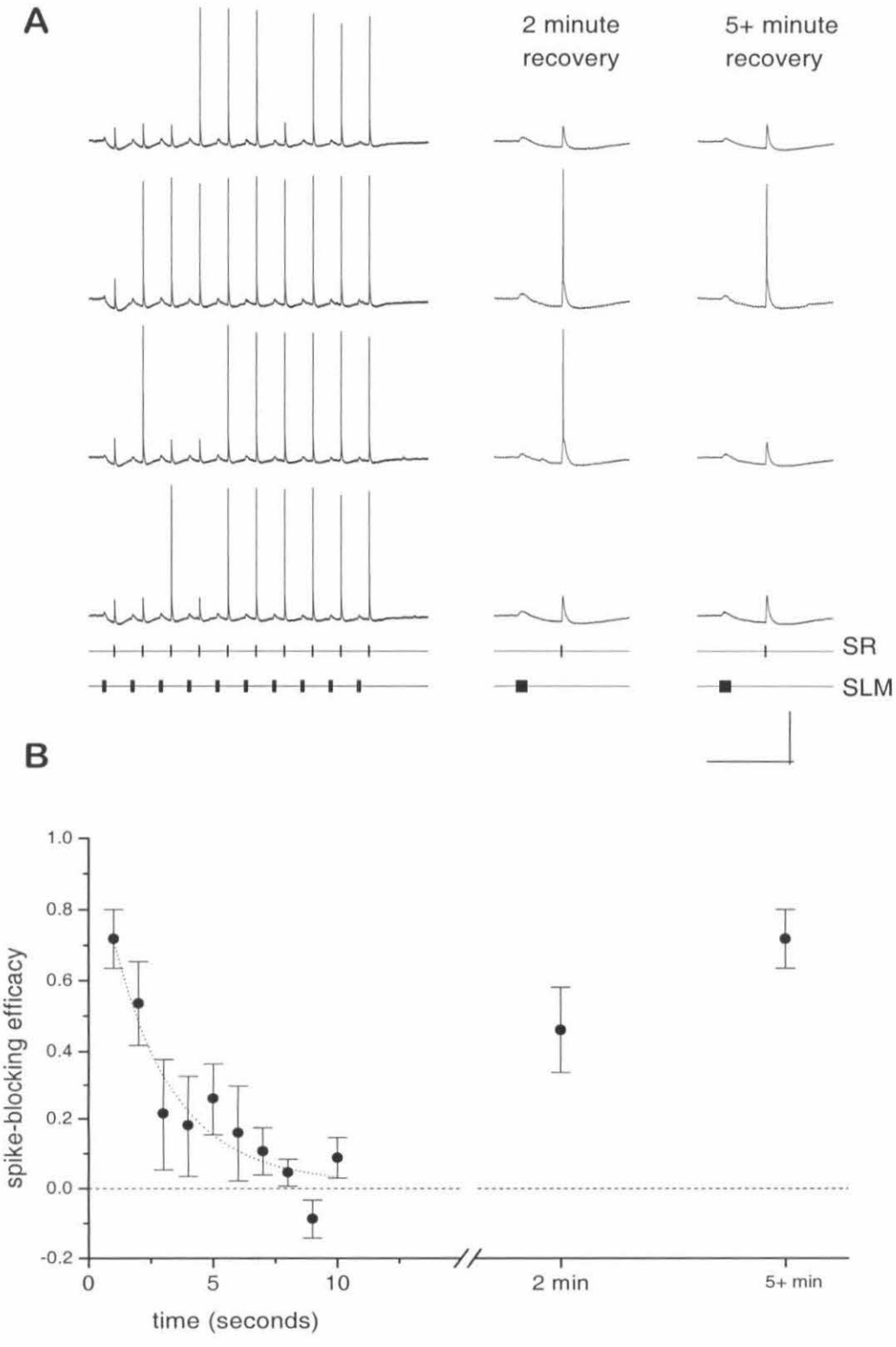
A
2 minute recovery
5+ minute recovery
SR
SLM
B
spike-blocking efficacy
1.0
0.8
0.6
0.4
0.2
0.0
-0.2
0
5
10
2 min
5+ min
time (seconds)

Figure 37. Example of an SR/SLM interneuron with synaptic responses to SLM stimulation. *A*, Synaptic responses to ten stimuli delivered at 100 Hz (*top*) and 25 Hz (*middle*), and to a single stimulus (*bottom*). Scale bar: 20 mV/200 ms. *B*, camera lucida reconstruction of the interneuron from a biocytin fill and DAB staining; note the location of the cell body near the SR/SLM border and the horizontal orientation of the presumed dendrites. No axon was recovered for this cell. Scale bar: 100 μm.

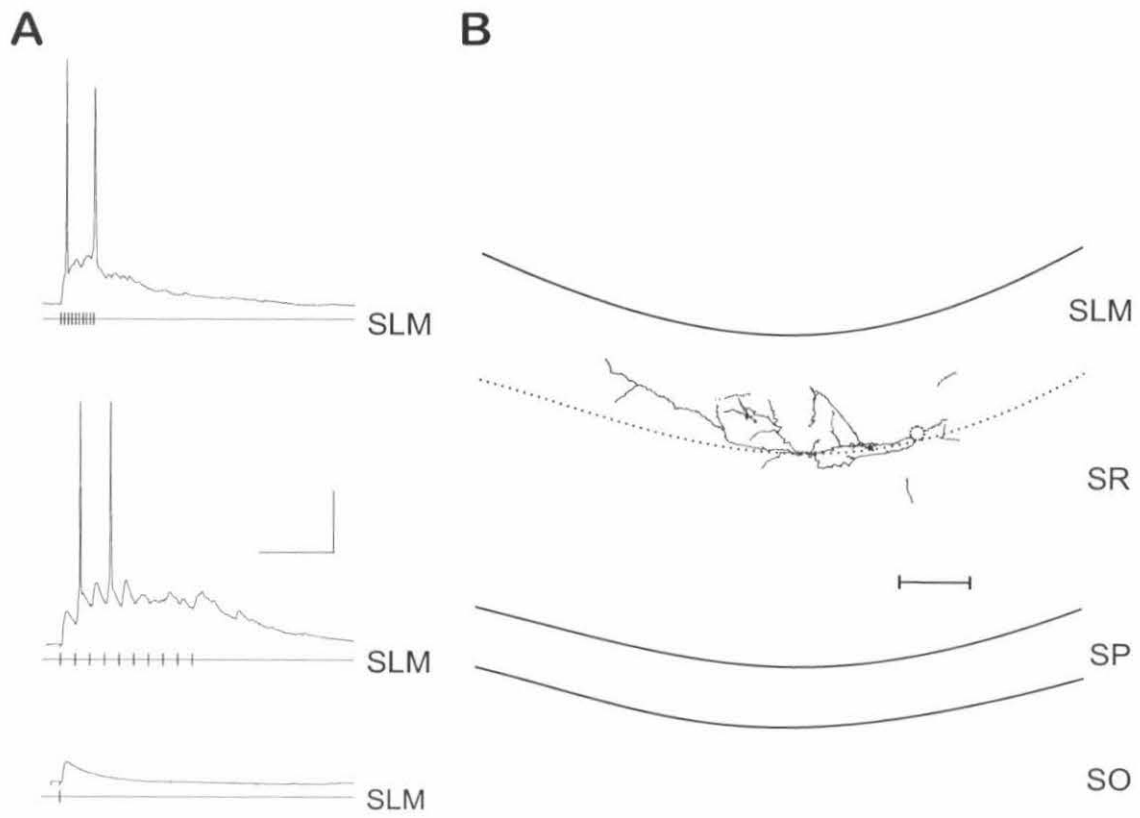
A
SLM
SLM
SLM
B
SLM
SR
SP
SO

5 General discussion and directions for further research

At about the time that I started my work in the Schuman lab, an issue (Volume 5, Number 2, 1995) of the journal "Hippocampus" came out that was entirely devoted to the monosynaptic projection from entorhinal cortex to CA1, the temporoammonic pathway (though that term does not appear anywhere in the journal). In an introductory essay, guest editors I. Soltesz and R. S. G. Jones asked the titular question, "The direct perforant path input to CA1: Excitatory or inhibitory?" After almost four years studying that pathway, my answer is an unequivocal "Both." Under certain circumstances, the TA input is likely to convey information to CA1 by means of excitatory input, whereas under other circumstances, the TA pathway can regulate information flow through the tri-synaptic pathway.

My preliminary results confirmed what others had seen. The TA response has an excitatory component, as demonstrated by the robust field EPSPs evoked in CA1 SLM by TA stimulation. And, the TA response has an inhibitory component, as demonstrated by the large IPSPs visible in intracellular recordings from pyramidal cells, especially in response to burst stimulation of the TA pathway.

5.1 TA LTD – directions for further research

5.1.1 How does TA LTD contribute to information processing in the hippocampus?

My observations, along with those of others (Yeckel and Berger 1990; Colbert and Levy 1992; Buzsáki *et al.* 1995) confirm the idea, motivated by the ultrastructural data showing a preponderance of TA synaptic inputs onto pyramidal cells (Desmond *et al.* 1994), that the TA input can be a strong, excitatory force in the hippocampus. As discussed in the introduction (section 1.3.2.5, p. 54), a strong, excitatory monosynaptic connection from EC to CA1 is key to several models of hippocampal information coding and retrieval (Levy 1989; Hasselmo *et al.* 1996; McClelland and Goddard 1996). In this context, the finding that the excitatory component of the TA response can be modulated in an activity-dependent manner (Colbert and Levy 1993; Leung *et al.* 1995; Dvorak-Carbone and Schuman 1999) takes on a new significance. Although the above models do not require activity-dependent plasticity of the TA pathway in order to function, they do describe a situation where different TA axons selectively activate a subset of CA1 pyramidal cells. It is possible that this selectivity could be hard-wired anatomically, and the TA projection is known to be organized in a point-to-point manner (Tamamaki and Nojyo 1995), but activity-dependent regulation such as LTD could certainly play a role in refining the connectivity. Field recording experiments can provide only a crude measure of changes in synaptic strength averaged over a population of pre- and postsynaptic neurons. However, the small size of the TA EPSPs as seen at the soma of pyramidal cells (section 2.3.2.2, p. 89) makes LTD of intracellular responses difficult to measure. A

potentially fruitful, but challenging, approach would be to record serially from pyramidal cells until one was found that was particularly responsive to TA stimulation. Other possible approaches include the use of Cs^+ and QX-314 in the intracellular solution to block K^+ and Na^+ channels; this block could amplify the EPSP recorded at the soma by reducing electrotonic decay due to passive leak conductances as well as active currents such as I_A (Hoffman *et al.* 1997). Intracellular TA responses would also likely be more robust in dendritic recordings, nearer to the site of synaptic input.

5.1.2 Differences between LTD in the TA and SC pathways

The discovery of robust TA LTD in slices from mature (6-8 week old) rats, an age at which SC LTD is difficult to induce, suggests directions for future research. In the SC pathway, developmental changes are observed in susceptibility to LTD induction, with LTD more easily induced in slices from younger animals (Dudek and Bear 1993; Wagner and Alger 1995; see Bear and Abraham 1996 for review). Is TA LTD also age-dependent? The experiments remain to be done.

Considering that SC and TA inputs converge on the same set of postsynaptic pyramidal cells, it would be interesting to determine what it is about the TA pathway that makes it more amenable to LTD induction. Another difference observed between TA and SC LTD was that, unlike SC LTD (Mulkey and Malenka 1992; Cummings *et al.* 1996) (Dudek and Bear 1992), TA LTD was not completely blocked by NMDA receptor antagonists. LTD induction is known to require elevated Ca^{2+} concentration in the postsynaptic cell, and some possible alternative sources for Ca^{2+}, such as voltage-gated calcium channels and release from intracellular stores, are discussed in section 3.5 (p.

215). However, this does not explain the difference between the TA and the SC inputs, unless there are different potential Ca^{2+} sources in SLM than in SR.

There may be some compartmentalization in the postsynaptic cells that makes the dendrites in SLM, site of the TA input, somehow different from the dendrites in SR, site of the SC input. Several differences have been described between basal (SO) and apical (SR and SLM) dendrites of CA1 pyramidal cells. For example, differences are observed in LTP induction in SO and SR, although these may be due to differences in inhibitory innervation of these layers (Kaibara and Leung 1993; Arai *et al.* 1994; Cavus and Teyler 1998), whereas the LTD observed in the TA response was independent of inhibitory inputs (section 3.4.1.2, p. 178). The endothelial form of nitric oxide synthase (NOS) is found at much higher levels in SR than in SO (Dinerman *et al.* 1994), and LTP in SO, unlike SR, is not NOS-dependent (Kantor *et al.* 1996). Apical and basal dendrites are separated by the soma, whereas SR and SLM dendrites are continuous, which would seem to make compartmentalization more difficult. However, the differential expression levels of at least one protein, the K^+ channel GIRK, between SR and SLM (Ponce *et al.* 1996; Drake *et al.* 1997) suggest that control of the biochemical makeup of dendrites at this scale is possible. Expression of different proteins in SR and SLM may perhaps be regulated by the differences in activity patterns of the afferent SC and TA inputs, respectively.

The dendrites of pyramidal cells ramify widely after reaching SLM (Ishizuka *et al.* 1995), and the fine, less spiny branches of these tufts may be somehow distinct from the more spiny dendritic branches in SR. The expression and activity of dendritic ion channels have been studied by the technique of patch-clamp recording in SR dendrites

(see Magee *et al.* 1998 for review), but it has so far proven impossible to record from the fine branches in SLM, so little is known about the properties of dendrites in this layer.

Differences between SC and TA LTD may also be attributable to differences on the presynaptic side of the two pathways. For example, TA axons differ from SC axons in their higher levels of mGluR2 expression (Neki *et al.* 1996; Petralia *et al.* 1996). A role for mGluR2 receptors in LTD is suggested by the finding that transgenic mice which do not express mGluR2 have impaired LTD in the mossy fiber input to CA3 (Yokoi *et al.* 1996).

Neuromodulatory afferents could also play a role in differences between these two pathways. ACh acting on mAChRs was shown not to contribute to TA LTD (section 3.4.1.4, p. 180). However, SLM also receives a high density of noradrenergic (Oleskevich *et al.* 1989) and serotonergic (Oleskevich and Descarries 1990) innervation, and the TA input can also be modulated by dopamine (Otmakhova and Lisman 1999); stimulation in SLM may have activated these neuromodulatory pathways, possibly contributing somehow to the observed LTD. LTD in other pathways can be affected by these neuromodulators. For example, in visual cortex, NE application facilitated LTD induction by a paired-pulse paradigm (Kirkwood *et al.* 1999), whereas in dentate gyrus, NE can induce LTD of the lateral perforant path and LTP of the medial perforant path in an activity-independent manner (Bramham *et al.* 1997). Conversely, NE prevented the induction of LTD by low-frequency stimulation of the SC pathway (Katsuki *et al.* 1997). In slices from kitten visual cortex, serotonin increased the probability of induction of LTP or LTD via an action on 5-HT_{2C} receptors (Kojic *et al.* 1997). Induction of an NMDA

receptor-independent form of activity-dependent LTD in prefrontal cortex was facilitated by the presence of dopamine (Otani *et al.* 1998), and D1 receptor activation increased the amount of LTD induced by low-frequency stimulation of SC axons in CA1 of the hippocampus (Chen *et al.* 1995).

5.2 Spike-blocking – directions for further research

Previous studies showed that the TA pathway can have an inhibitory effect on CA1 pyramidal cells (Empson and Heinemann 1995b; Paré and Llinás 1995; Soltesz 1995). I confirmed and extended these observations by showing that high-frequency stimulation in SLM can evoke inhibition in CA1 pyramidal cells sufficient to prevent their firing in response to SC excitatory input (Chapter 4). However, many questions remain about this phenomenon.

5.2.1 What are the mechanisms mediating spike-blocking and its decay?

In my study, I found that spike-blocking required the activation of $GABA_B$ receptors (section 4.4.1, p. 210), but did not determine whether the effect was due to postsynaptic hyperpolarization (e.g., Connors *et al.* 1988), presynaptic inhibition of SC transmission (Isaacson *et al.* 1993), or a combination of both mechanisms. This question could be resolved by the use of $GABA_B$ antagonists with different affinities for pre- and postsynaptic $GABA_B$ receptors, although this may be complicated by the fact that presynaptic $GABA_B$ receptors on excitatory terminals may be more like postsynaptic $GABA_B$ receptors than like the autoreceptors on inhibitory terminals (Kerr and Ong 1995). Another possibility would be to use Cs^+ in the intracellular recording electrode to

block K^+ channels. Since I found that $GABA_B$ IPSPs were still present in recordings made with sharp electrodes filled with CsAc (section 2.3.2.2, p. 89), whole-cell recording using, for example, a Cs-gluconate-based solution may be a better way to get Cs^+ into the postsynaptic cell. However, any non-specific blocking of K^+ channels may also change the excitability of the postsynaptic cell, confounding the issue.

The mechanism underlying the activity-dependent decay of spike-blocking efficacy (section 4.4.4, p. 213) also was not determined. A $GABA_B$ antagonist specific to presynaptic $GABA_B$ receptors on inhibitory axon terminals could be used to test whether $GABA_B$ autoreceptor regulation was involved. The exponential decay and slow time course of recovery of inhibition suggest that synaptic vesicle depletion may be involved. This could be tested by changing the extracellular calcium concentration to change the probability of vesicle release.

5.2.2 Which interneurons mediate spike-blocking?

Further work also could be done to better characterize which interneurons mediate the spike-blocking effect, how these interneurons are activated by synaptic inputs, and how many interneurons need to be activated in order for spike-blocking to occur. In our experiments, many SLM interneurons were unresponsive to TA input, and interneurons that were activated directly by the stimulating electrode may have contributed to the spike-blocking effect. It would be worthwhile to better characterize the conditions under which SLM interneurons are responsive to TA input. Given the strong serotonergic and noradrenergic innervation of SLM, and given that interneurons are excited by serotonin and NE, it would be interesting to see how the spike-blocking effect is modulated by

agonists or antagonists of these two neuromodulators. It has been shown that application of 5-HT (Ropert and Guy 1991) or NE (Bergles *et al.* 1996) to the hippocampal slice results in an inhibition of pyramidal cells. Some reports (Lacaille and Schwartzkroin 1988a; Fraser and MacVicar 1991) have suggested that SLM interneurons can switch between a regular-firing and a burst-firing mode, reminiscent of neurons in thalamus that become refractory to synaptic input when in a bursting mode, in a manner dependent on activation of low-threshold voltage-dependent Ca^{2+} channels (Steriade and Llinás 1988; Huguenard 1996). A low-threshold Ca^{2+} current in SLM interneurons is enhanced by 5-HT receptor activation (Fraser and MacVicar 1991), suggesting that serotonergic input may promote burst firing in SLM interneurons. It would be interesting to see how burst-mode firing in SLM interneurons affects CA1 network processing.

Recordings could also be made from the other types of interneurons with dendrites in SLM to see if they are activated by TA input. Basket and chandelier cells would be particularly good targets for investigation, given that they are known to receive synapses from TA axons (Kiss *et al.* 1996). The challenge in recording from these types of interneurons is that their somata are located in SP with the pyramidal cells (Ramón y Cajal 1893; Lorente de Nó 1934; Somogyi *et al.* 1983; Li *et al.* 1992; Han 1996) and are therefore difficult to target for intracellular or whole-cell recording. A new line of transgenic mice, whose GABAergic neurons selectively express green fluorescent protein (GFP) (Oliva *et al.* 1998), could be useful for targeting SP interneurons for recording. However, since basket and chandelier cells are thought to evoke primarily somatic or axo-axonic, $GABA_A$-mediated responses in pyramidal cells, they may in fact not contribute to the $GABA_B$-dependent spike-blocking process.

5.2.3 How does spike-blocking affect more complex patterns of SC input?

The spike-blocking effect could be further characterized by its effect on patterns of SC activity more complicated than a single stimulus. Preliminary results (data not shown) suggest that at stimulation strengths where spike firing in response to a single SC stimulus was blocked by TA-evoked inhibition, paired-pulse or burst stimulation of the SC pathway could overcome the inhibition and evoke a spike. This supports the idea that burst spiking may be important for reliable synaptic transmission (Lisman 1997; Usrey *et al.* 1998). More subtle effects on spike timing could also be examined. For example, a doublet stimulus in the absence of TA inhibition may result in a postsynaptic spike in response to the first stimulus, but in the presence of spike-blocking, perhaps only the second stimulus would evoke a spike. Timing of spikes can play an important role in information coding (e.g., Wehr and Laurent 1996) and in synaptic plasticity (e.g., Bi and Poo 1998) and so an interplay between TA-evoked inhibition and SC-evoked excitation could affect the temporal details of information coding in the hippocampus.

5.2.4 Possible interactions between TA LTD and spike-blocking

An unresolved question is whether there is an interaction between TA LTD and the spike-blocking effect. If low-frequency stimulation causes a persistent decrease in synaptic strength of the TA input to CA1, is there also a decrease in interneuron activation, and hence spike-blocking efficacy? Essentially, the question is whether TA synapses onto interneurons mediating the spike-blocking effect undergo the same depression as the TA field potential response. This could be measured directly in

interneuron recordings. Spike-blocking efficacy in pyramidal cells could also be measured directly before and after an LTD-inducing protocol. One concern is that, over the time required to induce LTD, the responsiveness of the pyramidal cell to SC inputs could change sufficiently to make a such a comparison uninformative. A way of working around this problem would be to use population spikes, rather than intracellular recordings, to assess spike-blocking efficacy. In this way, variability across neurons would be averaged out over a large population of pyramidal cells. Spike-blocking efficacy could be measured in a single trial, by comparing the amplitude of the SC-evoked population spike in the presence or absence of prior stimulation of the TA pathway. Preliminary results (not shown) suggest that population spikes evoked by SC stimulation can be reduced by TA burst activity; a similar protocol was used to study inhibition of evoked pyramidal cell activity in area CA3 (Kehl and McLennan 1985a).

The modulation of both excitatory (TA field potentials) and inhibitory (spike-blocking) responses by low-frequency stimulation occurs over very different time courses, with TA LTD lasting for at least an hour, while the depression of spike-blocking recovers within minutes. Nonetheless, the existence of both these activity-dependent phenomena suggests a complicated balance between excitation and inhibition in the TA input to CA1.

5.3 Other ideas

5.3.1 Other ways of studying the TA pathway

5.3.1.1 Mouse slices

One of the drawbacks of the slice preparation is that when the hippocampus is sliced, a portion of the intrinsic circuitry is lost (Amaral and Witter 1989). This can affect the general balance of excitation and inhibition in slice (e.g., see Lacaille and Schwartzkroin 1988a for contrasting results in transverse and longitudinal slices) as well as reducing the apparent strength of synaptic pathways that may not run parallel to the plane of the slice. As discussed previously, this may account for the lesser excitatory impact of the TA input *in vitro* than *in vivo*. One way to reduce the deleterious impact of slicing would be to prepare hippocampal slices from mice, rather than from rats. Because mice are so much smaller than rats, a 500 or even 400 μm thick slice from mouse hippocampus would preserve much more circuitry than an equally thick slice from rat hippocampus. However, any study of the TA pathway in mouse slices must take into account the different topography of the TA projection in mouse as compared to rat; whereas in rat, the mediolateral axis of the EC maps onto the CA3-subiculum axis of CA1, in mouse, the mediolateral axis of the EC maps onto the proximodistal axis of CA1 pyramidal cell dendrites (van Groen *et al.* 1998). Other differences between hippocampal circuitry in mouse and rat may well exist.

5.3.1.2 In vivo *studies*

Another way of getting around the limitations of the slice preparation would be to study the TA pathway *in vivo*. *In vivo* studies pose certain challenges. Intracellular or whole-cell recordings are much harder to obtain *in vivo* than *in vitro*. More expertise is required for proper placement of stimulating and recording electrodes *in vivo* than in slice, where the laminar structure of the hippocampus can be seen clearly. Field recordings may be complicated by volume conduction from other regions; in the case of the TA pathway, which can be activated by stimulating the angular bundle, which also contains the perforant path to dentate gyrus (Witter *et al.* 1989), care must be taken to distinguish between the TA response in CA1 and the volume-conducted perforant path response in dentate gyrus (Stringer and Colbert 1994; Leung *et al.* 1995). Pharmacological manipulations become more difficult to perform, and, especially, to reverse, in the absence of perfusion.

In vivo studies have the following advantages. The circuitry is intact; given the restricted topography of the TA projection (Tamamaki and Nojyo 1995), it may be easier to find a site responsive to TA stimulation in the hippocampus *in vivo* than in slice. Chronic recordings in awake, behaving animals provide neurophysiological data under completely natural conditions, and allow correlations to be made directly between neurophysiology, sensory inputs and motor outputs, and behavioral states. One issue directly relevant to the study of the TA pathway is the selectivity of activation of that particular pathway. In slice, stimulation in SLM activates other cortical and subcortical afferents (section 1.3.3, p. 60) in addition to the TA pathway. *In vivo*, each of these afferents could be stimulated independently at its site of origin, allowing one to differen-

tiate between the contributions of these pathways to hippocampal processing, as well as allowing the study of interactions between these inputs.

5.3.2 Temperature

The rat brain *in vivo* exists at a physiological temperature of about 37 °C (Moser *et al.* 1993). The Schuman lab electrophysiology room is generally a cool 20 °C, and that is the temperature at which my experiments were performed. Many biological processes simply become slower at lower temperatures, meaning that results obtained at room temperature are not qualitatively different from processes taking place *in vivo*. However, some inconsistencies in the literature have been attributed to temperature differences causing qualitative, rather than just quantitative, differences in results. For example, as described in section 1.1.4.2 (p. 24), the difficulty of inducing LTP in interneurons may be attributable to the low temperatures at which early experiments were performed (Franks *et al.* 1998). It would be interesting to know how my results would be affected if experiments were performed at a more physiological temperature. My prediction is that all synaptic responses would be scaled up, and that TA LTD would still occur, but starting with a higher baseline response; and spike-blocking would still be evoked by the TA pathway, though the balance in stimulus strengths needed to demonstrate spike-blocking might change. My attempts to record from slices at higher temperatures were initially stymied by my finding that, when the perfusion solution was heated, field and intracellular responses decreased dramatically (data not shown). I later reasoned that, at higher temperatures, the metabolic rate of the slice would increase, and a higher perfusion rate may be necessary to maintain sufficient oxygenation to keep the slice

healthy; preliminary experiments (data not shown) confirmed that healthy-looking recordings could be made from slices held at temperatures up to 36 °C. A recent report (Masino and Dunwiddie 1999) showed that synaptic transmission did decrease with increasing temperature; this decrease could be blocked with adenosine receptor antagonists, suggesting an effect similar to hypoxia, which increases adenosine levels (Winn *et al.* 1980). The perfusion rate (2 mL/min) used in those experiments is comparable to, or slower than, the perfusion rate I use. Higher perfusion rates may provide more oxygen and/or wash away the adenosine being released.

5.3.3 TA activity and hippocampal theta rhythms

Theta frequency (5-12 Hz) oscillations in the hippocampal EEG are associated with particular behavioral states, including those during which learning may be occurring (see Bland 1986; Vinogradova 1995 for review). The likely connection between the TA pathway and theta frequency oscillations in the hippocampus merits investigation. Synaptic input to the distal dendritic region of CA1, presumably via the TA pathway, contributes to the induction of theta *in vivo* (Bragin *et al.* 1995; Buzsáki *et al.* 1995; Ylinen *et al.* 1995a). Patterned stimulation in SLM, likely activating TA axons, can induce theta-like activity in the hippocampal slice (Heynen *et al.* 1993).

Cholinergic (as well as GABAergic) input to the hippocampus from the medial septum is also important in theta induction (Bland 1986; Vinogradova 1995). Theta-like activity can be induced in hippocampal slices by the application of the mAChR agonist CCh (see Konopacki *et al.* 1987; Bland *et al.* 1988; Huerta and Lisman 1993; Konopacki 1998 for review). SLM interneurons, putative targets of the TA pathway, are depolarized

and show membrane potential oscillations in the presence of CCh (Chapman and Lacaille 1998). The ease of induction of theta-like oscillations in slices appears to be age- and temperature-dependent, with oscillations more readily induced at higher temperatures and in slices from younger rats (Heynen and Bilkey 1991; Fellous and Sejnowski 1998). It should be noted, however, that doubts have been raised about whether oscillations recorded *in vitro* are truly analogous to *in vivo* theta activity, or instead resemble epileptiform activity (Williams and Kauer 1997).

The relative importance of the contributions of EC and septal input to the generation of theta in the hippocampus is still controversial. One way in which the TA input is thought to help drive theta is via the synchronous activation of interneurons which then inhibit pyramidal cells in a synchronized, rhythmic manner (Buzsáki 1984). However, the cholinergic septal input can also depolarize and activate interneurons (see Stewart and Fox 1990 for review), including SLM interneurons (Chapman and Lacaille 1998). It would be interesting to see how responses to TA activity, in both pyramidal cells and interneurons, are modulated by cholinergically-induced theta oscillations. Transmission through the trisynaptic pathway is reduced during theta (Winson and Abzug 1978), presumably at least partially because of the selective inhibition of Schaffer collateral transmission by the activation of mAChRs (Hasselmo and Schnell 1994). One would predict that TA responses during theta would be larger than those seen in quiet slices. It would also be of interest to see if the TA pathway is more easily potentiated during theta, just as the SC pathway is (Huerta and Lisman 1993).

5.3.4 Stratum radiatum giant cells

The role of SR giant cells in hippocampal processing remains to be elucidated. Unlike CA1 pyramidal cells, they seem to be strongly excited by TA inputs, even in slice (section 2.3.4.2, p. 105). However, since little is known about possible postsynaptic targets of SR giant cells (Gulyás *et al.* 1998b), it is difficult to speculate about the significance of a strong excitatory monosynaptic connection between EC and SR giant cells. SR giant cells, like pyramidal cells (Knowles and Schwartzkroin 1981a; Knowles and Schwartzkroin 1981b), appear to form synapses onto interneurons in SO (Gulyás *et al.* 1998b), suggesting a possible feedback inhibition of the TA input. It is possible that the axon collaterals of SR giant cells form synapses onto the basal dendrites of CA1 pyramidal cells, in which case they could help mediate a feed-forward excitation from the TA input. The greater responsiveness of SR giant cells to TA input, compared to pyramidal cells, suggests that studies of the plasticity of TA responses using intracellular techniques could be more readily performed on giant cells than on pyramidal cells; however, since it is not yet known just how similar giant cells really are to pyramidal cells, it may not be valid to extrapolate from results in giant cells to inferences about pyramidal cells. Further characterization of this novel cell type remains to be done.

5.3.5 Selective inhibition of SC vs. TA inputs to hippocampus

An intriguing possibility exists of a "competitive" interaction between the SC and the TA inputs to area CA1 of the hippocampus. As we have seen (Chapter 4), activation of the TA pathway can inhibit excitatory transmission in the SC pathway. Conversely, alvear stimulation, which evokes feedback activity of CA1 pyramidal cells, results in

activation of O-LM interneurons and inhibition of the TA field response (Maccaferri and McBain 1995). The question of whether the TA inhibitory, spike-blocking effect is selective for SC inputs remains an open one. Once again, the identification of circumstances under which TA inputs are strongly excitatory is required before this question can be answered. However, since it is not known how – or whether – pyramidal cells could distinguish between inputs coming from different dendritic layers (Yuste and Tank 1996), it is not obvious how the downstream targets of the CA1 pyramidal cells would "know" whether the activity was due to TA or SC input.

If the spike-blocking effect is, indeed, mediated by activation of presynaptic $GABA_B$ receptors on SC axons, then it seems likely that TA input would be unaffected, because TA responses in CA1 are insensitive to the $GABA_B$ agonist baclofen (Colbert and Levy 1992). Therefore, a situation exists where TA activity may selectively inhibit SC responses via the feedforward activation of SLM (and possibly other) interneurons, whereas SC activity may inhibit TA responses via the feedback activation of O-LM interneurons (Figure 2). This interaction could mediate the "switching" postulated in models of the function of the CA1 region in memory encoding and retrieval (Hasselmo and Schnell 1994; Hasselmo *et al.* 1996). A better understanding of how the balance between the excitatory and inhibitory components of these two afferent pathways to CA1 is determined by patterns of afferent activity would provide grist for more detailed models of hippocampal processing.

5.4 Summary and conclusions

The main findings of this thesis are:

1. The TA projection from EC to CA1, like the SC projection from CA3 to CA1, includes both glutamatergic excitatory components and GABAergic fast and slow inhibitory components. However, unlike the SC pathway, the inhibitory component dominates (at least *in vitro*) (Chapter 2).

2. In slice, the excitatory component of the TA pathway is best studied with field potential recordings, while the inhibitory component is more apparent in intracellular recordings from pyramidal cells (Chapter 2).

3. Short-term plasticity of the TA pathway is similar to that seen in the SC pathway. Some facilitation of the excitatory response is observed at short ISIs, but with longer trains of stimulation, a $GABA_B$-mediated IPSP dominates the response (Chapter 2).

4. In response to low-frequency stimulation, the excitatory TA response undergoes a robust long-term depression that is independent of GABAergic inhibition and partially mediated by NMDA receptors. This depression can be reversed by repeated high-frequency stimulation (Chapter 3).

5. Burst stimulation of the TA pathway evokes an inhibitory response that can prevent CA1 pyramidal cells from spiking in response to subsequent SC stimulation. This inhibition undergoes a form of short-term depression, with spike-blocking efficacy decreasing with repeated TA burst stimulation (Chapter 4).

How do these findings tie in to the themes of neuronal network processing and hippocampal function described in Chapter 1? Many of the forces controlling the balance

between excitation and inhibition in the brain are at play in the TA input to CA1. The excitatory component of the TA response is subject to activity-dependent regulation on both short and long time scales; differences observed between the TA and SC pathways may shed light on the importance of the spatial distribution of inputs to dendrites. The TA pathway also recruits feedforward inhibition in a stimulation pattern-dependent manner, showing the importance of bursts of activity in regulating information flow through neuronal networks. The dependence on timing of the inhibitory spike-blocking effect supports the idea that temporal patterning of activity is critical in determining the computation performed a neuronal network.

As described in section 1.3.2.5 (p. 54), some of the functions attributed to the TA pathway include memory encoding in an associative CA1 network, conveyance of spatial information from EC to CA1 place cells, and generation of theta and gamma oscillations in the hippocampus that may serve as a contextual background for information coding. The short- and long-term plasticity of the excitatory component of the TA input to CA1 described in this thesis demonstrates a capacity for activity-dependent regulation that may be critical in allowing the TA pathway to contribute to these processes. The recruitment of feedforward inhibition, as seen in the TA-SC spike-blocking effect, is likely be particularly important in the generation of oscillatory activity, and the discovery of short-term regulation of the efficacy of this inhibition may contribute to our understanding of the network properties giving rise to oscillations. The ability of the inhibitory component of the TA pathway to control output activity of the hippocampus suggests an important role in determining whether information will pass through the hippocampus via the mono- or the trisynaptic pathways; this switch may determine whether the hippocampus

is working in an encoding or in a recall state. Finally, the finding of control of CA1 excitation by the TA pathway is consistent with the loss of this pathway during conditions of runaway excitation, such as epilepsy.

The richness of network interactions and possible critical functions of the temporoammonic pathway show that this is, indeed, an "underestimated pathway" (Witter *et al.* 1988). It is to be hoped that the phenomena described here motivate further studies of the contribution of the TA pathway to hippocampal processing.

6 Literature cited

Abeliovich, A., Chen, C., Goda, Y., Silva, A.J., Stevens, C.F., and Tonegawa, S., 1993a. Modified hippocampal long-term potentiation in PKC-gamma mutant mice. Cell 75:1253-1262.

Abeliovich, A., Paylor, R., Chen, C., Kim, J.J., Wehner, J.M., and Tonegawa, S., 1993b. PKC-gamma mutant mice exhibit mild deficits in spatial and contextual learning. Cell 75:1263-1271.

Abraham, W.C., and Bear, M.F., 1996. Metaplasticity: the plasticity of synaptic plasticity. TINS 19:126-130.

Acsády, L., Arabadzisz, D., and Freund, T.F., 1996. Correlated morphological and neurochemical features identify different subsets of vasoactive intestinal polypeptide-immunoreactive interneurons in rat hippocampus. Neuroscience 73:299-315.

Aihara, T., Tsukada, M., Crair, M.C., and Shinomoto, S., 1997. Stimulus-dependent induction of long-term potentiation in CA1 area of the hippocampus: experiment and model. Hippocampus 7:416-426.

Aitken, P.G., Breese, G.R., Dudek, F.F., Edwards, F., Espanol, M.T., Larkman, P.M., Lipton, P., Newman, G.C., Nowak, T.S., Jr., Panizzon, K.L., Raley-Susman, K.M., Reid, K.H., Rice, M.E., Sarvey, J.M., Schoepp, D.D., Segal, M., Taylor, C.P., Teyler, T.J., and Voulalas, P.J., 1995. Preparative methods for brain slices: a discussion. J. Neurosci. Meth. 59:139-149.

Alger, B.E., and Nicoll, R.A., 1982. Feed-forward dendritic inhibition in rat hippocampal pyramidal cells studied *in vitro*. J. Physiol. (Lond.) 328:105-123.

Alkondon, M., Pereira, E.F.R., and Albuquerque, E.X., 1998. α-bungarotoxin- and methyllycaconitine-sensitive nicotinic receptors mediate fast synaptic transmission in interneurons of rat hippocampal slices. Brain Res. 810:257-263.

Alonso, A., and Garcia-Austt, E., 1987. Neuronal sources of theta rhythm in the entorhinal cortex of the rat. II. Phase relations between unit discharges and theta field potentials. Exp. Brain. Res. 67:502-509.

Amaral, D.G., Ishizuka, N., and Claiborne, B., 1990. Neurons, numbers, and the hippocampal network. In: Progress in Brain Research, vol. 83, edited by Storm-Mathisen, J., Zimmer, J. and Ottersen, O.P., Amsterdam: Elsevier Science Publishers B.V., pp. 1-11.

Amaral, D.G., and Witter, M.P., 1989. The three-dimensional organization of the hippocampal formation: a review of anatomical data. Neuroscience 31:571-591.

Andersen, P., 1975. Organization of hippocampal neurons and their interconnections. In: The Hippocampus - Volume 1: Structure and Development, edited by Isaacson, R.L. and Pribram, K.H., New York: Plenum Press, pp. 155-175.

Andersen, P., 1990. Synaptic integration in hippocampal CA1 pyramids. In: Progress in Brain Research, vol. 83, edited by Storm-Mathisen, J., Zimmer, J. and Ottersen, O.P., Elsevier Science Publishers B.V., pp. 215-222.

Andersen, P., Bliss, T.V.P., and Skrede, K.K., 1971. Lamellar organization of hippocampal excitatory pathways. Exp. Brain. Res. 13:222-238.

Andersen, P., Dingledine, R., Gjerstad, L., Langmoen, I.A., and Mostfled Laursen, A., 1980. Two different responses of hippocampal pyramidal cells to application of gamma-amino butyric acid. J. Physiol. (Lond.) 305:279-296.

Andersen, P., Holmqvist, B., and Voorhoeve, P.E., 1966. Excitatory synapses on hippocampal apical dendrites activated by entorhinal stimulation. Acta Physiol. Scand. 66:461-472.

Andersen, P., Sundberg, S.H., Sveen, O., and Wigström, H., 1977. Specific long-lasting potentiation of synaptic transmission in hippocampal slices. Nature 266:736-37.

Andre, P., Ferrat, T., Steinman, M., and Olpe, H.R., 1992. Increased acetylcholine and quisqualate responsiveness after blockade of $GABA_B$ receptors. Eur. J. Pharmacol. 218:137-143.

Arai, A., Black, J., and Lynch, G., 1994. Origins of the variation in long-term potentiation between synapses in the basal versus apical dendrites of hippocampal neurons. Hippocampus 4:1-10.

Arai, A., Silberg, J., and Lynch, G., 1995. Differences in the refractory period of two distinct inhibitory circuitries in field CA1 of the hippocampus. Brain Res. 704:298-306.

Artola, A., and Singer, W., 1993. Long-term depression of excitatory synaptic transmission and its relationship to long-term potentiation. TINS 16:480-487.

Atzori, M., 1996. Pyramidal cells and stratum lacunosum-moleculare interneurons in the CA1 hippocampal region share a GABAergic spontaneous input. Hippocampus 6:72-78.

Auerbach, J.M., and Segal, M., 1996. Muscarinic receptors mediating depression and long-term potentiation in rat hippocampus. J. Physiol. (Lond.) 492:479-493.

Ault, B., and Nadler, J.V., 1982. Baclofen selectively inhibits transmission at synapses made by axons of CA3 pyramidal cells in the hippocampal slice. J. Pharmacol. Exp. Ther. 223:291-297.

Ball, M.J., Hachinski, V., Fox, A., Kirshen, A.J., Fisman, M., Blume, W., Kral, V.A., Fox, H., and Merskey, H., 1985. A new definition of Alzheimer's disease: a hippocampal dementia. Lancet 5:14-16.

Banks, M.I., Li, T.-B., and Pearce, R.A., 1998. The synaptic basis of $GABA_{A,slow}$. J. Neurosci. 18:1305-1317.

Bannerman, D.M., Good, M.A., Butcher, S.P., Ramsay, M., and Morris, R.G.M., 1995. Distinct components of spatial learning revealed by prior training and NMDA receptor blockade. Nature 378:182-186.

Barnes, C.A., 1988. Spatial learning and memory processes: the search for their neurobiological mechanisms in the rat. TINS 11:163-169.

Barnes, C.A., McNaughton, B.L., Mizumori, S.J.Y., Leonard, B.W., and Lin, L.-H., 1990. Comparison of spatial and temporal characteristics of neuronal activity in sequential stages of hippocampal processing. In: Progress in Brain Research, vol. 83, edited by Storm-Mathisen, J., Zimmer, J. and Ottersen, O.P., Elsevier Science Publishers B.V., pp. 287-300.

Barrionuevo, G., and Brown, T.H., 1983. Associative long-term potentiation in hippocampal slices. Proc. Nat. Acad. Sci. USA 80:7347-7351.

Bear, M.F., and Abraham, W.C., 1996. Long-term depression in hippocampus. Annu. Rev. Neurosci. 19:437-462.

Benardo, L.S., 1995. *N*-methyl-D-aspartate transmission modulates $GABA_B$-mediated inhibition of rat hippocampal pyramidal neurons *in vitro*. Neuroscience 68:637-643.

Ben-Ari, Y., Krnjevic, K., and Reinhardt, W., 1979. Hippocampal seizures and failure of inhibition. Can. J. Physiol. Pharmacol 57:1462-1466.

Bergles, D.E., Doze, V.A., Madison, D.V., and Smith, S.J., 1996. Excitatory actions of norepinephrine on multiple classes of hippocampal CA1 interneurons. J. Neurosci. 16:572-585.

Bernasconi, R., Lauber, J., Marescaux, C., Vergnes, M., Martin, P., Rubio, V., Leonhardt, T., Reymann, N., and Bittiger, H., 1992. Experimental absence seizures: potential role of gamma-hydroxybutyric acid and $GABA_B$ receptors. In: Generalized Non-Convulsive Epilepsy: Focus on $GABA_B$ Receptors, edited by Marescaux, C., Vergnes, M. and Bernasconi, R., Vienna: Springer-Verlag, pp. 155-178.

Berry, M.S., and Pentreath, V.W., 1976. Criteria for distinguishing between monosynaptic and polysynaptic transmission. Brain Res. 105:1-20.

Bi, G.-q., and Poo, M.-m., 1998. Synaptic modifications in cultured hippocampal neurons: dependence on spike timing, synaptic strength, and postsynaptic cell type. J. Neurosci. 18:10464-10472.

Bland, B.H., 1986. The physiology and pharmacology of hippocampal formation theta rhythms. Prog. Neurobiol. 26:1-54.

Bland, B.H., Colom, L.V., Konopacki, J., and Roth, S.H., 1988. Intracellular records of carbachol-induced theta rhythm in hippocampal slices. Brain Res. 447:364-368.

Bliss, T.V.P., and Collingridge, G.L., 1993. A synaptic model of memory: long-term potentiation in the hippocampus. Nature 361:31-39.

Bliss, T.V.P., and Richter-Levin, G., 1993. Spatial learning and saturation of long-term potentiation. Hippocampus 3:123-126.

Boeijinga, P.H., and Boddeke, H.W.G.M., 1996. Activation of $5\text{-}HT_{1B}$ receptors suppresses low but not high frequency synaptic transmission in the rat subicular cortex *in vitro*. Brain Res. 721:59-65.

Bolshakov, V.Y., and Siegelbaum, S.A., 1994. Postsynaptic induction and presynaptic expression of hippocampal long-term depression. Science 264:1148-1152.

Bormann, J., and Feigenspan, A., 1995. $GABA_C$ receptors. TINS 18:515-519.

Bradford, H.F., 1995. Glutamate, GABA and epilepsy. Prog. Neurobiol. 47:477-511.

Bragin, A., Jando, G., Nadasdy, Z., Hetke, J., Wise, K., and Buzsáki, G., 1995. Gamma (40-100-Hz) oscillation in the hippocampus of the behaving rat. J. Neurosci. 15:47-60.

Bragin, A.G., and Otmakhov, N.A., 1979. Comparison of direct influences of the perforant path on hippocampal CA1 and CA3 neurons *in vitro*. Neurophysiology 11:220-226.

Bramham, C.R., Bacher-Svendsen, K., and Sarvey, J.M., 1997. LTP in the lateral perforant path is β-adrenergic receptor dependent. NeuroReport 8:719-724.

Bramham, C.R., Milgram, N.W., and Srebro, B., 1991. Activation of AP5-sensitive NMDA receptors is not required to induce LTP of synaptic transmission in the lateral perforant path. Eur. J. Neurosci. 3:1300-1308.

Bramham, C.R., and Sarvey, J.M., 1996. Endogenous activation of μ and δ-1 opioid receptors is required for long-term potentiation in the lateral perforant path: dependence on GABAergic inhibition. J. Neurosci. 16:8123-8131.

Brown, T.H., and Zador, A.M., 1990. Hippocampus. In: The Synaptic Organization of the Brain, edited by Shepherd, G.M., New York: Oxford University Press, pp. 346-388.

Buhl, E.H., Cobb, S.R., Halasy, K., and Somogyi, P., 1995. Properties of unitary IPSPs evoked by anatomically identified basket cells in the rat hippocampus. Eur. J. Neurosci. 7:1989-2004.

Buhl, E.H., Halasy, K., and Somogyi, P., 1994a. Diverse sources of hippocampal unitary inhibitory postsynaptic potentials and the number of synaptic release sites. Nature 368:823-828.

Buhl, E.H., Han, Z.S., Lörinczi, Z., Stezhka, V.V., Karnup, S.V., and Somogyi, P., 1994b. Physiological properties of anatomically identified axo-axonic cells in the rat hippocampus. J. Neurophysiol. 71:1289-1307.

Bunsey, M., and Eichenbaum, H., 1996. Conservation of hippocampal memory function in rats and humans. Nature 379:255-257.

Buonomano, D.V., and Merzenich, M.M., 1998. Net interaction between different forms of short-term synaptic plasticity and slow-IPSPs in the hippocampus and auditory cortex. J. Neurophysiol. 80:1765-1774.

Burke, J.P., and Hablitz, J.J., 1994. Presynaptic depression of synaptic transmission mediated by activation of metabotropic glutamate receptors in rat neocortex. J. Neurosci. 14:5120-5130.

Buzsáki, G., 1984. Feed-forward inhibition in the hippocampal formation. Prog. Neurobiol. 22:131-153.

Buzsáki, G., 1988. Polysynaptic long-term potentiation: a physiological role of the perforant path-CA3/CA1 pyramidal cell synapse. Brain Res. 455:192-195.

Buzsáki, G., 1997. Functions for interneuronal nets in the hippocampus. Can. J. Physiol. Pharmacol. 75:508-515.

Buzsáki, G., Penttonen, M., Bragin, A., Nadásdy, Z., and Chrobak, J.J., 1995. Possible physiological role of the perforant path-CA1 projection. Hippocampus 5:141-146.

Buzsáki, G., Penttonen, M., Nádasdy, Z., and Bragin, A., 1996. Pattern and inhibition-dependent invasion of pyramidal cell dendrites by fast spikes in the hippocampus *in vivo*. Proc. Nat. Acad. Sci. USA 93:9921-9925.

Carmant, L., Perez, Y., Chapman, C.A., and Lacaille, J.-C., 1998. Properties of AMPA receptors in subtypes of CA1 interneurons in rat hippocampal slices. Soc. Neurosci. Abstr. 24:91.

Carmant, L., Woodhall, G., Ouardouz, M., Robitaille, R., and Lacaille, J.C., 1997. Interneuron-specific Ca^{2+} responses linked to metabotropic and ionotropic glutamate receptors in rat hippocampal slices. Eur. J. Neurosci. 9:1625-1635.

Cash, S., and Yuste, R., 1998. Input summation by cultured pyramidal neurons is linear and position-independent. J. Neurosci. 18:10-15.

Cavus, I., and Teyler, T.J., 1998. NMDA receptor-independent LTP in basal versus apical dendrites of CA1 pyramidal cells in rat hippocampal slice. Hippocampus 8:373-379.

Chapman, C.A., and Lacaille, J.-C., 1998. Intrinsic theta-frequency membrane potential oscillations induced by carbachol in hippocampal interneurons in stratum lacunosum-moleculare. Soc. Neurosci. Abstr. 24:2020.

Chapman, C.A., and Lacaille, J.-C., 1999. Intrinsic theta-frequency membrane potential oscillations in hippocampal CA1 interneurons of stratum lacunosum-moleculare. J. Neurophysiol. 81:1296-1307.

Charpak, S., Paré, D., and Llinás, R., 1995. The entorhinal cortex entrains fast CA1 hippocampal oscillations in the anaesthetized guinea-pig: role of the monosynaptic component of the perforant path. Eur. J. Neurosci. 7:1548-1557.

Chavez-Noriega, L.E., Halliwell, J.V., and Bliss, T.V.P., 1990. A decrease in firing threshold observed after induction of the EPSP-spike (E-S) component of long-term potentiation in rat hippocampal slices. Exp. Brain. Res. 79:633-641.

Chen, Z., Fujii, S., Ito, K.-I., Kato, H., Kaneko, K., and Miyakawa, H., 1995. Activation of dopamine D1 receptors enhances long-term depression of synaptic transmission induced by low frequency stimulation in rat hippocampal CA1 neurons. Neurosci. Lett. 188:195-198.

Chikwendu, A., and McBain, C.J., 1996. Two temporally overlapping "delayed-rectifiers" determine the voltage-dependent potassium current phenotype in cultured hippocampal interneurons. J. Neurophysiol. 76:1477-1490.

Christie, B.R., and Abraham, W.C., 1994. L-type voltage-sensitive calcium channel antagonists block heterosynaptic long-term depression in the dentate gyrus of anesthetized rats. Neurosci. Lett. 167:41-45.

Christie, B.R., Schexnayder, L.K., and Johnston, D., 1997. Contribution of voltage-gated Ca^{2+} channels to homosynaptic long-term depression in the CA1 region *in vitro*. J. Neurophysiol. 77:1651-5.

Chrobak, J.J., and Buzsáki, G., 1998. Gamma oscillations in the entorhinal cortex of the freely behaving rat. J. Neurosci. 18:388-398.

Chu, D.C.M., Albin, R.L., Young, A.B., and Penney, J.B., 1990. Distribution and kinetics of $GABA_B$ binding sites in rat central nervous system: a quantitative autoradiographic study. Neuroscience 34:341-357.

Cobb, S.R., Buhl, E.H., Halasy, K., Paulsen, O., and Somogyi, P., 1995. Synchronization of neuronal activity in hippocampus by individual GABAergic interneurons. Nature 378:75-78.

Cobb, S.R., Halasy, K., Vida, I., Nyiri, G., Tamas, G., Buhl, E.H., and Somogyi, P., 1997. Synaptic effects of identified interneurons innervating both interneurons and pyramidal cells in the rat hippocampus. Neuroscience 79:629-648.

Cohen, G.A., Doze, V.A., and Madison, D.V., 1992. Opioid inhibition of GABA release from presynaptic terminals of rat hippocampal interneurons. Neuron 9:325-335.

Colbert, C.M., and Levy, W.B., 1992. Electrophysiological and pharmacological characterization of perforant path synapses in CA1: mediation by glutamate receptors. J. Neurophysiol. 68:1-8.

Colbert, C.M., and Levy, W.B., 1993. Long-term potentiation of perforant path synapses in hippocampal CA1 *in vitro*. Brain Res. 606:87-91.

Cole, A.E., and Nicoll, R.A., 1984. Characterization of a slow cholinergic post-synaptic potential recorded *in vitro* from rat hippocampal pyramidal cells. J. Physiol. (Lond.) 352:173-188.

Colino, A., and Malenka, R.C., 1993. Mechanisms underlying induction of long-term potentiation in rat medial and lateral perforant paths *in vitro*. J. Neurophysiol. 69:1150-1159.

Collingridge, G.L., Herron, C.E., and Lester, R.A.J., 1988. Frequency-dependent *N*-methyl-D-aspartate receptor-mediated synaptic transmission in rat hippocampus. J. Physiol. (Lond.) 399:301-312.

Congar, P., Khazipov, R., and Ben-Ari, Y., 1995. Direct demonstration of functional disconnection by anoxia of inhibitory interneurons from excitatory inputs in rat hippocampus. J. Neurophysiol. 73:421-426.

Congar, P., Leinekugel, X., Ben-Ari, Y., and Crépel, V., 1997. A long-lasting calcium-activated nonselective cationic current is generated by synaptic stimulation or exogenous activation of group I metabotropic glutamate receptors in CA1 pyramidal neurons. J. Neurosci. 17:5366-5379.

Connolly, P., Clark, P., Curtis, A.S.G., Dow, J.A.T., and Wilkinson, C.D.W., 1990. An extracellular microelectrode array for monitoring electrogenic cells in culture. Biosens. Bioelec. 5:223-234.

Connors, B.W., Malenka, R.C., and Silva, L.R., 1988. Two inhibitory postsynaptic potentials, and $GABA_A$ and $GABA_B$ receptor-mediated responses in neocortex of rat and cat. J. Physiol. (Lond.) 406:443-468.

Cowan, A.I., Stricker, C., Reece, L.J., and Redman, S.J., 1998. Long-term plasticity at excitatory synapses on aspinous interneurons in area CA1 lacks synaptic specificity. J. Neurophysiol. 79:13-20.

Creager, R., Dunwiddie, T., and Lynch, G., 1980. Paired-pulse and frequency facilitation in the CA1 region of the *in vitro* rat hippocampus. J. Physiol. (Lond.) 299:409-424.

Crunelli, V., and Leresche, N., 1991. A role for $GABA_B$ receptors in excitation and inhibition of thalamocortical cells. TINS 14:16-21.

Cummings, J.A., Mulkey, R.M., Nicoll, R.A., and Malenka, R.C., 1996. Ca^{2+} signaling requirements for long-term depression in the hippocampus. Neuron 16:825-833.

Dahl, D., and Lecompte, B.B., III, 1994. Cholecystokinin and response modifications in hippocampal field CA1. Psychobiology 22:134-140.

Dan, Y., and Poo, M.-m., 1992. Hebbian depression of isolated neuromuscular synapses in vitro. Science 256:1570-1573.

Davies, C.H., and Collingridge, G.L., 1993. The physiological regulation of synaptic inhibition by $GABA_B$ autoreceptors in rat hippocampus. J. Physiol. (Lond.) 472:245-265.

Davies, C.H., and Collingridge, G.L., 1996. Regulation of EPSPs by the synaptic activation of $GABA_B$ autoreceptors in rat hippocampus. J. Physiol. (Lond.) 496:451-470.

Davies, C.H., Davies, S.N., and Collingridge, G.L., 1990. Paired-pulse depression of monosynaptic GABA-mediated inhibitory postsynaptic responses in rat hippocampus. J. Physiol. (Lond.) 424:513-531.

Davies, C.H., Pozza, M.F., and Collingridge, G.L., 1993. CGP 55845A - a potent antagonist of $GABA_B$ receptors in the CA1 region of rat hippocampus. Neuropharmacology 32:1071-1073.

Davies, C.H., Starkey, S.J., Pozza, M.F., and Collingridge, G.L., 1991. $GABA_B$ autoreceptors regulate the induction of LTP. Nature 349:609-611.

De Leon, M.J., Convit, A., George, A.E., Golomb, J., De Santi, S., Tarshish, C., Rusinek, H., Bobinski, M., Ince, C., Miller, D., and Wisniewski, H., 1996. *In vivo* structural studies of the hippocampus in normal aging and in incipient Alzheimer's disease. Ann. N.Y. Acad. Sci. 777:1-13.

Deadwyler, S.A., and Hampson, R.E., 1998. Evidence for anatomical specificity of spatial representation in hippocampus. Soc. Neurosci. Abstr. 24:1908.

Debanne, D., Gahwiler, B.H., and Thompson, S.M., 1994. Asynchronous pre- and postsynaptic activity induces associative long-term depression in area CA1 of the rat hippocampus *in vitro*. Proc. Nat. Acad. Sci. USA 91:1148-1152.

Debanne, D., Guérineau, N.C., Gähwiler, B.H., and Thompson, S.M., 1996. Paired-pulse facilitation and depression at unitary synapses in rat hippocampus: quantal fluctuation affects subsequent release. J. Physiol. (Lond.) 491:163-176.

Deisz, R.A., and Prince, D.A., 1989. Frequency-dependent depression of inhibition in guinea-pig neocortex *in vitro* by $GABA_B$ receptor feed-back on GABA release. J. Physiol. (Lond.) 412:513-541.

Delaney, K.R., Zucker, R.S., and Tank, D.W., 1989. Calcium in motor nerve terminals associated with posttetanic potentiation. J. Neurosci. 9:3558-3567.

Derrick, B.E., and Martinez, J.L., Jr., 1996. Associative, bidirectional modifications at the hippocampal mossy fiber-CA3 synapse. Nature 381:429-434.

Desmond, N.L., Scott, C.A., Jane, J.A., and Levy, W.B., 1994. Ultrastructural identification of entorhinal cortical synapses in CA1 stratum lacunosum-moleculare of the rat. Hippocampus 4:594-600.

Dickinson, P.S., and Moulins, M., 1992. Interactions and combinations between different networks in the stomatogastric nervous system. In: Dynamic Biological Networks: The Stomatogastric Nervous System, edited by Harris-Warrick, R.M., Marder, E., Selverston, A.I. and Moulins, M., Cambridge: The MIT Press, pp. 139-160.

Dickson, C.T., Kirk, I.J., Oddie, S.D., and Bland, B.H., 1995. Classification of theta-related cells in the entorhinal cortex: cell discharges are controlled by the ascending brainstem synchronizing pathway in parallel with hippocampal theta-related cells. Hippocampus 5:306-319.

Dickson, C.T., Mena, A.R., and Alonso, A., 1997. Electroresponsiveness of medial entorhinal cortex layer III neurons *in vitro*. Neuroscience 81:937-950.

Dinerman, J.L., Dawson, T.M., Schell, M.J., Snowman, A., and Snyder, S.H., 1994. Endothelial nitric oxide synthase localized to hippocampal pyramidal cells: implications for synaptic plasticity. Proc. Nat. Acad. Sci. USA 91:4214-4218.

Dobrunz, L.E., and Stevens, C.F., 1997. Heterogeneity of release probability, facilitation and depletion at central synapses. Neuron 18:995-1008.

Doherty, J., and Dingledine, R., 1997. Regulation of excitatory input to inhibitory interneurons of the dentate gyrus during hypoxia. J. Neurophysiol. 77:393-404.

Dolleman-Van der Weel, M.J., Lopes da Silva, F.H., and Witter, M.P., 1997. Nucleus reuniens thalami modulates activity in hippocampal field CA1 through excitatory and inhibitory mechanisms. J. Neurosci. 17:5640-5650.

Dolleman-Van Der Weel, M.J., and Witter, M.P., 1996. Projections from the nucleus reuniens thalami to the entorhinal cortex, hippocampal field CA1, and the subiculum in the rat arise from different populations of neurons. J. Comp. Neurol. 364:637-650.

Doller, H.J., and Weight, F.F., 1982. Perforant pathway activation of hippocampal CA1 stratum pyramidale neurons: electrophysiological evidence for a direct pathway. Brain Res. 237:1-13.

Doller, H.J., and Weight, F.F., 1985. Perforant pathway-evoked long-term potentiation of CA1 neurons in the hippocampal slice preparation. Brain Res. 333:305-310.

Doyère, V., Errington, M.L., Laroche, S., and Bliss, T.V.P., 1996. Low-frequency trains of paired stimuli induce long-term depression in area CA1 but not in dentate gyrus of the intact rat. Hippocampus 6:52-57.

Drake, C.T., Bausch, S.B., Milner, T.A., and Chavkin, C., 1997. GIRK1 immunoreactivity is present predominantly in dendrites, dendritic spines, and somata in the CA1 region of the hippocampus. Proc. Nat. Acad. Sci. USA 94:1007-1012.

Dreier, J.P., and Heinemann, U., 1991. Regional and time dependent variations of low Mg^{2+} induced epileptiform activity in rat temporal cortex slices. Exp. Brain. Res. 87:581-596.

Du, F., Whetsell Jr., W.O., Abou-Khalil, B., Blumenkopf, B., Lothman, E.W., and Schwarcz, R., 1993. Preferential neuronal loss in layer III of the entorhinal cortex in patients with temporal lobe epilepsy. Epilepsy Res. 16:223-233.

Dudek, S.M., and Bear, M.F., 1992. Homosynaptic long-term depression in area CA1 of hippocampus and effects of *N*-methyl-D-aspartate receptor blockade. Proc. Nat. Acad. Sci. USA 89:4363-4367.

Dudek, S.M., and Bear, M.F., 1993. Bidirectional long-term modification of synaptic effectiveness in the adult and immature hippocampus. J. Neurosci. 13:2910-2918.

Dudek, S.M., Egelman, D., Montague, P.R., and Friedlander, M.J., 1996. Induction of LTD in visual cortical neurons with stochastic patterns of afferent stimulation. Soc. Neurosci. Abstr. 22:976-976.

Dutar, P., Bassant, M.H., Senut, M.C., and Lamour, Y., 1995. The septohippocampal pathway: structure and function of a central cholinergic system. Physiol. Rev. 75:393-427.

Dutar, P., and Nicoll, R.A., 1988. A physiological role for $GABA_B$ receptors in the central nervous system. Nature 332:156-158.

Dvorak, H., and Schuman, E.M., 1996. Long- and short-term plasticity of the temporoammonic pathway in rat hippocampal slice. Soc. Neurosci. Abstr. 22:1520-1520.

Dvorak, H., and Schuman, E.M., 1997. High-frequency stimulation in stratum lacunosum-moleculare gates Schaffer collateral-evoked spiking in hippocampal CA1 pyramidal cells. Soc. Neurosci. Abstr. 23:485-485.

Dvorak-Carbone, H., and Schuman, E.M., 1999. Long-term depression of temporoammonic-CA1 hippocampal synaptic transmission. J. Neurophysiol. 81:1036-1044.

Edwards, F.A., 1995. Patch-clamp recording in brain slices. In: Brain Slices in Basic and Clinical Research, edited by Schurr, A. and Rigor, B.M., Boca Raton, FL: CRC Press, Inc., pp. 99-116.

Eichenbaum, H., and Otto, T., 1993. LTP and memory: can we enhance the connection? TINS 16:163-164.

Eichenbaum, H., Otto, T., and Cohen, N.J., 1992. The hippocampus - what does it do? Behav. Neur. Biol. 57:2-36.

Empson, R.M., and Heinemann, U., 1995a. Perforant path connections to area CA1 are predominantly inhibitory in the rat hippocampal-entorhinal cortex combined slice preparation. Hippocampus 5:104-107.

Empson, R.M., and Heinemann, U., 1995b. The perforant path projection to hippocampal area CA1 in the rat hippocampal-entorhinal cortex combined slice. J. Physiol. (Lond.) 484:707-720.

Enz, R., and Cutting, G.R., 1999. $GABA_C$ receptor rho subunits are heterogeneously expressed in the human CNS and form homo- and heterooligomers with distinct physical properties. Eur. J. Neurosci. 11:41-50.

Fellous, J.-M., and Sejnowski, T.J., 1998. The involvement of CA1, CA3 and dentate gyrus cells in carbachol-induced oscillations in the hippocampal slice. Soc. Neurosci. Abstr. 24:1582.

Finch, D.M., Wong, E.E., Derian, E.L., and Babb, T.L., 1986. Neurophysiology of limbic system pathways in the rat: projections from the subicular complex and hippocampus to the entorhinal cortex. Brain Res. 397:205-213.

Fisher, S.A., Fischer, T.M., and Carew, T.J., 1997. Multiple overlapping processes underlying short-term synaptic enhancement. TINS 20:170-177.

Fortunato, C., Debanne, D., Scanziani, M., Gähwiler, B.H., and Thompson, S.M., 1996. Functional characterization and modulation of feedback inhibitory circuits in area CA3 of rat hippocampal slice cultures. Eur. J. Neurosci. 8:1758-1768.

Franks, K.M., Christie, B.R., Seamans, J., and Sejnowski, T.J., 1998. Long-term potentiation and long-term depression in interneurons within the rat hippocampal stratum radiatum. Soc. Neurosci. Abstr. 24:1070.

Fraser, D.D., and MacVicar, B.A., 1991. Low-threshold transient calcium current in rat hippocampal lacunosum-moleculare interneurons: kinetics and modulation by neurotransmitters. J. Neurosci. 11:2812-2820.

Frazier, C.J., Buhler, A.V., Weiner, J.L., and Dunwiddie, T.V., 1998. Synaptic potentials mediated via a-bungarotoxin-sensitive nicotinic acetylcholine receptors in rat hippocampal interneurons. J. Neurosci. 18:8228-8235.

Fredens, K., Stengaard-Pedersen, K., and Larsson, L.I., 1984. Localization of enkephalin and cholecystokinin immunoreactivities in the perforant path terminal fields of the rat hippocampal formation. Brain Res 304:255-63.

Freund, T.F., and Antal, M., 1988. GABA-containing neurons in the septum control inhibitory interneurons in the hippocampus. Nature 336:170-173.

Freund, T.F., and Buzsáki, G., 1996. Interneurons of the hippocampus. Hippocampus 6:347-470.

Freund, T.F., Gulyás, A.I., Acsády, L., Gorcs, T., and Tóth, K., 1990. Serotonergic control of the hippocampus via local inhibitory interneurons. Proc. Nat. Acad. Sci. USA 87:8501-8505.

Funahashi, M., and Stewart, M., 1998. GABA receptor-mediated post-synaptic potentials in the retrohippocampal cortices: regional, laminar and cellular comparisons. Brain Res. 787:19-33.

Gähwiler, B.H., and Brown, D.A., 1985. $GABA_B$-receptor-activated K^+ current in voltage-clamped CA3 pyramidal cells in hippocampal cultures. Proc. Nat. Acad. Sci. USA 82:1558-1562.

Galarreta, M., and Hestrin, S., 1998. Frequency-dependent synaptic depression and the balance of excitation and inhibition in the neocortex. Nature Neurosci. 1:587-594.

Geiger, J.R.P., Melcher, T., Koh, D.-S., Sakmann, B., Seeburg, P.H., Jonas, P., and Moyner, H., 1995. Relative abundance of subunit mRNAs determines gating and Ca^{2+} permeability of AMPA receptors in principal neurons and interneurons in rat CNS. Neuron 15:193-204.

Georgopoulos, A.P., 1991. Higher order motor control. Annu. Rev. Neurosci. 14:361-377.

Gereau, R.W., IV, and Conn, P.J., 1995. Multiple presynaptic metabotropic glutamate receptors modulate excitatory and inhibitory synaptic transmission in hippocampal area CA1. J. Neurosci. 15:6879-6889.

Gil, Z., Connors, B.W., and Amitai, Y., 1997. Differential regulation of neocortical synapses by neuromodulators and activity. Neuron 19:679-686.

Gilbert, C.D., 1993. Circuitry, architecture, and functional dynamics of visual cortex. Cereb. Cortex 3:373-386.

Gloveli, T., Schmitz, D., Empson, R.M., Dugladze, T., and Heinemann, U., 1997a. Morphological and electrophysiological characterization of layer III cells of the medial entorhinal cortex of the rat. Neuroscience 77:629-648.

Gloveli, T., Schmitz, D., Empson, R.M., and Heinemann, U., 1997b. Frequency-dependent information flow from the entorhinal cortex to the hippocampus. J. Neurophysiol. 78:3444-3449.

Gluck, M.A., 1993. Computational models of the neural bases of learning and memory. Annu. Rev. Neurosci. 16:667-706.

Golding, N.L., and Spruston, N., 1998. Dendritic sodium spikes are variable triggers of axonal action potentials in hippocampal CA1 pyramidal neurons. Neuron 21:1189-1200.

Gorelova, N., and Yang, C.R., 1998. Dopamine increases the excitability of fast-spiking interneurons in rat medial prefrontal cortex via D1/5 receptor activation. Soc. Neurosci. Abstr. 24:350.

Grant, S.G.N., O'Dell, T.J., Karl, K.A., Stein, P.L., Soriano, P., and Kandel, E.R., 1992. Impaired long-term potentiation, spatial learning, and hippocampal development in *fyn* mutant mice. Science 258:1903-1910.

Gray, R., Rajan, A.S., Radcliffe, K.A., Yakehiro, M., and Dani, J.A., 1996. Hippocampal synaptic transmission enhanced by low concentrations of nicotine. Nature 383:713-716.

Green, E.J., McNaughton, B.L., and Barnes, C.A., 1990. Exploration-dependent modulation of evoked responses in fascia dentata: dissociation of motor, EEG and sensory factors and evidence for a synaptic efficiency change. J. Neurosci. 10:1455-1471.

Gross, G.W., and Lucas, J.H., 1982. Long-term monitoring of spontaneous single unit activity from neuronal monolayer networks cultured on photoetched multielectrode surfaces. J. Electrophysiol. Tech. 9:55-67.

Grover, L.M., and Teyler, T.J., 1990. Two components of long-term potentiation induced by different patterns of afferent activation. Nature 347:477-479.

Gulyás, A.I., Megias, M., and Freund, T.F., 1998a. Convergence of excitatory and inhibitory synapses onto parvalbumin, calbindin and calretinin immunoreactive hippocampal CA1 interneurons. Soc. Neurosci. Abstr. 24:1418.

Gulyás, A.I., Tóth, K., McBain, C.J., and Freund, T.F., 1998b. Stratum radiatum giant cells: a type of principal cell in the hippocampus. Eur. J. Neurosci. 10:3813-3822.

Gustafsson, B., and Wigström, H., 1986. Hippocampal long-lasting potentiation produced by pairing single volleys and brief conditioning tetani evoked in separate afferents. J. Neurosci. 6:1575-1582.

Guyon, A., and Leresche, N., 1995. Modulation by different $GABA_B$ receptor types of voltage-activated calcium currents in rat thalamocortical neurons. J. Physiol. (Lond.) 485:29-42.

Hablitz, J.J., and Thalmann, R.H., 1987. Conductance changes underlying a late synaptic hyperpolarization in hippocampal CA3 neurons. J. Neurophysiol. 58:160-179.

Hájos, N., and Mody, I., 1997. Synaptic communication among hippocampal interneurons: properties of spontaneous IPSCs in morphologically identified cells. J. Neurosci. 17:8427-8442.

Hampson, R.E., Heyser, C.J., and Deadwyler, S.A., 1993. Hippocampal cell firing correlates of delayed-match-to-sample performance in the rat. Behav. Neurosci. 107:715-739.

Han, Z.S., 1996. Morphological heterogeneity of nonpyramidal neurons in the CA1 region of the rat hippocampus. Neurosci. Res. 25:51-65.

Hannay, T., Larkman, A., Stratford, K., and Jack, J., 1993. A common rule governs the synaptic locus of both short-term and long-term potentiation. Curr. Biol. 3:832-841.

Hargreaves, E.L., Cain, D.P., and Vanderwolf, C.H., 1990. Learning and behavioral-long-term potentiation: importance of controlling for motor activity. J. Neurosci. 10:1472-1478.

Harris-Warrick, R.M., and Marder, E., 1991. Modulation of neural networks for behavior. Annu. Rev. Neurosci. 14:39-57.

Hasselmo, M.E., and Schnell, E., 1994. Laminar selectivity of the cholinergic suppression of synaptic transmission in rat hippocampal region CA1: computational modeling and brain slice physiology. J. Neurosci. 14:3898-3914.

Hasselmo, M.E., Wyble, B.P., and Wallenstein, G.V., 1996. Encoding and retrieval of episodic memories: Role of cholinergic and GABAergic modulation in the hippocampus. Hippocampus 6:693-708.

Herkenham, M., 1978. The connections of the nucleus reuniens thalami: evidence for a direct thalamo-hippocampal pathway in the rat. J. Comp. Neurol. 177:589-610.

Hernandez, R.V., Jaffe, D.B., and Martinez, J.L., Jr., 1998. Mechanisms of perforant path-CA1 long-term potentiation in the rat hippocampal slice. Soc. Neurosci. Abstr. 24:2025.

Herreras, O., Solis, J.M., Martin del Rio, R., and Lerma, J., 1987. Characteristics of CA1 activation through the hippocampal trisynaptic pathway in the unanesthetized rat. Brain Res. 413:75-86.

Herron, C.E., Lester, R.A.J., Coan, E.J., and Collingridge, G.L., 1986. Frequency-dependent involvement of NMDA receptors in the hippocampus: a novel synaptic mechanism. Nature 322:265-268.

Heynen, A.J., and Bilkey, D.K., 1991. Induction of RSA-like oscillations in both the *in-vitro* and *in-vivo* hippocampus. Neuroreport 2:401-404.

Heynen, A.J., Sainsbury, R.S., and Bilkey, D.K., 1993. Stimulation-induced RSA-like field activity in region CA1 of the hippocampal slice: amplitude maxima and topography. Brain Res. Bull. 32:113-122.

Hill, D.R., and Bowery, N.G., 1981. ^{3}H-baclofen and ^{3}H-GABA bind to bicuculline-insensitive $GABA_B$ sites in rat brain. Nature 290:149-152.

Hille, B., 1992. Ionic Channels of Excitable Membranes, Second Edition, Sunderland, MA: Sinauer Associates Inc.

Hirayasu, Y., and Wada, J.A., 1992a. Convulsive seizures in rats induced by *N*-methyl-D-aspartate injection into the massa intermedia. Brain Res. 577:36-40.

Hirayasu, Y., and Wada, J.A., 1992b. *N*-methyl-D-aspartate injection into the massa intermedia facilitates development of limbic kindling in rats. Epilepsia 33:965-970.

Hoffman, D.A., Magee, J.C., Colbert, C.M., and Johnston, D., 1997. K^+ channel regulation of signal propagation in dendrites of hippocampal pyramidal neurons. Nature 387:869-875.

Honer, M., Fritschy, J.-M., Mohler, H., and Benke, D., 1998. Identification of $GABA_B$ receptor subunit proteins GB1A and GB1B in rat brain: differential developmental, regional and subcellular distribution. Soc. Neurosci. Abstr. 24:1587.

Huang, Y.-Y., Kandel, E.R., Varshavsky, L., Brandon, E.P., Qi, M., Idzerda, R.L., McKnight, G.S., and Bourtchouladze, R., 1995. A genetic test of the effects of mutation in PKA on mossy fiber LTP and its relation to spatial and contextual learning. Cell 83:1211-1222.

Hubel, D.H., 1982. Exploration of the primary visual cortex, 1955-78. Nature 299:515-524.

Huerta, P.T., and Lisman, J.E., 1993. Heightened synaptic plasticity of hippocampal CA1 neurons during a cholinergically induced rhythmic state. Nature 364:723-725.

Huguenard, J.R., 1996. Low-threshold calcium currents in central nervous system neurons. Annu. Rev. Physiol. 58:329-348.

Iijima, T., Witter, M.P., Ichikawa, M., Tominaga, T., Kajiwara, R., and Matsumoto, G., 1996. Entorhinal-hippocampal interactions revealed by real-time imaging. Science 272:1176-1179.

Isa, T., Itazawa, S., Iino, M., Tsuzuki, K., and Ozawa, S., 1996. Distribution of neurons expressing inwardly rectifying and Ca^{2+}-permeable AMPA receptors in rat hippocampal slices. J. Physiol. (Lond.) 491:719-733.

Isaacson, J.S., Solis, J.M., and Nicoll, R.A., 1993. Local and diffuse synaptic actions of GABA in the hippocampus. Neuron 10:165-175.

Ishizuka, N., Cowan, W.M., and Amaral, D.G., 1995. A quantitative analysis of the dendritic organization of pyramidal cells in the rat hippocampus. J. Comp. Neurol. 362:17-45.

Ito, M., Yoshida, M., and Obata, K., 1964. Monosynaptic inhibition of the intracerebellar nuclei induced from the cerebellar cortex. Experientia 21:325-326.

Jacobson, W., and Cottrell, G.A., 1993. Rapid visualization of NMDA receptors in the brain: characterization of (+)-3-[^{125}I]-indo-MK-801 binding to thin sections of rat brain. J. Neurosci. Meth. 46:17-27.

Jahr, C.E., and Stevens, C.F., 1987. Glutamate activates multiple single channel conductances in hippocampal neurons. Nature 325:522-525.

Jarvis, M.F., Murphy, D.E., and Williams, M., 1987. Quantitative autoradiographic localization of NMDA receptors in rat brain using [^{3}H]CPP: comparison with [^{3}H]TCP binding. Eur. J. Pharmacol. 141:149-152.

Jimbo, Y., and Kawana, A., 1992. Electrical stimulation and recording from cultured neurons using a planar electrode array. Biochem. Bioenerget. 29:193-204.

Johnston, D., Magee, J.C., Colbert, C.M., and Christie, B.R., 1996. Active properties of neuronal dendrites. Annu. Rev. Neurosci. 19:165-186.

Jones, E.G., 1985. The Thalamus. New York: Plenum Press.

Jones, K.A., Borowsky, B., Tamm, J.A., Craig, D.A., Durkin, M.M., Dai, M., Yao, W.-J., Johnson, M., Gundwalsen, C., Huang, L.-Y., Tang, C., Shen, Q., Salon, J.A., Morse, K., Laz, T., Smith, K.E., Nagarathnam, D., Noble, S.A., Blanchek, T.A., and Gerald, C., 1998. $GABA_B$ receptors function as a heteromeric assembly of the subunits $GABA_BR1$ and $GABA_BR2$. Nature 396:674-679.

Jones, R.S.G., 1993. Entorhinal-hippocampal connections - a speculative view of their function. TINS 16:58-64.

Jones, R.S.G., 1995. Frequency-dependent alterations in synaptic transmission in entorhinal-hippocampal pathways. Hippocampus 5:125-128.

Jørgensen, M.B., and Wright, D.C., 1988. The effect of unilateral and bilateral removal of the entorhinal cortex on the glucose utilization in various hippocampal regions in the rat. Neurosci. Lett. 87:227-232.

Jung, M.W., and McNaughton, B.L., 1993. Spatial selectivity of unit activity in the hippocampal granular layer. Hippocampus 3:165-182.

Kahle, J.S., and Cotman, C.W., 1989. Carbachol depresses synaptic responses in the medial but not the lateral perforant path. Brain Res. 482:159-163.

Kaibara, T., and Leung, L.S., 1993. Basal versus apical dendritic long-term potentiation of commissural afferents to hippocampal CA1 - a current-source density study. J. Neurosci. 13:2391-2404.

Kamondi, A., Horvath, Z., Bors, L., and Buzsáki, G., 1988. Perforant path activation of the hippocampus: spatial distribution, effects of urethane and atropine. Acta Physiol. Hung. 71:19-29.

Kandel, E.R., and Spencer, W.A., 1961. Electrophysiology of hippocampal neurons. II. After-potentials and repetitive firing. J. Neurophysiol. 24:243-259.

Kanter, E.D., Kapur, A., and Haberly, L.B., 1996. A dendritic $GABA_A$-mediated IPSP regulates facilitation of NMDA-mediated responses to burst stimulation of afferent fibers in piriform cortex. J. Neurosci. 16:307-312.

Kantor, D.B., Lanzrein, M., Stary, S.J., Sandoval, G.M., Smith, W.B., Sullivan, B.M., Davidson, N., and Schuman, E.M., 1996. A role for endothelial NO synthase in LTP revealed by adenovirus-mediated inhibition and rescue. Science 274:1744-1748.

Karlsson, G., and Olpe, H.R., 1989. Inhibitory processes in normal and epileptic-like rat hippocampal slices: the role of $GABA_B$ receptors. Eur. J. Pharmacol. 163:285-290.

Katona, I., Acsády, L., and Freund, T.F., 1999. Postsynaptic targets of somatostatin-immunoreactive interneurons in the rat hippocampus. Neuroscience 88:37-55.

Katsuki, H., Izumi, Y., and Zorumski, C.F., 1997. Noradrenergic regulation of synaptic plasticity in the hippocampal CA1 region. J. Neurophysiol. 77:3013-3020.

Katz, B., and Miledi, R., 1968. The role of calcium in neuromuscular facilitation. J. Physiol. (Lond.) 189:535-544.

Kauer, J.A., Malenka, R.C., and Nicoll, R.A., 1988. A persistent postsynaptic modification mediates long-term potentiation in the hippocampus. Neuron 1:911-917.

Kaupmann, K., Huggel, K., Heid, J., Flor, P.J., Bischoff, S., Mickel, S.J., McMaster, G., Angst, C., Bittiger, H., Froestl, W., and Bettler, B., 1997. Expression cloning of $GABA_B$ receptors uncovers similarity to metabotropic glutamate receptors. Nature 386:239-246.

Kaupmann, K., Malitschek, B., Schuler, V., Heid, J., Froestl, W., Beck, P., Mosbacher, J., Bischoff, S., Kulik, A., Shigemoto, R., Karschin, A., and Bettler, B., 1998. $GABA_B$-receptor subtypes assemble into functional heteromeric complexes. Nature 396:683-687.

Kawaguchi, Y., and Hama, K., 1988. Physiological heterogeneity of nonpyramidal cells in rat hippocampal CA1 region. Exp. Brain. Res. 72:494-502.

Kehl, S.J., and McLennan, H., 1985a. An electrophysiological characterization of inhibitions and postsynaptic potentials in rat hippocampal CA3 neurones *in vitro*. Exp. Brain. Res. 60:299-308.

Kehl, S.J., and McLennan, H., 1985b. A pharmacological characterization of chloride- and potassium-dependent inhibitions in the CA3 region of the rat hippocampus *in vitro*. Exp. Brain. Res. 60:309-317.

Kelso, S.R., Ganong, A.H., and Brown, T.H., 1986. Hebbian synapses in hippocampus. Proc. Nat. Acad. Sci. USA 83:5326-5330.

Kemp, N., and Bashir, Z.I., 1997. NMDA receptor-dependent and -independent long-term depression in the CA1 region of the adult rat hippocampus *in vitro*. Neuropharmacology 36:397-399.

Kerr, D.I.B., and Ong, J., 1995. $GABA_B$ receptors. Pharmac. Ther. 67:187-246.

Khazipov, R., Congar, P., and Ben-Ari, Y., 1995. Hippocampal CA1 lacunosum-moleculare interneurons: modulation of monosynaptic GABAergic IPSCs by presynaptic $GABA_B$ receptors. J. Neurophysiol. 74:2126-2137.

Kirkwood, A., Rozas, C., Kirkwood, J., Perez, F., and Bear, M.F., 1999. Modulation of long-term synaptic depression in visual cortex by acetylcholine and norepinephrine. J. Neurosci. 19:1599-1609.

Kiss, J., Buzsáki, G., Morrow, J.S., Glantz, S.B., and Leranth, C., 1996. Entorhinal cortical innervation of parvalbumin-containing neurons (basket and chandelier cells) in the rat Ammon's horn. Hippocampus 6:239-246.

Knowles, W.D., and Schwartzkroin, P.A., 1981a. Axonal ramifications of hippocampal CA1 pyramidal cells. J. Neurosci. 1:1236-1241.

Knowles, W.D., and Schwartzkroin, P.A., 1981b. Local circuit synaptic interactions in hippocampal brain slices. J. Neurosci. 1:318-322.

Koch, C., Douglas, R., and Wehmeier, U., 1990. Visibility of synaptically induced conductance changes: theory and simulations of anatomically characterized cortical pyramidal cells. J. Neurosci. 10:1728-1744.

Koch, C., Poggio, T., and Torre, V., 1983. Nonlinear interactions in a dendritic tree: localization, timing and role in information processing. Proc. Nat. Acad. Sci. USA 80:2799-2802.

Kojic, L., Gu, Q., Douglas, R.M., and Cynader, M.S., 1997. Serotonin facilitates synaptic plasticity in kitten visual cortex: an *in vitro* study. Dev. Brain Res. 101:299-304.

Konopacki, J., 1998. Theta-like activity in the limbic cortex *in vitro*. Neurosci. Biobehav. Rev. 22:311-323.

Konopacki, J., MacIver, B., Bland, B.H., and Roth, S.H., 1987. Carbachol-induced EEG "theta" activity in hippocampal brain slices. Brain Res. 405:196-198.

Krnjevic, K., 1997. Role of GABA in cerebral cortex. Can. J. Physiol. Pharmacol. 75:439-451.

Kuner, R., Köhr, G., Grünewald, S., Eisenhardt, G., Bach, A., and Kornau, H.-C., 1999. Role of heteromer formation in $GABA_B$ receptor function. Science 283:74-77.

Kunkel, D.D., Lacaille, J.-C., and Schwartzkroin, P.A., 1988. Ultrastructure of stratum lacunosum-moleculare interneurons of hippocampal CA1 region. Synapse 2:382-394.

Lacaille, J.-C., Kunkel, D.D., and Schwartzkroin, P.A., 1989. Electrophysiological and morphological characterization of hippocampal interneurons. In: The Hippocampus - New Vistas, edited by Chan-Palay, V. and Kohler, C., New York: Alan R. Liss, Inc., pp. 287-305.

Lacaille, J.-C., Mueller, A.L., Kunkel, D.D., and Schwartzkroin, P.A., 1988. Local circuit interactions between oriens/alveus interneurons and CA1 pyramidal cells in hippocampal slices: electrophysiology and morphology. J. Neurosci. 7:1979-1993.

Lacaille, J.-C., and Schwartzkroin, P.A., 1988a. Stratum lacunosum-moleculare interneurons of hippocampal CA1 region. I. Intracellular response characteristics, synaptic responses, and morphology. J. Neurosci. 8:1400-1410.

Lacaille, J.-C., and Schwartzkroin, P.A., 1988b. Stratum lacunosum-moleculare interneurons of hippocampal CA1 region. II. Intrasomatic and intradendritic recordings of local circuit synaptic interactions. J. Neurosci. 8:1411-1424.

Lambert, N.A., Borroni, A.M., Grover, L.M., and Teyler, T.J., 1991. Hyperpolarizing and depolarizing $GABA_A$ receptor-mediated dendritic inhibition in area CA1 of the rat hippocampus. J. Neurophysiol. 66:1538-1548.

Lambert, N.A., and Wilson, W.A., 1993a. Discrimination of post- and presynaptic $GABA_B$ receptor-mediated responses by tetrahydroaminoacridine in area CA3 of the rat hippocampus. J. Neurophysiol. 69:630-635.

Lambert, N.A., and Wilson, W.A., 1993b. Heterogeneity in presynaptic regulation of GABA release from hippocampal inhibitory neurons. Neuron 11:1057-1067.

Lambert, N.A., and Wilson, W.A., 1994. Temporally distinct mechanisms of use-dependent depression at inhibitory synapses in the rat hippocampus *in vitro*. J. Neurophysiol. 72:121-130.

Lambert, N.A., and Wilson, W.A., 1996. High-threshold Ca^{2+} currents in rat hippocampal interneurons and their selective inhibition by activation of $GABA_B$ receptors. J. Physiol. (Lond.) 492:115-127.

Lanthorn, T.H., and Cotman, C.W., 1981. Baclofen selectively inhibits excitatory synaptic transmission in the hippocampus. Brain Res. 225:171-178.

Larson, J., and Lynch, G., 1986a. Induction of synaptic potentiation in hippocampus by patterned stimulation involves two events. Science 232:985-988.

Lass, Y., Halevi, Y., Landau, E.M., and Gitter, S., 1973. A new model for transmitter mobilization in the frog neuromuscular junction. Pflügers Arch. 343:157-163.

Lester, R.A.J., Clements, J.D., Westbrook, G.L., and Jahr, C.E., 1990. Channel kinetics determine the time course of NMDA receptor-mediated synaptic currents. Nature 346:565-567.

Leung, L.S., and Fu, X.-W., 1994. Factors affecting paired-pulse facilitation in hippocampal CA1 neurons in vitro. Brain Res. 650:75-84.

Leung, L.S., Roth, L., and Canning, K.J., 1995. Entorhinal inputs to hippocampal CA1 and dentate gyrus in the rat: a current-source-density study. J. Neurophysiol. 73:2392-2403.

Leung, L.S., Shen, B., and Kaibara, T., 1992. Long-term potentiation induced by patterned stimulation of the commissural pathway to hippocampal CA1 region in freely moving rats. Neuroscience 48:63-74.

Levy, W.B., 1989. A computational approach to hippocampal function. In: Computational Models of Learning in Simple Neural Systems, edited by Hawkins, R.D. and Bower, G.H., Academic Press Inc., pp. 243-305.

Levy, W.B., and Colbert, C.M., 1992. Associative potentiation of Schaffer collaterals by paired conditioning with the perforant path in hippocampal CA1. Soc. Neurosci. Abstr. 18.

Levy, W.B., Colbert, C.M., and Desmond, N.L., 1995. Another network model bites the dust - entorhinal inputs are no more than weakly excitatory in the hippocampal CA1 region. Hippocampus 5:137-140.

Levy, W.B., Desmond, N.L., and Zhang, D.X., 1998. Perforant path activation modulates the induction of long-term potentiation of the Schaffer collateral-hippocampal CA1 response: Theoretical and experimental analyses. Learn. Mem. 4:510-518.

Levy, W.B., and Steward, O., 1983. Temporal contiguity requirements for long-term associative potentiation/depression in the hippocampus. Neuroscience 8:791-797.

Li, X.-G., Somogyi, P., Tepper, J.M., and Buzsáki, G., 1992. Axonal and dendritic arborization of an intracellularly labeled chandelier cell in the CA1 region of rat hippocampus. Exp. Brain. Res. 90:519-525.

Lind, R., Connolly, P., Wilkinson, C.D.W., and Thompson, R.D., 1991. Finite-element analysis applied to extracellular microelectrode design. Sens. Actuat. B 3:23-30.

Linden, D.J., 1994. Long-term synaptic depression in the mammalian brain. Neuron 12:457-472.

Ling, D.S.F., and Benardo, L.S., 1994. Properties of isolated $GABA_B$-mediated inhibitory postsynaptic currents in hippocampal pyramidal cells. Neuroscience 63:937-944.

Lingenhöhl, K., and Olpe, H.R., 1993. Blockade of the late inhibitory postsynaptic potential *in vivo* by the $GABA_B$ antagonist CGP 46 381. Pharmacol. Comm. 3:49-54.

Lippa, C.F., Hamos, J.E., Pulaski-Salo, D., Degennaro, L.J., and Drachman, D.A., 1992. Alzheimer's disease and aging: effects on perforant pathway perikarya and synapses. Neurobiol. Aging 13:405-411.

Lipton, P., Aitken, P.G., Dudek, F.E., Eskessen, K., Espanol, M.T., Ferchmin, P.A., Kelly, J.B., Kreisman, N.R., Landfield, P.W., Larkman, P.M., Leybaert, L., Newman, G.C., Panizzon, K.L., Payne, R.S., Phillips, P., Raley-Susman, K.M., Rice, M.E., Santamaria, R., Sarvey, J.M., Schurr, A., Segal, M.,

Sejer, V., Taylor, C.P., Teyler, T.J., Vasilenko, V.Y., Veregge, S., Wu, S.H., and Wallis, R., 1995. Making the best of brain slices: comparing preparative methods. J. Neurosci. Meth. 59:151-156.

Lisman, J.E., 1997. Bursts as a unit of neural information: Making unreliable synapses reliable. TINS 20:38-43.

Liu, G., and Tsien, R.W., 1995. Properties of synaptic transmission at single hippocampal synaptic boutons. Nature 375:404-408.

Liu, Y.-B., Disterhoft, J.P., and Slater, N.T., 1993. Activation of metabotropic glutamate receptors induces long-term depression of GABAergic inhibition in hippocampus. J. Neurophysiol. 69:1000-1004.

Livingstone, M., and Hubel, D., 1988. Segregation of form, color, movement, and depth: anatomy, physiology, and perception. Science 240:740-749.

Lopes da Silva, F.H., Witter, M.P., Boeijinga, P.H., and Lohman, A.H.M., 1990. Anatomic organization and physiology of the limbic cortex. Physiol. Rev. 70:453-511.

Lorente de Nó, R., 1934. Studies of the structure of the cerebral cortex II. Continuation of the study of the ammonic system. J. Psychol. Neurol. 46:113-177.

Lothman, E.W., III, E.H.B., and Stringer, J.L., 1991. Functional anatomy of hippocampal seizures. Prog. Neurobiol. 37:1-82.

Lu, X.-Y., Ghasemzadeh, M.B., and Kalivas, P.W., 1998. The regional distribution and cellular localization of $GABA_B1$ receptor messenger RNA in the rat brain. Soc. Neurosci. Abstr. 24:1587.

Lynch, G., Larson, J., Kelso, S., Barrionuevo, G., and Schottler, F., 1983. Intracellular injections of EGTA block induction of hippocampal long-term potentiation. Nature 305:719-721.

Maccaferri, G., and McBain, C.J., 1995. Passive propagation of LTD to stratum oriens-alveus inhibitory neurons modulates the temporoammonic input to the hippocampal CA1 region. Neuron 15:137-145.

Maccaferri, G., and McBain, C.J., 1996. Long-term potentiation in distinct subtypes of hippocampal nonpyramidal neurons. J. Neurosci. 16:5334-5343.

Macek, T.A., Winder, D.G., Gereau IV, R.W., Ladd, C.O., and Conn, P.J., 1996. Differential involvement of group II and group III mGluRs as autoreceptors at lateral and medial perforant path synapses. J. Neurophysiol. 76:3798-3806.

Magee, J., Hoffman, D., Colbert, C., and Johnston, D., 1998. Electrical and calcium signaling in dendrites of hippocampal pyramidal neurons. Annu. Rev. Physiol. 60:327-346.

Magee, J.C., 1998. Dendritic hyperpolarization-activated currents modify the integrative properties of hippocampal CA1 pyramidal neurons. J. Neurosci. 18:7613-7624.

Maguire, E.A., Frackowiak, R.S.J., and Frith, C.D., 1997. Recalling routes around London: activation of the right hippocampus in taxi drivers. J. Neurosci. 17:7103-7110.

Maher, M.P., Dvorak-Carbone, H., Pine, J., Wright, J.A., and Tai, Y.-C., 1999a. Microstructures for studies of cultured neural networks. Med. Biol. Eng. Comp. 37:110-118.

Maher, M.P., Pine, J., Wright, J.A., and Tai, Y.-C., 1999b. The neurochip: a new tool for studying neuronal circuits. J. Neurosci. Meth. 87:45-56.

Malenka, R.C., 1994. Synaptic plasticity in the hippocampus: LTP and LTD. Cell 78:535-538.

Malenka, R.C., Kauer, J.A., Zucker, R.S., and Nicoll, R.A., 1988. Postsynaptic calcium is sufficient for potentiation of hippocampal synaptic transmission. Science 242:81-84.

Malenka, R.C., and Nicoll, R.A., 1993. NMDA-receptor-dependent synaptic plasticity: multiple forms and mechanisms. TINS 16:521-527.

Manabe, T., Wyllie, D.J.A., Perkel, D.J., and Nicoll, R.A., 1993. Modulation of synaptic transmission and long-term potentiation: effects of paired pulse facilitation and EPSC variance in the CA1 region of the hippocampus. J. Neurophysiol. 70:1451-1459.

Mangan, P.S., and Lothman, E.W., 1996. Profound disturbances of pre- and postsynaptic $GABA_B$-receptor-mediated processes in region CA1 in a chronic model of temporal lobe epilepsy. J. Neurophysiol. 76:1282-1296.

Maren, S., and Fanselow, M.S., 1996. The amygdala and fear conditioning: has the nut been cracked? Neuron 16:237-240.

Marescaux, C., Vergnes, M., and Bernasconi, R., 1992a. $GABA_B$ receptor antagonists: potential new anti-absence drugs. In: Generalized Non-Convulsive Epilepsy: Focus on $GABA_B$ Receptors, edited by Marescaux, C., Vergnes, M. and Bernasconi, R., Vienna: Springer-Verlag, pp. 179-188.

Marescaux, C., Vergnes, M., and Bernasconi, R., 1992b. Generalized Non-Convulsive Epilepsy: Focus on $GABA_B$ Receptors. Journal of Neural Transmission, suppl. 35 (Vienna: Springer-Verlag).

Margulis, M., and Tang, C.M., 1998. Temporal integration can readily switch between sublinear and supralinear summation. J. Neurophysiol. 79:2809-2813.

Masino, S.A., and Dunwiddie, T.V., 1999. Temperature-dependent modulation of excitatory transmission in hippocampal slices is mediated by extracellular adenosine. J. Neurosci. 19:1932-1939.

Matsumura, N., Nishijo, H., Tamura, R., Eifuku, S., Endo, S., and Ono, T., 1999. Spatial- and task-dependent neuronal responses during real and virtual translocation in the monkey hippocampal formation. J. Neurosci. 19:2381-2393.

Matthews, D.A., Salvaterra, P.M., Crawford, G.D., Houser, C.R., and Vaughn, J.E., 1987. An immunocytochemical study of choline acetyltransferase-containing neurons and axon terminals in normal and partially deafferented hippocampal formation. Brain Res. 402:30-43.

Mayer, M.L., and Westbrook, G.L., 1987. Permeation and block of *N*-methyl-D-aspartic acid receptor channels by divalent cations in mouse cultured central neurones. J. Physiol. (Lond.) 394:501-527.

McBain, C.J., 1998. A short-term mechanism of plasticity for interneurones? J. Physiol. (Lond.) 511:331.

McBain, C.J., DiChiara, T.J., and Kauer, J.A., 1994. Activation of metabotropic glutamate receptors differentially affects two classes of hippocampal interneurons and potentiates excitatory synaptic transmission. J. Neurosci. 14:4433-4445.

McCarren, M., and Alger, B.E., 1985. Use-dependent depression of IPSPs in rat hippocampal pyramidal cells *in vitro*. J. Neurophysiol. 53:557-571.

McClelland, J.L., and Goddard, N.H., 1996. Considerations arising from a complementary learning systems perspective on hippocampus and neocortex. Hippocampus 6:654-665.

McDonald, R.J., and White, N.M., 1993. A triple dissociation of memory systems: hippocampus, amygdala, and dorsal striatum. Behav. Neurosci. 107:3-22.

McMahon, L.L., and Kauer, J.A., 1997a. Hippocampal interneurons are excited via serotonin-gated ion channels. J. Neurophysiol. 78:2493-2502.

McMahon, L.L., and Kauer, J.A., 1997b. Hippocampal interneurons express a novel form of synaptic plasticity. Neuron 18:295-305.

McNamara, J.O., 1994. Cellular and molecular basis of epilepsy. J. Neurosci. 14:3413-3425.

McNaughton, B.L., 1980. Evidence for two physiologically distinct perforant pathways to the fascia dentata. Brain Res. 199:1-19.

McNaughton, B.L., and Barnes, C.A., 1977. Physiological identification and analysis of dentate granule cell responses to stimulation of the medial and lateral perforant pathways in the rat. J. Comp. Neurol. 175:439-454.

McNaughton, B.L., Barnes, C.A., Meltzer, J., and Sutherland, R.J., 1989. Hippocampal granule cells are necessary for normal spatial learning but not for spatially-selective pyramidal cell discharge. Exp. Brain. Res. 76:485-496.

Mel, B.W., 1992. NMDA-based pattern discrimination in a modeled cortical neuron. Neural Comput. 4:502-517.

Michelson, H.B., and Wong, R.S.K., 1991. Excitatory synaptic responses mediated by $GABA_A$ receptors in the hippocampus. Science 253:1420-1423.

Miles, R., Tóth, K., Gulyás, A.I., Hájos, N., and Freund, T.F., 1996. Differences between somatic and dendritic inhibition in the hippocampus. Neuron 16:815-823.

Misgeld, U., 1988. Membrane properties and postsynaptic responses of hippocampal neurons. Adv. Anat. Embryol. Cell Biol. 111:20-39.

Misgeld, U., Bijak, M., Brunner, H., and Dembowsky, K., 1992. K-dependent inhibition in the dentate-CA3 network of guinea pig hippocampal slices. J. Neurophysiol. 68:1548-1557.

Misgeld, U., Bijak, M., and Jarolimek, W., 1995. A physiological role for $GABA_B$ receptors and the effects of baclofen in the mammalian central nervous system. Prog. Neurobiol. 46:423-462.

Misgeld, U., and Frotscher, M., 1986. Postsynaptic GABAergic inhibition of non-pyramidal neurons in the guinea-pig hippocampus. Neuroscience 19:193-206.

Miyahara, S., Nose, K., Ochiai, H., Kannan, H., and Wakisaka, S., 1998. Electrophysiology and morphology of rat's nucleus reuniens thalami neurons *in vitro*. Soc. Neurosci. Abstr. 24:1637.

Mizumori, S.J.Y., McNaughton, B.L., Barnes, C.A., and Fox, K.B., 1989. Preserved spatial coding in hippocampal CA1 pyramidal cells during reversible suppression of CA3c output: evidence for pattern completion in hippocampus. J. Neurosci. 9:3915-3928.

Mizumori, S.J.Y., Ward, K.E., and Lavoie, A.M., 1992. Medial septal modulation of entorhinal single unit activity in anesthetized and freely moving rats. Brain Res. 570:188-197.

Mody, I., De Koninck, Y., Otis, T.S., and Soltesz, I., 1994. Bridging the cleft at GABA synapses in the brain. TINS 17:517-524.

Monaghan, D.J., and Cotman, C.W., 1985. Distribution of *N*-methyl-D-aspartate-sensitive L-[^{3}H]glutamate-binding sites in rat brain. J. Neurosci. 5:2909-2919.

Morin, F., Beaulieu, C., and Lacaille, J.-C., 1996. Membrane properties and synaptic currents evoked in CA1 interneuron subtypes in rat hippocampal slices. J. Neurophysiol. 76:1-16.

Morris, R.G.M., Anderson, E., Lynch, G.S., and Baudry, M., 1986. Selective impairment of learning and blockade of long-term potentiation by an *N*-methyl-D-aspartate receptor antagonist, AP5. Nature 319:774-776.

Morris, R.G.M., Garrud, P., Rawlins, J.N.P., and O'Keefe, J., 1982. Place navigation impaired in rats with hippocampal lesions. Nature 297:681-683.

Morrisett, R.A., Mott, D.D., Lewis, D.V., Swartzwelder, H.S., and Wilson, W.A., 1991. $GABA_B$-receptor-mediated inhibition of the *N*-methyl-D-aspartate component of synaptic transmission in the rat hippocampus. J. Neurosci. 11:203-209.

Moser, E., Mathiesen, I., and Andersen, P., 1993. Association between brain temperature and dentate field potentials in exploring and swimming rats. Science 259:1324-1326.

Moser, M.B., Trommald, M., and Andersen, P., 1994. An increase in dendritic spine density on hippocampal CA1 pyramidal cells following spatial learning in adult rats suggests the formation of new synapses. Proc. Nat. Acad. Sci. USA 91:12673-12675.

Mott, D.D., Bragdon, A.C., and Lewis, D.V., 1990. Phaclofen antagonizes post-tetanic disinhibition in the rat dentate gyrus. Neurosci. Lett. 110:131-136.

Mott, D.D., and Lewis, D.V., 1991. Facilitation of the induction of long-term potentiation by $GABA_B$ receptors. Science 252:1718-1720.

Mott, D.D., and Lewis, D.V., 1994. The pharmacology and function of central $GABA_B$ receptors. Internat. Rev. Neurobiol. 36:97-223.

Mulkey, R.M., and Malenka, R.C., 1992. Mechanisms underlying induction of homosynaptic long-term depression in area CA1 of the hippocampus. Neuron 9:967-975.

Muller, R., 1996. A quarter of a century of place cells. Neuron 17:813-822.

Muller, R.U., and Kubie, J.L., 1989. The firing of hippocampal place cells predicts the future position of freely moving rats. J. Neurosci. 9:4101-4110.

Nakanishi, S., 1992. Molecular diversity of glutamate receptors and implications for brain function. Science 258:597-603.

Nathan, T., and Lambert, J.D.C., 1991. Depression of the fast IPSP underlies paired-pulse facilitation in area CA1 of the rat hippocampus. J. Neurophysiol. 66:1704-1715.

Nejtek, V., and Dahl, D., 1997. Pathway specificity of *l*-isoproterenol indicates beta-adrendergic modulation of the Schaffer collateral pathway in field CA1 in the rat hippocampal slice. NeuroReport 8:745-749.

Neki, A., Ohishi, H., Kaneko, T., Shigemoto, R., Nakanishi, S., and Mizuno, N., 1996. Presynaptic and postsynaptic localization of a metabotropic glutamate receptor, mGluR2, in the rat brain - an immunohistochemical study with a monoclonal antibody. Neurosci. Lett. 202:197-200.

Neveu, D., and Zucker, R.S., 1996. Postsynaptic levels of $[Ca^{2+}]_i$ needed to trigger LTD and LTP. Neuron 16:619-629.

Newberry, N.R., and Nicoll, R.A., 1984. A bicuculline-resistant inhibitory post-synaptic potential in rat hippocampal pyramidal cells *in vitro*. J. Physiol. (Lond.) 348:239-254.

Newberry, N.R., and Nicoll, R.A., 1985. Comparison of the action of baclofen with γ-aminobutyric acid on rat hippocampal pyramidal cells *in vitro*. J. Physiol. (Lond.) 360:161-185.

Nicoll, R.A., and Malenka, R.C., 1995. Contrasting properties of two forms of long-term potentiation in the hippocampus. Nature 377:115-119.

Nosten-Bertrand, M., Errington, M.L., Murphy, K.P.S.J., Tokugawa, Y., Barboni, E., Kozlova, E., Michalovich, D., Morris, R.G.M., Silver, J., Stewart, C.L., Bliss, T.V.P., and Morris, R.J., 1996. Normal spatial learning despite regional inhibition of LTP in mice lacking Thy-1. Nature 379:826-829.

Nowak, L., Bregestovski, P., Ascher, P., Herbet, A., and Prochiantz, A., 1984. Magnesium gates glutamate-activated channels in mouse central neurones. Nature 307:462-465.

O'Keefe, J., Burgess, N., Donnett, J.G., Jeffery, K.J., and Maguire, E.A., 1998. Place cells, navigational accuracy, and the human hippocampus. Phil. Trans. R. Soc. Lond. B 353:1333-1340.

O'Keefe, J., and Dostrovsky, J., 1971. The hippocampus as a spatial map. Preliminary evidence from unit activity in the freely-moving rat. Brain Res. 34:171-175.

Oleskevich, S., and Descarries, L., 1990. Quantified distribution of the serotonin innervation in adult rat hippocampus. Neuroscience 34:19-33.

Oleskevich, S., Descarries, L., and Lacaille, J.-C., 1989. Quantified distribution of the noradrenaline innervation in the hippocampus of adult rat. J. Neurosci. 9:3803-3815.

Oleskevich, S., and Lacaille, J.-C., 1992. Reduction of $GABA_B$ inhibitory postsynaptic potentials by serotonin via pre- and postsynaptic mechanisms in CA3 pyramidal cells of rat hippocampus *in vitro*. Synapse 12:173-188.

Oliet, S.H.R., Malenka, R.C., and Nicoll, R.A., 1997. Two distinct forms of long-term depression coexist in CA1 hippocampal pyramidal cells. Neuron 18:969-982.

Oliva, A.A., Jr., Smith, K.L., and Swann, J.W., 1998. Transgenic mice that express green fluorescent protein in GABAergic neurons: a new tool for studying hippocampal interneurons. Soc. Neurosci. Abstr. 24:1159.

O'Mara, S.M., Rowan, M.J., and Anwyl, R., 1995. Metabotropic glutamate receptor-induced homosynaptic long-term depression and depotentiation in the dentate gyrus of the rat hippocampus *in vitro*. Neuropharmacology 34:983-989.

Otani, S., Blond, O., Desce, J.-M., and Crépel, F., 1998. Dopamine facilitates long-term depression of glutamatergic transmission in rat prefrontal cortex. Neuroscience 85:669-676.

Otis, T.J., and Moody, I., 1992. Differential activation of $GABA_A$ and $GABA_B$ receptors by spontaneously released transmitter. J. Neurophysiol. 67:227-235.

Otis, T.S., De Koninck, Y., and Mody, I., 1993. Characterization of synaptically elicited $GABA_B$ responses using patch-clamp recordings in rat hippocampal slices. J. Physiol. (Lond.) 463:391-407.

Otmakhova, N.A., and Lisman, J.E., 1999. Dopamine selectively inhibits the direct cortical pathway to the CA1 hippocampal region. J. Neurosci. 19:1437-1445.

Otto, T., Eichenbaum, H., Wiener, S.I., and Wible, C.G., 1991. Learning-related patterns of CA1 spike trains parallel stimulation parameters optimal for inducing hippocampal long-term potentiation. Hippocampus 1:181-192.

Ouardouz, M., and Lacaille, J.-C., 1995. Mechanisms of selective long-term potentiation of excitatory synapses in stratum oriens/alveus interneurons of rat hippocampal slices. J. Neurophysiol. 73:810-819.

Ouardouz, M., and Lacaille, J.-C., 1997. Properties of unitary IPSCs in hippocampal pyramidal cells originating from different types of interneurons in young rats. J. Neurophysiol. 77:1939-1949.

Pacelli, G.J., Su, W., and Kelso, S.R., 1991. Activity-induced decrease in early and late inhibitory synaptic conductances in hippocampus. Synapse 7:1-13.

Papez, J.W., 1937. A proposed mechanism of emotion. Arch. Neurol. Psychiatry 38:725-743.

Paré, D., Dong, J.M., and Gaudreau, H., 1995. Amygdalo-entorhinal relations and their reflection in the hippocampal-formation - generation of sharp sleep potentials. J. Neurosci. 15:2482-2503.

Paré, D., and Llinás, R., 1994. Non-lamellar propagation of entorhinal influences in the hippocampal formation: multiple electrode recordings in the isolated guinea pig brain *in vitro*. Hippocampus 4:403-409.

Paré, D., and Llinás, R., 1995. Intracellular study of direct entorhinal inputs to field CA1 in the isolated guinea pig brain *in vitro*. Hippocampus 5:115-119.

Parra, P., Gulyás, A.I., and Miles, R., 1998. How many subtypes of inhibitory cells in the hippocampus? Neuron 20:983-993.

Pearce, R.A., 1993. Physiological evidence for two distinct $GABA_A$ responses in rat hippocampus. Neuron 10:189-200.

Penfield, W., and Jasper, H., 1954. Epilepsy and the Functional Anatomy of the Human Brain. Boston: Little, Brown and Company.

Petralia, R.S., Wang, Y.X., Niedzielski, A.S., and Wenthold, R.J., 1996. The metabotropic glutamate receptors, mGluR2 and mGluR3, show unique postsynaptic, presynaptic and glial localizations. Neuroscience 71:949-976.

Petrovich, G.D., Canteras, N.S., and Swanson, L.W., 1997. Organization of amygdalar projections to the hippocampal formation: a PHAL study in the rat. Soc. Neurosci. Abstr. 23:2101-2101.

Pfrieger, F.W., Gottman, K., and Lux, H.D., 1994. Kinetics of $GABA_B$ receptor-mediated inhibition of calcium currents and excitatory synaptic transmission in hippocampal neurons *in vitro*. Neuron 12:97-107.

Pham, T.M., and Lacaille, J.-C., 1996. Multiple postsynaptic actions of GABA via $GABA_B$ receptors on CA1 pyramidal cells of rat hippocampal slices. J. Neurophysiol. 76:69-80.

Pham, T.M., Nurse, S., and Lacaille, J.-C., 1998. Distinct $GABA_B$ actions via synaptic and extrasynaptic receptors in rat hippocampus *in vitro*. J. Neurophysiol. 80:297-308.

Pikkarainen, M., Ronkko, S., Savander, V., Insausti, R., and Pitkanen, A., 1999. Projections from the lateral, basal, and accessory basal nuclei of the amygdala to the hippocampal formation in rat. J. Comp. Neurol. 403:229-260.

Pin, J.-P., and Duvoisin, R., 1995. Review: Neurotransmitter receptors I - The metabotropic glutamate receptors: structure and functions. Neuropharmacology 34:1-26.

Pine, J., 1980. Recording action potentials from cultured neurons with extracellular microcircuit electrodes. J. Neurosci. Meth. 2:19-31.

Pohle, W., Ott, T., and Müller-Welde, P., 1984. Identification of neurons of origin providing the dopaminergic innervation of the hippocampus. J. Hirnforsch. 25:1-10.

Ponce, A., Bueno, E., Kentros, C., Demiera, E.V.S., Chow, A., Hillman, D., Chen, S., Zhu, L.X., Wu, M.B., Wu, X.Y., Rudy, B., and Thornhill, W.B., 1996. G protein-gated inward rectifier K^+ channel proteins (GIRK1) are present in the soma and dendrites as well as in nerve terminals of specific neurons in the brain. J. Neurosci. 16:1990-2001.

Pouzat, C., and Marty, A., 1999. Somatic recording of GABAergic autoreceptor current in cerebellar stellate and basket cells. J. Neurosci. 19:1675-1693.

Press, G.A., Amaral, D.G., and Squire, L.R., 1989. Hippocampal abnormalities in amnesic patients revealed by high-resolution magnetic resonance imaging. Nature 341:54-57.

Princivalle, A., Frassoni, C., Regondi, M.C., Raming, K., Bettler, B., Bowery, N.G., and Spreafico, R., 1998. Immunolocalization of $GABA_B$ receptors in rat brain. Soc. Neurosci. Abstr. 24:1587.

Proctor, W.R., and Dunwiddie, T.V., 1987. Presynaptic and postsynaptic actions of adenosine in the *in vitro* rat hippocampus. Brain Res. 426:187-190.

Quirk, G.J., Muller, R.U., Kubie, J.L., and Ranck, J.B., Jr., 1992. The positional firing properties of medial entorhinal neurons: description and comparison with hippocampal place cells. J. Neurosci. 12:1945-1963.

Radcliffe, K.A., and Dani, J.A., 1998. Nicotinic stimulation produces multiple forms of increased glutamatergic synaptic transmission. J. Neurosci. 18:7075-7083.

Rall, W., 1967. Distinguishing theoretical synaptic potentials computed for different soma-dendritic distributions of synaptic input. J. Neurophysiol. 30:1138-1168.

Ramón y Cajal, S., 1893. The Structure of Ammon's Horn, trans. Lisbeth M. Kraft. Springfield, Illinois: Charles C. Thomas.

Ramón y Cajal, S., 1911. Histologie du Système Nerveux de l'Homme et des Vertébrés, Volume II., trans. L. Azoulay. Paris: Maloine.

Ranck, J.B., Jr., 1973. Studies on single neurons in dorsal hippocampal formation and septum in unrestrained rats. Exp. Neurol. 41:461-531.

Reeves, T.M., Lyeth, B.G., Phillips, L.L., Hamm, R.J., and Povlishock, J.T., 1997. The effects of traumatic brain injury on inhibition in the hippocampus and dentate gyrus. Brain Res. 757:119-32.

Reyes, M., and Stanton, P.K., 1996. Induction of hippocampal long-term depression requires release of Ca^{2+} from separate presynaptic and postsynaptic intracellular stores. J. Neurosci. 16:5951-5960.

Reymann, K., Pohle, W., Müller-Welde, P., and Ott, T., 1983. Dopaminergic innervation of the hippocampus: evidence of midbrain raphe neurons as the site of origin. Biomed. Biochim. Acta 10:1247-1255.

Ribak, C.E., and Seress, L., 1983. Five types of basket cell in the hippocampal dentate gyrus: a combined Golgi and electron microscopic study. J. Neurocytol. 12:577-597.

Risso Bradley, S., Levey, A.I., Hersch, S.M., and Conn, P.J., 1996. Immunocytochemical localization of group III metabotropic glutamate receptors in the hippocampus with subtype-specific antibodies. J. Neurosci. 16:2044-2056.

Roepstorff, A., and Lambert, J.D.C., 1994. Factors contributing to the decay of the stimulus-evoked IPSC in rat hippocampal CA1 neurons. J. Neurophysiol. 72:2911-2926.

Rogan, M.T., Stäubli, U.V., and LeDoux, J.E., 1997. Fear conditioning induces associative long-term potentiation in the amygdala. Nature 390:604-607.

Ropert, N., and Guy, N., 1991. Serotonin facilitates GABAergic transmission in the CA1 region of rat hippocampus *in vitro*. J. Physiol. (Lond.) 441:121-136.

Rose, G.M., and Dunwiddie, T.V., 1986. Induction of hippocampal long-term potentiation using physiologically patterned stimulation. Neurosci. Lett. 69:244-248.

Rosenthal, J., 1969. Post-tetanic potentiation at the neuromuscular junction of the frog. J. Physiol. (Lond.) 203:121-133.

Rozov, A., Zilberter, Y., Wollmuth, L.P., and Burnashev, N., 1998. Facilitation of currents through rat Ca^{2+}-permeable AMPA receptor channels by activity-dependent relief from polyamine block. J. Physiol. (Lond.) 511:361-377.

Saint, D.A., Thomas, T., and Gage, P.W., 1990. $GABA_B$ agonists modulate a transient potassium current in cultured mammalian hippocampal neurons. Neurosci. Lett. 118:9-13.

Saucier, D., and Cain, D.P., 1995. Spatial learning without NMDA receptor-dependent long-term potentiation. Nature 378:186-189.

Scanziani, M., Salin, P.A., Vogt, K.E., Malenka, R.C., and Nicoll, R.A., 1997. Use-dependent increases in glutamate concentration activate presynaptic metabotropic glutamate receptors. Nature 385:630-633.

Scharfman, H.E., Goodman, J.H., Du, F., and Schwarcz, R., 1998. Chronic changes in synaptic responses of entorhinal and hippocampal neurons after amino-oxyacetic acid (AOAA)-induced entorhinal cortical neuron loss. J. Neurophysiol. 80:3031-3046.

Schmitz, D., Empson, R.M., Gloveli, T., and Heinemann, U., 1995a. Serotonin reduces synaptic excitation of principal cells in the superficial layers of rat hippocampal-entorhinal cortex combined slices. Neurosci. Lett. 190:37-40.

Schmitz, D., Empson, R.M., and Heinemann, U., 1995b. Serotonin reduces inhibition via 5-HT_{1A} receptors in area CA1 of rat hippocampal slices *in vitro*. J. Neurosci. 15:7217-7225.

Schoepp, D.D., and Conn, P.J., 1993. Metabotropic glutamate receptors in brain function and pathology. TiPS 14:13-20.

Schuman, E.M., 1997. Synapse specificity and long-term information storage. Neuron 18:339-342.

Schuman, E.M., and Madison, D.V., 1994. Locally distributed synaptic potentiation in the hippocampus. Science 263:532-536.

Schwartzkroin, P.A., 1975. Characteristics of CA1 neurons recorded intracellularly in the hippocampal *in vitro* slice preparation. Brain Res. 85:423-436.

Scoville, W.B., and Milner, B., 1957. Loss of recent memory after bilateral hippocampal lesions. J. Neurol. Neurosurg. Psychiat. 20:11-21.

Seeburg, P.H., 1993. The molecular biology of mammalian glutamate receptor channels. TINS 16:359-365.

Segal, M., 1972. Hippocampal unit responses to perforant path stimulation. Exp. Neurol. 35.

Segal, M., 1987. Repetitive inhibitory postsynaptic potentials evoked by 4-aminopyridine in hippocampal neurons *in vitro*. Brain Res. 414:285-293.

Séguéla, P., Wadishe, J., Dineley-Miller, K., Dani, J.A., and Patrick, J.W., 1993. Molecular cloning, functional properties, and distribution of rat brain α_7: a nicotinic cation channel highly permeable to calcium. J. Neurosci. 13:596-604.

Shepherd, G.M., and Koch, C., 1990. Introduction to synaptic circuits. In: The Synaptic Organization of the Brain, third edition, edited by Shepherd, G.M., New York: Oxford University Press, pp. 3-31.

Shigemoto, R., Kulik, A., Tamaru, Y., Malitschek, B., Kuhn, R., and Bettler, B., 1998. Immunohistochemical distribution of $GABA_BR1$ in the rat CNS. Soc. Neurosci. Abstr. 24:1587.

Shors, T.J., and Matzel, L.D., 1997. Long-term potentiation: What's learning got to do with it? Behav. Brain Sci. 20:597-655.

Siegelbaum, S.A., and Kandel, E.R., 1991. Learning-related synaptic plasticity: LTP and LTD. Curr. Op. Neurobiol. 1:113-120.

Sík, A., Hájos, N., Gulácsi, A., Mody, I., and Freund, T.F., 1998. The absence of a major Ca^{2+} signaling pathway in GABAergic neurons of the hippocampus. Proc. Nat. Acad. Sci. USA 95:3245-3250.

Sík, A., Penttonen, M., Ylinen, A., and Buzsáki, G., 1995. Hippocampal CA1 interneurons: an *in vivo* intracellular labeling study. J. Neurosci. 15:6651-6665.

Silva, A.J., Paylor, R., Wehner, J.M., and Tonegawa, S., 1992. Impaired spatial learning in α-calcium-calmodulin kinase II mutant mice. Science 257:206-211.

Sirvio, J., Larson, J., Quach, C.N., Rogers, G.A., and Lynch, G., 1996. Effects of pharmacologically facilitating glutamatergic transmission in the trisynaptic intrahippocampal circuit. Neuroscience 74:1025-1035.

Sivilotti, L., and Nistri, A., 1990. GABA receptor mechanisms in the central nervous system. Prog. Neurobiol. 36:35-92.

Skaggs, W.E., and McNaughton, B., 1996. Replay of neuronal firing sequences in rat hippocampus during sleep following spatial experience. Science 271:1870-1873.

Skrede, K.K., and Westgaard, R.H., 1971. The transverse hippocampal slice: a well-defined cortical structure maintained *in vitro*. Brain Res. 35:589-593.

Sloviter, R.S., 1991. Feedforward and feedback inhibition of hippocampal principal cell activity evoked by perforant path stimulation: GABA-mediated mechanisms that regulate excitability *in vivo*. Hippocampus 1:31-40.

Sodickson, D.L., and Bean, B.P., 1996. $GABA_B$ receptor-activated inwardly rectifying potassium current in dissociated hippocampal CA3 neurons. J. Neurosci. 16:6374-6385.

Solís, J.M., and Nicoll, R.A., 1992. Pharmacological characterization of $GABA_B$-mediated responses in the CA1 region of the rat hippocampal slice. J. Neurosci. 12:3466-3472.

Soltesz, I., 1995. Brief history of cortico-hippocampal time with a special reference to the direct entorhinal input to CA1. Hippocampus 5:120-124.

Soltesz, I., and Jones, R.S.G., 1995. The direct perforant path input to CA1 - excitatory or inhibitory? Hippocampus 5:101-103.

Somogyi, P., Nunzi, M.G., Gorio, A., and Smith, A.D., 1983. A new type of specific interneuron in the monkey hippocampus forming synapses exclusively with the axon initial segments of pyramidal cells. Brain Res. 259:137-142.

Squire, L.R., and Zola-Morgan, S., 1991. The medial temporal lobe memory system. Science 253:1380-1386.

Staubli, U., and Scafidi, J., 1997. Studies on long-term depression in area CA1 of the anesthetized and freely moving rat. J. Neurosci. 17:4820-4828.

Stelzer, A., Simon, G., Kovacs, G., and Rai, R., 1994. Synaptic disinhibition during maintenance of long-term potentiation in the CA1 hippocampal subfield. Proc. Nat. Acad. Sci. USA 91:3058-3062.

Stelzer, A., Slater, N.T., and ten Bruggencate, G., 1987. Activation of NMDA receptors blocks GABAergic inhibition in an *in vitro* model of epilepsy. Nature 326:698-701.

Stenger, D.A., and McKenna, T.M., 1994. Enabling Technologies for Cultured Neural Networks, San Diego: Academic Press.

Stephenson, F.A., 1995. The $GABA_A$ receptors. Biochem. J. 310:1-9.

Steriade, M., and Llinás, R.R., 1988. The functional states of the thalamus and the associated neuronal interplay. Physiol. Rev. 68:649-742.

Stevens, C.F., and Tsujimoto, T., 1995. Estimates for the pool size of releasable quanta at a single central synapse and for the time required to refill the pool. Proc. Nat. Acad. Sci. USA 92:846-849.

Steward, O., and Scoville, S.A., 1976. Cells of origin of entorhinal cortical afferents to the hippocampus and fascia dentata of the rat. J. Comp. Neurol. 169:347-370.

Steward, O., Tomasulo, R., and Levy, W.B., 1990. Blockade of inhibition in a pathway with dual excitatory and inhibitory action unmasks a capability for LTP that is otherwise not expressed. Brain Res. 516:292-300.

Stewart, M., and Fox, S.E., 1990. Do septal neurons pace the hippocampal theta rhythm? TINS 13:163-168.

Stewart, M., Quirk, G.J., Barry, M., and Fox, S.E., 1992. Firing relations of medial entorhinal neurons to the hippocampal theta rhythm in urethane anesthetized and walking rats. Exp. Brain. Res. 90:21-28.

Stringer, J.L., and Colbert, C.M., 1994. Analysis of field potentials-evoked in CA1 by angular bundle stimulation in the rat. Brain Res. 641:289-294.

Stuart, G., Spruston, N., Sakmann, B., and Hausser, M., 1997. Action potential initiation and backpropagation in neurons of the mammalian CNS. TINS 20:125-131.

Svoboda, K.R., and Lupica, C.R., 1998. Opioid inhibition of hippocampal interneurons via modulation of potassium and hyperpolarization-activated cation (I_h) currents. J. Neurosci. 18:7084-7098.

Swandulla, D., Hans, M., Zipser, K., and Augustine, G.J., 1991. Role of residual calcium in synaptic depression and posttetanic potentiation: fast and slow calcium signaling in nerve terminals. Neuron 7:915-926.

Swanson, T.H., Drazba, J.A., and Rivkees, S.A., 1995. Adenosine A1 receptors are located predominantly on axons in the rat hippocampal formation. J. Comp. Neurol. 363:517-531.

Taira, T., Lamsa, K., and Kaila, K., 1997. Posttetanic excitation mediated by $GABA_A$ receptors in rat CA1 pyramidal neurons. J. Neurophysiol. 77:2213.

Takahashi, T., Kajikawa, Y., and Tsujimoto, T., 1998. G-protein-coupled modulation of presynaptic calcium currents and transmitter release by a $GABA_B$ receptor. J. Neurosci. 18:3138-3146.

Tamamaki, N., and Nojyo, Y., 1995. Preservation of topography in the connections between the subiculum, field CA1, and the entorhinal cortex in rats. J. Comp. Neurol. 353:379-390.

Tang, C.-M., Dichter, M., and Morad, M., 1989. Quisqualate activates a rapidly inactivating high conductance ionic channel in hippocampal neurons. Science 243:1474-1477.

Tecott, L.H., Maricq, A.V., and Julius, D., 1993. Nervous system distribution of the serotonin-$5HT_3$ receptor mRNA. Proc. Nat. Acad. Sci. USA 90:1430-1434.

Thiels, E., Barrionuevo, G., and Berger, T.W., 1994. Excitatory stimulation during postsynaptic inhibition induces long-term depression in hippocampus *in vivo*. J. Neurophysiol. 72:3009-3016.

Thiels, E., Xie, X., Yeckel, M.F., Barrionuevo, G., and Berger, T.W., 1996. NMDA receptor-dependent LTD in different subfields of hippocampus *in vivo* and *in vitro*. Hippocampus 6:43-51.

Thomas, M.J., Moody, T.D., Makhinson, M., and O'Dell, T.J., 1996. Activity-dependent β-adrenergic modulation of low frequency stimulation induced LTP in the hippocampal CA1 region. Neuron 17:475-482.

Thomas, M.J., Watabe, A.M., Moody, T.D., Makhinson, M., and O'Dell, T.J., 1998. Postsynaptic complex spike bursting enables the induction of LTP by theta frequency synaptic stimulation. J. Neurosci. 18:7118-7126.

Thompson, S.M., 1994. Modulation of inhibitory synaptic transmission in the hippocampus. Prog. Neurobiol. 42:575-609.

Thompson, S.M., and Gähwiler, B.H., 1989. Activity-dependent disinhibition. I. Repetitive stimulation reduces IPSP driving force and conductance in the hippocampus *in vitro*. J. Neurophysiol. 61:501-511.

Thompson, S.M., Haas, H.L., and Gahwiler, B.H., 1992. Comparison of the actions of adenosine at presynaptic and postsynaptic receptors in the rat hippocampus invitro. J. Physiol. (Lond.) 451:347-363.

Thomson, A.M., 1997. Activity-dependent properties of synaptic transmission at two classes of connections made by rat neocortical pyramidal axons *in vitro*. J. Physiol. (Lond.) 502:131-147.

Thomson, A.M., Deuchars, J., and West, D.C., 1993. Large, deep layer pyramid-pyramid single axon EPSPs in slices of rat motor cortex display paired pulse and frequency-dependent depression, mediated presynaptically, and self-facilitation, mediated postsynaptically. J. Neurophysiol. 70:2354-2369.

Thomson, A.M., West, D.C., Hahn, J., and Deuchars, J., 1996. Single axon IPSPs elicited in pyramidal cells by three classes of interneurones in slices of rat neocortex. J. Physiol. (Lond.) 496:81-102.

Tomasulo, R.A., Ramirez, J.J., and Steward, O., 1993. Synaptic inhibition regulates associative interactions between afferents during the induction of long-term potentiation and depression. Proc. Nat. Acad. Sci. USA 90:11578-11582.

Tomasulo, R.A., and Steward, O., 1996. Homosynaptic and heterosynaptic changes in driving of dentate gyrus interneurons after brief tetanic stimulation *in vivo*. Hippocampus 6:62-71.

Torre, E.R., and Steward, O., 1992. Demonstration of local protein synthesis within dendrites using a new cell culture system that permists the isolation of living axons and dendrites from their cell bodies. J. Neurosci. 12:762-772.

Tóth, K., Freund, T.F., and Miles, R., 1997. Disinhibition of rat hippocampal pyramidal cells by GABAergic afferents from the septum. J. Physiol. (Lond.) 500:463-474.

Trussell, L.O., and Fischbach, G.D., 1989. Glutamate receptor desensitization and its role in synaptic transmission. Neuron 3:209-218.

Tsubokawa, H., and Ross, W.N., 1996. IPSPs modulate spike backpropagation and associated $[Ca^{2+}]_i$ changes in the dendrites of hippocampal CA1 pyramidal neurons. J. Neurophysiol. 76:2896-2906.

Turner, D.A., 1990. Feed-forward inhibitory potentials and excitatory interactions in guinea-pig hippocampal pyramidal cells. J. Physiol. (Lond.) 422:333-350.

Turner, R.W., Meyers, D.E.R., Richardson, T.L., and Barker, J.L., 1991. The site for initiation of action potential discharge over the somatodendritic axis of rat hippocampal CA1 pyramidal neurons. J. Neurosci. 11:2270-2280.

Urban, N.N., Henze, D.A., and Barrionuevo, G., 1998. Amplification of perforant-path EPSPs in CA3 pyramidal cells by LVA calcium and sodium channels. J. Neurophysiol. 80:1558-1561.

Usrey, W.M., Reppas, J.B., and Reid, R.C., 1998. Paired-spike interactions and synaptic efficacy of retinal inputs to the thalamus. Nature 395:384-387.

van Groen, T., Kadish, I., and Riekkinen, P., Jr., 1998. The projections from the entorhinal cortex to the hippocampus in the mouse. Soc. Neurosci. Abstr. 24:677.

van Groen, T., and Wyss, J.M., 1990. Extrinsic projections from area CA1 of the rat hippocampus: olfactory, cortical, subcortical, and bilateral hippocampal formation projections. J. Comp. Neurol. 302:515-528.

Van Hoesen, G.W., Hyman, B.T., and Damasio, A.R., 1986. Cell-specific pathology in neural systems of the temporal lobe in Alzheimer's disease. In: Progress in Brain Research, vol. 70, edited by Swaab, D.F., Fliers, E., Mirmiran, M., Van Gool, W.A. and Van Haaren, F., Elsevier Science Publishers B. V., pp. 321-335.

Vida, I., Halasy, K., Szinyei, C., Somogyi, P., and Buhl, E.H., 1998. Unitary IPSPs evoked by interneurons at the stratum radiatum-stratum lacunosum-moleculare border in the CA1 area of the rat hippocampus *in vitro*. J. Physiol. (Lond.) 506:755-773.

Vinogradova, O.S., 1995. Expression, control, and probable functional significance of the neuronal theta-rhythm. Prog. Neurobiol. 45:523-583.

Vizi, S., and Kiss, J.P., 1998. Neurochemistry and pharmacology of the major hippocampal transmitter systems: synaptic and nonsynaptic interactions. Hippocampus 8:566-607.

Wagner, J.J., and Alger, B.E., 1995. GABAergic and developmental influences on homosynaptic LTD and depotentiation in rat hippocampus. J. Neurosci. 15:1577-1586.

Wagner, J.J., and Alger, B.P., 1996. Homosynaptic LTD and depotentiation: Do they differ in name only? Hippocampus 6:24-29.

Wang, L.-Y., and Kaczmarek, L.K., 1998. High-frequency firing helps replenish the readily releasable pool of synaptic vesicles. Nature 394:384-388.

Wang, Y., Rowan, M.J., and Anwyl, R., 1997. Induction of LTD in the dentate gyrus *in vitro* is NMDA receptor independent, but dependent on Ca^{2+} influx via low-voltage-activated Ca^{2+} channels and release of Ca^{2+} from intracellular stores. J. Neurophysiol. 77:812-825.

Watson, P.L., Weiner, J.L., and Carlen, P.L., 1997. Effects of variations in hippocampal slice preparation protocol on the electrophysiological stabiligy, epileptogenicity and graded hypoxia responses of CA1 neurons. Brain Res. 775:134-143.

Wehr, M., and Laurent, G., 1996. Odour encoding by temporal sequences of firing in oscillating neural assemblies. Nature 384:162-166.

White, G., Levy, W.B., and Steward, O., 1988. Evidence that associative interactions between synapses during the induction of long-term potentiation occur within local dendritic domains. Proc. Nat. Acad. Sci. USA 85:2368-2372.

White, J.H., Wise, A., Main, M.J., Green, A., Fraser, N.J., Disney, G.H., Barnes, A.A., Emson, P., Foord, S.M., and Marshall, F.H., 1998. Heterodimerization is required for the formation of a functional $GABA_B$ receptor. Nature 397:679-682.

Wickens, J.R., and Abraham, W.C., 1991. The involvement of L-type calcium channels in heterosynaptic long-term depression in the hippocampus. Neurosci. Lett. 130:128-132.

Wigström, H., and Gustafsson, B., 1981. Two types of synaptic facilitation recorded in pyramidal cells of *in vitro* hippocampal slices from guinea pigs. Neurosci. Lett. 26:73-78.

Wigström, H., and Gustafsson, B., 1983. Facilitated induction of hippocampal long-lasting potentiation during blockade of inhibition. Nature 301:603-604.

Wilcox, K.S., and Dichter, M.A., 1994. Paired pulse depression in cultured hippocampal neurons is due to a presynaptic mechanism independent of $GABA_B$ autoreceptor activation. J. Neurosci. 14:1775-1788.

Wiley, R.G., Spencer, C., and Pysh, J.J., 1987. Time course and frequency dependence of synaptic vesicle depletion and recovery in electrically stimulated sympathetic ganglia. J. Neurocytol. 16:359-372.

Williams, J.H., and Kauer, J.A., 1997. Properties of carbachol-induced oscillatory activity in rat hippocampus. J. Neurophysiol. 78:2631-2640.

Williams, S., and Lacaille, J.-C., 1992. $GABA_B$ receptor-mediated inhibitory postsynaptic potentials evoked by electrical stimulation and by glutamate stimulation of interneurons in stratum lacunosum-moleculare in hippocampal CA1 pyramidal cells *in vitro*. Synapse 11:249-258.

Williams, S., Samulack, D.D., Beaulieu, C., and Lacaille, J.-C., 1994. Membrane properties and synaptic responses of interneurons located near the stratum lacunosum-moleculare/radiatum border of area CA1 in whole-cell recordings from rat hippocampal slices. J. Neurophysiol. 71:2217-2235.

Wilson, M.A., and McNaughton, B.L., 1993. Dynamics of the hippocampal ensemble code for space. Science 261:1055-1058.

Wilson, M.A., and McNaughton, B.L., 1994. Reactivation of hippocampal ensemble memories during sleep. Science 265:676-679.

Winn, H.R., Welsh, J.E., Rubio, R., and Berne, R.M., 1980. Changes in brain adenosine during bicuculline-induced seizures in rats. Effects of hypoxia and altered systemic blood pressure. Circulat. Res. 47:568-577.

Winson, J., and Abzug, C., 1978. Neuronal transmission through hippocampal pathways dependent on behavior. J. Neurophysiol. 41:716-732.

Witter, M.P., 1993. Organization of the entorhinal-hippocampal system: a review of current anatomical data. Hippocampus 3:33-44.

Witter, M.P., Griffioen, A.W., Jorritsma-Byham, B., and Krijnen, J.L.M., 1988. Entorhinal projections to the hippocampal CA1 region in the rat: an underestimated pathway. Neurosci. Lett. 85:193-198.

Witter, M.P., Groenewegen, H.J., Lopes da Silva, F.H., and Lohman, A.H.M., 1989. Functional organization of the extrinsic and intrinsic circuitry of the parahippocampal region. Prog. Neurobiol. 33:161-253.

Wong, R.K.S., and Watkins, D.J., 1982. Cellular factors influencing GABA response in hippocampal pyramidal cells. J. Neurophysiol. 48:938-951.

Wood, E.R., Dudchenko, P.A., and Eichenbaum, H., 1999. The global record of memory in hippocampal neuronal activity. Nature 397:613-617.

Woodson, W., Nitecka, L., and Ben-Ari, Y., 1989. Organization of the GABAergic system in the rat hippocampal formation: a quantitative immunocytochemical study. J. Comp. Neurol. 280:254-271.

Wouterlood, F.G., Saldana, E., and Witter, M.P., 1990. Projection from the nucleus reuniens thalami to the hippocampal region: light and electron microscopic tracing study in the rat with the anterograde tracer *Phaseolus vulgaris*-leucoagglutinin. J. Comp. Neurol. 296:179-203.

Wright, J.A., Tatic-Lucic, S., Tai, Y.-C., Maher, M.P., Dvorak, H., and Pine, J., 1996. Towards a functional MEMS neurowell by physiological experimentation. Tech. Dig.: Internat. Mech. Eng. Congr. Expo. (Atlanta, GA), DSC-Vol. 59, pp. 333-338.

Wu, H.Q., and Schwarcz, R., 1998. Focal microinjection of γ-acetylenic GABA into the rat entorhinal cortex: Behavioral and electroencephalographic abnormalities and preferential neuron loss in layer III. Exp. Neurol. 153:203-213.

Wu, K., and Leung, L.S., 1998. Monosynaptic activation of CA3 by the medial perforant path. Brain Res. 797:35-41.

Wu, L.G., and Saggau, P., 1994. Presynaptic calcium is increased during normal synaptic transmission and paired-pulse facilitation, but not in long-term potentiation in area CA1 of hippocampus. J. Neurosci. 14:645-654.

Xiang, Z., Huguenard, J.R., and Prince, D.A., 1998. Cholinergic switching within neocortical inhibitory networks. Science 281:985-988.

Xu, L., Anwyl, R., and Rowan, M.J., 1998. Spatial exploration induces a persistent reversal of long-term potentiation in rat hippocampus. Nature 394:891-894.

Yanovsky, Y., Sergeeva, O.A., Freund, T.F., and Haas, H.L., 1997. Activation of interneurons at the stratum oriens/alveus border suppresses excitatory transmission to apical dendrites in the CA1 area of the mouse hippocampus. Neuroscience 77:87-96.

Yeckel, M.F., and Berger, T.W., 1990. Feedforward excitation of the hippocampus by afferents from the entorhinal cortex: Redefinition of the role of the trisynaptic pathway. Proc. Nat. Acad. Sci. USA 87:5832-5836.

Yeckel, M.F., and Berger, T.W., 1995. Monosynaptic excitation of hippocampal CA1 pyramidal cells by afferents from the entorhinal cortex. Hippocampus 5:108-114.

Ylinen, A., Bragin, A., Nadasdy, Z., Jando, G., Szabo, I., Sík, A., and Buzsáki, G., 1995a. Sharp wave-associated high-frequency oscillation (200 Hz) in the intact hippocampus: network and intracellular mechanisms. J. Neurosci. 15:30-46.

Ylinen, A., Soltesz, I., Bragin, A., Penttonen, M., Sík, A., and Buzsáki, G., 1995b. Intracellular correlates of hippocampal theta rhythm in identified pyramidal cells, granule cells, and basket cells. Hippocampus 5:78-90.

Yokoi, M., Kobayashi, K., Manabe, T., Takahashi, T., Sakaguchi, I., Katsuura, G., Shigemoto, R., Ohishi, H., Nomura, S., Nakamura, K., Nakao, K., Katsuki, M., and Nakanishi, S., 1996. Impairment of hippocampal mossy fiber LTD in mice lacking mGluR2. Science 273:645-647.

Yukie, M., and Iwai, E., 1988. Direct projections from the ventral TE area of the inferotemporal cortex to hippocampal field CA1 in the monkey. Neurosci. Lett. 88:6-10.

Yuste, R., and Tank, D.W., 1996. Dendritic integration in mammalian neurons, a century after Cajal. Neuron 16:701-716.

Zhang, D.X., Colbert, C.M., and Levy, W.B., 1992. Associative potentiation of perforant path responses by conditioning with the Schaffer collaterals in hippocampal CA1. Soc. Neurosci. Abstr. 18.

Zhang, J.Y., Zeise, M.L., and Wang, R.Y., 1994. Serotonin$_3$ receptor agonists attenuate glutamate-induced firing in rat hippocampal CA1 pyramidal cells. Neuropharmacology 33:483-491.

Zhang, N., Tahtakran, S.A., and Houser, C.R., 1998. Interneurons in CA1 of the human hippocampus as revealed by immunohistochemical localization of a neuronal nuclear protein and GABA. Soc. Neurosci. Abstr. 24:716.

Zola-Morgan, S.M., and Squire, L.R., 1990. The primate hippocampal formation: evidence for a time-limited role in memory storage. Science 250:288-290.

Appendix A: The neurochip

A.1 Background and motivation

The nervous system transforms sensory inputs into appropriate motor outputs and memories. Nervous systems have a hierarchical organization, whose levels range from single macromolecules and ions, through individual neurons and synapses, local circuits, and behavioral subsystems (Shepherd and Koch 1990). Input-output transformations, or computations, are performed at each of these levels. Much is known about these transformations at the level of single neurons and synapses. However, relatively little is known about the input-output characteristics of local circuits, which consist of small networks of neurons. It is very difficult to study circuit behavior in an intact animal; the neurons in the circuit may not be easily accessible, and their activity will be affected by their surroundings, which are beyond the experimenter's control. Even in a slice preparation, much complexity is retained. Networks formed by dissociated neurons in culture are a model system that allows much greater access to, and control over, the neurons, while retaining enough of their *in vivo* characteristics to make studies on them relevant to more physiological situations (Stenger and McKenna 1994).

In order to study network properties of a neuronal culture, it is necessary to record the electrical activity of many neurons simultaneously and non-invasively, and to be able to stimulate neurons in the culture. Standard electrophysiological techniques such as intracellular or whole-cell recording are not suited to recording from multiple sites, because of the bulky manipulators required to hold each electrode in place; furthermore,

penetrations with glass electrodes are damaging to the neurons and limit the period of data acquisition to no more than a few hours. Optical recording with voltage-sensitive dyes is another option; however, the dyes tend to be phototoxic, are fairly poor indicators of membrane potential, and provide no convenient way to stimulate neurons.

An alternative approach to studying cultured neuronal networks is the multielectrode array. Such an array consists of multiple thin-film metal electrodes, insulated from each other, embedded in a substrate on which a network of cultured neurons can be grown. The electrodes record action potentials extracellularly and are thus non-invasive. The signals seen are due to the current flow in the extracellular medium; this is the return path for current that flows into the spike initiation zone of a neuron during the action potential. By far the greatest part of the voltage drop in this current loop takes place across the high-resistance cell membrane. The extracellular signal consists only of the voltage drop due to the current flow through the fairly conductive extracellular medium, and is therefore small. For example, a typical action potential with an amplitude of 100 mV and a rise time of 0.5 ms will be driven by an inward current on the order of 10 nA; given a typical resistivity of extracellular medium of 100 Ω-cm, this will result in a signal of a few hundred microvolts at 5 μm from the cell.

An extracellular signal is thus very small compared to an intracellular one, but still large enough to be distinguishable from the typical 5-10 μV noise of a good recording and amplification system. Extracellular signals have been recorded with microelectrode arrays from several types of dissociated, cultured cells. Examples include

30-100 μV signals from rat superior cervical ganglion (SCG) neurons up to 40 μm from the electrode (Pine 1980); 100-400 μV signals from cardiac cells (Connolly *et al.* 1990); and 50-350 μV signals from mouse spinal cord neurons up to 20 μm from the electrode (Gross and Lucas 1982). Extracellular electrodes can also be used to stimulate cultured neurons (Pine 1980; Jimbo and Kawana 1992).

In most multielectrode arrays, the cultured neurons are positioned randomly with respect to the electrodes. The neurochip developed in the Pine lab, on the other hand, has an array of 16 gold electrodes, each recessed in a 16 μm deep well in the silicon substrate (Figure A-1) (Wright *et al.* 1996). Dissociated neurons can be manually positioned into each well. As they grow, they are trapped inside the well by silicon nitride grillwork that lies over the well; the processes (axons and dendrites) are free to leave the well and grow across the silicon surface to make contact with other neurons. This arrangement provides three important advantages over the typical flat multielectrode dish. First, holding the neuron in place over the electrode improves the signal size, because the extracellular signal decreases with distance from the cell body; the geometry of the substrate may also increase signal size as compared with that recorded on a flat surface (Lind *et al.* 1991). Second, the positioning of the neurons eliminates uncertainty as to the origin of a recorded signal seen at the electrode. Third, the proximity of each neuron to an electrode allows selective stimulation of any neuron in the network.

The ability to record from and stimulate each and every neuron in a small neuronal network containing more than two neurons is unprecedented. With such a system, many questions that were formerly beyond the scope of experimentation can be

addressed. One example is the elucidation of the input-output transformations, or computations, that can be performed by a small network of neurons. Much is known about the transformation that occurs at a single synapse, that is, the relationship between the activity of a presynaptic and a postsynaptic neuron. However, extrapolation to complicated neuronal systems requires more than a simple extrapolation from such pairwise interactions. To bridge the gap from neuron to brain, it is necessary to determine what emergent properties arise from the interactions of neurons in increasingly more complicated networks. It is therefore of great interest to see whether complex computations can be predicted from the functional connectivity of a cultured neuronal network.

The computations performed by neuronal networks are not invariant in time. Changes in the connectivity between neurons, and hence changes in the input-output transformations performed by those neurons, are thought to be a cellular substrate for learning and memory (Gluck 1993). Much of our knowledge about the rules governing synaptic plasticity derives from *in vitro* studies. However, traditional techniques limit the sort of data that can be obtained to changes in synaptic strength either averaged over a large population of neurons, or in only a single pair of neurons. Consequently, most rules for the conditions required to modulate synaptic strength have been phrased in such a way as to account explicitly for the behavior of only two or three neurons. For example, Hebbian learning, the potentiation of a synapses when the pre- and postsynaptic neurons are synchronously active, has been demonstrated in the hippocampus (see Malenka 1994 for review). Heterosynaptic depression, the weakening of a synapse when it is asynchronously active with respect to the postsynaptic cell and another synaptic input,

has been demonstrated in an *in vitro* model of the neuromuscular junction (Dan and Poo 1992). The simultaneous access to several neurons provided by the neurochip will allow the testing of more complicated theories about changes in connectivity that are likely to occur in intact nervous systems.

Descriptions of the neurochip project have been published (Wright *et al.* 1996; Maher *et al.* 1999a); the results published in these two papers are summarized in the next section, with my contributions to the project described. All neurochip experiments were performed in the laboratory of Dr. Jerome Pine, with the collaboration of technicians Cory Noll and Sheri McKinney, and post-doctoral fellows Dr. Michael Maher and Dr. Steve Potter; neurochips were designed and fabricated by graduate students John Wright and Svetlana Tatic-Lucic in the laboratory of Dr. Yu-Chong Tai at Caltech.

A.2 Neurochip design and testing

A.2.1 Cell growth and survival

The design and testing of the neurochip was an iterative process. The basic structure of the neurochip comprises an array of 16 wells in a silicon substrate. Each well is a truncated pyramid shape 16 μm deep with a 30 μm square top and 8 μm square base, somewhat larger than the cell body of a neuron. Grillwork over the top of the hole includes a central hole for loading of neurons into the well, as well as corner holes to allow the growth of dendrites and axons out of each well. A gold electrode at the bottom of each well allows recording and stimulation of neuronal activity (Figure A-1).

My primary contributions to the neurochip project were to help develop the technique of loading neurons into wells and to monitor their growth and survival. Although our goal was to eventually use the neurochip to record from networks of central nervous system neurons, namely hippocampal neurons, preliminary experiments were done using dissociated SCG neurons, because we found them to be hardier and easier to maintain in culture than hippocampal neurons. Many experiments investigating growth and survival were performed on "dummy" neurochips with no electrodes, because the difficulty of fabrication of neurochips with electrodes made them a scarce resource.

The method for loading SCG neurons into neurochip wells is as follows. All procedures were performed under conditions as sterile as possible to minimize the chances of fungal or bacterial contamination. The neurochip was prepared by hydration with ethanol (because the high surface tension of water would otherwise prevent aqueous solutions from entering the tiny wells), rinsing with de-ionized water, coating with poly-DL-lysine (Sigma; 1 mg/mL solution, left on overnight), sterilization with UV radiation, and rehydration and coating with laminin (Sigma) to promote cell adhesion. SCG neurons were obtained from newborn (postnatal days 1-4) rats. Rats were decapitated following Halothane anesthesia and the SCG on each side removed. Following a brief incubation in trypsin, the ganglia were rinsed in a medium based on L-15 (Irvine Scientific) containing rat serum and nerve growth factor, and then triturated gently with a sterile Pasteur pipette to produce a suspension of dissociated neurons. This suspension was plated onto the neurochip as well as onto control dishes so that growth and survival of sibling cultures could be compared to that of the neurochip cultures. Later

experiments were performed using hippocampal neurons prepared by a similar technique from E18 rats; hippocampal cultures were maintained in a medium based on Neurobasal + B27 (Gibco).

Following plating, the neurochip was carried to the stage of an upright microscope. We developed two tools for manipulation of neurons into wells. The first was a glass microelectrode heated over a hot filament such that the tip melted back into a club-like end approximately 10 μm in diameter; the pipette was then heated about 50 μm from its end so that it would bend at about a 30° angle, resulting in an implement shaped like a tiny hockey stick. This tool was used to nudge neurons over the central hole of a neurochip well and, if necessary, push them into the well (Figure A-2). The second tool was a glass microelectrode cut back to a tip diameter of about 40 μm, and attached by tubing to a microsyringe to provide suction. This pipette was used to "vacuum" up extraneous neurons from the surface of the neurochip in the vicinity of the wells. Because of the difficulty of visualizing neuron cell bodies inside of wells, and because processes from neurons outside of the wells could easily grow into wells, elimination of neurons from the vicinity of the wells helped confirm that processes seen around wells came from neurons inside those wells. Both tools were coated by evaporation of tri-n-butylchlorosilane (Heraeus, Germany) to prevent neurons from sticking to them.

In initial neurochip experiments, disappointingly low levels of outgrowth were observed from neurochip wells. We wished to determine whether neurons placed into wells were somehow escaping rather than attaching to the substrate and growing processes, or if neurons in wells were dying or in a dormant phase where they were not extending processes. The optical properties of the neurochip precluded answering this

question by simple observation. Therefore, it was necessary to stain neurons with fluorescent dyes to see if there were, indeed, cells in wells. I used the fluorescent, lipophilic dye DiI to stain neuronal membranes and look for neurons in wells. This allowed me to confirm that in neurochips where each well had been loaded with a neuron, many wells did not contain neurons a few days after loading. (DiI also appears to stain cellular debris, and so this staining also revealed that many neurons remained in wells but died.) This discovery motivated us to modify our technique for loading neurons into wells; we subsequently allowed the neurochip to stay undisturbed on the microscope stage for several hours after neuron loading to give the neurons sufficient time to attach to the substrate. We also delayed the changing of the medium, which may also have washed cells out of wells. I also used the fluorescent, membrane-permeable vital dye calcein AM to verify that living neurons were present inside of wells (Figure A-3).

The observation that some cells were staying in wells but not developing processes, and eventually dying, led us to the conclusion that some factor was preventing the outgrowth of processes from wells. Scanning electron microscopy (SEM) of the neurochips revealed that the original method of etching wells in the silicon substrate resulted in an overhang of the top surface of the silicon past the inside edges of the well (Figure A-1b). We concluded that this sharply angled barrier presented an insurmountable obstacle to the developing growth cone, and this motivated the development of new microfabrication techniques to eliminate the overhang.

Initial studies using the redesigned neurochips showed substantially more outgrowth from wells (Figure A-4). I used SEM to take a better look at the way in which processes were emerging from wells. To do this, I fixed neurochip cultures in 2%

glutaraldehyde in phosphate-buffered saline, followed by postfixation in 1% OsO_4 on ice. I then dehydrated the sample in an ethanol series; it was then critical point dried and coated with gold. Although the sample preparation process does introduce some distortion, scanning electron micrographs clearly reveal neurons in wells with processes emerging (Figure A-5).

The success of neuron survival and outgrowth in the redesigned neurochips led to a new problem. We found that after several days in culture, neuron cell bodies would appear in the vicinity of the wells, far from any neurons in the rest of the dish. This led us to suspect that neurons were now escaping from the wells due to the tension of the growing processes. The grillwork over the wells was redesigned to reduce the size of the holes through which processes could emerge. However, by taking series of photographs of the same neurochip culture over several days, I confirmed that neurons could escape neurochip wells through a hole as small as 1 x 3 μm (Figure A-6).

This discovery motivated a further redesign of the wells. A previous study (Torre and Steward 1992) had shown that hippocampal cell bodies could not pass through 3 μm diameter, 10 μm long pores in a filter membrane, whereas axons and dendrites could readily grow through these pores. The final neurochip well design included an extension of the grillwork, called the canopy, which constrained neuron growth to tunnels of dimension similar to such pores.

A.2.2 Electrophysiological testing

The signal recorded by a neurochip well electrode of an action potential will be very small (see section A.1, p. A-1) and difficult to distinguish from background noise.

The most direct way to determine whether a neurochip electrode can record an action potential from a neuron in a well is to record using the neurochip electrode and an intracellular, sharp electrode simultaneously.

We performed electrophysiological tests on neurochip cultures of SCG neurons. After a few weeks in culture, SCG neurons develop thick (>5 μm diameter), unbranched dendrites that can be clearly assigned to their cell of origin. We used the presence of these dendrites in the vicinity of a well (Figure A-3) to verify, without having to use the somewhat cytotoxic fluorescent dyes described above (section A.2.1, p. A-5), that a particular well contained a neuron. The shallow angle of approach of the electrode to the cell in the well, necessitated by the geometry of the microscope, made successful penetrations difficult. I developed a bent intracellular electrode, made in a similar way to the hockey-stick-shaped neuron pusher described above; a standard sharp electrode was heated over a red-hot filament until the end of the electrode was bent at an angle of about 60°. Using this kind of electrode, I was able to successfully record action potentials in SCG neurons in wells. However, we found that these signals could not be detected by the neurochip electrodes. This observation led to the discovery of a design flaw in the neurochip that resulted in a capacitive shunt to ground. This discovery led to further revisions in the neurochip design.

A.3 Current status

Work performed since I left the Pine lab has shown that action potentials can be evoked and recorded by neurochip electrodes in a hippocampal culture on a redesigned neurochip (Maher *et al.* 1999b). Both spontaneous action potentials, as well as action

potentials evoked by the puffing of 1 M KCl onto the axon of a cell in a well, were recorded by well electrodes with a signal-to-noise ratio of 35-70:1 and no detectable cross-talk between electrodes. Voltage-sensitive dyes were used to confirm that action potentials could be elicited in neurons in wells by the passage of current through the well electrode. However, neurochip experiments are still hampered by the difficulty of maintaining hippocampal cultures for more than a week.

Figure A-1. Schematic diagram of cross-section through a neurochip well.

A, cross-section showing relative size of neuron soon after implantation; the neuron fits through the central hole in the grillwork. *B*, in an early neurochip design, overhanging grillwork prevents process outgrowth. *C*, in the absence of overhang, processes leave the well while the cell body is confined to the well.

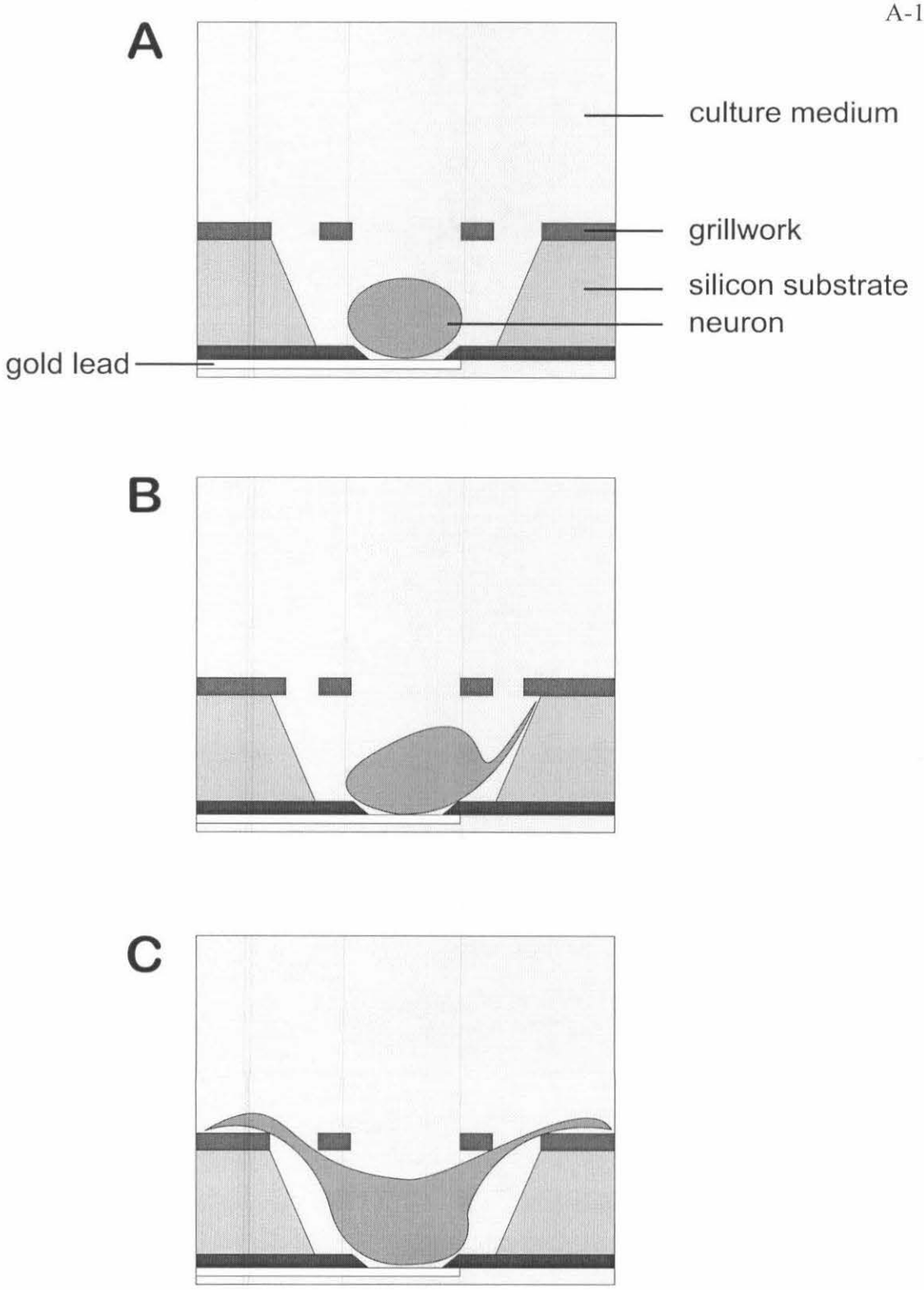
A
culture medium
grillwork
silicon substrate
neuron
gold lead
B
C

Figure A-2. A bent, rounded-off microelectrode is used to maneuver freshly dissociated neurons into wells. The tip of the tool is in focus; the double out-of-focus image is of the rest of the electrode and its reflection in the silicon neurochip surface. Scale: neurochip wells are 100 μm apart.

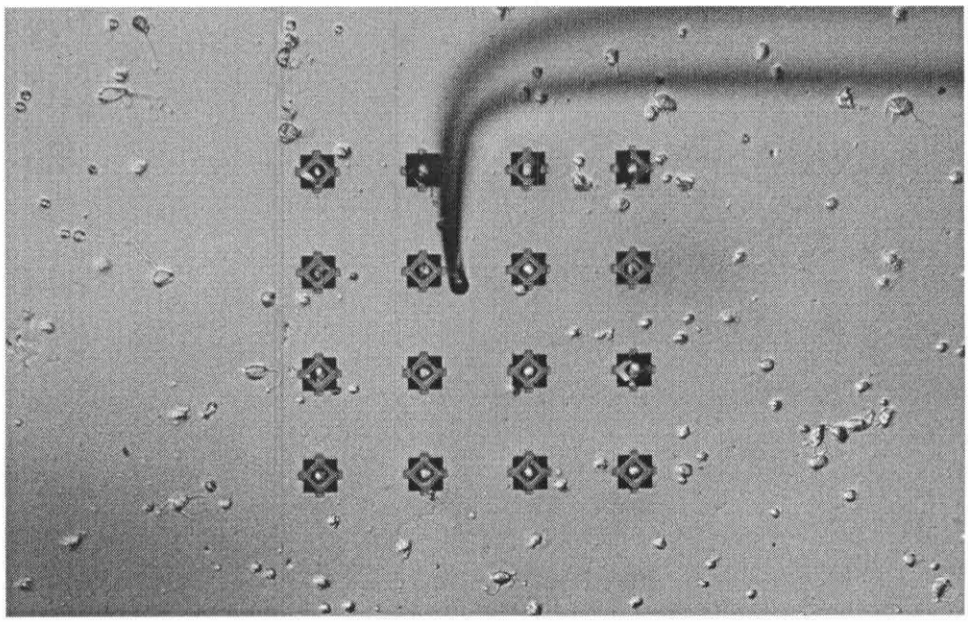

Figure A-3. Calcein AM staining of a mature SCG culture in a neurochip. *A*, differential interference contrast micrograph showing mature dendrites emerging from the center and rightmost wells (black squares) of the top row. Note that in this particular design, the grillwork is made of silicon oxide and becomes transparent when the chip is hydrated. *B*, fluorescence image showing calcein AM staining of the cells seen in *A*. *C*, overlay of *A* and *B* showing that the other four wells visible in this picture do not contain neurons. Scale: neurochip wells are 100 μm apart.

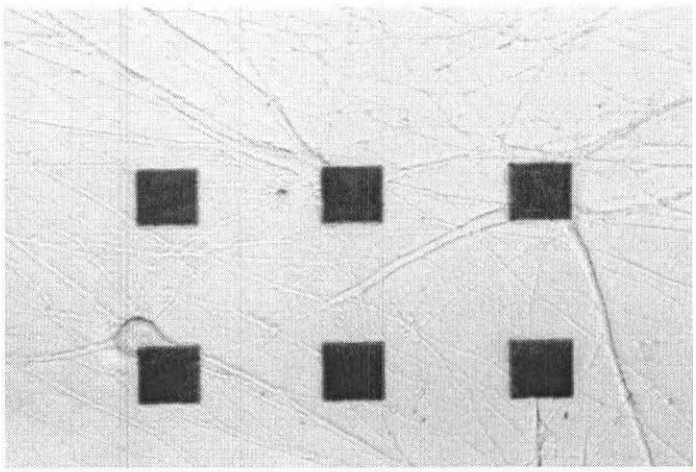

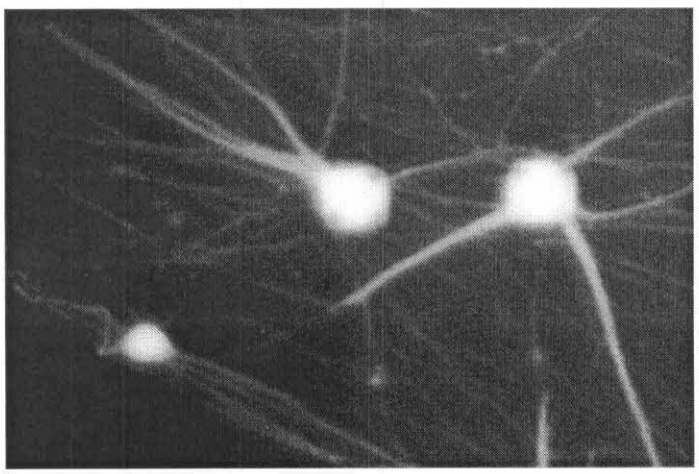

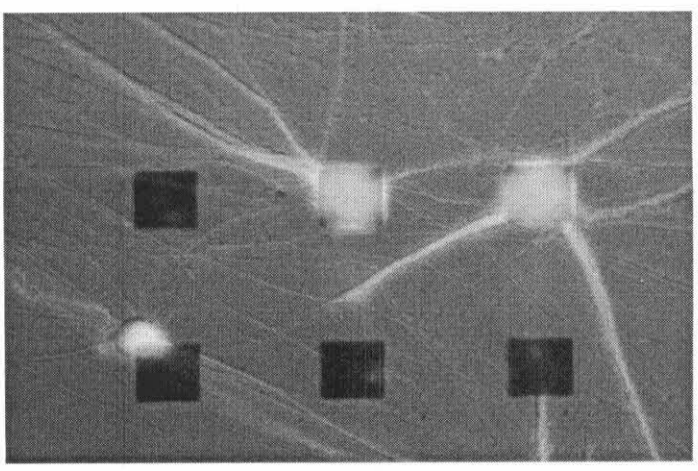

Figure A-4. Differential interference contrast micrograph of a three day hippocampal culture in a neurochip without overhanging grillwork. Processes, and cell bodies, can be seen emerging from most wells. Scale bar: 100 μm.

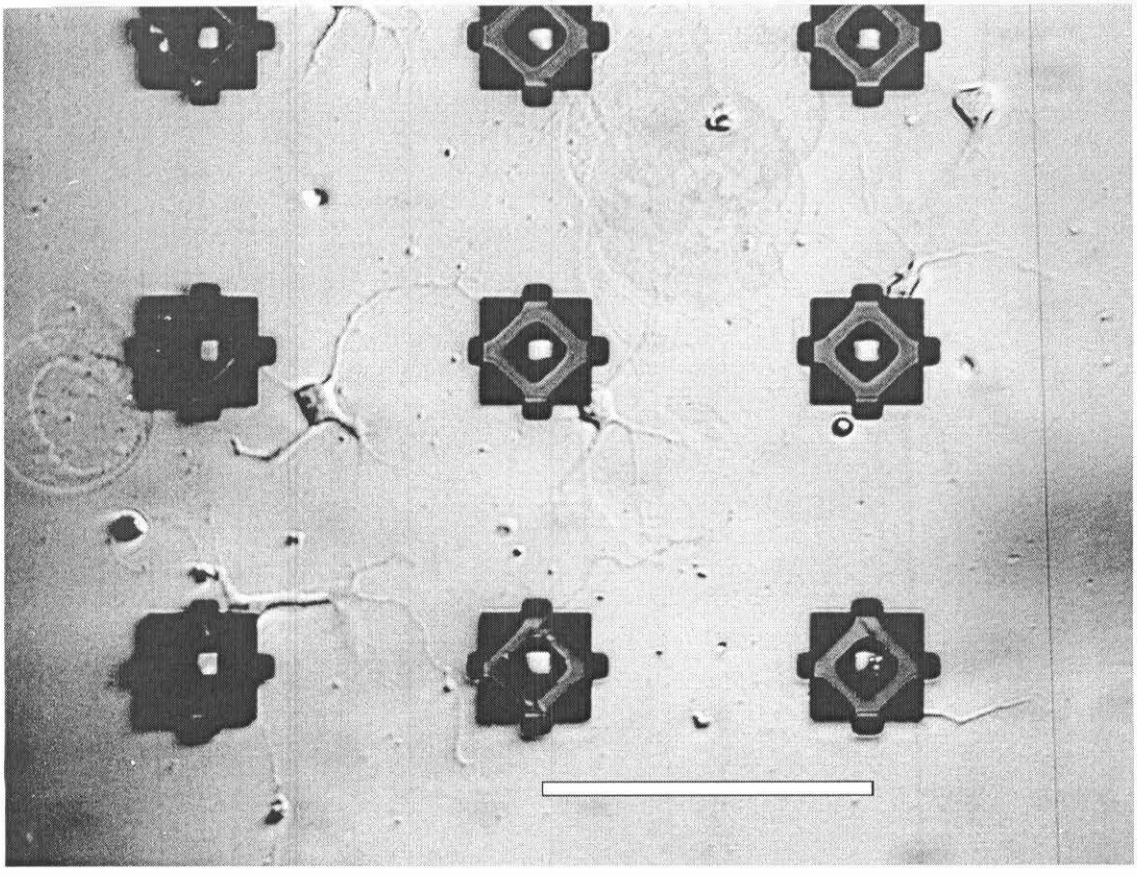

Figure A-5. Scanning electron micrographs of SCG neurons in wells without overhanging grillwork. *A*, cell body is clearly visible inside well along with growth cones emerging through corner hole as well as through center of grillwork. Scale bar: 10 μm. *B*, axons emerging through corner holes of a well. Scale bar: 10 μm. *C*, higher-magnification view of well in *B*, showing cell body inside well. Scale bar: 1 μm.

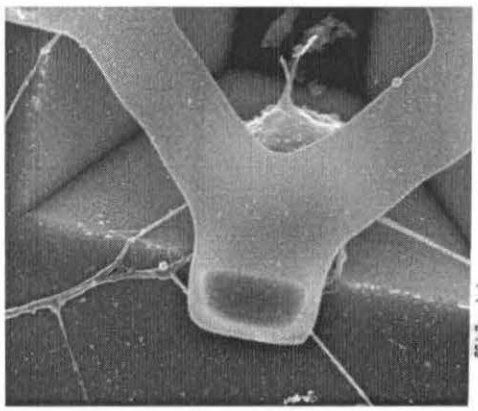

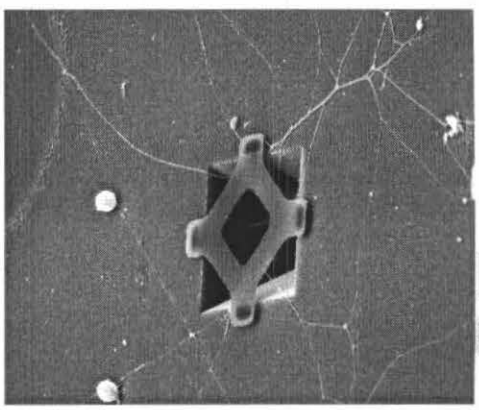

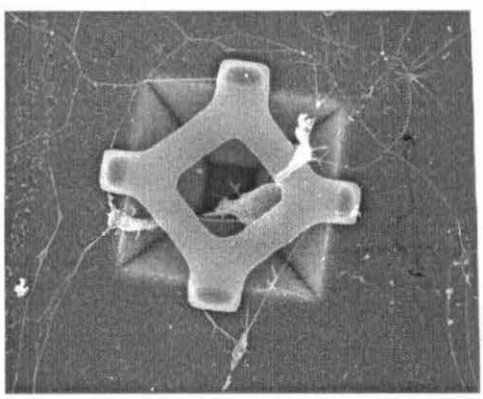

Figure A-6. Differential interference contrast micrographs showing that hippocampal neurons can escape from wells through holes as small as 1 x 3 μm. *A*, after three days in culture, a long process can be seen emerging through the top left corner of the well. *B*, same well after four days in culture; the cell body has escaped the well. Scale bar: 25 μm.

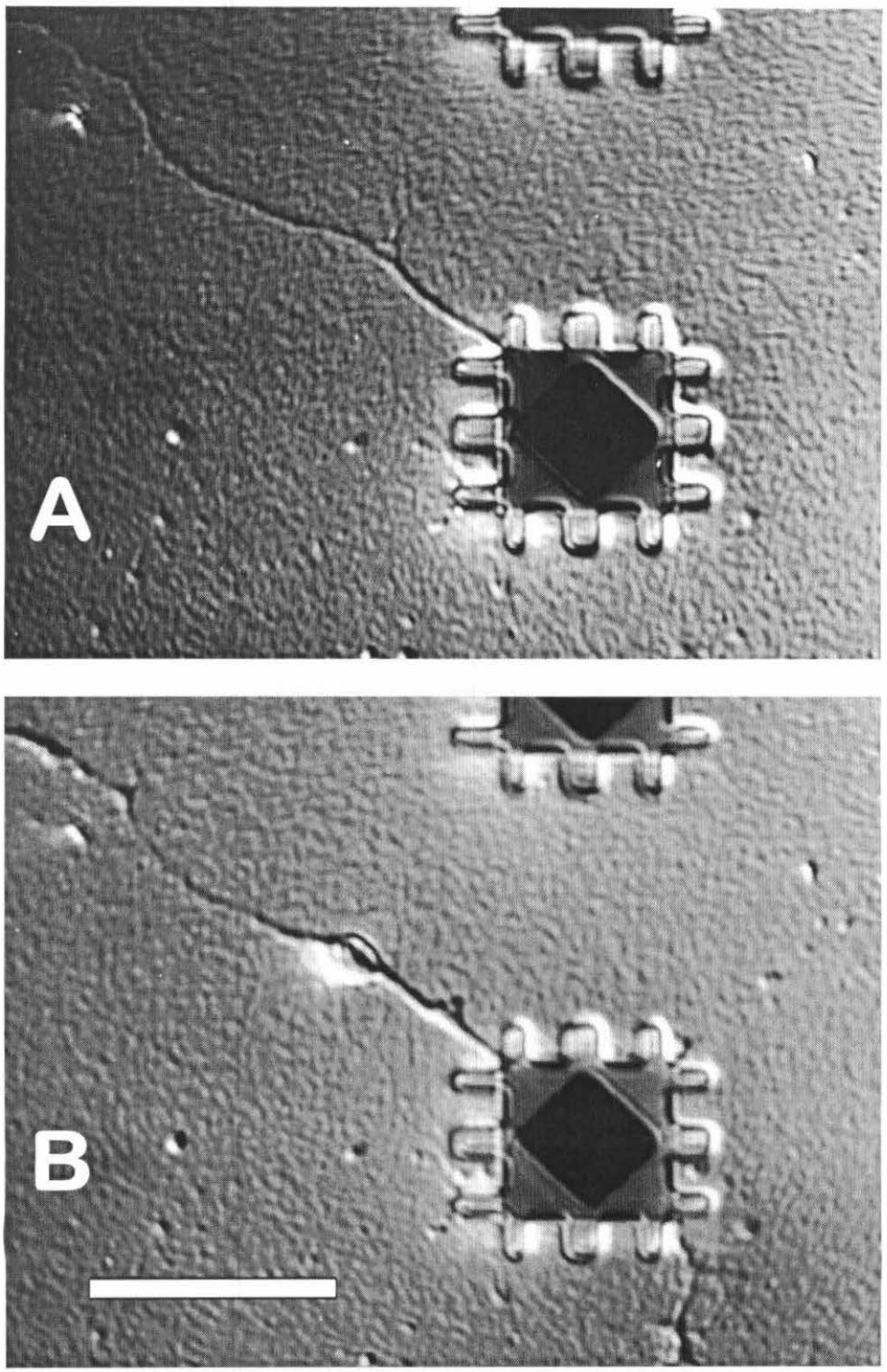
A
B